

AWARD NUMBER: W81XWH-20-1-0394

TITLE: Regulation of Prostate Cancer Dormancy and Recurrence by Hippo Signaling

PRINCIPAL INVESTIGATOR: Frank Cackowski, M.D., Ph.D.

CONTRACTING ORGANIZATION: Wayne State Universtiy

REPORT DATE: July-2021

TYPE OF REPORT: Annual Technical Report, first year

PREPARED FOR: U.S. Army Medical Research and Development Command
Fort Detrick, Maryland 21702-5012

DISTRIBUTION STATEMENT: Approved for Public Release;
Distribution Unlimited

The views, opinions and/or findings contained in this report are those of the author(s) and should not be construed as an official Department of the Army position, policy or decision unless so designated by other documentation.

REPORT DOCUMENTATION PAGE				Form Approved OMB No. 0704-0188	
Public reporting burden for this collection of information is estimated to average 1 hour per response, including the time for reviewing instructions, searching existing data sources, gathering and maintaining the data needed, and completing and reviewing this collection of information. Send comments regarding this burden estimate or any other aspect of this collection of information, including suggestions for reducing this burden to Department of Defense, Washington Headquarters Services, Directorate for Information Operations and Reports (0704-0188), 1215 Jefferson Davis Highway, Suite 1204, Arlington, VA 22202-4302. Respondents should be aware that notwithstanding any other provision of law, no person shall be subject to any penalty for failing to comply with a collection of information if it does not display a currently valid OMB control number. PLEASE DO NOT RETURN YOUR FORM TO THE ABOVE ADDRESS.					
1. REPORT DATE July-2021		2. REPORT TYPE Annual Technical Report		3. DATES COVERED 15-June-2020 to 14-June-2021	
4. TITLE AND SUBTITLE Regulation of Prostate Cancer Dormancy and Recurrence by Hippo Signaling				5a. CONTRACT NUMBER W81XWH-20-1-0394	
				5b. GRANT NUMBER PC190093	
				5c. PROGRAM ELEMENT NUMBER	
6. AUTHOR(S) Frank Cackowski E-Mail: cackowskif@karmanos.org				5d. PROJECT NUMBER	
				5e. TASK NUMBER	
				5f. WORK UNIT NUMBER	
7. PERFORMING ORGANIZATION NAME(S) AND ADDRESS(ES) Wayne State University Carole Bach 5057 Woodward Ave Suite 13001 Detroit, MI 48202-4050				8. PERFORMING ORGANIZATION REPORT NUMBER	
9. SPONSORING / MONITORING AGENCY NAME(S) AND ADDRESS(ES) U.S. Army Medical Research and Development Command Fort Detrick, Maryland 21702-5012				10. SPONSOR/MONITOR'S ACRONYM(S)	
				11. SPONSOR/MONITOR'S REPORT NUMBER(S)	
12. DISTRIBUTION / AVAILABILITY STATEMENT Approved for Public Release; Distribution Unlimited					
13. SUPPLEMENTARY NOTES					
14. ABSTRACT In prostate cancer patients with disease apparently localized to the prostate, cancer cells can spread early in the disease process, lie dormant in distant sites and then grow decades after a patient was thought to be cured. In the application for this proposal, <u>we hypothesized that; inhibition of hippo signaling or YAP1 and TAZ activation stimulates dormancy escape in prostate cancer.</u> We proposed to; Aim 1: Determine which hippo pathway components stimulate or inhibit dormancy escape in vivo, Aim 2: Delineate how tissue mechanics regulate prostate cancer dormancy through the hippo pathway, and Aim 3: Investigate how non-coding RNAs regulate prostate cancer dormancy through the hippo pathway. Thus far, we have found that culture of prostate cancer cells on medium stiffness matrix induces maximal cell cycle activity and transcription of YAP/TAZ target genes. Knockdown of the non-coding RNA, SNHG1, induces quiescence, but unexpectedly decreases YAP1 and TAZ mRNA levels. We have also have institutional approval for our animal protocol and have created stable cell lines.					
15. SUBJECT TERMS Hippo, dormancy, prostate cancer recurrence, non-coding RNA, mechanobiology					
16. SECURITY CLASSIFICATION OF:			17. LIMITATION OF ABSTRACT	18. NUMBER OF PAGES	19a. NAME OF RESPONSIBLE PERSON
a. REPORT	b. ABSTRACT	c. THIS PAGE			USAMRMC
Unclassified	Unclassified	Unclassified	Unclassified	192	19b. TELEPHONE NUMBER (include area code)

TABLE OF CONTENTS

	<u>Page</u>
1. Introduction	4
2. Keywords	5
3. Accomplishments	6
4. Impact	14
5. Changes/Problems	14
6. Products	15
7. Participants & Other Collaborating Organizations	16
8. Special Reporting Requirements	17
9. Appendices	18

1. INTRODUCTION:

Though some patients with prostate cancer are cured by surgical removal or radiation of the prostate, some patients have recurrences as long as decades after initial treatment¹. These recurrences are usually incurable if they occur at distant sites (outside the pelvis). Prostate cancer disseminated tumor cells (DTCs) display a dormant phenotype and act as an important reservoir for distant recurrence after curative intent surgery or radiation²⁻⁴. However, there are no specific treatments able to inactivate or eradicate these cells. In the preliminary data for this proposal, we used RNA-seq to compare macroscopic vs. microscopic prostate cancer tumors, analyzed TCGA data, and predicted the cell cycle phase in single cell RNA-seq data; and found that the hippo pathway and its downstream transcriptional coactivators YAP1 and TAZ appear to regulate prostate cancer dormancy and recurrence. We hypothesized that; **inhibition of hippo signaling or YAP1 and TAZ activation stimulates dormancy escape in prostate cancer**, and organized the proposed studies around the following specific aims.

Specific Aim 1: *Determine which hippo pathway components stimulate or inhibit dormancy escape in vivo.*

Specific Aim 2: *Delineate how tissue mechanics regulate PCa dormancy through the hippo pathway.*

Specific Aim 3: *Investigate how non-coding RNAs regulate PCa dormancy escape through the hippo pathway.*

Because this is an early career award, the training and career development of the principal investigator (Dr. Cackowski) is also particularly important. As guided by primary mentor, Dr. Evan Keller, co-mentors and consultants, Dr. Cackowski's career development will be structured around the following training objectives:

Training Objective 1: *Develop expertise in analyzing cell signaling of prostate cancer DTCs in vivo.*

Training Objective 2: *Learn techniques to study signaling modulation by mechanical forces and non-coding RNAs.*

Training Objective 3: *Hone skills in scientific communication and laboratory management.*

2. KEYWORDS:

Hippo kinases	MST1/MST2; Protein products of <i>STK4</i> and <i>STK3</i> genes
PCa	Prostate Cancer
PCR	Polymerase chain reaction
qRT- PCR	Real-time reverse transcriptase polymerase chain reaction
s.c.	Subcutaneous
SCID	Severe Combined Immune Deficient
YAP1	Product of <i>YAP1</i> gene, a hippo pathway downstream effector
TAZ	Product of the <i>WWTR1</i> gene, a hippo pathway downstream effector
Myc-CaP	Prostate cancer cell line derived from the FVB high myc mouse
PC3	Human patient derived prostate cancer cell line
RNA-Seq	RNA sequencing
scRNA-Seq	Single cell RNA sequencing
<i>SNHG1</i>	A long non-coding RNA gene
LATS1	Large tumor suppressor kinase 1, negatively regulates YAP1 and TAZ
LATS2	Large tumor suppressor kinase 2, negatively regulates YAP1 and TAZ
DTC	Disseminated tumor cell
DCC	Disseminated cancer cell (synonym of DTC)
Young's modulus	Physics and engineering term to describe the stiffness of a substance
lncRNA	Long non-coding RNA

3. ACCOMPLISHMENTS:

What were the major goals of the project?

Below are the tasks in the current statement of work, proposed timeline and the current status for each.

Training-Specific Tasks

Major Task 1: Training and career development in prostate cancer research	Months	Status
Subtask 1: Learn techniques to modify gene expression in prostate cancer disseminated tumor cells after the cells home to metastatic sites such as bone marrow.	1-24	Pending
Subtask 2: Learn how to use archived patient samples to assess a potential biomarker	1-12	Pending
Subtask 3: Learn how to use acoustic tweezing cytometry to modulate signaling pathways.	13-36	Pending
Subtask 4: Learn techniques to vary strength and composition of the extracellular matrix to modulate signaling pathways	13-36	Ongoing; approx. 30% completed, February, 2021
Subtask 5: Learn ultrasound imaging techniques to measure mechanical properties of tissues.	25-36	Pending
Subtask 6: Obtain proficiency with analysis of bulk and single cell RNA-sequencing data including statistics	1-48	Ongoing; approx. 30% completed, including manuscript submitted June, 2021
Subtask 7: Learn how to study how the cell cycle is controlled by non-coding RNAs	13-48	Ongoing, approx. 30% completed
Subtask 8: Learn how to use reporter constructs to assess signaling pathway activity	13-48	Pending
Subtask 9: Peer review at least two manuscripts per year with mentor feedback	1-48	Completed for year 1
Subtask 10: Complete Wayne State University "Academic Leadership Academy"	25-36	Pending
Subtask 11: Attend at least one national meeting per year	1-48	Completed for year 1 (virtual); Prostate Cancer Foundation (10/2020) and ASCO (6/2021)
Subtask 12: Attend Wayne State University seminar: "Planning and Writing Successful Grant Proposals for Biomedical Research"	24-36	Pending
<i>Milestone 1: Submit first manuscript from this proposal</i>	24	Completed: Corresponding author manuscript submitted to J Bone Oncology in May, 2021 and Co-Corresponding author manuscript submitted to Frontiers in Cell Dev Biology in June, 2021
<i>Milestone 2: Obtain NIH R01, DoD IDEA or equivalent funding</i>	36-48	Pending

Research-Specific Tasks:

Major Task 1: Determine which hippo pathway components stimulate or inhibit dormancy escape <i>in vivo</i>.	Months	Status
Subtask 1: Submit animal protocol to Wayne State IACUC and make any necessary revisions for approval. Also applies to Major tasks 2, 3 and 4.	1-3	Completed, approved 10/2020
Subtask 2: Obtain ACURO approval. Will be completed before any animal work. Also applies to Major tasks 2, 3 and 4.	4-6	Ongoing (submitted 7/14/2021)
Subtask 3: Finish preparation and testing of dominant negative and constitutively active hippo pathway constructs. For all experiments, established, de-identified human cell lines will be used: C42B, LNCaP, PC3 and Du145. The mouse prostate cancer cell line FVB MyC-CaP may also be used.	1-12	Pending
Subtask 4: Complete testing of which hippo pathway members affect the cell cycle <i>in vitro</i> . This will include analysis of single cell RNA sequencing data and use of the hippo pathway constructs	1-12	Ongoing, approx. 20% complete
Subtask 5: Perform <i>in vivo</i> experiments using the constructs tested in Subtasks 3 and 4. Mice: 120 male CB17 SCID.	7-24	Pending
Subtask 6: Establish immunofluorescence methods for tissue micro-arrays.	1-6	Pending
Subtask 7: Use tissue microarrays from PCBN, corresponding patient data and immunofluorescence to test if YAP and TAZ protein expression or localization predict time to biochemical recurrences	7-12	Pending
Subtask 8: Prepare inducible CRISPR-Cas9 cell lines if necessary depending on results from Subtask 1.	12-15	Pending
<i>Milestone: Publication submission</i>	24	Pending
Major Task 2: Delineate how mechanics of the tumor microenvironment regulate PCa dormancy through the hippo pathway	Months	Status
Subtask 1: Use acoustic tweezing cytometry to assess the effect of mechanical stress and strain on the hippo pathway and cell cycle. Cell lines are as described for Major Task 1.	13-24	Pending
Subtask 2: Determine the effect of substrate stiffness on the hippo pathway and cell cycle	13-24	Ongoing; approx. 30% completed, February, 2021
Subtask 3: Validate techniques to modulate the stiffness of the extracellular matrix <i>in vivo</i> . Mice: 30 FVB and 10 CB17 SCID	13-18	Pending
Subtask 4: Determine the effect of ECM stiffness on	19-24	Pending

prostate cancer dormancy escape. Mice: 30 CB17 SCID		
Subtask 5: Determine if DTCs' location and cell cycle status correlates with ECM stiffness <i>in vivo</i> . Uses tissues from Subtask 4.	28-36	Pending
Subtask 6: Determine if the hippo pathway is required for the effects of ECM stiffness on cell cycle <i>in vitro</i> .	13-18	Pending
Subtask 7: Determine if the hippo pathway is required for the effects of ECM stiffness on dormancy escape <i>in vivo</i> . Mice: 30 CB17 SCID	31-36	Pending
Subtask 8: Determine if the actin cytoskeleton mediates the effect of mechanics on proliferation	24-30	Pending
Subtask 9: Use Inducible CRISP/Cas9 or shRNA to determine if <i>RHOA</i> is involved in mechanical stimulation of dormancy escape <i>in vivo</i> . Mice: 60 CB17 SCID	24-36	Pending
<i>Milestone: Publication submission</i>	36	Pending
Major Task 3: Investigate how non-coding RNAs regulate PCa dormancy escape through the hippo pathway.	Months	Status
Subtask 1: Determine how SNHG1 knockdown and overexpression alters hippo signaling, and the cell cycle <i>in vitro</i> .	13-24	Ongoing; 50% completed; June, 2021
Subtask 2: Determine if other candidate non-coding RNAs interact with the hippo pathway in the experimental systems used.	16-36	Pending
Subtask 3: Create an SNHG1 inducible knockdown or over-expressing PCa cell line	31-36	Pending
Subtask 4: Determine the effect of SNHG1 modulation on prostate cancer recurrence <i>in vivo</i> . Mice: 30 CB17 SCID	37-48	Pending
<i>Milestone: Publication submission</i>	48	Pending
Major Task 4: Ensure publication of at least one manuscript per specific aim	Months	Status
Subtask 1: Additional experiments requested by reviewers	24-48	Pending
Subtask 2: Resubmission of manuscripts(s)	24-48	Pending

What was accomplished under these goals?

Training-Specific Tasks:

Major Task 1: Training and career development in prostate cancer research

We have made significant progress in Subtask 4: Learn techniques to vary strength and composition of the extracellular matrix to modulate signaling pathways. On culture with silicone matrices of varying stiffness coated with either collagen or fibronectin, we observed changes in both cell cycle and transcription of YAP/TAZ target genes (see also Figure 2).

Similarly, we are pleased to report experiential learning and experimental progress under Subtask 7: Learn how to study how the cell cycle is controlled by non-coding RNAs (see also Figures 3-6). Prior to this proposal, I had no experience in this complex and rapidly changing research area.

Although travel was severely limited by the COVID-19 pandemic, I did fulfill Subtask 11: Attend at least one national meeting per year, by attending both the Prostate Cancer Foundation Scientific Retreat and the American Society for Clinical Oncology Annual Meeting in the virtual format.

In reference to Milestone 1: Submit first manuscript from this proposal, I am pleased to report submission of two manuscripts; 1) *Use of FVB MycCaP Cells as an Immune Competent, Androgen Receptor Positive, Mouse Model of Prostate Cancer Bone Metastasis* to *Journal of Bone Oncology* as the corresponding author, and 2) *Monitoring spontaneous quiescence and asymmetric proliferation-quiescence decisions in prostate cancer cells*, to *Frontiers in Cell and Developmental Biology* as the co-corresponding author along with Co-Mentor, Dr. Laura Buttitta (see also APPENDIX p 19 – 38 and 39 – 72 respectively). The first manuscript (*Use of FVB Myc-CaP cells...*) includes data presented in Figure 4 of the initial application and figures prominently into most of the animal studies for the entire project. This manuscript describes a new model rather than findings concerning hippo signaling. However, establishment of the model in a publication first will greatly expedite subsequent studies from this project because it will allow subsequent publications to focus on the “science” rather than description and validation of the experimental model. The manuscript received favorable reviews (see APPENDIX p 73 - 75) such that we expect it to be accepted on revision. The second manuscript (*Monitoring spontaneous quiescence...*) includes data presented in figures 2 and 3 of the original proposal. This manuscript focuses on cell cycle decisions and differential regulation of quiescent (G0 cell cycle phase) cells and describes the hippo pathway as being differentially regulated in quiescence and differentially regulated between macroscopic and microscopic tumors. We found that the mRNA for multiple genes affecting the hippo pathway in both positive and negative directions are increased in G0, but that the pathway appears to be held in check by protein phosphorylation and degradation. This manuscript will establish the rationale for the study of the hippo pathway in prostate cancer dormancy and recurrence so the future publications from this study can focus on how the pathway works and cite the article in *Frontiers in Cell and Developmental Biology* as the Reason for studying hippo signaling in prostate cancer dormancy.

Research-Specific Tasks:

Major Task 1: Determine which hippo pathway components stimulate or inhibit dormancy escape *in vivo*.

Subtask 1: Submit animal protocol to Wayne State IACUC and make any necessary revisions for approval. Our protocol for the studies in this proposal was approved by the Wayne State IACUC in October, 2020 (see APPENDIX p 95 - 192). We have an amendment pending to add Kristina Ibrahim to the personnel on the protocol. She joined the group after initial approval of the protocol.

Subtask 2: Obtain ACURO approval. Will be completed before any animal work: We submitted our protocol and other required documentation to ACURO on July 14, 2021.

Subtask 4: Complete testing of which hippo pathway members affect the cell cycle *in vitro*. This will include analysis of single cell RNA sequencing data and use of the hippo pathway constructs: In figure 3 of the initial application for this project, we presented data that knockdown of *YAP1* increases the number of cells in the G0 phase of the cell cycle in PC3 prostate cancer cells. Subsequently, we have confirmed and extended this finding using alternative techniques and showed that total cell number and growth rate are also decreased by *YAP1* knockdown by siRNA and measurement of total viable cell number in PC3 cells and also in a second cell line, C42B. (**Figure 1**). We seeded cells at 50,000 cells per ml and transiently transfected with control or *YAP1* targeting siRNAs (Thermo-Fisher) using Lipofectamine RNAi MAX reagents. We trypsinized triplicate wells and changed the culture media to RPMI with 10% FCS after one day. We trypsinized triplicate wells each day for 7 days and counted total viable cell number with a Countess™ automated cell counter.

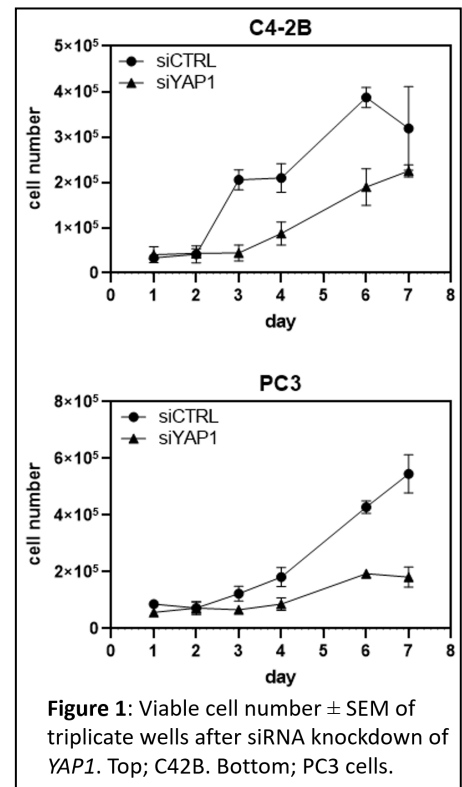


Figure 1: Viable cell number \pm SEM of triplicate wells after siRNA knockdown of *YAP1*. Top; C42B. Bottom; PC3 cells.

Major Task 2: Delineate how mechanics of the tumor microenvironment regulate PCa dormancy through the hippo pathway

Subtask 2: Determine the effect of substrate stiffness on the hippo pathway and cell cycle:

We began our studies of the effects of the stiffness of the extracellular matrix on hippo signaling in prostate cancer

cells. We were able to purchase (Advanced Biomatrix) pre-made six well culture plates coated with silicone of defined stiffness (Young's modulus) ranging from 0.5 to 64 kilo-Pascals (kPa). To allow cell attachment, we coated these substrates with two common matrix molecules; collagen or fibronectin. We seeded PC3 cells on these protein coated matrices, cultured for 2 days in RPMI with 1% FCS, lysed the cells, isolated RNA and conducted qRT-PCR with Taqman primer probes for the *YAP/TAZ* target genes; *CCN1* (*CYR61*) and *CCN2* (*CTGF*). For genes and for both protein coatings, we saw increased mRNA

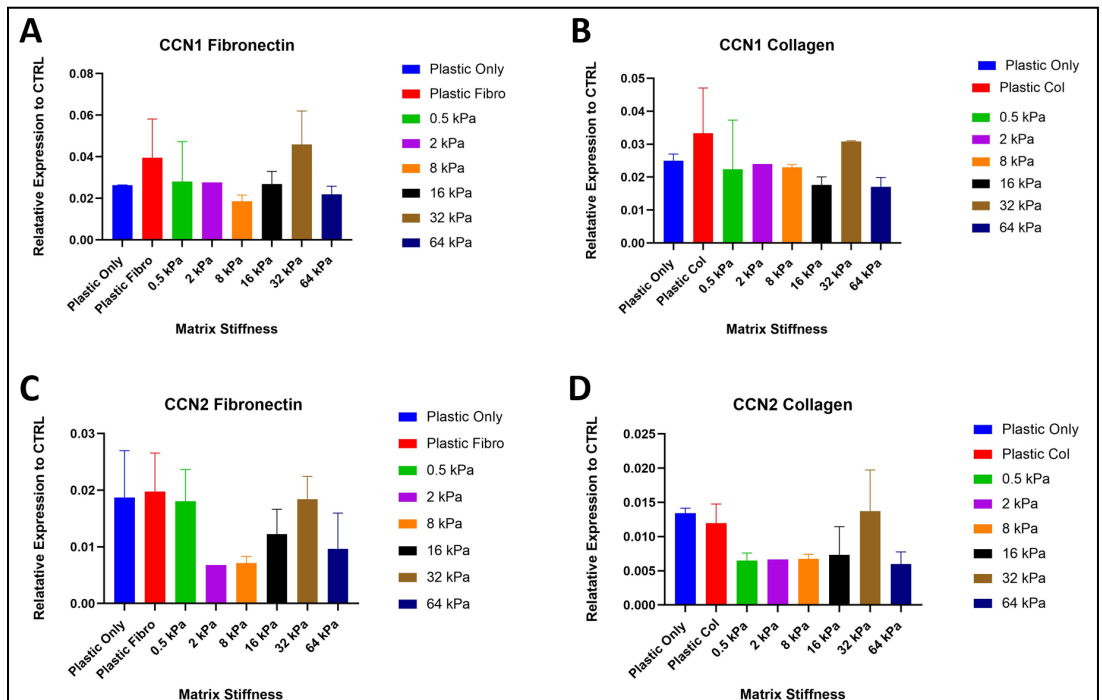


Figure 2: Relative mRNA expression *YAP/TAZ* target genes in response to matrix stiffness. (A) *CCN1* on fibronectin coated wells (B) *CCN1* on collagen coated wells (C) *CCN2* on fibronectin (D) *CCN2* on collagen. Data indicate mean \pm SD of triplicate wells.

expression at only 32 kPa (**Figure 2**). Curiously, this is well within the expected range for the stiffness of pre-calcified bone (the matrix surrounding pre-osteoblasts), which is 20-50 kPa⁵. We also note that investigators have also proposed pre-calcified bone and the osteoblastic niche to be an especially important location for homing of prostate cancer disseminated tumor cells⁶. We think that these future studies will be especially important for studies on the mechanism of prostate cancer recurrence.

Major Task 3: Investigate how non-coding RNAs regulate PCa dormancy escape through the hippo pathway.

Subtask 1: Determine how *SNHG1* knockdown and overexpression alters hippo signaling, and the cell cycle in vitro.

Effect of SNHG1 on hippo signaling

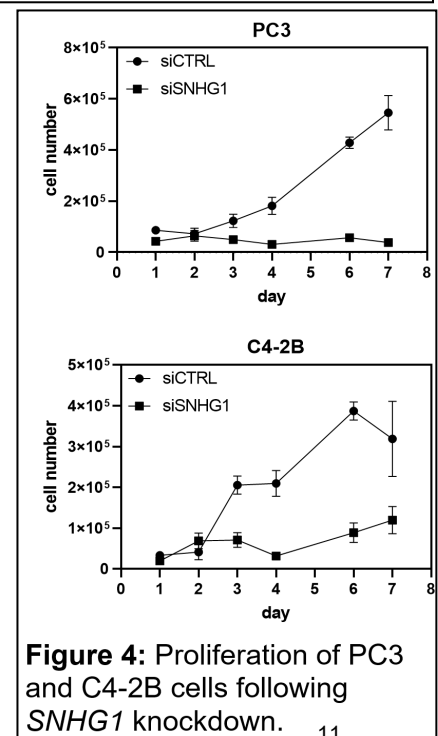
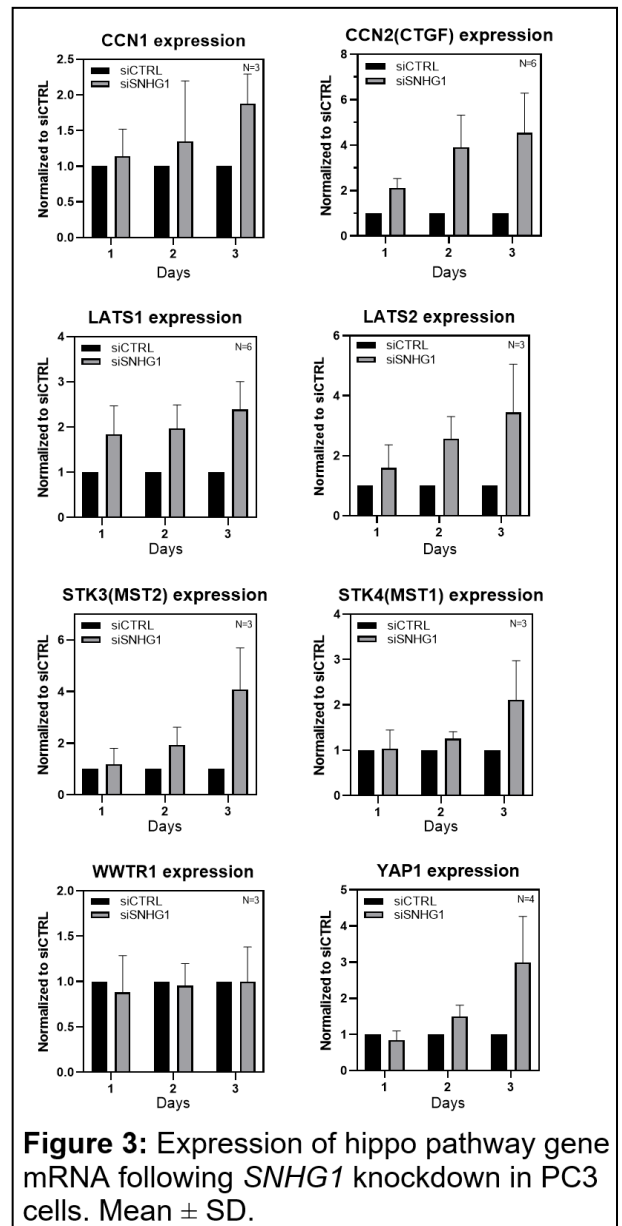
One of the ways lncRNAs regulate pathways is by altering the expression of components of the target pathway. This is done primarily through post-transcriptional regulation. The lncRNA such as *SNHG1* can competitively bind specific miRNAs and prevent them from inhibiting their target mRNA.

To determine how *SNHG1* alters the hippo pathway, we used RNAi to knockdown expression of *SNHG1* in prostate cancer cell lines, then measured expression of hippo pathway genes by RT-qPCR. As a surrogate for hippo pathway signaling, we measured expression levels of the downstream hippo-regulated genes *CCN1* and *CCN2 (CTGF)*. In PC3 cells, we obtain a 51-64% knockdown of *SNHG1* over a 3 day period. Knockdown resulted in increased expression of *CCN1* and *CCN2*, up to 1.9-fold and 4.5-fold, respectively (**Figure 3**). This indicates reduced hippo pathway signaling resulting in transcriptional activation by YAP1/TAZ/TEAD proteins. When we analyzed the expression of other hippo pathway genes following *SNHG1* knockdown, we found increased expression of *LATS1*, *LATS2*, *STK3*, *STK4*, and *YAP1* (2.1-4.0-fold increase), while *WWTR1* (gene for TAZ protein) expression was unchanged. Similar results were obtained in C4-2B cells. Investigations into the mechanisms used by *SNHG1* to affect hippo pathway signaling are ongoing.

Effect of SNHG1 on cell cycle

We analyzed the effect of *SNHG1* on cell cycle first by following growth of PC3 and C4-2B cells *in vitro* after *SNHG1* knockdown. Little to no proliferation was observed in PC3 and C4-2B cells deficient in *SNHG1* over a 7 d period (**Figure 4**). However, in control cells, cell counts increased 6-11-fold over 7 d. This was not due to greater cell death, as viability was similar to controls cells following siRNA transfection, and cell counts reported are viable cell counts.

The lack of proliferation of *SNHG1*-deficient cells led us to investigate cell cycle status of these cells. Non-proliferating cells may be senescent, or in G₀ or G₁ phase of the cell cycle. Analysis of senescence found no significant numbers of senescent cells (<1% in control and knockdown). We then used PC3 cells with “venus / cherry” reporters (PC3-VC) engineered to doubly fluoresce Venus and mCherry fluorescent proteins when they are in the G₀ cell cycle phase (quiescent) based on expression of fluorescent protein reporters for CDKN1B (p27) and CDT1. G1 phase cells are singly positive for CDT1-mCherry. The double negative population contains cells in the S, G2 and M phases. This is the same cell cycle reporter system that we presented in figure 3 of the preliminary data in the application for this project. It was originally tested in mouse



fibroblasts⁷ and has been validated for use in prostate cancer cells by our group and collaborators⁸. Cells were then analyzed by flow cytometry (**Figure 5**). In control-siRNA transfected PC3-VC cells (left), the proportion of double positive G₀ cells was found to be 13%, while in *SNHG1*-deficient cells (right), the proportion increased to 48%, a nearly 4-fold increase in quiescent cells.

In addition to analysis of G₀ and other cell cycle phases, the venus / cherry cell cycle reporter system allows us to use FACS to isolate cells in each of the cell cycle phase populations. We FACS to isolate PC3-VC cells in G₀, G₁, and S/G₂/M phases of the cell cycle. After isolation of mRNA and cDNA synthesis, we used qRT-PCR to analyze expression of *SNHG1* based on cell cycle phase. We found *SNHG1* expression correlated with cycling cells, with the lowest expression in G₀ cells and the highest expression in S/G₂/M phase cells (**Figure 6**).

Overall, these data suggest *SNHG1* is part of a regulatory network involved in cell cycle and quiescence, potentially through the hippo pathway. Further investigation will elucidate the role of *SNHG1* in this process.

Subtask 2: Determine if other candidate non-coding RNAs interact with the hippo pathway in the experimental systems used.

These experiments are ongoing. We are investigating *SNHG15* and other lncRNAs for interaction with the hippo pathway. *SNHG15* has been reported to interact with *YAP1* (Wu *et al.*, Cell Death Dis 2018).

Subtask 3: Create an *SNHG1* inducible knockdown or over-expressing PCa cell line.

These experiments are ongoing. We have constructed *SNHG1* knockout PC3, PC3-VC, C4-2B, Du45, and LnCaP cells using CRISPR technology. These cell lines are undergoing validation. We have also constructed cell lines (PC3, PC3-VC, C4-2B, Du45, LnCaP) stably expressing dCas9-SAM, a mutant Cas9 with a synergistic activation mediator (SAM) which will enable overexpression of the genomic copy of *SNHG1*. The next step in this process is to transduce the guide RNA for *SNHG1* and select for stable expression. We will generate inducible versions of these cell lines and this work is ongoing.

Subtask 4: Determine the effect of *SNHG1* modulation on prostate cancer recurrence *in vivo*.

We have acquired protocol approval by the Wayne State Institutional Animal Care and Use Committee (IACUC) for performance of these experiments.

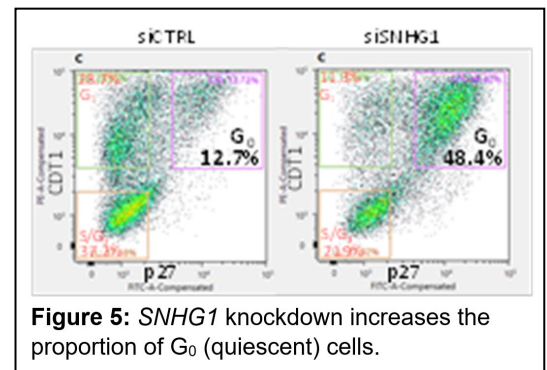


Figure 5: *SNHG1* knockdown increases the proportion of G₀ (quiescent) cells.

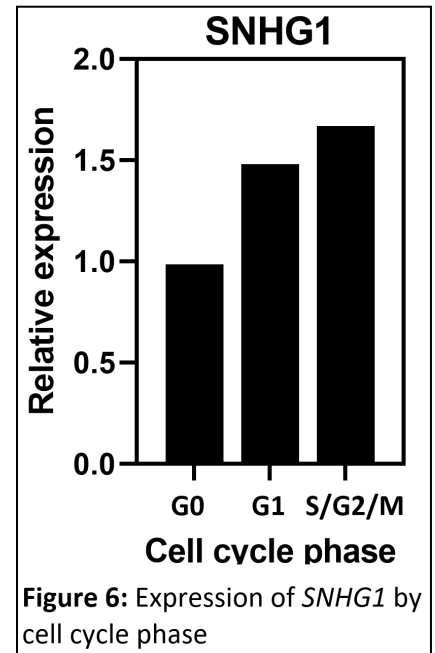


Figure 6: Expression of *SNHG1* by cell cycle phase

What opportunities for training and professional development has the project provided?

In addition to the specific skills acquired, this project has been instrumental in my career development in other critical ways – especially in the assistance it provided in achieving promotion, an independent research laboratory and a competitive start-up package. When I received the positive funding decision for this award, I was a Clinical Lecturer at University of Michigan and did not have independent laboratory space. The Clinical Lecturer title at University of Michigan is intended to give new physician researchers time to develop a research portfolio and is limited to five years. Before receiving the positive funding decision on this award, I had an active Prostate Cancer Foundation Young Investigator Award for \$225K of direct costs over three years, which was crucial to my career development. However, laboratory based researchers almost always need a career development award over twice this size in order to negotiate a physician scientist appointment, competitive start-up package, and workable clinic schedule for long term independent success. With the support of this Department of Defense Physician Research Award, I was able to successfully begin my independent career at Wayne State University and Karmanos Cancer Institute; with an appointment on the Clinical Scholar (tenure) Track, 750 square feet of laboratory space, a \$750,000 start-up package, and a 25% clinical commitment; consisting of 1.5 days per week of genitourinary medical oncology clinic and not more than six weeks of hospital consult rounding per year. In my experience and the experience of my peers, this position would not have been possible without my DoD Physician Research Award or another similarly sized grant.

With this position have come other invaluable opportunities not specifically listed in the objectives of the grant. In addition to the expected opportunities at a research university and NCI Designated Comprehensive Cancer Center, Wayne State and Karmanos Cancer Institute (WSU / KCI) have unique opportunities beneficial to a prostate cancer researcher. We are a site for the DoD funded Prostate Cancer Clinical Trials Consortium (PCCTC), which greatly eases translating laboratory based discoveries to clinical trials. Along with this are opportunities to design investigator initiated trials under the mentoring of our GU disease group lead and PCCTC site PI, Dr. Elisabeth Heath. Also, there are multiple advantages afforded by the geographic proximity to my previous institution (University of Michigan). This has allowed easy transfer of samples between me and my mentors and collaborators at University of Michigan. In the future, the geographic proximity will be useful when I require hands on teaching and use of equipment at University of Michigan. WSU/KCI also share a NCI Prostate Cancer SPORE grant with the University of Michigan, which further facilitates collaboration between institutions including with my mentors and collaborators. As an illustration of this collaboration, I published a co-first author publication with Dr. Arul Chinnaiyan and others at University of Michigan⁹ (see also APPENDIX p 76 - 82). Lastly, WSU/KCI would not be so strong in prostate cancer research if not for the leadership and insight from our Genitourinary disease group lead, Dr. Elisabeth Heath. Her presence has also created multiple opportunities for both collaborative projects and funding. For example, I was first author on a chapter published in the 2021 ASCO Educational Book¹⁰ (see also APPENDIX p 83 - 94).

Although not specifically listed in the Statement of Work, a major career development during the first year was setting up my independent research laboratory at Wayne State University and Karmanos Cancer Institute. I began laboratory set-up after my appointment began on May 1, 2021 and was ready to begin experiments in August. Laboratory set-up was critical for the experiential learning of laboratory management described in the Researcher Development Plan. During laboratory setup and hiring of personnel, I frequently consulted with members of my mentoring team, especially, Dr. Russell Taichman, who is now a Dental School Dean.

How were the results disseminated to communities of interest?

Nothing to report

What do you plan to do during the next reporting period to accomplish the goals?

We are well positioned to progress at an even faster rate during the next reporting period. We are through the initial laboratory set up period including instrument and general supply purchases and regulatory approvals. In addition to the PI's efforts, Dr. Steven Zielske has made steady progress on Research Major Task 3. Ms. Kristina Ibrahim, the newest addition to the group has played a minor role in this project thus far but will devote about half of her time to this work going forward, and will primarily work on the studies described under Research Major Task 2.

4. **IMPACT:**

- **What was the impact on the development of the principal discipline(s) of the project?**

Nothing to Report

- **What was the impact on other disciplines?**

Nothing to Report

- **What was the impact on technology transfer?**

Nothing to Report

- **What was the impact on society beyond science and technology?**

Nothing to Report

5. **CHANGES/PROBLEMS:**

- **Changes in approach and reasons for change**

Nothing to Report

- **Actual or anticipated problems or delays and actions or plans to resolve them**

Wet bench productivity was mildly reduced due to COVID-19 safety precautions. We were able to access the laboratory during most of the reporting period. However, institutional safety requirements dictated that only one person be present in the laboratory at a given time, which did reduce the amount of benchwork that could be conducted. Fortunately, because this is a new laboratory, we have start-up (discretionary) funds available. If necessary, some of these funds can be utilized in the future for personnel or supplies to ensure that we meet study objectives.

- **Changes that had a significant impact on expenditures**

Nothing to report

- **Significant changes in use or care of human subjects, vertebrate animals, biohazards, and/or select agents**

- **Significant changes in use or care of human subjects:** Nothing to report

- **Significant changes in use or care of vertebrate animals:**

The animal protocol was approved by the Wayne State University IACUC on 10/23/2020.

- **Significant changes in use of biohazards and/or select agents:** Nothing to report

6. PRODUCTS:

○ Publications, conference papers, and presentations

▪ Journal publications.

Pulianmackal AJ, Sun D, Yumoto K, Li Z, Chen YC, Patel M, Wang Y, Yoon E, Pearson A, Yang Q, Taichman R, Cackowski FC, and Buttitta L. Monitoring spontaneous quiescence and asymmetric proliferation-quiescence decisions in prostate cancer cells. *Frontiers in Cell and Developmental Biology*, 2021

Status: submitted

Federal support acknowledged: yes

Wang Y, Zielske S, Ellis L, Taichman R, and Cackowski FC. Use of FVB Myc-CaP Cells as an Immune Competent, Androgen Receptor Positive, Mouse Model of Prostate Cancer Bone Metastases. *Journal of Bone Oncology*. 2021

Status: under review

Federal support acknowledged: yes

Jung Y, Cackowski FC, Yumoto K, et al. Absciscic acid regulates dormancy of prostate cancer disseminated tumor cells in the bone marrow. *Neoplasia* 2021; **23**(1): 102-11.

Status: published

Federal support acknowledged: yes

Cackowski FC, Kumar-Sinha C, Mehra R, Wu YM, Robinson D, Alumkal J, and Chinnaiyan A. Double-Negative Prostate Cancer Masquerading as a Squamous Cancer of Unknown Primary: A Clinicopathologic and Genomic Sequencing-Based Case Study. *JCO Precis Oncol* 2020; **4**.

Status: published

Federal support acknowledged: yes

▪ Books or other non-periodical, one-time publications.

Cackowski FC, Mahal B, Heath EI, Carthon B. Evolution of Disparities in Prostate Cancer Treatment: Is This a New Normal? *Am Soc Clin Oncol Educ Book* 2021; **41**: 1-12.

Status: published

Federal support acknowledged: yes

▪ Other publications, conference papers, and presentations.

Nothing to report

○ Website(s) or other Internet site(s)

Nothing to Report

○ Technologies or techniques

Nothing to Report

○ Inventions, patent applications, and/or licenses

Nothing to Report

○ Other Products

Nothing to Report

7. PARTICIPANTS & OTHER COLLABORATING ORGANIZATIONS

- What individuals have worked on the project?

Name:	Frank Cackowski, MD, PhD
Project Role:	PI
Researcher Identifier (e.g. ORCID ID):	0000-0002-0075-3745
Nearest person month worked:	6
Contribution to Project:	Supervision, overall direction, benchwork, student mentoring
Funding Support:	This grant, Prostate Cancer Foundation Young Investigator Award, and Karmanos Cancer Institute start-up funds

Name:	Steven Zielske, PhD
Project Role:	Scientist
Researcher Identifier (e.g. ORCID ID):	none
Nearest person month worked:	4
Contribution to Project:	Benchwork predominantly on Major Task 3, and student mentoring
Funding Support:	This grant, Prostate Cancer Foundation Young Investigator Award, and Karmanos Cancer Institute start-up funds

Name:	Alexis Wilson
Project Role:	Graduate student
Researcher Identifier (e.g. ORCID ID):	none
Nearest person month worked:	2
Contribution to Project:	Benchwork predominantly on Major Task 2
Funding Support:	NCI T32 training grant

Name:	Kristina Ibrahim, MS
Project Role:	Technician
Researcher Identifier (e.g. ORCID ID):	none
Nearest person month worked:	1
Contribution to Project:	Cell culture maintenance, ordering supplies
Funding Support:	Karmanos Cancer Institute start-up funds

Has there been change in active other support of the PD/PI(s) or senior/key personnel since the last reporting period?

Nothing to Report

- **What other organizations were involved as partners?**

Nothing to Report

8. SPECIAL REPORTING REQUIREMENTS

- Nothing to Report

REFERENCES

1. Pound CR, Partin AW, Eisenberger MA, Chan DW, Pearson JD, Walsh PC. Natural history of progression after PSA elevation following radical prostatectomy. *JAMA* 1999; **281**(17): 1591-7.
2. Cackowski FC, Taichman RS. Minimal Residual Disease in Prostate Cancer. *Adv Exp Med Biol* 2018; **1100**: 47-53.
3. Chery L, Lam HM, Coleman I, et al. Characterization of single disseminated prostate cancer cells reveals tumor cell heterogeneity and identifies dormancy associated pathways. *Oncotarget* 2014; **5**(20): 9939-51.
4. Morgan TM, Lange PH, Porter MP, et al. Disseminated tumor cells in prostate cancer patients after radical prostatectomy and without evidence of disease predicts biochemical recurrence. *Clin Cancer Res* 2009; **15**(2): 677-83.
5. Engler AJ, Sen S, Sweeney HL, Discher DE. Matrix elasticity directs stem cell lineage specification. *Cell* 2006; **126**(4): 677-89.
6. Shiozawa Y, Pedersen EA, Havens AM, et al. Human prostate cancer metastases target the hematopoietic stem cell niche to establish footholds in mouse bone marrow. *J Clin Invest* 2011; **121**(4): 1298-312.
7. Oki T, Nishimura K, Kitaura J, et al. A novel cell-cycle-indicator, mVenus-p27K-, identifies quiescent cells and visualizes G0-G1 transition. *Sci Rep* 2014; **4**: 4012.
8. Takahashi H, Yumoto K, Yasuhara K, et al. Anticancer polymers designed for killing dormant prostate cancer cells. *Sci Rep* 2019; **9**(1): 1096.
9. Cackowski FC, Kumar-Sinha C, Mehra R, et al. Double-Negative Prostate Cancer Masquerading as a Squamous Cancer of Unknown Primary: A Clinicopathologic and Genomic Sequencing-Based Case Study. *JCO Precis Oncol* 2020; **4**.
10. Cackowski FC, Mahal B, Heath EI, Carthon B. Evolution of Disparities in Prostate Cancer Treatment: Is This a New Normal? *Am Soc Clin Oncol Educ Book* 2021; **41**: 1-12.

9. APPENDICES:

Journal of Bone Oncology

Use of FVB Myc-CaP Cells as an Immune Competent, Androgen Receptor Positive, Mouse Model of Prostate Cancer Bone Metastasis --Manuscript Draft--

Manuscript Number:	
Article Type:	Research Paper
Keywords:	prostate cancer; metastasis; bone; model system; androgen receptor; immune competent
Corresponding Author:	Frank Cameron Cackowski, MD, PhD Wayne State University School of Medicine Detroit, MI UNITED STATES
First Author:	Yu Wang, PhD
Order of Authors:	Yu Wang, PhD Steven P Zielske, PhD Leigh Ellis, PhD Russell S Taichman, DDS, DMSc Frank Cameron Cackowski, MD, PhD
Manuscript Region of Origin:	North America
Abstract:	Prostate cancer (PCa) metastasis research has been hamstrung by lack of animal models that closely resemble the disease present in most patients – that metastasizes to bone, are dependent on the androgen receptor (AR), and grow in an immune competent host. Here, we adapt the Myc-CaP cell line for use as a PCa androgen dependent, immune competent bone metastases model and characterize the metastases. After injection into the left cardiac ventricle of syngeneic FVB/NJ mice, these cells formed bone metastases in the majority of animals; easily visible on H&E sections and confirmed by immunohistochemistry for the AR and epithelial cell adhesion molecule. Mediastinal tumors were also observed. We also labeled Myc-CaP cells with tdTomato, and confirmed the presence of cancer cells in bone by flow cytometry. To adapt the model to a bone predominant metastasis pattern and further examine the bone phenotype, we labeled the cells with luciferase, injected in the tibia and observed tumor formation only in tibia with a mixed osteolytic / osteoblastic phenotype. The presence of Myc-CaP tumors significantly increased tibia bone volume as compared to sham injected controls. The osteoclast marker, TRAcP-5b was not significantly changed in plasma from tibial tumor bearing animals vs. sham animals. However, conditioned media from Myc-CaP cells stimulated osteoclast formation in vitro from FVB/NJ mouse bone marrow. Overall, Myc-CaP cells injected in the left ventricle or tibia of syngeneic mice recapitulate key aspects of human metastatic PCa.
Suggested Reviewers:	John Chirgwin, PhD Professor, Indiana University School of Medicine jmchirgw@iu.edu Extensive experience in cancer bone metastasis research Jesús Delgado-Calle, PhD Assistant Professor, University of Arkansas for Medical Sciences JDelgadocalle@uams.edu Research in myeloma bone disease Hernan Roca, PhD Assistant Research Scientist, University of Michigan School of Dentistry rocah@umich.edu Multiple publications on prostate cancer bone metastases Matthew Drake, MD, PhD Associate Professor, Mayo Clinic College of Medicine and Science Drake.Matthew@mayo.edu

	Multiple publications on osteoporosis and cancer bone disease
	<p>Jolele Windle, PhD Professor, Virginia Commonwealth University School of Medicine jolene.windle@vcuhealth.org Extensive experience in bone metastases and particular expertise in animal models.</p>
	<p>Deborah Galson, PhD Associate Professor, University of Pittsburgh School of Medicine galson@pitt.edu Experience with bone biology and bone metastasis research</p>



Re; Cover letter for manuscript entitled, **Use of FVB Myc-CaP Cells as an Immune Competent, Androgen Receptor Positive, Mouse Model of Prostate Cancer Bone Metastasis**

May 21, 2021

Dear Drs. Coleman, Hadji, and Heymann,

Please find enclosed our manuscript for consideration for publication as a Research Paper in *Journal of Bone Oncology*. Here, we describe use of murine Myc-CaP cells injected into FVB mice as a model system for prostate cancer bone metastasis. We view this model as a significant contribution because of the relative paucity of prostate cancer metastatic models and because of the characteristics of this particular system including; an intact immune system, dependence of the cancer cells on the androgen receptor, mixed osteolytic and osteoblastic bone tumor phenotype, and reduced cost as compared to immune deficient mouse models. Additionally, the use of a cell line in its syngeneic host, as opposed to genetically modified mouse models, will allow investigators to rapidly determine the effect of gene alterations introduced into cancer cells.

We have received uniformly positive feedback from colleagues regarding this work and are confident that it will be noticed by other investigators to the mutual benefit of the journal, authors and the prostate cancer research field. I look forward to your favorable reply and am happy to answer any questions.

Sincerely,

Frank Cackowski, M.D., Ph.D.

Assistant Professor of Oncology

Karmanos Cancer Institute and Wayne State University School of Medicine

715 Hudson Webber Cancer Research Center

4100 John R. Street

Detroit, MI, USA, 48201

Phone: 1-313-576-8321

Email: cackowskif@karmanos.org

4100 John R
Detroit, Michigan 48201
1-800-KARMANOS (1-800-527-6266)
info@karmanos.org | www.karmanos.org



- Mouse prostate cancer Myc-CaP cells readily form bone tumors in FVB/NJ mice
- Tumors are grossly confined to bone after intraosseous injection
- Myc-CaP bone tumors have a mixed osteolytic / osteosclerotic morphology
- Syngeneic Myc-CaP tumors model key aspects of prostate cancer bone metastases

Use of FVB Myc-CaP Cells as an Immune Competent, Androgen Receptor Positive, Mouse Model of Prostate Cancer Bone Metastasis

Yu Wang¹, Steven P. Zielske², Leigh Ellis³, Russell S. Taichman^{1,4} and Frank C. Cackowski^{*,2,5}

¹Department of Periodontics and Oral Medicine, University of Michigan School of Dentistry, Ann Arbor, MI, USA

²Department of Oncology, Wayne State University School of Medicine and Karmanos Cancer Institute, Detroit, MI, USA

³Department of Medicine, Cedars-Sinai Medical Center, Los Angeles, CA, USA

⁴Department of Periodontology, University of Alabama at Birmingham School of Dentistry, Birmingham, AL, USA

⁵Department of Medicine; Division of Hematology & Oncology, University of Michigan School of Medicine, Ann Arbor, MI, USA

*Corresponding author

Frank C. Cackowski, M.D., Ph.D.

Wayne State University and Karmanos Cancer Institute

Department of Oncology

Room 715 Hudson Webber Cancer Research Center

Detroit, MI, USA

Phone: 1-313-576-8321, Fax: 1-313-576-8381

email: cackowskif@karmanos.org

Twitter: @karmanoscancer

Abstract:

Prostate cancer (PCa) metastasis research has been hamstrung by lack of animal models that closely resemble the disease present in most patients – that metastasizes to bone, are dependent on the androgen receptor (AR), and grow in an immune competent host. Here, we adapt the Myc-CaP cell line for use as a PCa androgen dependent, immune competent bone metastases model and characterize the metastases. After injection into the left cardiac ventricle of syngeneic FVB/NJ mice, these cells formed bone metastases in the majority of animals; easily visible on H&E sections and confirmed by immunohistochemistry for the AR and epithelial cell adhesion molecule. Mediastinal tumors were also observed. We also labeled Myc-CaP cells with tdTomato, and confirmed the presence of cancer cells in bone by flow cytometry. To adapt the model to a bone predominant metastasis pattern and further examine the bone phenotype, we labeled the cells with luciferase, injected in the tibia and observed tumor formation only in tibia with a mixed osteolytic / osteoblastic phenotype. The presence of Myc-CaP tumors significantly increased tibia bone volume as compared to sham injected controls. The osteoclast marker, TRAcP-5b was not significantly changed in plasma from tibial tumor bearing animals vs. sham animals. However, conditioned media from Myc-CaP cells stimulated osteoclast formation *in vitro* from FVB/NJ mouse bone marrow. Overall, Myc-CaP cells injected in the left ventricle or tibia of syngeneic mice recapitulate key aspects of human metastatic PCa.

Keywords: prostate cancer, metastasis, bone, model system, androgen receptor, immune competent

Introduction:

Prostate cancer (PCa) causes over 33,000 deaths per year in the United States[1]. However, there are relatively few models available to study its pathophysiology, especially for metastatic disease, and with characteristics that closely mimic the disease of most patients[2]. Genetically engineered mouse models of PCa have been developed based on expression of the SV40 large T antigen; (transgenic adenocarcinoma of the mouse prostate (TRAMP)), or deletion of *Pten* targeted to the prostate gland[3-5]. Xenograft models metastasize to bone and other tissues but lack a normal immune system and are almost completely devoid of signaling downstream of the androgen receptor (AR)[6-8].

A basis for improvement in PCa mouse models came with the development of the Myc-CaP cell line[9]. This line was initially developed from a spontaneous prostate tumor of a c-myc overexpressing mouse and shows overexpression of wild type AR[9] and also AR splice variants[10]. Mammary fat pad tumors developed from this cell line partially regress after animals are castrated[9]. Additionally, because they are syngeneic, they have been used in studies of tumor immunology and immunotherapy when injected subcutaneously or as an intraosseous injection into the femur, but with minimal characterization of bone tumors formed after femur intraosseous injection [11-13]. However, adaptation of the FVB Myc-CaP cell line to model disseminated PCa has progressed at a slower pace. A recent report describes use of the cell line to induce liver tumors after injection in the spleen[14]. The same cell line on the C57/BL6 rather than the original FVB/NJ background was recently shown to form bone tumors after systemic (intra-cardiac) inoculation, but only from a single cell suspension of an existing tumor – which limits the studies that can be performed with the model[15]. Here, we inject FVB Myc-CaP cells maintained under routine culture conditions in the left cardiac ventricle of syngeneic mice and observe metastases to multiple bones. To better study the bone phenotype of the cells, we directly injected the cells in the tibia of mice and observed formation of large mixed osteolytic / osteoblastic tumors and characterized their bone phenotype. Therefore, we expect these models to be invaluable for future studies of PCa bone metastases.

Materials and Methods:

Cell culture and *in vitro* assays: The Myc-CaP cell line on the FVB background (#CRL-3255) was obtained from ATCC and cultured as recommended in DMEM with 10% FCS. PC3 cells were obtained from ATCC (#CRL-1435) and cultured in RPMI with 10% FCS. Myc-CaP cells were labeled by lentiviral transduction with either; tdTomato (CloneTech Lenti-LVX-IRES) and selected by FACS, or labeled with firefly luciferase (Genecopoeia hLUC-Lv105) and selected with puromycin. To model mouse osteoclast (OCL) formation, bone marrow cells from FVB/NJ mice not adherent to tissue culture plastic were used as previously described[16]. The cells were cultured for 7 days in α -MEM with 10% FCS and 10 mg/ml of rhM-CSF (R&D Systems) and rhRANKL (R&D Systems) at a sub-maximal concentration of 10 ng/ml to allow for stimulation by added conditioned media (CM). 2×10^5 cells were seeded per well in 200 μ l volume in 96 well plates. Media was changed every other day. For conditioned media collection, 5×10^5 Myc-CaP or PC3 cells were seeded in 10 cm dishes in their usual growth media (DMEM or RPMI respectively) containing 10% FCS and cultured for one day. For CM collection, the media was changed to α -MEM with 10% FCS and cells were cultured for an additional day prior

to CM collection. CM was added to OCL cultures at 25% of the total volume (50 μ l per well). Cultures were fixed with 10% neutral buffered formalin, and stained for tartrate resistant acid phosphate (TRAP) as previously described[17]. TRAP⁺ cells with three or more nuclei were counted as OCLs. To assay TRAP activity secreted into culture media, 100 μ l of media collected after 5 days of culture was combined with 200 μ l of TRAP substrate and absorbance at 562 nm was determined with a microplate reader[17]. Bone resorption and formation markers were evaluated by ELISA of plasma samples; TRAP-5b (Immunodiagnostic Systems #SB-TR103), type 1 collagen pro-peptide (Immunodiagnostic Systems #AC-33F1) and osteocalcin (Novus Biologicals #NBP2-68151).

Animal models and imaging: All studies were approved by the Institutional Animal Care and Use Committee of the University of Michigan. 5×10^5 or 5×10^4 cells recovered from *in vitro* culture were injected in the cardiac left ventricle or left tibia respectively of male syngeneic FVB/NJ mice (Jackson Labs) as previously described[18]. Bioluminescence *in vivo* imaging or fluorescence *ex vivo* imaging were conducted with a Perkin Elmer IVIS 2000 instrument. For bioluminescence imaging, 200 mg/kg of Promega VivoGloTM luciferin was injected 10 minutes prior to imaging. After injection, mice were anesthetized with 2% isoflurane in oxygen. Mice were euthanized by CO₂ asphyxiation if they became moribund from disease or at experiment endpoint. After euthanasia, blood was collected into EDTA tubes and centrifuged to collect plasma. Tissues were drop fixed in 10% neutral buffered formalin for one day at 4 °C and then stored in 70% ethanol. Bone specimens were imaged with a microCT system (μ CT100, Scanco Medical, Bassersdorf, Switzerland). Scan settings were: voxel size 12 μ m, 70 kVp, 114 μ A, 0.5 mm AL filter, and integration time 500 ms. Analysis was performed using the manufacturer's evaluation software, and a fixed global threshold of 18% (180 on a grayscale of 0–1000) was used to segment bone from non-bone. A 6 mm region of bone was analyzed beginning immediately below the growth plate for 500 slices. Bone volume and tissue mineral density were generated and compared with the control tibiae for each animal.

Histology and immunohistochemistry: Bones were then decalcified in multiple changes of 10% EDTA pH 8 for 3 weeks at 4 °C and then embedded in paraffin. 5 μ m sections stained with hematoxylin and eosin were used for general morphologic assessment. Blue staining on Masson's Trichrome was used to assess collagen. TRAP cytochemistry was used to visualize OCLs, followed by hematoxylin counterstaining and aqueous mounting as described [17]. PCa origin of tumors was confirmed by immunohistochemistry. After de-waxing and permeabilization with PBS with 0.1% Triton X-100 (PBT), antigen retrieval was performed with pepsin (Invitrogen #003009) for 15 minutes at 37°C. Endogenous peroxidases were blocked with 3% hydrogen peroxide in PBS for 15 minutes at room temperature. Slides were blocked with 5% goat serum in PBT overnight at 4°C. Primary antibodies for androgen receptor (Millipore antibody #06-680, diluted 1:50) and EPCAM (Abcam antibody #71916, diluted 1:250) or the corresponding concentrations of rabbit IgG were diluted in PBT and applied at room temperature for one hour. Slides were washed with PBT and visualized using reagents provided with the Vector rabbit ABC EliteTM kit (#PK-6101). Slides were subsequently counterstained with hematoxylin, dehydrated and mounted.

FACS and flow cytometric analysis: All analyses were conducted on a BD FACS AriaIIu cell sorter and analyzer with 405 nm, 488 nm, and 630 nm lasers and non-co-linear detectors. After transduction, successive rounds of FACS for tdTomato (PE channel) were performed until a uniform population was obtained. Unlabeled Myc-CaP cells were used as a negative control. To detect tdTomato positive tumor cells *in vivo*, lungs or bones (tibia, femur and lumbar

vertebrae) were disrupted with a mortar and pestle and strained. The cells were labeled with DAPI and mouse PE/Cy7 conjugated Ter119 (Biolegend #116222) and APC conjugated CD45 (Biolegend #103112) antibodies. Putative tumor cells were defined as single viable cells, negative for Ter119, and successively negative for CD45 but positive for tdTomato.

Statistical analyses: Student's unpaired equal variance *t*-test was used to compare two means. Multiple means were analyzed with one-way ANOVA with Tukey post-hoc testing. The log-rank test was used for survival analyses. All analyses were conducted with GraphPad Prism software.

Results:

We injected half a million Myc-CaP cells into the left cardiac ventricle of eight FVB/NJ mice and injected 4 mice with phosphate buffered saline (PBS) as sham controls. The animals injected with Myc-CaP cells died or were moribund at a median of 30 days after injection (Figure 1A). Upon necropsy of these animals, with the aid of H&E histology, we observed tumors in bones of 4 of 7 animals and in the chest of all 7 animals analyzed (Figure 1B). We did not observe tumors in the kidneys, livers, gastrointestinal tracts, or genitourinary tracts by gross analysis or H&E histology. We confirmed the presence of bone metastases by immunohistochemistry (IHC) for both androgen receptor and epithelial cell adhesion molecule (EPCAM) (Figure 1C). At the level of gross anatomic analysis, the tumors in the chest cavities, appeared to be in the mediastinum rather than arising from heart or lung. Histologically, the majority of the tumor volume was in the mediastinum, but we did observe small tumors in lung parenchyma as well (Figure 1D). To further validate the distribution of metastases in the left cardiac ventricle injection model, we labeled Myc-CaP cells with tdTomato for *in vivo* imaging and isolation and performed left cardiac ventricle injections. Gross analysis, as aided by *ex vivo* fluorescent imaging, showed tumor cells in the bone; with putative tumor cells defined as tdTomato positive and negative for Ter119 (erythroid marker) and CD45 (leukocyte marker) (Figure 1F). We consistently found in excess of an order of magnitude more events in the tumor cell gate in Myc-CaP injected animals as compared to PBS injected controls.

To explore the potential of Myc-CaP cells as a bone metastasis model and to quantify the bone phenotype, we next examined their growth after intra-tibial intraosseous injection. To increase the sensitivity of *in vivo* imaging, we labeled the Myc-CaP cells with luciferase (Figure 2A) before performing intra-tibial injections of Myc-CaP cells or sham injections of PBS into FVB/NJ mice. These animals died or required euthanasia after about two months and had large tibial tumors at the time of necropsy (Figure 2B). Tumor growth as measured by bioluminescence was detectable 5 days after injection and was only detectable in the left legs of Myc-CaP injected – but not sham injected animals (Figure 2C). On micro computed tomography (μ -CT) analysis, the lesions had areas of both bone loss and apparent new bone formation including areas outside of the prior boundary of bone cortex (Figure 2D). Because of the surprising finding of suspected extra-cortical bone formation, we analyzed the bones histologically. The extra-cortical bone areas stained as expected (pink) on hematoxylin and eosin (H&E) stains, and also as expected (blue) on Masson's trichrome stain, which selectively stains collagen (Figure 2E). Therefore, from the histologic findings and high attenuation on μ -CT analyses, we concluded that Myc-CaP bone tumors induce extra-osseous calcification in addition to abnormal bone formation within the existing bone cavity.

To further evaluate the presence of abnormal bone remodeling, we labeled sections from these specimens for tartrate resistant acid phosphatase (TRAP), as a marker of mouse osteoclasts and observed increased TRAP staining of osteoclasts (OCLs) at many of the areas of extra-cortical ossification (Figure 2E). However, we did not detect a difference in TRAP-5b in plasma from control compared to Myc-CaP tumor bearing animals (Figure 2F).

To better determine if the Myc-CaP bone tumor phenotype is osteosclerotic, osteolytic, or mixed, we quantified bone remodeling parameters. The concentration of bone formation markers, osteocalcin and pro-peptide of type 1 collagen, trended higher in the plasma of mice injected with luciferase labeled Myc-CaP cells but was not statistically significant (Figure 3A and 3B). Therefore, we quantified μ -CT images of the sham or Myc-CaP tumor bearing tibiae (Figure 2D). Presence of the Myc-CaP tumor increased the bone volume in a statistically significant fashion (Figure 3C). However, the ratio of the bone volume to total volume (BV/TV) remained unchanged (Figure 3D). Therefore, we concluded that the volume of new bone induced by the tumors was approximately balanced by the increased bone area caused by extra-cortical ossification. To further assess the contribution of Myc-CaP cells to OCL formation, we assayed formation of OCLs *in vitro* from bone marrow of FVB/NJ mice. As assessed by microscopy, counted TRAP⁺ multi-nuclear cells, and activity of TRAP secreted into the media of the OCL cultures; conditioned media (CM) from Myc-CaP cells significantly induced OCL formation as compared to control media, but induced less OCL formation than the strongly osteolytic cell line, PC3 (Figure 3E – 3G).

Discussion:

Here we describe a new mouse model of PCa bone metastases, which shares important features of the disease of many metastatic prostate cancer patients. This model utilizes the Myc-CaP prostate cancer cell line inoculated into syngeneic FVB/NJ mice and therefore produces a model that requires androgen signaling and is immune competent. The FVB background Myc-CaP cell line models the most common type of deadly PCa; disease which initially responds to androgen deprivation, then becomes castration resistant (can grow in the presence of a low concentration of testosterone), but continues to require transcription regulated by the androgen receptor. Subcutaneous FVB Myc-CaP tumors established in intact FVB/NJ mice initially shrink after medical or surgical castration, but then uniformly progress within two months[19]. In patients, selective pressure of continual hormonal based therapies can induce the development of small cell neuroendocrine prostate cancer, or alternatively “double negative” prostate cancer which has neither androgen signaling nor neuroendocrine markers. However, even in modern patients, androgen receptor positive PCa remains the most common subtype of castration resistant disease[20]. One of the ways that prostate cancers become castration resistant while retaining androgen receptor related signaling is through ligand independent splice variants of the *AR* gene including *AR-v7*. FVB background Myc-CaP cells express splice variants of the *AR* gene, whereas B6 background Myc-CaP cells do not[10]. This might explain why FVB Myc-CaP cells rapidly become castrate resistant *in vivo*, and in the current study, FVB Myc-CaP cells formed bone tumors after routine cell culture, but in another study, the investigators only observed bone tumor formation after preparing a single cell suspension of an existing tumor[15]. We expect this tumor growth from routine culture to expedite future mechanistic studies using this model.

Furthermore, because of the syngeneic and immune competent host, FVB Myc-CaP models are also well suited to studies of the immune system and immune therapy in prostate cancer[19]. This is unlike the more commonly used xenograft based models of metastatic PCa[6]. These studies are especially of interest because modern immune checkpoint inhibitors have not been effective enough in most PCa patients to garner approval from the U.S. F.D.A. or regulatory bodies in other countries, though many investigators are trying to understand the mechanisms of resistance. Of unique interest to PCa, androgens are reported to partially regulate tumor immunology, with androgen suppression favoring a more robust immune response[21]. Therefore, the previously reported ability of the FVB Myc-CaP model to respond to castration and later progress makes the model particularly attractive in studies of immunotherapy.

Lastly, development of a bone metastatic model of PCa is also notable because bone is the most common metastatic site for the disease. Indeed, 90% of patients who die of PCa have bone metastases[22]. Our studies showed that FVB Myc-CaP cells form bone metastases when administered both systemically (left ventricle intracardiac injection) and in a directed fashion when injected in the tibia. The results of our characterization of these tumors resembled the appearance of bone metastases in many PCa patients. We characterize the tumors as mixed osteosclerotic / osteolytic and quantitatively demonstrated new calcified bone formation, which curiously included areas outside of the prior cortical boundary. Although PCa bone metastases are predominantly osteosclerotic, mixed osteolytic / osteosclerotic PCa bone metastases, like our model, are not rare either and comprised 12.7% of patients in one series[23]. We also found that Myc-CaP conditioned media induced osteoclast formation *in vitro*, though not to the extent induced by the purely osteolytic cell line, PC3[8]. While others have begun to use a femoral intraosseous injection adaptation of FVB Myc-CaP cells, there has been minimal description of the bone phenotype and no reports of bone metastases after systemic (intracardiac) administration as we describe here[12, 13]. Overall, the FVB Myc-CaP cell promises to be a clinically relevant and practical model of PCa bone metastases.

Conclusions:

In these studies, we found that androgen receptor positive, murine FVB Myc-CaP cells form bone metastases in syngeneic FVB/NJ hosts with a mixed osteolytic / osteosclerotic appearance after systemic and localized intraosseous injection of cells cultured *in vitro*. The model therefore promises great utility for prostate cancer research involving bone, androgen signaling, or the immune system.

Figure Legends:

Figure 1: Distribution of tumors formed by FVB Myc-CaP cells after left ventricle injection by gross analysis, histology, fluorescence imaging, and flow cytometry. (A) Kaplan-Meier curve of time to death or humane endpoint of FVB mice injected with parental FVB Myc-CaP cells ($n = 8$) or PBS as a negative control ($n = 4$). * indicates $p < 0.05$ by the log rank test. (B) Number of animals injected with tumor cells with tumor visible on H&E sections at each listed anatomic site. (C) Immunohistochemical (IHC) validation of tumor identity of suspected bone metastases. Representative images for sections stained with H&E or IHC staining against either androgen receptor or EPCAM (brown) with hematoxylin counterstain (blue). Original magnification 100x (10x objective), or 400x (40x objective). Area of higher magnification is indicated by the boxes. (D) IHC validation of tumor identity of suspected lung metastases. (E) *ex vivo* fluorescent imaging of the CNS and MSK systems of a mouse injected in the left ventricle with tdTomato labeled FVB Myc-CaP cells. (F) Flow cytometry plots showing detection of tumor cells at metastatic sites (lung or bone) from sham (PBS) or tumor injected animals.

Figure 2: Myc-CaP tumor formation after intra-tibial injection. (A) Example bioluminescence image of mouse injected with luciferase labeled Myc-CaP cells. (B) Kaplan-Meier curve of time to death or humane endpoint of FVB mice injected with parental FVB Myc-CaP cells ($n = 14$) or PBS ($n = 4$) as a negative control. * indicates $p < 0.05$ by the log rank test. (C) Mean bioluminescence \pm SEM over time of Myc-CaP or PBS (sham) tumors. (D) Sample axial micro-CT images of tibia injected with PBS or Myc-CaP cells. (E) Sample sections stained with hematoxylin and eosin (left), Masson's trichrome (middle), or tartrate resistant acid phosphatase (TRAP) with hematoxylin counterstain (right) of sham (top) or Myc-CaP injected mouse tibiae (bottom). (F) Osteoclast activity as measured by TRAcP-5b ELISA of peripheral blood from sham injected or Myc-CaP intra-tibial tumor bearing animals, mean \pm SEM.

Figure 3: Quantification of the Myc-CaP bone tumor phenotype. (A) and (B) Osteocalcin or type 1 collagen pro-peptide concentration in plasma of mice injected in the tibia with luciferase labeled Myc-CaP cells ($n = 14$) or PBS ($n = 4$). (C) and (D) Bone volume or the ratio of bone volume to total volume (BV/TV) in tibia injected with sham or luciferase Myc-CaP cells. (E) 100 x original magnification images of osteoclast cultures stained for TRAP (red). (F) TRAP+ multinucleated cells per low power field of mouse OCL cultures with or without addition of conditioned media from Myc-CaP or PC3 cells. (G) Colorimetric assay of secreted TRAP activity in the mouse OCL cultures. Data is represented as mean \pm SEM. * indicates $p < 0.05$. Data from *in vitro* studies represents quadruplicate wells from one of four independent experiments.

Acknowledgements:

The authors wish to thank Christopher Strayhorn of the University of Michigan School of Dentistry Histology Core for tissue processing, sectioning, and H&E and trichrome staining. We also thank Michelle Lynch of the University of Michigan School of Dentistry micro CT Core, funded in part by NIH/NCRR S10RR026475-01, for CT analyses.

Funding:

Direct funding was provided by the University of Michigan Prostate Cancer S.P.O.R.E. NIH/NCI 5 P50CA18678605, PI Arul Chinnaiyan, Career Enhancement sub-award to F.C.C. F048931, and NIH/NCI P01-CA093900. F.C.C. and R.S.T. received support from The Prostate Cancer Foundation Challenge award 16CHAL05. R.T. received support as the Major McKinley Ash Colligate Professor at The University of Michigan. F.C.C. received support from The Prostate Cancer Foundation Young Investigator Award 18YOUN04, Department of Defense Prostate Cancer Research Program Physician Research Award W81XWH2010394, and start-up funds from The University of Michigan and Karmanos Cancer Institute.

References:

1. *SEER Cancer Statistics Factsheets: Prostate Cancer*. National Cancer Institute. Bethesda, MD. August 10, 2020]; Available from: <https://seer.cancer.gov/statfacts/html/prost.html>.
2. Grabowska, M.M., et al., *Mouse models of prostate cancer: picking the best model for the question*. *Cancer Metastasis Rev*, 2014. **33**(2-3): p. 377-97.
3. Hurwitz, A.A., et al., *The TRAMP mouse as a model for prostate cancer*. *Curr Protoc Immunol*, 2001. **Chapter 20**: p. Unit 20 5.
4. Kido, L.A., et al., *Transgenic Adenocarcinoma of the Mouse Prostate (TRAMP) model: A good alternative to study PCa progression and chemoprevention approaches*. *Life Sci*, 2019. **217**: p. 141-147.
5. Ma, X., et al., *Targeted biallelic inactivation of Pten in the mouse prostate leads to prostate cancer accompanied by increased epithelial cell proliferation but not by reduced apoptosis*. *Cancer Res*, 2005. **65**(13): p. 5730-9.
6. Park, S.H., M.R. Eber, and Y. Shiozawa, *Models of Prostate Cancer Bone Metastasis*. *Methods Mol Biol*, 2019. **1914**: p. 295-308.
7. Havens, A.M., et al., *An in vivo mouse model for human prostate cancer metastasis*. *Neoplasia*, 2008. **10**(4): p. 371-80.
8. Fradet, A., et al., *A new murine model of osteoblastic/osteolytic lesions from human androgen-resistant prostate cancer*. *PLoS One*, 2013. **8**(9): p. e75092.
9. Watson, P.A., et al., *Context-dependent hormone-refractory progression revealed through characterization of a novel murine prostate cancer cell line*. *Cancer Res*, 2005. **65**(24): p. 11565-71.
10. Ellis, L., et al., *Generation of a C57BL/6 MYC-Driven Mouse Model and Cell Line of Prostate Cancer*. *Prostate*, 2016. **76**(13): p. 1192-202.
11. Dudzinski, S.O., et al., *Combination immunotherapy and radiotherapy causes an abscopal treatment response in a mouse model of castration resistant prostate cancer*. *J Immunother Cancer*, 2019. **7**(1): p. 218.
12. Jiao, S., et al., *Differences in Tumor Microenvironment Dictate T Helper Lineage Polarization and Response to Immune Checkpoint Therapy*. *Cell*, 2019. **179**(5): p. 1177-1190 e13.
13. Vardaki, I., et al., *Radium-223 Treatment Increases Immune Checkpoint Expression in Extracellular Vesicles from the Metastatic Prostate Cancer Bone Microenvironment*. *Clin Cancer Res*, 2021.
14. Simons, B.W., et al., *A hemi-spleen injection model of liver metastasis for prostate cancer*. *Prostate*, 2020.
15. Simons, B.W., et al., *A mouse model of prostate cancer bone metastasis in a syngeneic immunocompetent host*. *Oncotarget*, 2019. **10**(64): p. 6845-6854.
16. Oba, Y., et al., *Eosinophil chemotactic factor-L (ECF-L): a novel osteoclast stimulating factor*. *J Bone Miner Res*, 2003. **18**(7): p. 1332-41.
17. Cackowski, F.C., et al., *Osteoclasts are important for bone angiogenesis*. *Blood*, 2010. **115**(1): p. 140-9.
18. Cackowski, F.C., et al., *Mer Tyrosine Kinase Regulates Disseminated Prostate Cancer Cellular Dormancy*. *J Cell Biochem*, 2017. **118**(4): p. 891-902.

19. Shen, Y.C., et al., *Combining intratumoral Treg depletion with androgen deprivation therapy (ADT): preclinical activity in the Myc-CaP model*. Prostate Cancer Prostatic Dis, 2018. **21**(1): p. 113-125.
20. Labrecque, M.P., et al., *Molecular profiling stratifies diverse phenotypes of treatment-refractory metastatic castration-resistant prostate cancer*. J Clin Invest, 2019. **129**(10): p. 4492-4505.
21. Graff, J.N., et al., *A phase II single-arm study of pembrolizumab with enzalutamide in men with metastatic castration-resistant prostate cancer progressing on enzalutamide alone*. J Immunother Cancer, 2020. **8**(2).
22. Bubendorf, L., et al., *Metastatic patterns of prostate cancer: an autopsy study of 1,589 patients*. Hum Pathol, 2000. **31**(5): p. 578-83.
23. Cheville, J.C., et al., *Metastatic prostate carcinoma to bone: clinical and pathologic features associated with cancer-specific survival*. Cancer, 2002. **95**(5): p. 1028-36.

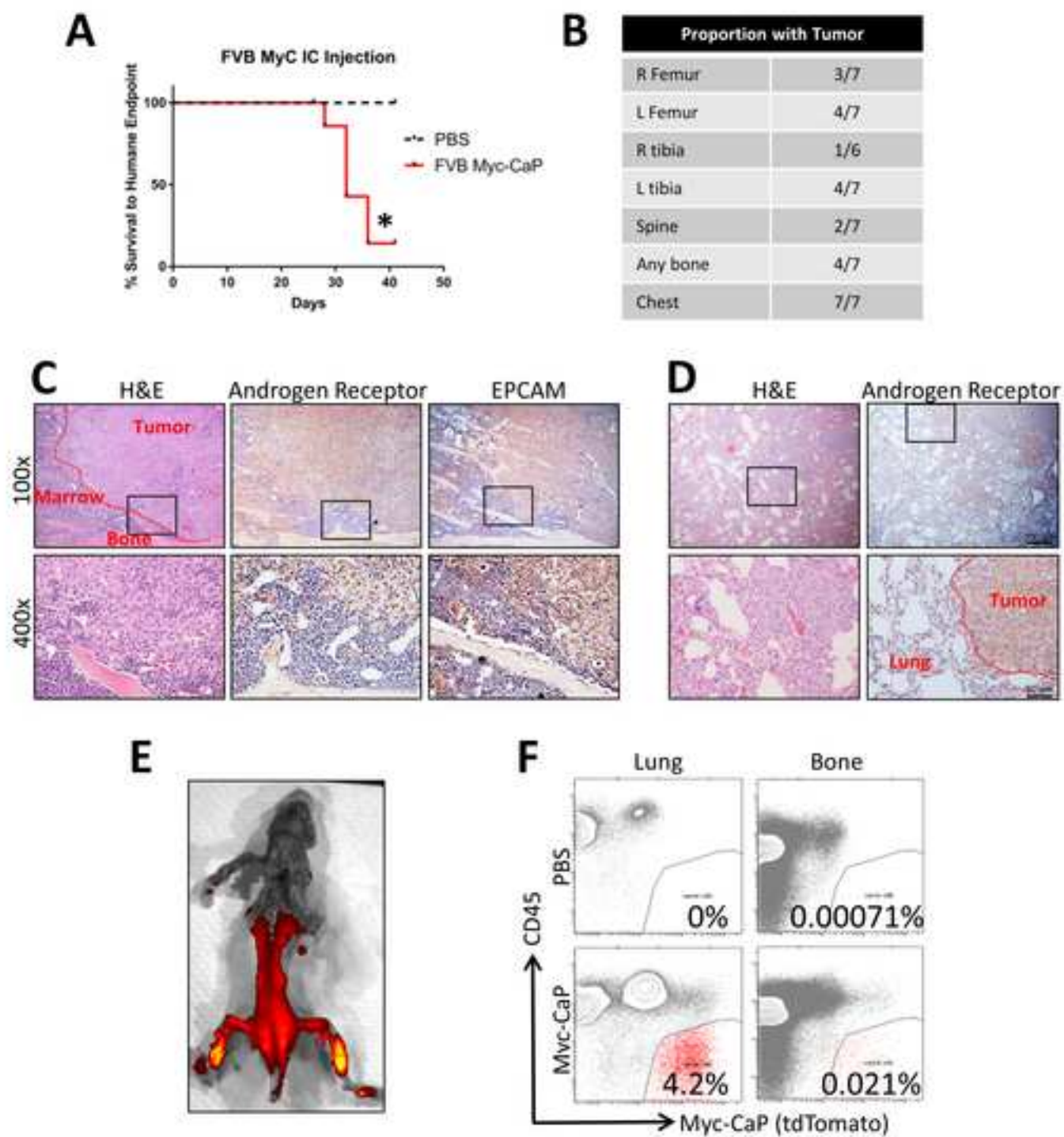
Figure 1

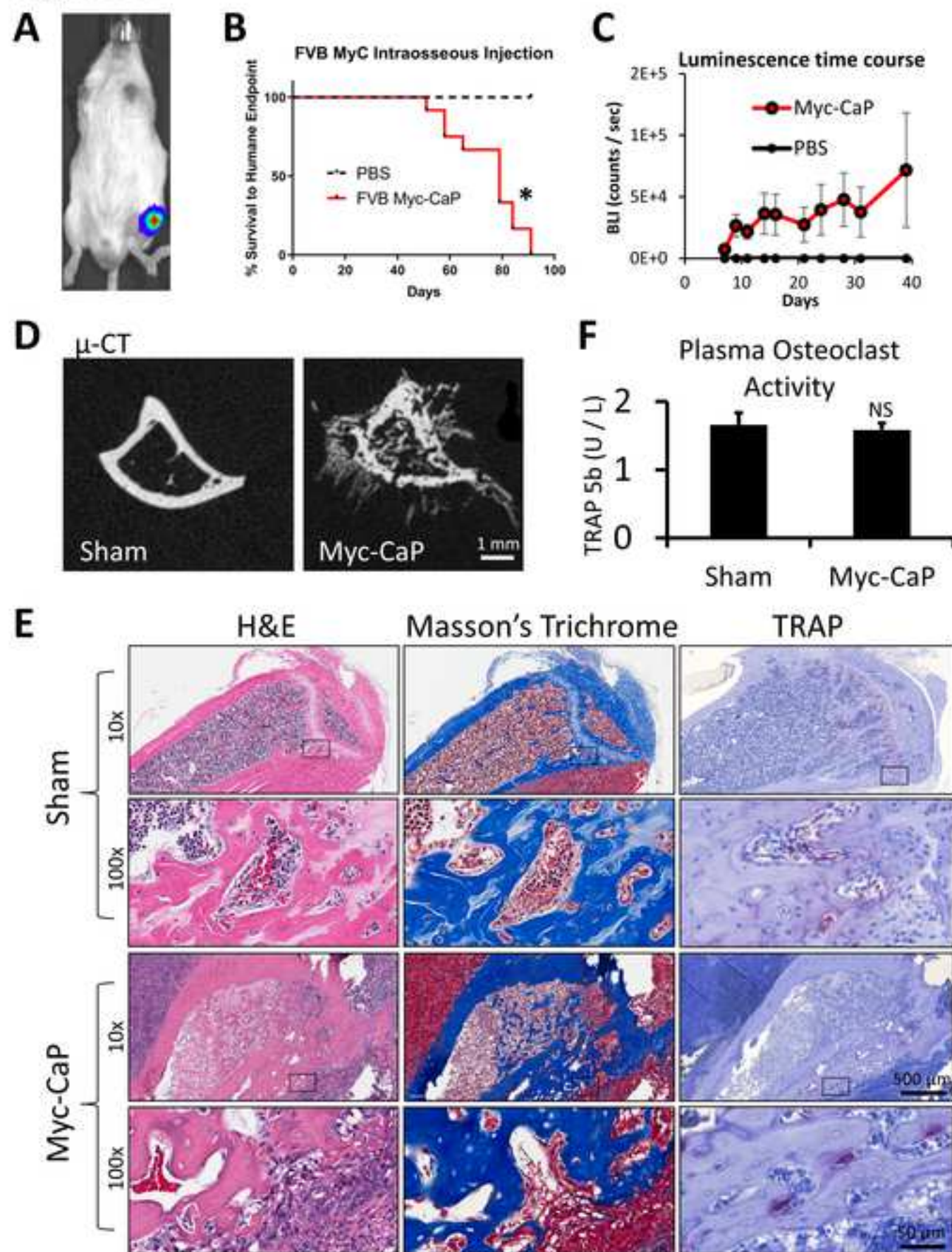
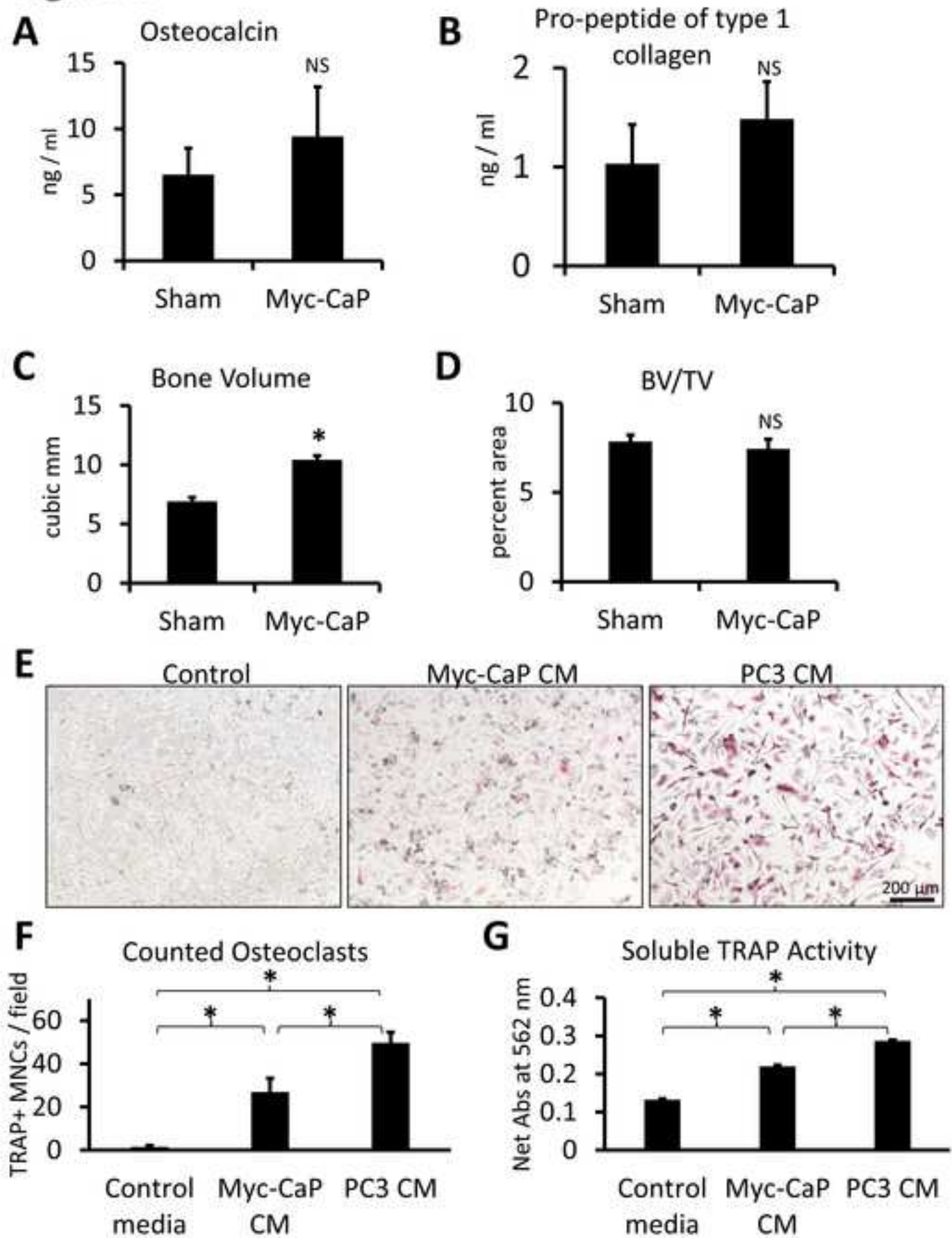
Figure 2

Figure 3

Declaration of interests

☒ The authors declare that they have no known competing financial interests or personal relationships that could have appeared to influence the work reported in this paper.

☐ The authors declare the following financial interests/personal relationships which may be considered as potential competing interests:

Author Contributions:

Yu Wang: Investigation, Visualization, Methodology, and Writing – Review and Editing. **Steven Zielske:** Investigation, Visualization, and Writing – Review and Editing. **Leigh Ellis:** Conceptualization, Methodology, Resources, and Writing – Review and Editing. **Russell Taichman:** Conceptualization, Supervision, Funding acquisition, and Writing – Review and Editing. **Frank Cackowski:** Conceptualization, Supervision, Investigation, Visualization, Methodology, Funding acquisition, Writing – Original draft preparation, and Writing – Review and Editing. All authors gave approval of the final version of the manuscript.

Monitoring spontaneous quiescence and asymmetric proliferation-quiescence decisions in prostate cancer cells

Ajai J. Pulianmackal¹, Dan Sun¹, Kenji Yumoto², Zhengda Li³, Yu-Chih Chen^{4, 5}, Meha V. Patel¹, Yu Wang^{2, 6}, Euisik Yoon^{4, 7, 8}, Alexander Pearson^{9, 10}, Qiong Yang³, Russell Taichman^{2, 11}, Frank C. Cackowski^{2, 12*}, Laura Buttitta^{1*}

¹Department of Molecular, Cellular and Developmental Biology, College of Literature, Science, and the Arts, University of Michigan, United States, ²School of Dentistry, University of Michigan, United States, ³Department of Biophysics, College of Literature, Science, and the Arts, University of Michigan, United States, ⁴Department of Electrical Engineering and Computer Science, University of Michigan, United States, ⁵Hillman Cancer Center, University of Pittsburgh Medical Center, United States, ⁶Division of Hematology and Oncology, Department of Internal Medicine, University of Michigan, United States, ⁷Department of Biomedical Engineering, University of Michigan, United States, ⁸Center for Nanomedicine, Institute for Basic Science (IBS), South Korea, ⁹University of Chicago Medical Center, United States, ¹⁰Department of Medicine, Section of Hematology/Oncology, University of Chicago Medical Center, United States, ¹¹Department of Periodontology, School of Dentistry, University of Alabama at Birmingham, United States, ¹²Karmanos Cancer Institute and Wayne State University, Dept. of Oncology, United States

Submitted to Journal:

Frontiers in Cell and Developmental Biology

Specialty Section:

Cell Growth and Division

Article type:

Original Research Article

Manuscript ID:

728663

Received on:

21 Jun 2021

Journal website link:

www.frontiersin.org

Conflict of interest statement

The authors declare that the research was conducted in the absence of any commercial or financial relationships that could be construed as a potential conflict of interest

Author contribution statement

AJP, DS, KY, ZL, AP, FCC and LB conceived of the study. AJP, DS, KY, ZL, AP, Y-CC, MVP, YW and FCC performed experiments. DS, ZL, QY, and AP developed ATCO and performed data analysis. Y-CC and EY developed the microfluidics chamber for live imaging. EY, QY, AP, RT, FCC and LB supervised research. All authors contributed to the writing of the manuscript.

Keywords

quiescence, dormancy, prostate cancer, Cell Cycle, live imaging

Abstract

Word count: 234

The proliferation-quiescence decision is a dynamic process that remains incompletely understood. Live-cell imaging with fluorescent cell cycle sensors now allows us to visualize the dynamics of cell cycle transitions and has revealed that proliferation-quiescence decisions can be highly heterogeneous, even among clonal cell lines in culture. Under normal culture conditions, cells often spontaneously enter non-cycling G0 states of varying duration and depth. This also occurs in cancer cells and G0 entry in tumors may underlie tumor dormancy and issues with cancer recurrence. Here we show that a cell cycle indicator previously shown to indicate G0 upon serum starvation, mVenus-p27K-, can also be used to monitor spontaneous quiescence in untransformed and cancer cell lines. We find that the duration of spontaneous quiescence in untransformed and cancer cells is heterogeneous and that a portion of this heterogeneity results from asymmetric proliferation-quiescence decisions after mitosis, where one daughter cell enters or remains in temporary quiescence while the other does not. We find that cancer dormancy signals influence both entry into quiescence and asymmetric proliferation-quiescence decisions after mitosis. Finally, we show that spontaneously quiescent prostate cancer cells may be poised to respond to proliferative signals via the Hippo pathway and are enriched for the stem cell markers CD133 and CD44. This suggests that dormancy signals may promote cancer recurrence by increasing the proportion of quiescent tumor cells poised for cell cycle re-entry with stem cell characteristics in cancer.

Contribution to the field

A G0 sensor, mVenus-p27K, can be used to monitor and enrich for spontaneously quiescent cells in culture. Spontaneous quiescence is heterogeneous and daughter cells resulting from a single mitosis may make asymmetric proliferation-quiescence decisions. Tumor dormancy signals can influence quiescence and asymmetric proliferation-quiescence decisions. Quiescent cancer cells are enriched for stem cell markers and express high levels of Hippo pathway signaling components.

Funding statement

This work in the Buttitta Lab was supported by funding from the American Cancer Society (RSG-15-161-01-DDC), and the Dept. of Defense (W81XWH1510413). Work in the Yang Lab is supported by the National Science Foundation (Early CAREER Grant #1553031 and MCB#1817909) and the National Institutes of Health (MIRA GM119688). Work in the Pearson lab is supported by the National Institutes of Health (K08-DE026500). Work in the Yoon Lab was in part supported by the National Institute of Health (R01-CA-203810). Work in the Cackowski Lab is supported by a Prostate Cancer Foundation Challenge award, University of Michigan Prostate Cancer S.P.O.R.E. NIH/NCI 5 P50CA18678605, Career Enhancement sub-award to F.C.C. F048931, Prostate Cancer Foundation Young Investigator Award 18YOUN04, Department of Defense Prostate Cancer Research Program Physician Research Award W81XWH2010394, and start-up funds from The University of Michigan and Karmanos Cancer Institute. Work in the Taichman lab was supported by National Institutes of Health (3P01CA093900-06) and the Prostate Cancer Foundation (16CHAL05).

Ethics statements

Studies involving animal subjects

Generated Statement: The animal study was reviewed and approved by University of Michigan Committee for the Use and Care of Animals.

Studies involving human subjects

Generated Statement: No human studies are presented in this manuscript.

Inclusion of identifiable human data

Generated Statement: No potentially identifiable human images or data is presented in this study.

In review

Data availability statement

Generated Statement: The authors acknowledge that the data presented in this study must be deposited and made publicly available in an acceptable repository, prior to publication. Frontiers cannot accept a manuscript that does not adhere to our open data policies.

Monitoring spontaneous quiescence and asymmetric proliferation-quiescence decisions in prostate cancer cells

Ajai Pulianmackal^{*1}, Dan Sun^{*1}, Kenji Yumoto², Zhengda Li³, Yu-Chih Chen^{4,5}, Meha Patel¹, Yu Wang², Euisik Yoon^{4,6,7}, Alexander Pearson^{#8}, Qiong Yang^{#3}, Russell Taichman^{2,9}, Frank C. Cackowski^{#2,10} and Laura Buttitta^{#1}

1. Molecular, Cellular and Developmental Biology, University of Michigan, Ann Arbor, MI
2. School of Dentistry, University of Michigan, Ann Arbor, MI
3. Department of Biophysics, University of Michigan, Ann Arbor, MI
4. Department of Electrical Engineering and Computer Science, University of Michigan, Ann Arbor, MI
5. Hillman Cancer Center, Department of Computational and Systems Biology, University of Pittsburgh School of Medicine, Pittsburgh, PA
6. Department of Biomedical Engineering, University of Michigan, Ann Arbor, MI
7. Center for Nanomedicine, Institute for Basic Science (IBS) and Graduate Program of Nano Biomedical Engineering (Nano BME), Advanced Science Institute, Yonsei University, Seoul, Korea.
8. Department of Medicine, Section of Hematology/Oncology, University of Chicago Medical Center, Chicago, IL
9. Department of Periodontology, School of Dentistry, University of Alabama at Birmingham, Birmingham, AL
10. Karmanos Cancer Institute and Wayne State University, Dept. of Oncology, Detroit, MI

^{*}These authors contributed equally

[#]Co-corresponding authors

Summary

The proliferation-quiescence decision is a dynamic process that remains incompletely understood. Live-cell imaging with fluorescent cell cycle sensors now allows us to visualize the dynamics of cell cycle transitions and has revealed that proliferation-quiescence decisions can be highly heterogeneous, even among clonal cell lines in culture. Under normal culture conditions, cells often spontaneously enter non-cycling G0 states of varying duration and depth. This also occurs in cancer cells and G0 entry in tumors may underlie tumor dormancy and issues with cancer recurrence. Here we show that a cell cycle indicator previously shown to indicate G0 upon serum starvation, mVenus-p27K-, can also be used to monitor spontaneous quiescence in untransformed and cancer cell lines. We find that the duration of spontaneous quiescence in

untransformed and cancer cells is heterogeneous and that a portion of this heterogeneity results from asymmetric proliferation-quiescence decisions after mitosis, where one daughter cell enters or remains in temporary quiescence while the other does not. We find that cancer dormancy signals influence both entry into quiescence and asymmetric proliferation-quiescence decisions after mitosis. Finally, we show that spontaneously quiescent prostate cancer cells may be poised to respond to proliferative signals via the Hippo pathway and are enriched for the stem cell markers CD133 and CD44. This suggests that dormancy signals may promote cancer recurrence by increasing the proportion of quiescent tumor cells poised for cell cycle re-entry with stem cell characteristics in cancer.

Highlights:

- The G0 sensor, mVenus-p27K, can be used to monitor and enrich for spontaneously quiescent cells in culture.
- Spontaneous quiescence is heterogeneous and daughter cells resulting from a single mitosis may make asymmetric proliferation-quiescence decisions
- Tumor dormancy signals can influence quiescence and asymmetric proliferation-quiescence decisions
- Quiescent cancer cells are enriched for stem cell markers and express high levels of Hippo pathway signaling components.

Introduction

Cycling cells tend to enter quiescence, a reversible, non-cycling state in response to contact inhibition, reduced levels of mitogens, or under various stress conditions. Quiescent cells retain the ability to re-enter the cycle upon the addition of serum or under favorable conditions (Coller et al., 2006; Yao, 2014). However, studies of mammalian cells in the past few years have found that many cells enter a spontaneous reversible G0-like state in cell culture even in the presence of mitogens and abundant nutrients (Spencer et al., 2013; Overton et al., 2014; Min and Spencer,

2019). This suggests that the proliferation-quiescence decision is constantly regulated - even under optimal growth conditions.

The relative percentage of cells that enter a temporary G0-like state after mitosis varies with cell type and culture conditions, suggesting many signaling inputs influence the proliferation-quiescence decision (Spencer et al., 2013). This is also consistent with findings in several cancer cell lines, where some cells enter a temporary quiescent state while others do not (Dey-Guha et al., 2011). This leads to heterogeneity in cell culture, with a subpopulation of cells entering and leaving temporary quiescent states (Overton et al., 2014). This proliferative heterogeneity may underlie states of dormancy in cancer and has been shown to be related to cancer therapeutic resistance (Recasens and Munoz, 2019;Risson et al., 2020;Nik Nabil et al., 2021). This is particularly relevant in prostate cancer, where it is thought that early spreading of tumor cells to the bone marrow and other tissues may provide signals leading to quiescence and tumor dormancy (Chen et al., 2021). Prostate cancer dormancy in tissues such as the bone are problematic as a percentage of patients will later develop recurrent cancer with significant metastases from these cells, which are often also resistant to treatment (Lam et al., 2014). Understanding how and why quiescent cancer cells reside in environments such as the bone marrow for long periods of time, and finding ways to eliminate them, is an important ongoing challenge in prostate cancer research and treatment.

The difficulties in monitoring the proliferation-quiescence decision and distinguishing different states and lengths of G0 has limited our ability to understand how signals impact the heterogeneity of quiescence in cell populations. Most assays for cell cycling status use immunostaining of cell cycle phase markers or nucleotide analogue incorporation, both of which assess static conditions in fixed samples (Matson and Cook, 2017). Cell cycle reporters such as the FUCCI system (Fluorescent Ubiquitination-based Cell Cycle Indicator), have become widely used to track cell cycle dynamics live in individual cells (Sakaue-Sawano et al., 2008). The FUCCI system and related systems such as CycleTrak and others including a constitutive nuclear marker are able to differentially label cells in G₁, S and G₂/M phases, allowing us to visualize the G₁-M transition, however G0 cannot be distinguished from G₁ in these approaches (Ridenour et al., 2012;Chittajallu et al., 2015).

Recent methods to monitor quiescence heterogeneity have used live cell imaging with sensors for Cdk2 activity, Ki-67 expression, and expression of Cdk inhibitors such as p21 and

p27 (Spencer et al., 2013;Overton et al., 2014;Stewart-Ornstein and Lahav, 2016;Miller et al., 2018;Zambon et al., 2020). Here we take advantage of the cell cycle indicator, mVenus-p27K⁻, which was generated to work in combination with the G0/G1 FUCCI reporter mCherry-hCdt1(30/120), to specifically label quiescent cells (Oki et al., 2014). This probe is a fusion protein consisting of a fluorescent protein mVenus and a Cdk binding defective mutant of p27 (p27K⁻). p27 accumulates during quiescence and is degraded by two ubiquitin ligases: the Kip1 ubiquitination-promoting complex (KPC) at the G0-G1 transition, and the SCF^{Skp2} complex at S/G2/M phases (Kamura et al., 2004). When used in combination with the G0/G1 FUCCI reporter, cells can be tracked from a few hours after mitosis until early S phase with distinct colors. This allows us to examine the dynamics of the proliferation-quiescence transition after mitosis on a single-cell level without artificial synchronization.

Prior work with a Cdk2 sensor and monitoring p21 levels revealed that both non-transformed and cancer cells in culture can enter “spontaneously” quiescent states of variable length, even under optimal growth conditions (Spencer et al., 2013;Overton et al., 2014;Yang et al., 2017;Min and Spencer, 2019). The proportion of spontaneously quiescent cells in a population and their variability in the length of quiescence leads to cell cycle heterogeneity (Overton et al., 2014), which may in part also underlie cell cycle heterogeneity within clonal tumors (Dey-Guha et al., 2011;Dey-Guha et al., 2015). This led us to examine whether we could monitor spontaneous quiescence using the mVenus-p27K⁻ G0 reporter. Here we show that by tracking the trajectory of this reporter activity, we can monitor spontaneous quiescence in non-transformed and prostate cancer cells. While measuring the heterogeneity of spontaneous quiescence, we also observed that daughter cells resulting from a single mitosis can make asymmetric proliferation-quiescence decisions. In this type of asymmetric decision, one daughter from a mitosis enters G0, while the other enters G1, further increasing cell cycle heterogeneity within a clonal population. We find that signals associated with promoting or releasing tumor dormancy can influence quiescence and asymmetric proliferation-quiescence decisions in prostate cancer cells. Using the mVenus-p27K⁻ G0 reporter, we isolate populations containing quiescent cancer cells and find they are enriched for stem cell markers and express high levels of Hippo pathway signaling components, but with inactivated YAP, which may indicate a state poised for cell cycle re-entry. Finally, we show that the expression of immune recognition

signals is decreased in populations containing quiescent cancer cells, suggesting a way these cancer cells may preferentially evade the immune system.

Results

mVenus-p27K⁻ based G0/G1 cell cycle indicators track spontaneous quiescence

To characterize the proliferation-quiescence transition at single-cell resolution in mouse 3T3 cells under full serum conditions without synchronization, we used the G0 cell cycle indicator mVenus-p27K⁻ combined with the G0/G1 reporter from the FUCCI cell cycle system, mCherry-hCdt1(30/120) to distinguish G0 cells from G1 cells as previously described (Oki et al., 2014). We first manually examined movies of asynchronously proliferating 3T3 cells stably expressing these reporters to monitor reporter dynamics (Supp. [Movie 1,2](#)). With this combination of cell cycle reporters, mVenus-p27K⁻ expression begins approximately 2-6h after cytokinesis is complete, followed by mCherry-hCdt1 expression approximately 2-6h later. Most cells then exhibit a rapid reduction in mVenus-p27K⁻ within approximately 3h, signaling G1 entry followed by mCherry-hCdt1 degradation at G1 exit (Fig 1 A,B). However, for a fraction of cells (ranging between 20-65% in different movies) we observed both mVenus-p27K⁻ and mCherry-hCdt1 to both continue to accumulate for up to 14h and beyond, without division or evidence of S/G2/M entry for 20h or more, signaling spontaneous G0 entry (Fig 1 C). This progression of reporter expression in order from mVenus-p27K⁻ positive to mVenus-p27K⁻ and mCherry-hCdt1 double positive to mCherry-hCdt1 was invariant in the movies, although we did observe some cell to cell variation in reporter expression intensity, despite using a clonal cell line.

To monitor and quantitatively measure the dynamic transitions of cell cycle states—from cytokinesis to S phase entry, we developed an Automated Temporal Tracking of Quiescence (ATCQ) analysis platform. This platform includes a computational framework for automated cell segmentation (identification of individual cells in an image), tracking, cell cycle state identification, and quantification from movies ([Supp. Fig 1](#)). The cell segmentation and tracking allows us to record the fluorescent reporter intensity changes within individual cells in real-time imaging, without the aid of a constitutive nuclear marker. The single-cell fluorescence changes over time, in turn, are used to obtain cell cycle state identification (G0, G1, or early S phase) and

quantification, which allows us to examine the kinetics of the proliferation-quiescence transition. The single-cell traces of fluorescent reporters, mVenus-p27K⁻ and mCherry-hCdt1, graphed by ATCQ is consistent with trajectories of G0 entry (increasing Venus and Cherry), G0 exit/G1 entry (degradation of Venus, increasing Cherry), and G1 exit/S-phase progression (degradation of Cherry) we manually observed in movies (Fig 1D).

To confirm that the Venus/Cherry- double positive population represents G0 phase, we performed a short-term (24h, 1%FBS) serum starvation treatment followed by 48 h of live imaging. As expected in low serum, the reporter trajectories collapsed into predominantly G0 entry (Fig 1E). When we measure the timing of the reporter trajectories we find that the timing of G0 is heterogeneous compared to G1 entry and G1 exit and becomes further prolonged under low serum (Fig 1F,G).

We next examined whether the mVenus-p27K⁻ / mCherry-hCdt1 double positive population under full serum conditions exhibits molecular markers of G0. To do this, we sorted cells into Venus/Cherry double-positive, Cherry single-positive, and Venus/Cherry double-negative populations and performed western blots for markers of G0 vs. G1 phase. As a positive control for G0, cells cultured under serum deprivation were sorted in a similar manner (Supp. Fig 2). We found that Venus/Cherry double-positive cells under full serum conditions exhibited hypophosphorylated pocket proteins RB and p130, increased endogenous p27, and reduced phosphorylation of Cdk2 on the activating T-Loop (Jeffrey et al., 1995; Sherr and Roberts, 1999; Tedesco et al., 2002). We also confirmed reduced expression of cell cycle genes, and upregulated expression of genes associated with G0 in the double positive cells in full serum by qRT-PCR on sorted cells (Supp. Fig. 2) (Oki et al., 2014). Altogether our tracking and molecular data suggests that many of the Venus/Cherry double-positive cells under full serum conditions enter a temporary G0 of variable length. We therefore conclude that this reporter combination also captures temporary, spontaneous quiescence in a fraction of asynchronously proliferating cells.

Asymmetry in the proliferation-quiescence decision

In the manual tracking of dividing cells, we noticed several instances of daughters, born of a single mitosis, making asymmetric proliferation-quiescence decisions. In this asymmetry, one daughter will remain G0, while the other daughter born at the same time will degrade the mVenus-p27K⁻ reporter and enter G1, followed by S/G2 and mitosis (Fig 1H). Under normal culture conditions we observe this in 20-40% of 3T3 cells entering G0, with the differences in the timing of G1 entry between asymmetric daughters varying from 1-15 hours. We also find that daughters can exhibit varying lengths of the Venus/Cherry double-positive state (from 5h – 24h) before one enters G1 asymmetrically. We next examined whether such asynchrony in the cell cycle progression of two daughters born of the same mitosis could be observed in other cell types. We manually examined movies of published live cell imaging and observed instances of cell cycle asynchrony in pairs of daughters in BT549 and MCF10A cells (Supp. Table 1). Asymmetric cell division rates in daughters born of the same mitosis have also been reported in MCF7 and HCT116 cells (Dey-Guha et al., 2011; Dey-Guha et al., 2015). We suggest that both spontaneous G0 and asymmetric proliferation-quiescence decisions in daughters after mitosis both contribute to cell cycle heterogeneity in clonal cell populations.

PC3 prostate cancer cells exhibit spontaneous quiescence and asymmetry in the proliferation-quiescence decision

Cellular quiescence in prostate cancer is thought to contribute to tumor dormancy and issues with metastatic cancer recurrence. However, it is not well understood how and why prostate cancer cells enter and exit quiescence. We wondered whether spontaneous quiescence and asymmetric proliferation-quiescence decisions may, in part, underlie cell cycle heterogeneity in prostate cancer cells. To examine this, we transduced the mVenus-p27K⁻ G0 and mCherry-hCdt1 G1 reporters into PC3 cells. We initially selected pools of transduced cells expressing both reporters under reduced serum conditions by FACS. We found that sorted, pooled cells quickly lost expression of one or the other reporter after a limited number of passages. We therefore isolated clones and selected a clonal PC3 Venus-Cherry cell line, stably expressing both reporters at visible levels with normal cell cycle dynamics (i.e a cell doubling time similar to parental PC3). In this line, we readily observe double positive Venus/Cherry cells under normal full-serum

culture conditions (Fig 2 A). We also confirmed that the reporters exhibited the expected G0/G1 dynamics during serum withdrawal and serum re-addition (Fig 2C).

We next attempted to track the reporter dynamics in PC3 cells with live cell imaging and found that these cancer cells were too motile to be tracked accurately for more than a few hours. We therefore used a microfluidic device we term the “cell hotel,” to capture one or a few cells and trap them in a chamber, to allow for manual tracking of individual cells and their daughters (Cheng et al., 2016). Each cell hotel slide allows simultaneous recording of up to 27 chambers under 10X magnification. We confirmed that the PC3 Venus-Cherry cells in the cell hotel exhibited similar growth and cell doubling times as previously reported for PC3 cells in bulk cell culture. In addition we repeated measurements of 3T3 Venus/Cherry cells in the cell hotel for all comparisons to PC3 (Fig. 2 E-G).

Similar to the 3T3 cells, we observed a nearly invariant reporter progression of mVenus-p27K⁻ expression 2h after cytokinesis, followed by mCherry-hCdt1 expression approximately 2h later. Cells that enter the cell cycle, degrade mVenus-p27K⁻ within approximately 4h, followed by mCherry-hCdt1 degradation and ultimately cell division (Fig 2B). As in 3T3 cells, we observed 20% of cells with stabilized mVenus-p27K⁻ and mCherry-hCdt1 for 14h and beyond, without division or evidence of S/G2/M entry for 20h or more, suggestive of spontaneous G0 entry in PC3 cells (Fig.2D). We also observed evidence of asymmetric proliferation-quiescence decisions, with 30% of daughters making asymmetric G0/G1 decisions within 1-6 hours of each other (Fig 2B). Notably, spontaneous quiescence in PC3 cells tends to be more rare and shorter than in 3T3 cells (Fig 2E). This could reflect the important role for p53 signaling in spontaneous quiescence (Arora et al., 2017; Yang et al., 2017), as PC3 cells lack functional p53 (Carroll et al., 1993). Interestingly, the asymmetric proliferation-quiescence decisions were also more rare and the difference in timing between asymmetric daughters was less dramatic in PC3 cells (Fig. 2 F, G). This may also suggest a partial role for p53 in asymmetric proliferation-quiescence decisions.

Tumor dormancy signals can influence quiescence and asymmetric proliferation-quiescence decisions

Bone is a common site for prostate cancer metastasis and work from our group and others have shown that signals from osteoblasts can influence prostate cancer dormancy and PC3 cell cycle dynamics (Jung et al., 2016; Lee et al., 2016; Yumoto et al., 2016). Our previous work on PC3 cell cycle dynamics used the FUCCI cell cycle reporters, which could not distinguish between G0 and G1 arrest (Jung et al., 2016). We therefore examined whether PC3 Venus-Cherry cells co-cultured with osteoblasts increased entry into G0 quiescence. We found that co-culture with mouse MC3T3-E1 pre-osteoblasts under full serum conditions significantly increased the fraction of double positive PC3 Venus-Cherry cells consistent with increased entry into G0 (Fig. 3A-C). We next examined whether Gas6, a signal from osteoblasts we have previously shown to induce a G0/G1 cell cycle arrest, induced entry into G0. Indeed, exposure to Gas6 increased the fraction of double positive PC3 Venus-Cherry cells after 48h, suggesting the G0/G1 arrest we previously observed was indeed arrest in G0 (Fig 3D).

In the marrow, Gas6 promotes prostate cancer dormancy (Jung et al., 2012; Taichman et al., 2013) while GM-CSF promotes stem cell release from the bone marrow, which may provide cues for metastatic cancer cells in the marrow to exit from dormancy and proliferate (Dai et al., 2010). While some of the role for GM-CSF is thought to be due to indirect effects on the bone marrow stem cell niche, studies of GM-CSF directly added to cultured PC3 cells also show increased S-phase entry, proliferation and clonogenic growth consistent with exit from dormancy (Lang et al., 1994; Savarese et al., 1998). To test whether the increased G0 we observe from Gas6 reflects prolonged G0 or increased G0 entry, we used the cell hotel to track cell cycle dynamics 6 hours after addition of Gas 6. We found an increase in the fraction of cells entering into G0 for more than 14 hours (Fig. 3D). In parallel, we also examined the response to GM-CSF and surprisingly found an increase in the fraction of cells entering G0 for more than 14h, suggesting the initial 6h response to GM-CSF may differ from the prolonged responses published previously (1-4 days). For comparison, we also measured the fraction of 3T3 cells entering G0 for more than 14h in the cell hotel and obtained results similar to those in Fig.1 (Fig. 3E).

We next examined whether signals within the bone marrow may influence asymmetric proliferation-quiescence decisions to impact cell cycle heterogeneity in metastatic prostate cancer. We found that within 6 hours of exposure, both Gas6 and GM-CSF influence asymmetric proliferation-quiescence decisions, but in opposing ways (Fig 3 F,G). Gas6 suppressed

asymmetry in favor of symmetric G0 entry and GM-CSF suppressed asymmetry in favor of symmetric G1 entry. The effect of GM-CSF on cell cycle entry in a subset of the population during the 30h of imaging was also reflected by an increase in the number of cell divisions per hour, and may reflect the initiation of the pro-proliferative effects of GM-CSF on PC3 cells shown previously (Lang et al., 1994;Savarese et al., 1998).

Quiescent cancer cells are enriched for stem cell markers and express high levels of Hippo pathway signaling components.

Identifying molecular markers of quiescent cancer cells that could be assayed in patient samples is an attractive approach to identify those at risk for metastasis and recurrence. Toward this goal, we used the PC3 Venus-Cherry cells to isolate populations enriched for quiescent cancer cells by FACS, to examine their cell surface markers and gene expression changes. (Fig. 4). We first used the prostate cancer stem cell markers CD133 and CD44 to determine whether quiescence was correlated with expression of these markers (Jung et al., 2016). We observed a strong correlation, with most CD133/CD44 double positive cells also being Venus/Cherry double positive. Although we also observe a smaller fraction of CD133/CD44 double positive cells in G1 (Fig 4A). While this is a correlation and we cannot infer whether cell cycle influences the stem cell markers or vice versa, this suggests the quiescent fraction in prostate cancer may be enriched for cancer stem cells that could underlie recurrence.

We previously established a mouse xenograft model of prostate cancer bone metastasis using Du-145 cells, that recapitulates aspects of dormancy and recurrence (Cackowski et al., 2017). We attempted to use the PC3 Venus/Cherry cells in this model, but found that the cells quickly silenced the cell cycle reporters in vivo, despite retaining the constructs. We therefore used this xenograft model with Du-145 cells as a tool to compare gene expression profiles for cells in actively growing bone metastases as assessed by bioluminescence imaging (“involved”) vs. bones without imaging detected metastases, but which still contained cancer cells that were fewer in number and presumably more slowly growing (“uninvolved”). Use of this approach of comparing cancer cells from high burden / involved vs. low burden / uninvolved sites was previously used in a breast cancer model and showed that cancer cells from the uninvolved sites

had more stem-like properties (Lawson et al., 2015). We isolated cells from mouse marrow under both conditions and performed RNAseq to compare global gene expression changes in the growing vs. dormant state. Due to the small number of human cells recovered from uninvolved bones, we were only able to accurately assign differences in expression for 117 genes (Supp. Fig. 3). Nonetheless using DAVID and the KEGG database to perform pathway analysis of differentially expressed genes, we found an enrichment of genes involved in extracellular matrix interactions and the TGF-beta signaling pathway, known to be involved in prostate cancer dormancy (Bragado et al., 2013). We noted that several of the genes falling into these enriched categories also interface with Hippo signaling, which is a key regulator of cell cycle entry and exit (Zheng and Pan, 2019). We therefore decided to examine whether components of Hippo signaling may be altered in quiescent prostate cancer cells.

To examine differences in gene expression between G0, G1, and S/G2/M populations, we sorted populations and examined gene expression differences using a Hippo signaling Pathway qRT-PCR array (Fig. 4B). In G0 cells, we noted a widespread increase in transcripts for Hippo signaling pathway components (e.g. DCHS1, FAT3, MST1, MOB1A, SAV1), transcriptional regulators (TEAD3, MEIS1) as well as targets (AMOTL1, AMOTL2) (Wang et al., 2018). The increased expression of some transcriptional targets of Hippo signaling is surprising, since these cells are in G0 and therefore would be expected to have Hippo signaling on. Hippo signaling acts via phosphorylation to suppress the activity of the downstream transcriptional effectors YAP1 and TAZ (encoded by the *WWTR1* gene in humans) (Zheng and Pan, 2019). We therefore confirmed that YAP and TAZ are indeed suppressed via phosphorylation in G0 cells through active Hippo signaling, by performing westerns for the inactivating phosphorylations on YAP1 and TAZ in G0, G1 and S/G2/M sorted cells (Fig 4C). We suggest the increased expression of Hippo pathway components may poise quiescent cells to re-enter the cell cycle upon receipt of a dormancy escape signal, but that during G0, active Hippo signaling restrains YAP and TAZ transcriptional activity through inhibitory phosphorylation. (Fig 4 and Supp. Fig 4).

Hippo signaling in cancer has been associated with restraining proliferation (Zheng and Pan, 2019), but also has been shown to alter immune response, with active Hippo signaling suppressing tumor immunogenicity (Moroishi et al., 2016; Yamauchi and Moroishi, 2019). We therefore next examined whether G0 cells exhibited alterations in expression of immune

response-associated signals. Using the Qiagen Cancer Immunology array on sorted G0, G1 and S/G2/M PC3 cells vs. the mixed population as a reference, we observed a moderate but widespread decrease in the expression of immune-related genes including signals known to target cancer cells for host immune destruction, such as CXCR3, CXCL8, and HLA-c (Fig 4D) in G0 cells. This suggests that the spontaneously quiescent cancer cells also exhibit altered immunoreactivity. Interestingly, one pro-inflammatory gene, PTGS2 (Cox-2), was strongly upregulated in G0 cells (Fig 4D), consistent with the previous work showing this target to be de-repressed when upstream Hippo signaling is active and YAP/TAZ are suppressed by phosphorylation (Zhang et al., 2018). Taken together, our results suggest the inherent cell cycle heterogeneity of metastatic prostate cancer includes a fraction of spontaneously quiescent cells that are enriched for potential cancer stem cells and exhibit gene expression changes consistent with a state poised to re-enter the cell cycle, but potentially less visible to the host immune system.

Discussion

Several cancers contain heterogeneous populations with varying levels of proliferation (Davis et al., 2019). Some studies suggest that quiescent tumor cells contribute to drug-resistance, by providing a population of non-cycling cells that survive cytotoxic chemotherapy (De Angelis et al., 2019; Talukdar et al., 2019; Hen and Barkan, 2020). Understanding the molecular basis of proliferative heterogeneity therefore may assist in developing better therapeutic approaches for cancer. Here, we show that untransformed 3T3 cells and PC3 prostate cancer cells show spontaneous quiescence and heterogeneous G0 lengths under pro-proliferative culture conditions. We propose that spontaneous quiescence may be related to quiescence in cancer, since quiescent cancer cells must leave the cell cycle in the presence of pro-proliferative growth factor and oncogenic signaling.

Spontaneous quiescence has been shown to underlie clonal cell cycle heterogeneity (Overton et al., 2014) and may in part underlie cell cycle heterogeneity in tumors. Here we show an additional mechanism to create heterogeneity, asymmetric G0/G1 decisions, where one daughter from a mitotic event remains in G0, while the other enters G1. These asymmetric decisions are somewhat surprising, since recent work has suggested the signals that influence the proliferation-

quiescence decision are integrated over the previous cell cycle phases prior to mitosis and therefore would be expected to be inherited equally in daughters after mitosis (Yang et al., 2017;Min et al., 2020). The asynchrony in asymmetric PC3 cell divisions is generally only a few hours and may possibly be explained by fluctuations resulting in unequal protein and transcript inheritance at mitosis. However, this is a less satisfying hypothesis for G0/G1 asymmetry in 3T3 cells, where differences in G0 exit between daughters born at the same time can exceed 10h. Previous work in MCF7 breast and HCT116 colon cancer cells has shown a population of dormant cells resulting from asymmetric Akt signaling after cell divisions (Dey-Guha et al., 2011). In this example, about 1% of cell divisions exhibit asymmetry, resulting in a daughter with low Akt signaling. Importantly, elimination of Akt prevented proliferative heterogeneity in these lines in cell culture (Dey-Guha et al., 2015), and inhibition of asymmetric Akt signaling reduced tumor recurrence after treatment in a xenograft model (Alves et al., 2018). It is worth noting that PC3 cells lack functional PTEN (Huang et al., 2001;Dubrovskaya et al., 2009) and therefore may have higher endogenous Akt signaling that suppresses some degree of asymmetry. In addition, Gas6 and other TYRO3/AXL/MERTK ligands signal in part through Akt, and therefore may impact Akt asymmetry (Cosemans et al., 2010;Kasikara et al., 2017). Inhibition of Akt signaling can lead to up regulation of p27 in PC3 cells (van Duijn and Trapman, 2006), while over expression of p27 can also inhibit Akt signaling (Chen et al., 2009). Further work will be needed to determine if asymmetric Akt signaling may be a cause or consequence of asymmetric proliferation-quiescence decisions in prostate cancer.

The relationship of dormancy and cellular quiescence remains unclear. Here we show that a dormancy-associated signal in prostate cancer, Gas6, rapidly within 6h, induces quiescence entry in cells after mitosis. We further show that exposure to Gas6 tips the balance of asymmetric proliferation-quiescence decisions in favor of symmetric G0 entry. By contrast, a pro-proliferative signal for PC3 cells, GM-CSF tips the balance in favor of symmetric divisions into G1. We suggest that in addition to altering G0/G1 choice after mitosis, extracellular signals that influence G0/G1 asymmetry could influence tumor cell cycle heterogeneity.

Understanding the gene expression changes in dormant cancer cells will be essential to understanding their biology, but will also be useful tools as molecular markers for identifying

them in patient samples. Here we show that quiescent PC3 cells are enriched for prostate cancer stem cell markers CD133 and 44, and exhibit increased expression of many Hippo pathway components, while the Hippo pathway remains on to restrain cell cycle entry. This finding in cell culture was also supported by our gene expression analysis in an *in vivo* xenograft model for prostate cancer tumor dormancy (Supp. Fig 3). Interestingly, this is correlated with suppressed levels of mRNA for immune targeting factors, and may in part explain how dormant cancer cells evade host immune attack. Whether there is a direct or indirect relationship between the Hippo signaling status and expression of immune targets in quiescent cells remains to be examined.

Materials and Methods

Cells and cell culture

The mouse embryonic fibroblast 3T3 cell line containing the G0 and G1 cell cycle reporters were kindly provided by Dr. Toshihiko Oki (University of Tokyo). These cells were grown in Dulbecco's modified Eagle's medium (DMEM; Gibco) supplemented with 10% fetal bovine serum (FBS) and 1% penicillin-streptomycin. Serum levels were reduced as indicated in the figures and text for serum starvation experiments. PC3 prostate cancer cells were cultured and transduced with the G0 and G1 cell cycle reporters as previously described (Takahashi et al., 2019).

Live Cell Imaging

NIH3T3 cells were cultured at low density (to avoid contact inhibition) on 12-well plates in phenol red-free DMEM/10%FBS or 1%DMEM. Experiments in Fig.1 (and Supplements to Fig 1) were performed using an EVOS FL cell imaging system with a 20X objective lens or an IncuCyte Zoom at 37°C, 5% CO₂. The imaging intervals were 20-30 minutes.

For experiments using the “Cell Hotel” (Figs. 2 and 3), 10,000 PC3 cells in RPMI medium with 10% serum were loaded into the inlet of the microfluidic chamber. The chamber loading was monitored until most of the chambers were occupied with single cells (~5mins). Remaining cells were then removed from the inlet and the outlet and replenished with fresh media. Imaging was performed using a Leica DMI 6000 with a Tokai Hit stage-top environmental chamber at 37°C,

5% CO₂. Gas6 (R&D systems) and GM-CSF were reconstituted according to the manufacturer's guidelines. For Gas6 and GM-CSF treatments, 10,000 PC3 cells were mixed with media containing the ligand (0.5 µg/mL for Gas6 and 10 µg/mL for GM-CSF) and introduced into the chamber. Cells were then incubated in media with the indicated ligand for 6h of pre-equilibration prior to imaging every 20 minutes.

Fabrication of the Microfluidic Device for Single-Cell Tracking

The microfluidic device used for single-cell tracking was developed in our previous work (Cheng et al., 2016). The device was built by bonding a PDMS (Polydimethylsiloxane, Sylgard 184, Dow Corning) layer with microfluidic patterns to a glass slide. The PDMS layer was formed by standard soft lithography. The SU-8 mold used for soft-lithography was created by a 3-layer photolithography process with 10 µm, 40 µm, and 100 µm thick SU-8 (Microchem) following the manufacturer's protocol. PDMS was prepared by mixing with 10 (elastomer): 1 (curing agent) (w/w) ratio, poured on SU-8 molds, and cured at 100°C overnight. Inlet and outlet holes are created by biopsy punch cutting. The PDMS with microfluidic channel structures and the glass slide were treated using oxygen plasma (80W for 60 seconds) and bonded. The devices after bonding were heated at 80°C for an hour to ensure bonding quality. The microfluidic chips were sanitized using UV radiation and primed using either a Collagen solution (1.45mL Collagen (Collagen Type 1, 354236, BD Biosciences) or Fibronectin solution, 0.1mL acetic acid in 50mL DI Water) overnight before use.

Flow Cytometry analysis and FACS

For cell sorting and assays in Figs. 2-4, cells were cultured in RPMI supplemented with either 10% FBS or 1% as indicated and subpopulations were sorted according to the intensity of their fluorescent reporters, using a BD FACS Aria II system. Cells were sorted into SDS-PAGE loading buffer or RLT (Qiagen) for immediate protein extraction or RNA isolation. A minimum of ~10⁵ cells were collected for each experiment. Antibodies used for PC3 isolation from osteoblasts co-culture in Fig. 2 were APC/Cy7 anti-human HLA A,B,C antibody (Biolegend #311426). Antibodies used in Fig. 4 were PE-anti-CD133 antibody (cat. 130-080-901, Miltenyi Biotec, San Diego, CA) and APC-anti-CD44 antibody (cat. 559942, BD Biosciences, San Jose, CA).

Western Blotting: Cleared cell lysates in SDS loading buffers were separated on 4-20% SDS PAGE gels under reducing conditions and transferred to PVDF membranes. Membranes were blocked with 5% milk in TBST and probed with primary antibodies diluted 1:1000 in 5% BSA TBST; YAP1 phospho-serine 127 (Cell Signaling Technology #4911) and TAZ phosphor-serine 89 (Cell Signaling Technology #59971). The secondary antibody was Cell Signaling #7074 diluted 1:1000 in 1% milk TBST. Blots were developed in Pierce Supersignal Pico ECL substrate and visualized with a Biorad Image Doc Touch system. The membranes were subsequently stripped and reprobed for total YAP1 (CST #14074), total TAZ (CST #83669), beta actin (CST #4970), or vinculin (CST #13901) as indicated.

qRT-PCR Arrays: PC3 Venus/Cherry cells were seeded at 10^5 cells per dish in 10 cm dishes and cultured for 3 days in RPMI media with 1% FCS. Cells were seeded on different days for biologic triplicate or quadruplicate samples. After three days of culture, cells were released by trypsinization, stained with DAPI for viability and sorted by FACS into either the total (mixed) viable cell population, G0, G1, or S/G2/M phases using the Venus/Cherry markers. 10^5 viable cell events for each population were collected directly into Qiagen RLT buffer containing β -mercaptoethanol. Total RNA was isolated with Qiagen RNeasy kits. The samples were analyzed with the Human Hippo Signaling RT2 Profiler PCR array (Qiagen #PAHS-172ZA) or Human Cancer Inflammation and Immunity Crosstalk array (Qiagen #PAHS-181ZA) using the recommended cDNA synthesis and PCR reagents. Data are presented as biologic quadruplicate or triplicate samples of expression relative to the total viable population sample. Visualization and hierarchical clustering was prepared with Morpheus software (Broad Institute).

Additional Methods and details for ATCQ and Supplemental Figures are included in the Supplemental Data file.

Acknowledgements:

This work in the Buttitta Lab was supported by funding from the American Cancer Society (RSG-15-161-01-DDC), and the Dept. of Defense (W81XWH1510413). Work in the Yang Lab is supported by the National Science Foundation (Early CAREER Grant #1553031 and MCB#1817909) and the National Institutes of Health (MIRA GM119688). Work in the Pearson lab is supported by the National Institutes of Health (K08-DE026500). Work in the Yoon Lab

was in part supported by the National Institute of Health (R01-CA-203810). Work in the Cackowski Lab is supported by a Prostate Cancer Foundation Challenge award, University of Michigan Prostate Cancer S.P.O.R.E. NIH/NCI 5 P50CA18678605, Career Enhancement sub-award to F.C.C. F048931, Prostate Cancer Foundation Young Investigator Award 18YOUN04, Department of Defense Prostate Cancer Research Program Physician Research Award W81XWH2010394, and start-up funds from The University of Michigan and Karmanos Cancer Institute. Work in the Taichman lab was supported by National Institutes of Health (3P01CA093900-06) and the Prostate Cancer Foundation (16CHAL05). We thank Dr. T. Oki for providing the G0-Venus vector and Venus/Cherry labeled 3T3 cell line. We thank Chris A. Edwards, manager of Microscopy & Image-analysis Laboratory (MIL) from University of Michigan for help with live-cell imaging. We thank Abbey Roelofs (U. Michigan LSA-IT) for help with improving the cell tracking and analysis program. We thank Melissa Coon and the University of Michigan DNA Sequencing Core Facility for preparation of libraries and sequencing for the Du-145 experiment, and Rebecca Tagett of the University of Michigan Bioinformatics Core Facility for quality control, alignment, and differential expression analysis of the Du-145 RNA sequencing data. We thank “The Tribe” (ATCQ) for musical inspiration.

Figure Legends:

Figure 1. The G0 sensor, mVenus-p27K-, can be used to monitor spontaneous quiescence and asymmetric proliferation-quiescence decisions in untransformed cells.

(A) The proliferation-quiescence decision as monitored with the G0 sensor, mVenus-p27K- (G0-Venus) and G1 sensor hCdt1₍₃₀₋₁₂₀₎-Cherry (G1-Cherry) in over 400 cells. For NIH3T3 cells, on average, 2-4 hours after cytokinesis, G0-Venus expression begins increasing, followed approximately 3-4 hours later by G1-Cherry expression. For cells entering G1, the Venus/Cherry double-positive phase lasts 5-10h. For quantification purposes we define a Venus/Cherry double-positive phase prolonged beyond 14 hours as spontaneous G0. **(B)** Example traces of G0-Venus/G1-Cherry reporter dynamics in cells entering the cell cycle. 0h is relative time, aligned to the start of G0-Venus reporter increase. **(C)** Example traces of G0-Venus/G1-Cherry reporter

dynamics in cells under full serum conditions. Left shows a transient spontaneous G0 state of less than 15 hours, while right shows an example of prolonged, spontaneous quiescence lasting over 24 hours. **(D)** Cell trajectories followed over time from several movies show reporter behaviors consistent with G0 entry, G0 exit and G1 entry, and exit from G1 and early S-phase under full serum conditions. **(E)** Under serum starvation for 24h, multiple trajectories collapse into G0 entry. **(F)** Under full serum conditions, time spent in G0 is highly variable. **(G)** Under serum starvation for 24h G0 is prolonged. **(H)** Frames from movies showing examples of mitoses followed by a symmetric G0/G1 decision (top), symmetric G1 decision (middle) and symmetric G0 decision (bottom).

Figure 2. Spontaneous quiescence and asymmetric proliferation-quiescence decisions occur in p53-deficient Prostate Cancer PC3 cells.

(A) G0-Venus and G1-Cherry reporters were transduced into PC3 cells and a clone exhibiting normal growth rate and strong, stable reporter expression was isolated. PC3 Venus/Cherry cells exhibit reporter dynamics similar to 3T3 cells, including 15-25% of cells double positive for G0-Venus/G1-Cherry under full serum conditions. **(B)** PC3 Venus/Cherry cells were cultured in a microfluidics chamber termed the “cell hotel” for single cell tracking and imaging of daughters. Examples of asymmetric G0/G1 decisions, as well as symmetric spontaneous G0 and symmetric G1 entry are observed in PC3 cells under full serum conditions. **(C)** G0-Venus and G1-Cherry reporters in PC3 cells respond to serum starvation and re-stimulation as expected. G1 (Cherry-only) cells were isolated by FACS and cultured in serum free media for 3 days. By 3 days, 90% of cells become Venus/Cherry double positive demonstrating that nearly all cells retain the dual reporters. In parallel, double negative late S, G2/M cells were isolated by FACS and cultured in serum free media. By 3 days, 85% of cells become Venus/Cherry double positive, demonstrating that actively proliferating cells retain the dual reporters. Serum was then added back to G0 arrested cells, and within 2-3 days (days 5 and 7 of the entire timecourse) the distribution of G0, G1, S, G2/M cells returns to normal. **(D)** To measure heterogeneity of G0 in PC3 cells under full serum conditions, we quantified time spent in a double-positive Venus/Cherry state for 90 cells. We found G0 length to be highly heterogeneous, compared to the rest of the cell cycle timing for G1, S and G2/M. **(E)** We measured the length of the double Venus/Cherry positive G0 state for ~50 PC3 and 3T3 cells under full serum conditions in the cell hotel. For PC3, we found that most

cells transitioned to G1 by 14 hours after the initial rise in G0-Venus fluorescence, with a small number of cells (27.5%) exhibiting longer G0-Venus fluorescence consistent with spontaneous quiescence. By contrast, for 3T3 cells we observed 64.4% of cells to exhibit spontaneous quiescence, a double-positive state lasting more than 14h (dotted line). (P=0.0005 by Mann-Whitney test.) (F) We also compared the frequency of asymmetric proliferation-quiescence decisions in PC3 vs. 3T3 cells (P<0.0001 by Mann-Whitney test) and (G) the length of the time difference until G1 entry between asymmetric daughters in PC3 and 3T3 cells.

Figure 3. Tumor dormancy signals influence quiescence and asymmetric proliferation-quiescence decisions.

(A) PC3 Venus/Cherry cells were either cultured alone or co-cultured with mouse osteoblasts, which were excluded from cell cycle analysis by negative human HLA staining and positive anti-mouse MHC staining. (B,C) PC3 co-culture with osteoblasts induced a significant increase in G0 cells under full serum conditions. (D) PC3 cells treated with Gas6 also exhibit a significant increase in G0 cells. (E) G0-Venus reporter dynamics were tracked using the cell hotel for cells exposed to Gas 6 (n=140), GM-CSF (n=300) or vehicle only controls (n=128) and compared to 3T3 cells. Gas6 and GM-CSF increased the percentage of PC3 cells entering quiescence under full serum, defined as a G0-Venus/G1-Cherry double positive state for >14h. As shown in Fig 2, 3T3 cells exhibit more spontaneous quiescence than PC3 cells. (F) Using the cell hotel, we also measured the length of time spent in G0 prior to G1 entry and whether transitions were symmetric (black) or asymmetric (red) under the indicated conditions. Similar to what we observe for 3T3 cells, the length of time spent in the G0-Venus/G1-Cherry double positive state does not seem to correlate with whether G1 entry will be symmetric or asymmetric. (G) Symmetric G0 entry, symmetric G1 entry and asymmetric G0/G1 entry was tracked for the indicated number of cell divisions under each treatment. For Gas 6 we observed an increase in symmetric G0 entry, while treatment with GM-CSF dramatically decreased symmetric entry into G0 by increasing symmetric entry into G1 and reduced asymmetric proliferation-quiescence decisions.

Figure 4. Quiescent prostate cancer cells are enriched for stem cell markers, expression of Hippo pathway components and exhibit an “immuno-cold” phenotype.

(A) FACS analysis of PC3 Venus/Cherry cells under normal culture conditions shows an enrichment ($P < 0.02$, t-test) for CD133+44+ cells, suggested to be PC3 prostate cancer stem cells (PCSCs), in the G0 cell population. (B, D) PC3 Venus/Cherry cells were sorted into G0, G1 and S,G2/M fractions for gene expression analysis using Qiagen qRT-PCR arrays. Biological quadruplicates were run on the Hippo Signaling Pathway array and triplicates were run on the Qiagen Cancer Immunology qRT-PCR array. All changes in expression are normalized to asynchronous cells. Selected genes are shown here, the full dataset is shown in the Supp. Fig. 4B. (B) G0 cells show a consistent increase in transcripts for Hippo signaling pathway components including positive and negative regulators as well as feedback targets. (C) PC3 Venus/Cherry cells were sorted into G0, G1 and S,G2/M fractions for protein isolation and western blotting. G0 cells exhibit an increase in phosphorylated YAP and TAZ (note TAZ protein encoded by WWTR1 gene), consistent with active Hippo signaling repressing their transcriptional activity. (D) G0 cells exhibit an altered immune expression profile while G1, S and G2/M cells exhibit few significant changes.

Supplemental Figure 1: Automated Tracking of Cellular Quiescence (ATCQ) can be used to quantify and monitor G0 entry and exit in adherent cell culture.

(A) A workflow of the ATCQ system. (B) (a-e) partitioning images from the single-cell tracking process. White arrow points out the same cell traced at different time points. Representative single-cell trajectory of two fluorescent probes in time-lapse, live-cell imaging. Each circle depicts one fluorescent intensity reading at a given time in either mVenus or mCherry channel. (C) Representative images show the same cells traced at two adjacent time frames. The calculation is generated to convert fluorescent intensity readouts to radial readings over time. (D) Three distinct cell cycle behaviors in order were observed from G0/G1 cell cycle reporter fluorescent intensity changes in asynchronously growing cells. When cells in state G0, both mVenus reporter and mCherry accumulate together, colored in blue. Then cells transit into G1 when mVenus fluorescent signal decreases while mCherry remains high, colored in orange. The

third state is S phase entry, when mCherry signal decreases, colored in grey. (E) The radial histogram shows the conversion of the two fluorescent intensity readouts from each time frame to the radian readings over two adjacent time frames. The length of the spikes depicts the frequency of individual cells exhibiting a certain cell cycle behavior at a particular radian. The transition from one state to another is marked by the local minima of the frequency in radial histogram. (F) The dot plot shows all the cell-level, post-smoother radian assignment values for temporally adjacent movie frames. In this plot, all the radian values defining cell state can be compared among all cells in any movie frame t and the next frame $t+1$. (G) A model to explain the variability observed in the G0 state vs other cell cycle states. (H) The Kaplan-Meier curves of each state estimates the time cells remaining in each state under either full serum (10%) or low serum (1%) conditions. The analysis shows that cells tend to spend longer times in both G₀ and G₁ states in response to serum starvation (p value<0.001). To test the sensitivity of ATCQ, 50nM Okadaic Acid (OA) was used to inhibit PP2A function for 30min prior to live, time-lapse imaging. Inhibition of PP2A has previously been shown to mildly reduce G0 entry in response to serum starvation by 10%. The Kaplan-Meier curves confirm that cells treated with OA are less likely to enter spontaneous G₀ than cells with vehicle treatment. However, consistent with previous work on PP2A, cells with OA treatment exhibit no significant difference in time spent in G₁.

Supplemental Figure 2: Cells expressing mVenus-p27K exhibit molecular markers of quiescence.

(A) A representative flow cytometry dot plot of NIH3T3 cells expressing mVenus-p27K⁻ (G0-Venus) and mCherry-hCdt1(30/120) (G1-Cherry), cultured under reduced 1% serum for 72h to induce G0 entry. (B) Quantifications of cells in G0, G1 or S,G2/M in full 10% serum, after 24h of reduced (1%) serum (S-) or 72h of reduced (1%) serum. Experiments were performed in triplicate, and averages are plotted with error bars indicating SEM. The sub-population of double positive G0 cells increases as cells are treated with serum starvation. (C) Western blots confirm molecular markers of G0 in Venus/Cherry double positive cells under full and low (1%) or no serum conditions. Quantifications confirm an increase in the ratio of un/hypo-phosphorylated to hyper-phosphorylated form p130 in double positive cells. The un/hypo-phosphorylated form and

hyper-phosphorylated form are indicated by the black and red arrows, respectively. The active form of Cdk2, phospho-Cdk2^{T160}, is reduced in Venus/Cherry double positive cells compared to Cherry single positive cells. Endogenous p27 is also highly expressed in double positive cells. Phosphorylation of Rb is also low in G0 Venus/Cherry double-positive cells under serum starvation or full serum compared to single Cherry positive cells (G1) or double negative cells in S/G2/M. **(D)** qRT-PCR on sorted cell populations under normal serum (S+) or 1% serum (S-) conditions shows that active cell cycle regulators PCNA, Ki67 and Geminin are downregulated in G0 Venus/Cherry double positive cells even in spontaneous quiescence (S+), when compared to asynchronously proliferating cells. Conversely, two genes previously associated with G0, Sod3 and Pcd4 are enriched in spontaneous G0 and low serum G0. $\Delta CT = \log_2$ of the fold difference from asynchronous unsorted cell samples normalized to Gapdh transcript levels. **(F)** G0-Venus reporter dynamics were tested in a timecourse of serum starvation followed by re-stimulation. By 48h of serum starvation most cells are entering G0, with nearly 90% exhibiting a Venus/Cherry double positive state by 72h. Upon serum addition, cells begin exhibiting significant cell cycle re-entry and G1 entry (Cherry single positive) by 14h. By 20h after serum addition, the majority of cells exhibit S/G2 or M states (double negative).

Supplemental Fig. 3 – Identifying differentially expressed genes in growing vs. dormant tumors in the Du-145 mouse xenograft model.

(A) Experimental schema. **(B)** Results of pathway analysis of differentially expressed genes in tumor cells from microscopic vs. macroscopic tumors using NIH DAVID software and the KEGG pathway collection. Left; negative log base 10 of the p-value for enrichment in each pathway. Right; Genes responsible for the enrichment in each pathway.

Supplemental Fig. 4 – The complete dataset for qRT-PCR arrays

PC3 Venus/Cherry cells were sorted into G0, G1 and S,G2/M fractions for gene expression analysis using Qiagen qRT-PCR arrays. Biological triplicates were run on the Qiagen Cancer Immunology qRT-PCR array **(A)** and quadruplicates were run on the Hippo Signaling Pathway array **(B)**. Changes in expression were normalized to asynchronous cells and represented as a heatmap of the log₂Fold Change.

References

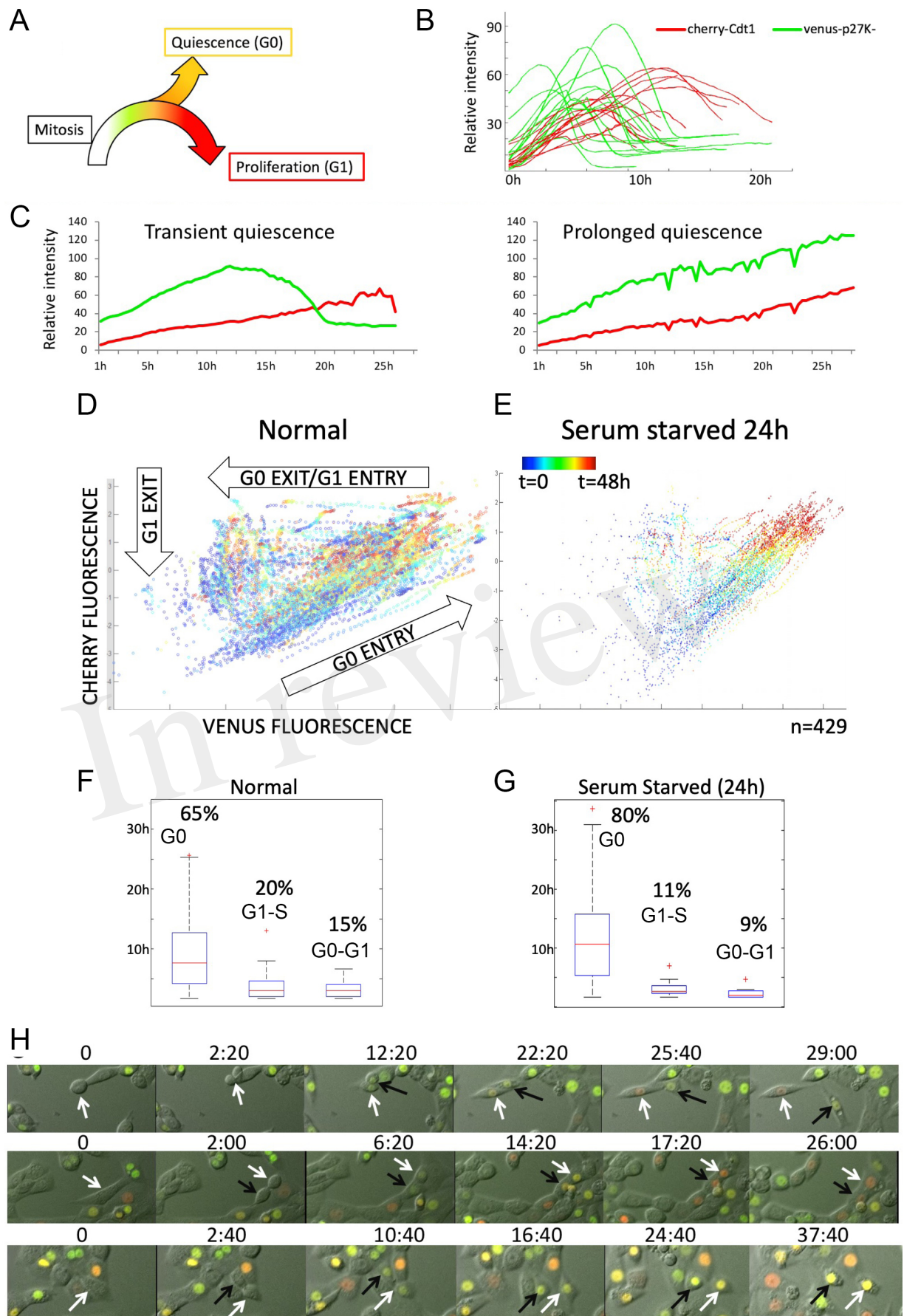
- Alves, C.P., Dey-Guha, I., Kabraji, S., Yeh, A.C., Talele, N.P., Sole, X., Chowdhury, J., Mino-Kenudson, M., Loda, M., Sgroi, D., Borresen-Dale, A.L., Russnes, H.G., Ross, K.N., and Ramaswamy, S. (2018). AKT1(low) Quiescent Cancer Cells Promote Solid Tumor Growth. *Mol Cancer Ther* 17, 254-263.
- Arora, M., Moser, J., Phadke, H., Basha, A.A., and Spencer, S.L. (2017). Endogenous Replication Stress in Mother Cells Leads to Quiescence of Daughter Cells. *Cell Rep* 19, 1351-1364.
- Bragado, P., Estrada, Y., Parikh, F., Krause, S., Capobianco, C., Farina, H.G., Schewe, D.M., and Aguirre-Ghiso, J.A. (2013). TGF-beta2 dictates disseminated tumour cell fate in target organs through TGF-beta-RIII and p38alpha/beta signalling. *Nat Cell Biol* 15, 1351-1361.
- Cackowski, F.C., Eber, M.R., Rhee, J., Decker, A.M., Yumoto, K., Berry, J.E., Lee, E., Shiozawa, Y., Jung, Y., Aguirre-Ghiso, J.A., and Taichman, R.S. (2017). Mer Tyrosine Kinase Regulates Disseminated Prostate Cancer Cellular Dormancy. *J Cell Biochem* 118, 891-902.
- Carroll, A.G., Voeller, H.J., Sugars, L., and Gelmann, E.P. (1993). p53 oncogene mutations in three human prostate cancer cell lines. *Prostate* 23, 123-134.
- Chen, F., Han, Y., and Kang, Y. (2021). Bone marrow niches in the regulation of bone metastasis. *Br J Cancer* 124, 1912-1920.
- Chen, J., Xia, D., Luo, J.D., and Wang, P. (2009). Exogenous p27KIP1 expression induces anti-tumour effects and inhibits the EGFR/PI3K/Akt signalling pathway in PC3 cells. *Asian J Androl* 11, 669-677.
- Cheng, Y.H., Chen, Y.C., Brien, R., and Yoon, E. (2016). Scaling and automation of a high-throughput single-cell-derived tumor sphere assay chip. *Lab Chip* 16, 3708-3717.
- Chittajallu, D.R., Florian, S., Kohler, R.H., Iwamoto, Y., Orth, J.D., Weissleder, R., Danuser, G., and Mitchison, T.J. (2015). In vivo cell-cycle profiling in xenograft tumors by quantitative intravital microscopy. *Nat Methods* 12, 577-585.
- Coller, H.A., Sang, L., and Roberts, J.M. (2006). A new description of cellular quiescence. *PLoS Biol* 4, e83.
- Cosemans, J.M., Van Kruchten, R., Olieslagers, S., Schurgers, L.J., Verheyen, F.K., Munnix, I.C., Waltenberger, J., Angelillo-Scherrer, A., Hoylaerts, M.F., Carmeliet, P., and Heemskerk, J.W. (2010). Potentiating role of Gas6 and Tyro3, Axl and Mer (TAM) receptors in human and murine platelet activation and thrombus stabilization. *J Thromb Haemost* 8, 1797-1808.
- Dai, J., Lu, Y., Yu, C., Keller, J.M., Mizokami, A., Zhang, J., and Keller, E.T. (2010). Reversal of chemotherapy-induced leukopenia using granulocyte macrophage colony-stimulating factor promotes bone metastasis that can be blocked with osteoclast inhibitors. *Cancer Res* 70, 5014-5023.
- Davis, J.E., Jr., Kirk, J., Ji, Y., and Tang, D.G. (2019). Tumor Dormancy and Slow-Cycling Cancer Cells. *Adv Exp Med Biol* 1164, 199-206.
- De Angelis, M.L., Francescangeli, F., La Torre, F., and Zeuner, A. (2019). Stem Cell Plasticity and Dormancy in the Development of Cancer Therapy Resistance. *Front Oncol* 9, 626.
- Dey-Guha, I., Alves, C.P., Yeh, A.C., Salony, Sole, X., Darp, R., and Ramaswamy, S. (2015). A mechanism for asymmetric cell division resulting in proliferative asynchronicity. *Mol Cancer Res* 13, 223-230.
- Dey-Guha, I., Wolfer, A., Yeh, A.C., J, G.A., Darp, R., Leon, E., Wulfschuhle, J., Petricoin, E.F., 3rd, Wittner, B.S., and Ramaswamy, S. (2011). Asymmetric cancer cell division regulated by AKT. *Proc Natl Acad Sci U S A* 108, 12845-12850.

- Dubrovskaya, A., Kim, S., Salamone, R.J., Walker, J.R., Maira, S.M., Garcia-Echeverria, C., Schultz, P.G., and Reddy, V.A. (2009). The role of PTEN/Akt/PI3K signaling in the maintenance and viability of prostate cancer stem-like cell populations. *Proc Natl Acad Sci U S A* 106, 268-273.
- Hen, O., and Barkan, D. (2020). Dormant disseminated tumor cells and cancer stem/progenitor-like cells: Similarities and opportunities. *Semin Cancer Biol* 60, 157-165.
- Huang, H., Chevillet, J.C., Pan, Y., Roche, P.C., Schmidt, L.J., and Tindall, D.J. (2001). PTEN induces chemosensitivity in PTEN-mutated prostate cancer cells by suppression of Bcl-2 expression. *J Biol Chem* 276, 38830-38836.
- Jeffrey, P.D., Russo, A.A., Polyak, K., Gibbs, E., Hurwitz, J., Massague, J., and Pavletich, N.P. (1995). Mechanism of CDK activation revealed by the structure of a cyclinA-CDK2 complex. *Nature* 376, 313-320.
- Jung, Y., Decker, A.M., Wang, J., Lee, E., Kana, L.A., Yumoto, K., Cackowski, F.C., Rhee, J., Carmeliet, P., Buttitta, L., Morgan, T.M., and Taichman, R.S. (2016). Endogenous GAS6 and Mer receptor signaling regulate prostate cancer stem cells in bone marrow. *Oncotarget*.
- Jung, Y., Shiozawa, Y., Wang, J., McGregor, N., Dai, J., Park, S.I., Berry, J.E., Havens, A.M., Joseph, J., Kim, J.K., Patel, L., Carmeliet, P., Daignault, S., Keller, E.T., Mccauley, L.K., Pienta, K.J., and Taichman, R.S. (2012). Prevalence of prostate cancer metastases after intravenous inoculation provides clues into the molecular basis of dormancy in the bone marrow microenvironment. *Neoplasia* 14, 429-439.
- Kamura, T., Hara, T., Matsumoto, M., Ishida, N., Okumura, F., Hatakeyama, S., Yoshida, M., Nakayama, K., and Nakayama, K.I. (2004). Cytoplasmic ubiquitin ligase KPC regulates proteolysis of p27(Kip1) at G1 phase. *Nat Cell Biol* 6, 1229-1235.
- Kasikara, C., Kumar, S., Kimani, S., Tsou, W.I., Geng, K., Davra, V., Sriram, G., Devoe, C., Nguyen, K.N., Antes, A., Krantz, A., Rymarczyk, G., Wilczynski, A., Empig, C., Freimark, B., Gray, M., Schlunegger, K., Hutchins, J., Kotenko, S.V., and Birge, R.B. (2017). Phosphatidylserine Sensing by TAM Receptors Regulates AKT-Dependent Chemoresistance and PD-L1 Expression. *Mol Cancer Res* 15, 753-764.
- Lam, H.M., Vessella, R.L., and Morrissey, C. (2014). The role of the microenvironment-dormant prostate disseminated tumor cells in the bone marrow. *Drug Discov Today Technol* 11, 41-47.
- Lang, S.H., Miller, W.R., Duncan, W., and Habib, F.K. (1994). Production and response of human prostate cancer cell lines to granulocyte macrophage-colony stimulating factor. *Int J Cancer* 59, 235-241.
- Lawson, D.A., Bhakta, N.R., Kessenbrock, K., Prummel, K.D., Yu, Y., Takai, K., Zhou, A., Eyob, H., Balakrishnan, S., Wang, C.Y., Yaswen, P., Goga, A., and Werb, Z. (2015). Single-cell analysis reveals a stem-cell program in human metastatic breast cancer cells. *Nature* 526, 131-135.
- Lee, E., Decker, A.M., Cackowski, F.C., Kana, L.A., Yumoto, K., Jung, Y., Wang, J., Buttitta, L., Morgan, T.M., and Taichman, R.S. (2016). Growth Arrest-Specific 6 (GAS6) Promotes Prostate Cancer Survival by G Arrest/S Phase Delay and Inhibition of Apoptotic Pathway During Chemotherapy in Bone Marrow. *J Cell Biochem*.
- Matson, J.P., and Cook, J.G. (2017). Cell cycle proliferation decisions: the impact of single cell analyses. *FEBS J* 284, 362-375.
- Miller, I., Min, M., Yang, C., Tian, C., Gookin, S., Carter, D., and Spencer, S.L. (2018). Ki67 is a Graded Rather than a Binary Marker of Proliferation versus Quiescence. *Cell Rep* 24, 1105-1112 e1105.
- Min, M., Rong, Y., Tian, C., and Spencer, S.L. (2020). Temporal integration of mitogen history in mother cells controls proliferation of daughter cells. *Science* 368, 1261-1265.
- Min, M., and Spencer, S.L. (2019). Spontaneously slow-cycling subpopulations of human cells originate from activation of stress-response pathways. *PLoS Biol* 17, e3000178.
- Moroishi, T., Hayashi, T., Pan, W.W., Fujita, Y., Holt, M.V., Qin, J., Carson, D.A., and Guan, K.L. (2016). The Hippo Pathway Kinases LATS1/2 Suppress Cancer Immunity. *Cell* 167, 1525-1539 e1517.

- Nik Nabil, W.N., Xi, Z., Song, Z., Jin, L., Zhang, X.D., Zhou, H., De Souza, P., Dong, Q., and Xu, H. (2021). Towards a Framework for Better Understanding of Quiescent Cancer Cells. *Cells* 10.
- Oki, T., Nishimura, K., Kitaura, J., Togami, K., Maehara, A., Izawa, K., Sakaue-Sawano, A., Niida, A., Miyano, S., Aburatani, H., Kiyonari, H., Miyawaki, A., and Kitamura, T. (2014). A novel cell-cycle-indicator, mVenus-p27K-, identifies quiescent cells and visualizes G0-G1 transition. *Sci Rep* 4, 4012.
- Overton, K.W., Spencer, S.L., Noderer, W.L., Meyer, T., and Wang, C.L. (2014). Basal p21 controls population heterogeneity in cycling and quiescent cell cycle states. *Proc Natl Acad Sci U S A* 111, E4386-4393.
- Recasens, A., and Munoz, L. (2019). Targeting Cancer Cell Dormancy. *Trends Pharmacol Sci* 40, 128-141.
- Ridenour, D.A., McKinney, M.C., Bailey, C.M., and Kulesa, P.M. (2012). CycleTrak: a novel system for the semi-automated analysis of cell cycle dynamics. *Dev Biol* 365, 189-195.
- Risson, E., Nobre, A.R., Maguer-Satta, V., and Aguirre-Ghiso, J.A. (2020). The current paradigm and challenges ahead for the dormancy of disseminated tumor cells. *Nat Cancer* 1, 672-680.
- Sakaue-Sawano, A., Kurokawa, H., Morimura, T., Hanyu, A., Hama, H., Osawa, H., Kashiwagi, S., Fukami, K., Miyata, T., Miyoshi, H., Imamura, T., Ogawa, M., Masai, H., and Miyawaki, A. (2008). Visualizing spatiotemporal dynamics of multicellular cell-cycle progression. *Cell* 132, 487-498.
- Savarese, D.M., Valinski, H., Quesenberry, P., and Savarese, T. (1998). Expression and function of colony-stimulating factors and their receptors in human prostate carcinoma cell lines. *Prostate* 34, 80-91.
- Sherr, C.J., and Roberts, J.M. (1999). CDK inhibitors: positive and negative regulators of G1-phase progression. *Genes Dev* 13, 1501-1512.
- Spencer, S.L., Cappell, S.D., Tsai, F.C., Overton, K.W., Wang, C.L., and Meyer, T. (2013). The proliferation-quiescence decision is controlled by a bifurcation in CDK2 activity at mitotic exit. *Cell* 155, 369-383.
- Stewart-Ornstein, J., and Lahav, G. (2016). Dynamics of CDKN1A in Single Cells Defined by an Endogenous Fluorescent Tagging Toolkit. *Cell Rep* 14, 1800-1811.
- Taichman, R.S., Patel, L.R., Bedenis, R., Wang, J., Weidner, S., Schumann, T., Yumoto, K., Berry, J.E., Shiozawa, Y., and Pienta, K.J. (2013). GAS6 receptor status is associated with dormancy and bone metastatic tumor formation. *PLoS One* 8, e61873.
- Takahashi, H., Yumoto, K., Yasuhara, K., Nadres, E.T., Kikuchi, Y., Buttitta, L., Taichman, R.S., and Kuroda, K. (2019). Anticancer polymers designed for killing dormant prostate cancer cells. *Sci Rep* 9, 1096.
- Talukdar, S., Bhoopathi, P., Emdad, L., Das, S., Sarkar, D., and Fisher, P.B. (2019). Dormancy and cancer stem cells: An enigma for cancer therapeutic targeting. *Adv Cancer Res* 141, 43-84.
- Tedesco, D., Lukas, J., and Reed, S.I. (2002). The pRb-related protein p130 is regulated by phosphorylation-dependent proteolysis via the protein-ubiquitin ligase SCF(Skp2). *Genes Dev* 16, 2946-2957.
- Van Duijn, P.W., and Trapman, J. (2006). PI3K/Akt signaling regulates p27(kip1) expression via Skp2 in PC3 and DU145 prostate cancer cells, but is not a major factor in p27(kip1) regulation in LNCaP and PC346 cells. *Prostate* 66, 749-760.
- Wang, Y., Xu, X., Maglic, D., Dill, M.T., Mojumdar, K., Ng, P.K., Jeong, K.J., Tsang, Y.H., Moreno, D., Bhavana, V.H., Peng, X., Ge, Z., Chen, H., Li, J., Chen, Z., Zhang, H., Han, L., Du, D., Creighton, C.J., Mills, G.B., Cancer Genome Atlas Research, N., Camargo, F., and Liang, H. (2018). Comprehensive Molecular Characterization of the Hippo Signaling Pathway in Cancer. *Cell Rep* 25, 1304-1317 e1305.
- Yamauchi, T., and Moroishi, T. (2019). Hippo Pathway in Mammalian Adaptive Immune System. *Cells* 8.

- Yang, H.W., Chung, M., Kudo, T., and Meyer, T. (2017). Competing memories of mitogen and p53 signalling control cell-cycle entry. *Nature* 549, 404-408.
- Yao, G. (2014). Modelling mammalian cellular quiescence. *Interface Focus* 4, 20130074.
- Yumoto, K., Eber, M.R., Wang, J., Cackowski, F.C., Decker, A.M., Lee, E., Nobre, A.R., Aguirre-Ghiso, J.A., Jung, Y., and Taichman, R.S. (2016). Axl is required for TGF-beta2-induced dormancy of prostate cancer cells in the bone marrow. *Sci Rep* 6, 36520.
- Zambon, A.C., Hsu, T., Kim, S.E., Klinck, M., Stowe, J., Henderson, L.M., Singer, D., Patam, L., Lim, C., Mcculloch, A.D., Hu, B., and Hickerson, A.I. (2020). Methods and sensors for functional genomic studies of cell-cycle transitions in single cells. *Physiol Genomics* 52, 468-477.
- Zhang, Q., Han, X., Chen, J., Xie, X., Xu, J., Zhao, Y., Shen, J., Hu, L., Xu, P., Song, H., Zhang, L., Zhao, B., Wang, Y.J., and Xia, Z. (2018). Yes-associated protein (YAP) and transcriptional coactivator with PDZ-binding motif (TAZ) mediate cell density-dependent proinflammatory responses. *J Biol Chem* 293, 18071-18085.
- Zheng, Y., and Pan, D. (2019). The Hippo Signaling Pathway in Development and Disease. *Dev Cell* 50, 264-282.

Figure 1.JPEG



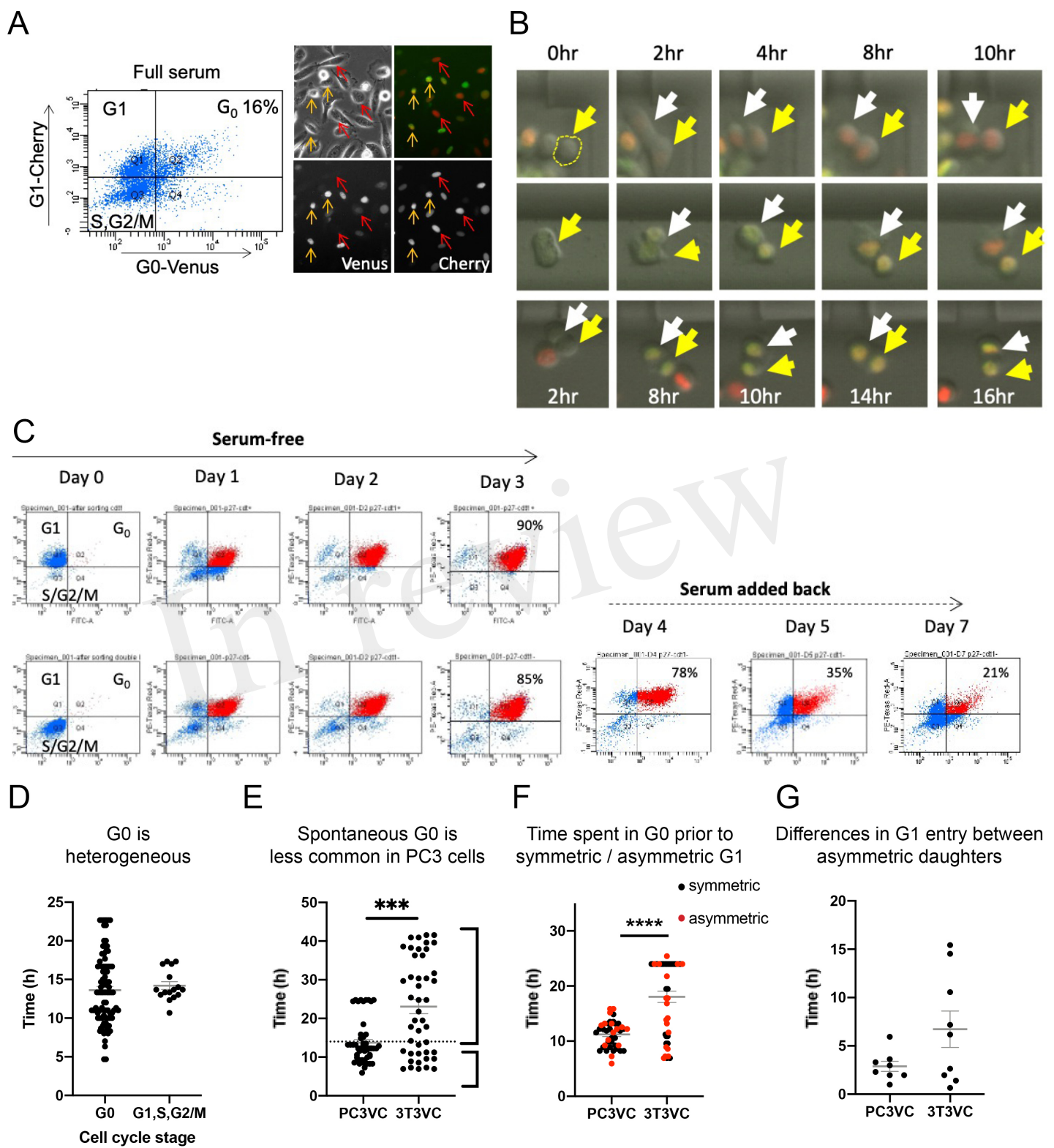


Figure 3.JPEG

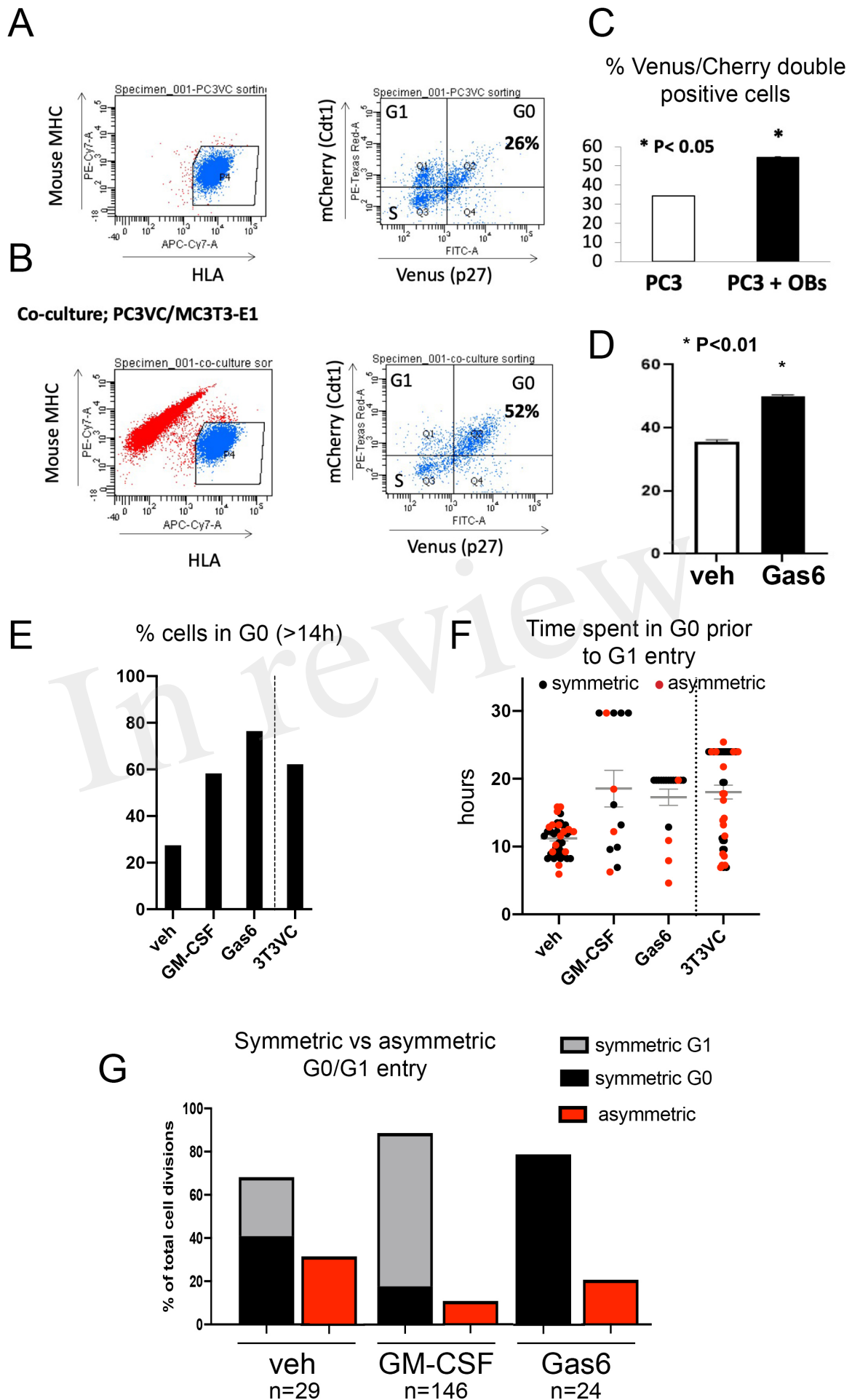
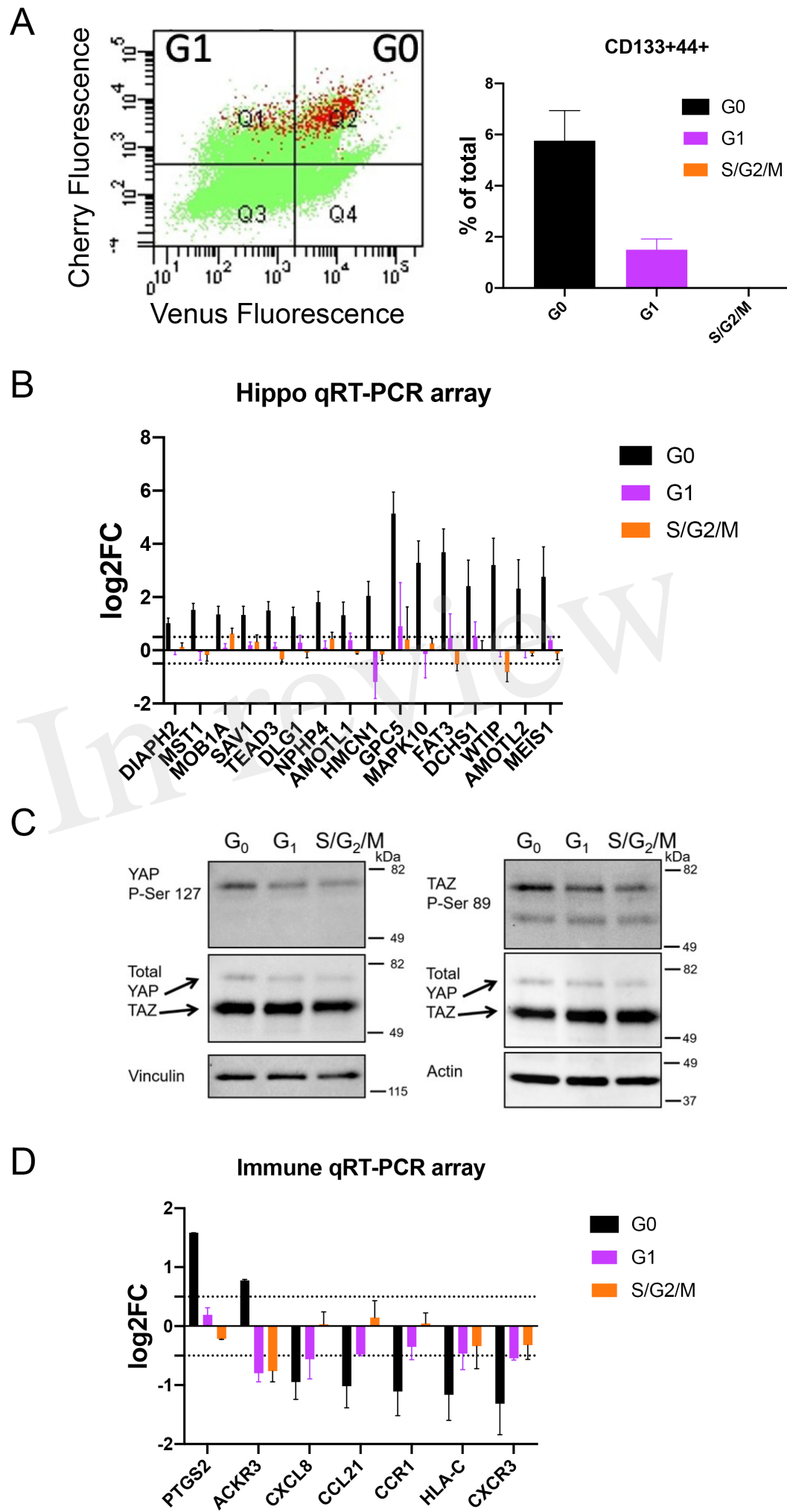


Figure 4.JPEG



Manuscript Number: JBO-D-21-00113

Use of FVB Myc-CaP Cells as an Immune Competent, Androgen Receptor Positive, Mouse Model of Prostate Cancer Bone Metastasis

Dear Dr. Cackowski,

Thank you for submitting your manuscript to Journal of Bone Oncology.

I have completed my evaluation of your manuscript. The reviewers recommend reconsideration of your manuscript following minor revision and modification. I invite you to resubmit your manuscript after addressing the comments below. Please resubmit your revised manuscript by Aug 06, 2021.

When revising your manuscript, please consider all issues mentioned in the reviewers' comments carefully: please outline every change made in response to their comments and provide suitable rebuttals for any comments not addressed. Please note that your revised submission may need to be re-reviewed.

To submit your revised manuscript, please log in as an author at <https://www.editorialmanager.com/jbo/>, and navigate to the "Submissions Needing Revision" folder under the Author Main Menu.

Journal of Bone Oncology values your contribution and I look forward to receiving your revised manuscript.

Kind regards,

Robert Coleman

Editor-in-Chief

Journal of Bone Oncology

Editor and Reviewer comments:

Reviewer #1: This is a clearly written paper that addresses an unmet need in the prostate cancer field. It is brief and to the point. I found only two very minor written errors: Line two of the Abstract, 'metastasizes' should drop its final 's' so that it matches the

rest of the sentence.

In the 3rd Highlight, 'osteolytic' is missing its 'e'.

The metastatic phenotype in bone is adequately characterized, although the image quality provided to the reviewer is not of high enough resolution to say very much. It is probably that the chest tumors in the intracardiac experiment in Fig 1 are due to leakage during injection, which those who are more expert in the technique would say is a problem. To my mind the intratibial model is more sensible anyway and to be encouraged. An attraction of the submission is that the model can be reproduced by other laboratories without needing specially developed mice or cancer subline.

In fig 2B, can the authors comment on the cause of death/need for euthanasia? It is curious that tumor restricted to the tibia (even if extraosseous) is lethal. Was there paraplegia, muscle cachexia or other systemic sign of morbidity?

If there is a weakness to the paper, it is its failure to address obvious mechanistic questions. Were the conditioned media in Fig 3F positive for the usual suspects: PTHrP, sRANKL, or IL8? Since the paper argues for the value of an immunocompetent metastasis model, what about some basic IHC for B & T cells and macrophages in the sections of bone adjacent to tumor vs the contralateral bone?

Reviewer #2: Major

Page 5, paragraph 3: The authors report that eight animals were injected with Myc-CaP cells. Two sentences later, it mentions that seven animals were analyzed. What happened to the other mouse?

Page 5, paragraph 4: Please report how many animals received intra-tibial inoculations and how many of these were found to have detectable Myc-CaP growth.

Minor

Page 3, paragraph 2: For mouse genes, the first letter is capitalized, and subsequent letters are lower case. Please change AR to Ar.

Page 3, Paragraph 2: Change C57/BL6 to C57BL/6

Page 4, paragraph 2: Change C02 to CO2. I think the O is a zero rather than the letter.

Figure 2E: Please increase the inset box line sizes in the 10X figures. These are difficult to see.

More information and support

FAQ: How do I revise my submission in Editorial Manager?

https://service.elsevier.com/app/answers/detail/a_id/28463/supporthub/publishing/

You will find information relevant for you as an author on Elsevier's Author

Hub: <https://www.elsevier.com/authors>

FAQ: How can I reset a forgotten password?

https://service.elsevier.com/app/answers/detail/a_id/28452/supporthub/publishing/

For further assistance, please visit our customer service

site: <https://service.elsevier.com/app/home/supporthub/publishing/>

Here you can search for solutions on a range of topics, find answers to frequently asked questions, and learn more about Editorial Manager via interactive tutorials. You can also talk 24/7 to our customer support team by phone and 24/7 by live chat and email

In compliance with data protection regulations, you may request that we remove your personal registration details at any time. (Use the following URL: <https://www.editorialmanager.com/jbo/login.asp?a=r>). Please contact the publication office if you have any questions.

Double-Negative Prostate Cancer Masquerading as a Squamous Cancer of Unknown Primary: A Clinicopathologic and Genomic Sequencing-Based Case Study

Frank C. Cackowski, MD, PhD^{1,2}; Chandan Kumar-Sinha, PhD³; Rohit Mehra, MD^{3,4,5}; Yi-Mi Wu, PhD^{3,4,5}; Dan R. Robinson, PhD^{3,4,5}; Joshi J. Alumkal, MD¹; and Arul M. Chinnaiyan, MD, PhD^{4,5}

Case Description

In January 2018, a 79-year-old man was referred to our genitourinary medical oncology clinic for management of his prostate adenocarcinoma metastatic to multiple bones. His case was complicated by a concurrent diagnosis of melanoma metastatic to a distant skin site, for which he had started pembrolizumab immunotherapy the week previously. His prostate cancer had originally been diagnosed in November 2011 after a transurethral resection of the prostate performed for urinary obstruction revealed Gleason score 7 prostate adenocarcinoma. In June 2015, he was found to have biopsy-proven prostate adenocarcinoma from a rib metastasis. The patient elected to defer all medical therapy and had his rib metastasis treated with radiation alone. He then had definitive radiation to the prostate in June 2016. His prostate cancer spread to additional bony sites, which were likewise treated with radiation, including radiation to the thoracic spine in July 2017 and the proximal humerus in August 2017, rather than any systemic therapy. In December 2017, he had prophylactic nipple irradiation to prevent gynecomastia in preparation for noncastrating medical therapy with single-agent bicalutamide. On meeting the patient for the first time in January 2018, we elected to continue with the plan for single-agent bicalutamide 50 mg per day, given the patient's preference and the uncertain prognosis from his metastatic melanoma. His prostate-specific antigen (PSA) was 30.8 ng/mL at the time of treatment initiation and responded rapidly to bicalutamide, reaching a nadir of 1.1 ng/mL in September 2018 (Fig 1A).

His melanoma was diagnosed from a shave biopsy of the right superior lateral lower back in August 2015 as localized ulcerated malignant melanoma, unclassified, with nevoid features. It was invasive to at least 1.45 mm and at least Clark level IV, and it had five mitoses/mm². He subsequently had a microstaging excision and a right back excision with a negative sentinel lymph node in the right groin. In 2017, the

patient noticed a new lump on his right lower back scar in 2017. In November 2017, excisional biopsies of his right lower back and right groin both showed metastatic melanoma, as confirmed by immunohistochemistry (IHC) showing positive staining for SOX-10 and MART-1. A 7-mm lesion was also detected on his posterior scalp and was also visible on magnetic resonance imaging of his brain and metabolically active on positron emission tomography (PET)/computed tomography (CT); hence, it was diagnosed as stage IV melanoma. Mutation testing showed an atypical N581I mutation in the *BRAF* gene, but wild-type status at the *BRAF* V600 codon. His PET/CT showed extensive osteosclerotic lesions, most of which were not fluorodeoxyglucose (FDG) avid, consistent with metastatic prostate cancer. The most avid lesion in the right ischium had a maximum standardized uptake value (SUV max) of 7.2 but was biopsied and found to be metastatic prostate adenocarcinoma, as confirmed by IHC assessment that demonstrated NKX3.1 expression. He began treatment of his metastatic melanoma with pembrolizumab 200 mg intravenous every 3 weeks and received four treatments before the pembrolizumab was stopped because of the development of pneumonitis. This treatment resulted in a complete response in his melanoma as assessed by physical examination of his scalp lesion. His pneumonitis was treated with a taper of prednisone, which was reduced to physiologic dosing by August 2018.

However, despite evidence of response in his melanoma by physical examination, there was concern for progression on PET/CT in June 2018, with FDG update in the descending colon/small bowel wall, perisplenic region, a mildly FDG-avid left internal iliac lymph node, and a right external iliac nodal conglomerate encasing the right ureter, 4.1 cm in diameter and with an SUV max of 11.7. By December 2018, the right pelvic mass had increased in size to 4.4 cm and in metabolic activity to SUV max 19.8 (Fig 1B). At this time, he was also noted to have multiple small lung nodules of unclear etiology. Because the appearance of the right

Author affiliations and support information (if applicable) appear at the end of this article.

Accepted on September 30, 2020 and published at ascopubs.org/journal/po on November 16, 2020; DOI <https://doi.org/10.1200/P0.20.00309>


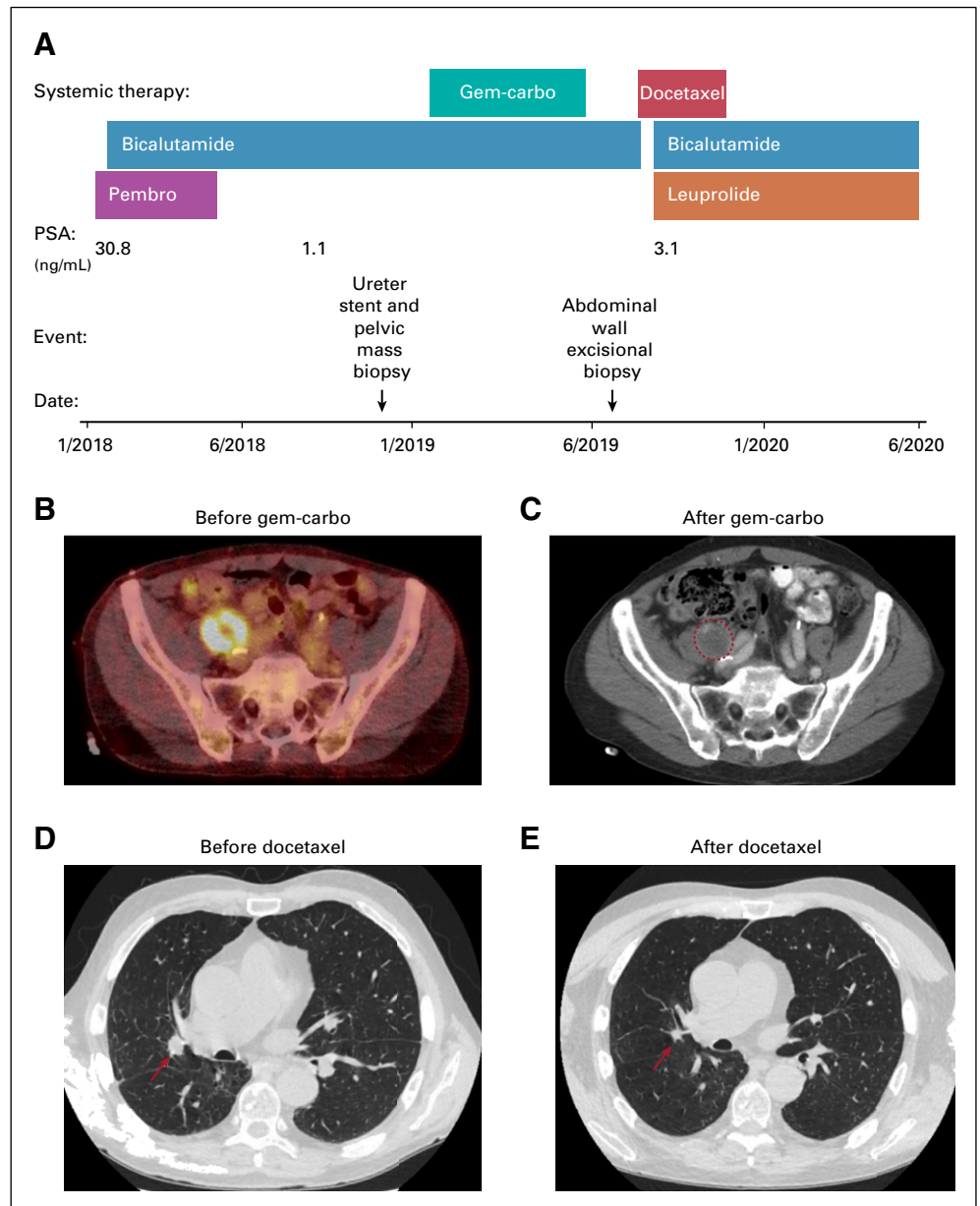
Licensed under the Creative Commons Attribution 4.0 License 

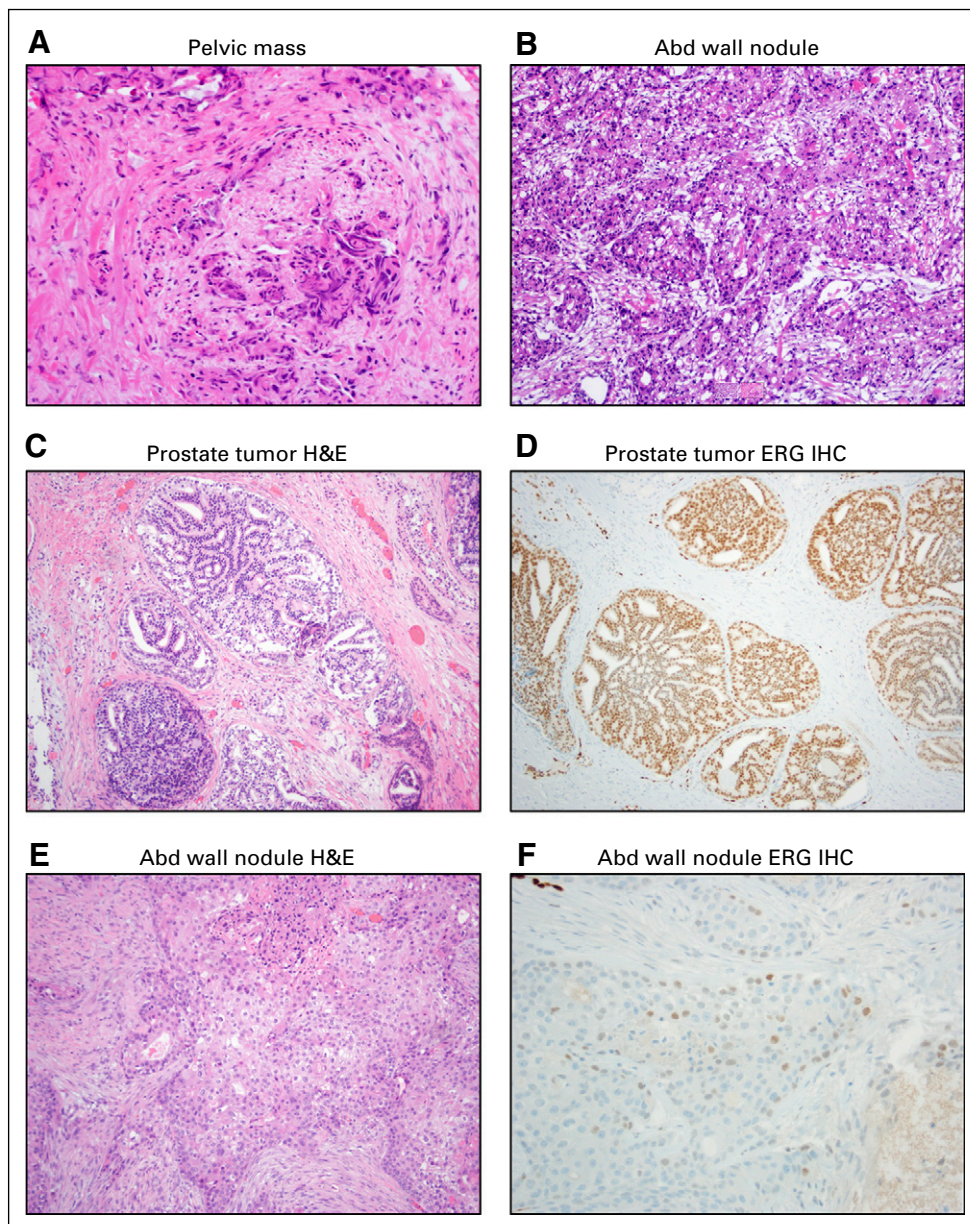
FIG 1. Clinical timeline and cross-sectional imaging. (A) Summary of the clinical course and systemic therapy. (B) Positron emission tomography (PET)/computed tomography (CT) showing the right pelvic mass before treatment in December 2018. Dark orange/white color indicates metabolic activity. (C) CT with oral and intravenous contrast showing the right pelvic mass after treatment with carboplatin and gemcitabine (Gem-carbo) chemotherapy. Dashed red circle indicates the metabolically active lesion in the previous PET scan. (D) Noncontrast chest CT before docetaxel chemotherapy in September 2019. (E) Noncontrast chest CT after three cycles of docetaxel chemotherapy. Red arrows in (D) and (E) indicate a lesion responsive to docetaxel. PSA, prostate-specific antigen.



pelvic mass was judged to be atypical for either prostate cancer or melanoma, it was biopsied by pelvic laparoscopy in November 2018 and was found on surgical pathology assessment to be consistent with a high-grade carcinoma with squamous features (Fig 2A). IHC assessment demonstrated neoplastic cells positive for p63 and GATA3, but negative for PSA and NKX3-1 expression. Urine cytology also showed atypical urothelial cells. We performed exome sequencing using the University of Michigan OncoSeq panel (MI-OncoSeq) and whole transcriptome analysis on formalin-fixed paraffin-embedded tissue from this biopsy. All patients enrolled in the MI-OncoSeq study provided written informed consent approved by the University of Michigan Institutional Review Board. Consent is inclusive of publishing information and/or

images from participants (or their designate). However, results were limited because of low tumor content, estimated to be less than 10%. The variant allele fraction of mutations spanned 1% to 6%, and no copy number aberrations were detected (Table 1). Because the pelvic mass was causing pain and urinary obstruction, we elected to treat it with a platinum doublet active in urothelial carcinoma and carcinoma of unknown primary, despite not knowing the tissue of origin. In January 2019, we began carboplatin area under the curve 5 mg/mL/minute on day 1 and gemcitabine 1,000 mg/m² on days 1 and 8 of 21-day cycles, and we completed six cycles before stopping because of progressive fatigue. The patient experienced some improvement in pain, but the size of the right pelvic mass was largely unchanged (Fig 1C).

FIG 2. Histology and immunohistochemistry (IHC). (A) Hematoxylin and eosin (H&E) histology of pelvic mass biopsy showing squamous cell carcinoma. (B) H&E histology of the excisional biopsy of an abdominal (Abd) wall nodule, also showing squamous cell carcinoma. (C) H&E histology of the patient's (untreated) prostate tumor at initial diagnosis showing prostate adenocarcinoma. (D) IHC for ERG of the primary prostate tumor showing strong labeling. (E) H&E histology of the Abd wall nodule biopsy specimen used for molecular analysis. (F) IHC for ERG of the Abd wall nodule showing much weaker labeling.



In June 2019, while being treated only with bicalutamide, the patient was noted on CT scan as having a 1.4-cm nodule in the superficial anterior abdominal wall, which subsequently became easily palpable and caused skin erythema. This nodule, together with smaller adjacent nodules, was removed by excisional biopsy in July 2019, where surgical pathology assessment demonstrated tumor features consistent with metastatic squamous cell carcinoma (Fig 2B). A fresh portion of this specimen was sent for analysis using the MI-OncoSeq platform. This specimen showed a much higher tumor content of 54%, allowing the discovery of additional molecular alterations.

Precision Medicine Tumor Board Discussion

Results were discussed at the University of Michigan Precision Medicine Tumor Board in September 2019.

Somatic aberrations detected in the previous sample were detected in the new biopsy specimen, suggesting clonal relatedness, and additional alterations consistent with the increased tumor content were noted as well (Table 2). Most curiously, we noted a few reads of chimeric transcripts supporting a gene fusion between TMPRSS2 exon 1 and ERG exon 2, accompanied by a focal deletion located in the intergenic region between the two genes and breakpoint visible on the copy number profile (Table 2 and Fig 3A). Fusions between the TMPRSS2 locus and Ets family transcription factors occur in nearly one half of prostate cancers in the United States and, to our knowledge, do not occur in other cancers.^{1,2} Given the presence of this pathognomonic gene fusion and the patient's history of prostate adenocarcinoma, we concluded that his squamous cell carcinoma had arisen from his prostate cancer.

TABLE 1. Summary of OncoSeq Findings From the Pelvic Mass

Mutation Class	Gene/Aberration
Somatic point mutations (Total: 4) 1.3 Mutations/Mb	<i>PIK3CA</i> : p.E542K, activating <i>SF3B1</i> : p.K666Q (hotspot, also detected in blood) Mutations of uncertain significance: <i>ETV3</i> (p. L90P), <i>HOXA3</i> (p. P295L)
Somatic indels (Total: 2)	<i>ELK4</i> : Frameshift deletion, p.L353fs <i>NFKB1</i> : Frameshift deletion, p.E63fs
Copy-number aberrations	Insufficient tumor content for analysis
Gene fusions	No gene fusion detected
Outlier gene expression	Insufficient tumor content for analysis
Germline variants for disclosure	No pathogenic variants detected

To further confirm the findings, we subsequently performed IHC analysis, which showed positive ERG expression on the patient's initial prostate transurethral resection, which was strongly positive for ERG protein (Figs 2C and 2D). We further performed ERG IHC assessment on the patient's recent abdominal biopsy, which demonstrated focal and weak-to-moderate ERG protein expression, supporting a clonal phenotypic origin and evolution from the patient's original conventional (acinar) prostatic adenocarcinoma (Figs 2E and 2F).

Armed with the knowledge that this patient's squamous cell carcinoma was either a trans-differentiated or metaplastic variant of prostate cancer, we discussed the possible therapeutic implications at this point, when the patient was taking only single-agent bicalutamide. For prostate adenocarcinoma, the addition of medical castration, likely in addition to either abiraterone and prednisone or a non-steroidal second-generation antiandrogen, would have been a reasonable next line of therapy. However, the transcriptomics data of the MI-OncoSeq platform showed low expression of the androgen receptor and androgen responsive genes *KLK2*, *KLK3* (PSA), *TMPRSS2*, *ACPP*, and *SLC45A3* (Fig 3B). In keeping with these findings, his PSA level was only 3.1 ng/mL at this point. Therefore, we concluded that additional therapy targeting androgens or the androgen receptor was unlikely to be successful. Similarly, we examined markers for neuroendocrine carcinoma, the most common nonadenocarcinoma type of prostate cancer. However, expression of the neuroendocrine markers *SYP*, *CHGA*, *CHGB*,

and *NCAM1* were also low (Fig 3C). Therefore, we did not plan chemotherapy with a regimen such as carboplatin and etoposide, which is active against small-cell neuroendocrine carcinomas.

We examined the remainder of the molecular results in an effort to find alternative, clinically actionable molecular targets. We noted two alterations associated with PTEN and Akt signaling: an activating mutation in *PIK3CA* and a homozygous deletion in *PTEN* itself (Table 2). Inhibitors of mammalian target of rapamycin (mTOR) have been suggested for use in *PTEN*-deficient tumors. However, overall, the results for mTOR inhibitors in prostate cancer have been disappointing.³ Some randomized data support the use of PI3K inhibitors in metastatic castration-resistant prostate cancer.⁴ However, this was in combination with abiraterone, which made PI3K inhibitors less attractive in this case, given the patient's near total lack of androgen signaling. Last, the homozygous deletion of *CDKN2B* could theoretically sensitize to CDK4/6 inhibitors. However, we decided against this option because CDK4/6 inhibitors have thus far shown disappointing results in prostate cancer.⁵ Therefore, we elected to treat with docetaxel, the most common cytotoxic chemotherapy drug for castration-resistant prostate cancer.

At this point, the patient's lung nodules, which were previously indeterminate, had enlarged greatly (Fig 1D). We started treatment with docetaxel at 75 mg/m² for one cycle, then decreased the dose to 60 mg/m² because of fatigue, and completed three more cycles. We also attempted bicalutamide withdrawal for the adenocarcinoma component of his disease but resumed bicalutamide and added

TABLE 2. Summary of OncoSeq Findings From the Abdominal Wall Nodule

Mutation Class	Gene/Aberration
Somatic point mutations (Total: 14) 3.9 mutations/Mb	<i>PIK3CA</i> p.E542K, activating 13 nonrecurrent SNVs of unknown significance
Somatic indels	<i>ELK4</i> : Frameshift deletion, p.L353fs <i>NFKB1</i> : Frameshift deletion, p.E63fs
Copy-number aberrations	Extensive polyploidy, UPDs, and focal deletions: <i>CDKN2A</i> homozygous deletion <i>PTEN</i> ; homozygous deletion; copy gain: chr1q, 2q, 4q, 3, 7, 8q, 12 to 16, 17q, 19 to 22 UPD: chr1p, 2p, 6, 8p, 9 to 11, 17p, 18
Gene fusions	<i>TMPRSS2</i> (exon 1) – <i>ERG</i> (exon 2), low (8) chimeric reads; minimal expression of both genes
Outlier gene expression	No expression of AR signaling genes and <i>ERG</i> ; no expression of neuroendocrine markers; high expression of keratins KRT4, 5, 13, 14, 15, 19, 8; high expression of TP63 (basal cell marker)
Germline variants for disclosure	No cancer associated pathogenic variants

Abbreviations: SNV, single-nucleotide variant; UPD, uniparental disomy.

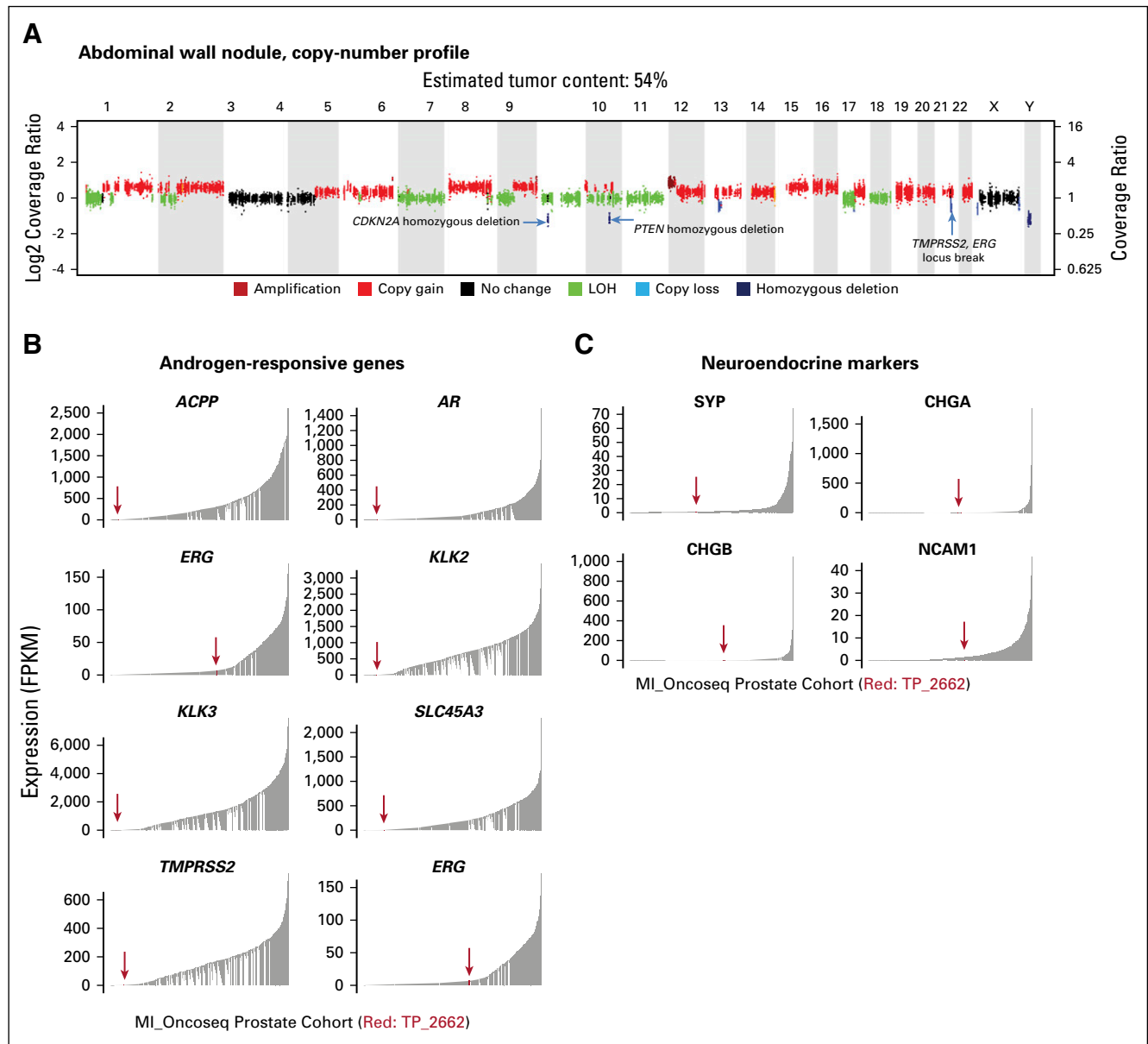


FIG 3. Next-generation sequencing. (A) Copy-number profile from the abdominal wall nodule highlighting the *TMPRSS2-ERG* locus break, a *PTEN* homozygous deletion, and a *CDKN2A* homozygous deletion. (B) Expression of androgen-responsive genes in the patient's second sample OncoSeq transcriptomics data. (C) Expression of neuroendocrine marker genes in the patient's second sample OncoSeq transcriptomics data. FPKM, fragments per kilobase of transcript per million mapped reads; LOH, loss of heterozygosity.

leuprolide a month later after his PSA continued to rise. The patient reported improvement in right groin pain shortly after initiation of docetaxel. CT completed after three cycles showed an interval decrease in the size of multiple bilateral lung nodules, and a decrease in size of his right pelvic mass, compatible with a therapeutic response (Fig 1E).

Discussion

In this case, we used next-generation sequencing to determine that the patient's squamous cell carcinoma was actually of prostate origin, because of the presence of a gene fusion between *TMPRSS2* and *ERG*. Transcriptomic

and histologic analysis showed minimal evidence of androgen receptor signaling, but it also showed a lack of evidence of neuroendocrine differentiation. Such prostate cancers without evidence of androgen receptor signaling and without neuroendocrine markers have been termed "double-negative" prostate cancers.⁶ In more recent work profiling rapid autopsy specimens, investigators identified a squamous subtype of double-negative prostate cancer present in eight of 98 patients.⁷ Squamous histology prostate cancer was reported previously but was a rare finding before the development of advanced antiandrogens.⁸ However, the detection of squamous and other nonadenocarcinoma

prostate cancer subtypes has become more common since the development of abiraterone and nonsteroidal second-generation antiandrogens,⁶ possibly as a means to escape continual selective pressure against androgen signaling, a phenomenon that had been described rarely in the past.⁹ Some of these double-negative prostate cancer (DNPC) tumors seem to be driven by fibroblast growth factor (FGF) alterations, and trials of FGF inhibitors have recently begun in advanced prostate cancer.¹⁰ Our patient did not have an FGF abnormality. Platinum-based chemotherapy is also commonly used to treat squamous cell neoplasms. In the current case, despite having squamous differentiation, this patient had only stable disease in response to platinum-based chemotherapy.

After using whole exome sequencing and RNA sequencing to identify this tumor as a squamous neoplasm of prostate origin, we elected to treat him with an agent approved for prostate cancer (docetaxel), an agent we would not have elected to use without knowing the tissue of origin. We elected not to pursue the therapies that could target molecular alterations in his tumor because of the known survival benefit of docetaxel in men with advanced prostate cancer, but therapies targeting his tumor's molecular alterations remain options down the road if his disease progresses. In summary, this report demonstrates a case of transdifferentiation of a prostate adenocarcinoma to a DNPC tumor with squamous differentiation without evidence of an FGF alteration. Consideration should be given to docetaxel in patients with tumors of a similar phenotype.

AFFILIATIONS

¹Department of Medicine, Division of Hematology & Oncology, and Rogel Cancer Center, University of Michigan School of Medicine, Ann Arbor, MI

²Department of Oncology, Wayne State University School of Medicine and Karmanos Cancer Institute, Detroit, MI

³Michigan Center for Translational Pathology, University of Michigan School of Medicine, Ann Arbor, MI

⁴Department of Pathology and Rogel Cancer Center, University of Michigan School of Medicine, Ann Arbor, MI

⁵Michigan Center for Translational Pathology, Department of Computational Medicine and Bioinformatics, Howard Hughes Medical Institute, Department of Urology, and Rogel Cancer Center, University of Michigan School of Medicine, Ann Arbor, MI

CORRESPONDING AUTHOR

Arul M. Chinnaiyan, MD, PhD, 5309 Rogel Cancer Center, 1500 E Medical Center Dr, Ann Arbor, MI 48109; e-mail: arul@umich.edu; Twitter: @UMRogelCancer.

EQUAL CONTRIBUTION

F.C.C. and C.K.-S. are co-first authors of this article.

SUPPORT

Supported by a Career Enhancement Award from the NIH/NCI Prostate Cancer Specialized Program in Research Excellence (SPORE) at the University of Michigan F048931, sub-award F036250, Prostate Cancer Foundation Young Investigator Award 18YOUN04, and Department of Defense Prostate Cancer Research Program Physician Research Award W81XWH2010394 (F.C.C.); NIH R01CA251245, NIH P50CA097186, and a University of Michigan Rogel Scholar Award (J.J.A.); and Prostate SPORE Grant P50 CA186786, NCI Outstanding Investigator Award R35 CA231996, and the Prostate Cancer Foundation (A.M.C.).

AUTHOR CONTRIBUTIONS

Conception and design: Frank C. Cackowski, Chandan Kumar-Sinha, Rohit Mehra, Dan R. Robinson, Arul M. Chinnaiyan

Collection and assembly of data: All authors

Data analysis and interpretation: All authors

Manuscript writing: All authors

Final approval of manuscript: All authors

Accountable for all aspects of the work: All authors

AUTHORS' DISCLOSURES OF POTENTIAL CONFLICTS OF INTEREST

The following represents disclosure information provided by authors of this manuscript. All relationships are considered compensated unless otherwise noted. Relationships are self-held unless noted. I = Immediate Family Member, Inst = My Institution. Relationships may not relate to the subject matter of this manuscript. For more information about ASCO's conflict of interest policy, please refer to www.asco.org/rwc or ascopubs.org/po/author-center.

Open Payments is a public database containing information reported by companies about payments made to US-licensed physicians ([Open Payments](http://OpenPayments.org)).

Chandan Kumar-Sinha

Patents, Royalties, Other Intellectual Property: Royalty for UM Agr No.3199.101 - "Recurrent Gene Fusions In Prostate Cancer" licensed to Gen-Probe

Rohit Mehra

Patents, Royalties, Other Intellectual Property: Co-inventor on a patent on the detection of ETS gene fusions in prostate cancer issued to The University of Michigan.

Joshi J. Alumkal

Consulting or Advisory Role: Merck Sharp & Dohme, Dendreon

Research Funding: Aragon Pharmaceuticals (Inst), Astellas Pharma (Inst), Zenith Epigenetics (Inst), Gilead Sciences (Inst)

Travel, Accommodations, Expenses: Astellas Pharma, Merck Sharp & Dohme

Other Relationship: Astellas Pharma

Arul Chinnaiyan

Stock and Other Ownership Interests: Oncopia, Tempus, Esanik, OncoFusion Therapeutics, Medsyn

Consulting or Advisory Role: Tempus

Patents, Royalties, Other Intellectual Property: Co-inventor on a patent on the detection of ETS gene fusions in prostate cancer issued to The University of Michigan.

No other potential conflicts of interest were reported.

ACKNOWLEDGMENT

We thank the MI-OncoSeq clinical sequencing team, Leslie Fecher, MD, Jeff Montgomery, MD, and Michael Sabel, MD, for collaborative clinical care and discussion; Alex Hopkins for assistance with figures; and Jyoti Athanikar for assistance with scientific editing and manuscript preparation. Most importantly, we recognize the generosity and kindness of the patient and his family for participating in this study.

REFERENCES

1. Tomlins SA, Rhodes DR, Perner S, et al: Recurrent fusion of TMPRSS2 and ETS transcription factor genes in prostate cancer. *Science* 310:644-648, 2005
2. Robinson D, Van Allen EM, Wu YM, et al: Integrative clinical genomics of advanced prostate cancer. *Cell* 161:1215-1228, 2015 [Erratum: *Cell* 162:454, 2015]
3. Statz CM, Patterson SE, Mockus SM: mTOR inhibitors in castration-resistant prostate cancer: A systematic review. *Target Oncol* 12:47-59, 2017
4. de Bono JS, De Giorgi U, Rodrigues DN, et al: Randomized phase II study evaluating Akt blockade with ipatasertib, in combination with abiraterone, in patients with metastatic prostate cancer with and without PTEN loss. *Clin Cancer Res* 25:928-936, 2019
5. ClinicalTrials.gov: A phase II study of androgen deprivation therapy with or without palbociclib in RB-positive metastatic prostate cancer. <https://clinicaltrials.gov/ct2/show/NCT02059213>
6. Bluemn EG, Coleman IM, Lucas JM, et al: Androgen receptor pathway-independent prostate cancer is sustained through FGF signaling. *Cancer Cell* 32:474-489.e6, 2017
7. Labrecque MP, Coleman IM, Brown LG, et al: Molecular profiling stratifies diverse phenotypes of treatment-refractory metastatic castration-resistant prostate cancer. *J Clin Invest* 129:4492-4505, 2019
8. Parwani AV, Kronz JD, Genega EM, et al: Prostate carcinoma with squamous differentiation: An analysis of 33 cases. *Am J Surg Pathol* 28:651-657, 2004
9. Weindorf SC, Taylor AS, Kumar-Sinha C, et al: Metastatic castration resistant prostate cancer with squamous cell, small cell, and sarcomatoid elements—a clinicopathologic and genomic sequencing-based discussion. *Med Oncol* 36:27, 2019
10. ClinicalTrials.gov: Erdafitinib and abiraterone acetate or enzalutamide in treating patients with double negative prostate cancer. <https://clinicaltrials.gov/ct2/show/NCT03999515>



Evolution of Disparities in Prostate Cancer Treatment: Is This a New Normal?

Frank C. Cackowski, MD, PhD¹; Brandon Mahal, MD²; Elisabeth I. Heath, MD¹; and Bradley Carthon, MD, PhD³

OVERVIEW

Despite notable screening, diagnostic, and therapeutic advances, disparities in prostate cancer incidence and outcomes remain prevalent. Although commonly discussed in the context of men of African descent, disparities also exist based on socioeconomic level, education level, and geographic location. The factors in these disparities span systemic access issues affecting availability of care, provider awareness, and personal patient views and mistrust. In this review, we will discuss common themes that patients have noted as impediments to care. We will review how equitable access to care has helped improve outcomes among many different groups of patients, including those with local disease and those with metastatic castration-resistant prostate cancer. Even with more advanced presentation, challenges with recommended screening, and lower rates of genomic testing and trial inclusion, Black populations have benefited greatly from various modalities of therapy, achieving comparable and at times superior outcomes with certain types of immunotherapy, chemotherapy, androgen receptor–based inhibitors, and radiopharmaceuticals in advanced disease. We will also briefly discuss access to genomic testing and differences in patterns of gene expression among Black patients and other groups that are traditionally underrepresented in trials and genomic cohort studies. We propose several strategies on behalf of providers and institutions to help promote more equitable care access environments and continued decreases in prostate cancer disparities across many subgroups.

Prostate cancer continues to be the leading cancer among men in the United States, with 33,000 deaths and 191,000 cases occurring in 2020.¹ One in nine men overall in the United States develops prostate cancer in his lifetime. In Black men, however, this rate is one in seven, and the incidence rate among Black men is 2.2 times that in White men, with the death rate 1.7 times higher.¹ Moreover, although Black men are diagnosed at younger ages, they present routinely with more advanced disease and higher prostate-specific antigen (PSA) levels at presentation than other groups.²⁻⁷

Disparities have been shown to exist not only between ethnic groups but also based on socioeconomic level,^{8,9} education level,¹⁰ and rural versus urban residency.¹¹ Here, we will examine common areas of disparity in prostate cancer. We will also address some of the systemic and personal patient views that contribute to these disparities. We will show how equitable access to care may alleviate some of these areas of disparity, especially in the context of challenges brought on by the COVID-19 pandemic. Lastly, we will examine molecular signatures and the trends and roles they may play in disparate outcomes in patients with prostate cancer.

CHANGING TRENDS

Over the last few decades, technologic and screening advances have led to a decrease in some of the noted

prostate cancer disparities.¹² U.S. Surveillance, Epidemiology, and End Results database analyses show that at a peak in 1992, there were approximately 237 new cases per 100,000 patients. This decreased markedly over time to a nadir of 102 cases per 100,000 patients.^{13,14} Five-year overall survival increased during the same period of time, from 96% to greater than 98% for all patients registered.^{13,15} Moreover, the disparities between Black and White patients have narrowed over time, with recent analyses of prostate cancer survival rates between 2001 and 2016 showing Black men with metastatic prostate cancer are surviving at a similar rate to White men, with approximately 31% of men alive at 5 years.^{12,15} There are likely several reasons for this, including screening increases as well as treatment advances being available. The rates and any differences in incidence and mortality in the future remain to be seen. Changes in screening recommendations by the U.S. Preventive Services Task Force in 2012 against general PSA screening and later in 2018 to favor open-ended discussion on screening for most men at general risk of prostate cancer may have played a role in a disproportionate effect within Black populations, which had a 29% decrease in screening rates after the recommendation changes, despite being at higher risk.¹⁶ Decreases in screening have previously been shown to have an effect on later presentation patterns. Indeed, in the 5 years after the initial

Author affiliations and support information (if applicable) appear at the end of this article.

Accepted on April 8, 2021, and published at ascopubs.org on May 13, 2021; DOI https://doi.org/10.1200/EDBK_321195

PRACTICAL APPLICATIONS

- Prostate cancer disparities exist in the context not only of race and ethnicity but also of socioeconomic level, education level, and geographic location.
- Systemic hurdles to access with regard to screening, diagnostics, and therapeutics, as well as personal patient views and medical hesitancy, may play a role in noted disparities.
- Despite presenting with more advanced disease, Black patients demonstrate favorable outcomes in trial formats and equal access environments with regard to multiple types of therapy.
- Genomic trial data and information useful for all patients depend on diverse patient inclusion to ensure applicability to a wide population.

decreased PSA screening recommendation, there was a decrease in incidence of local stage disease but increases in regional and distant metastases.¹⁷⁻¹⁹ Drops in screening rates have also become more problematic during the COVID-19 pandemic. Data demonstrate that prostate cancer screening rates dropped approximately 60% to 75% in different series during the COVID-19 pandemic when compared with prior time periods.^{20,21} Prostate cancer pathologic diagnoses have also decreased in several series examined, with declines ranging from 20% to 39% lower than the preceding year.^{20,22} The total effects of the COVID-19 pandemic on overall outcomes are not yet clear, but early analyses paint a challenging picture. A recent case control analysis of more than 73 million electronic medical records showed that Black patients with prostate cancer were five times more likely to be infected with COVID-19 (odds ratio, 5.10; 95% CI, 4.34–5.98; $p < .001$). There was a synergistic adverse effect of COVID-19 and cancer with regard to patient rates of hospitalization (Black patients, 55.56% vs. White patients, 43.24%; $p = .003$).²³ The life expectancy for all men in the United States is estimated to have dropped by approximately 1.13 years during the early parts of the COVID-19 pandemic, but the life expectancy for Black men decreased by approximately 2.10 years and the life expectancy for Latino men decreased by approximately 3.05 years during the same period.²⁴ This rapid decrease in life expectancy has been suggested to be due in large part to COVID-19 effects. The long-term effects of delayed care with regard to the most common medical comorbidities, such as cardiovascular disease, chronic kidney disease, diabetes, and cancer, present in these groups remain to be seen, but indeed, these groups seem to have increased COVID-19–related mortality in the short term in meta-

analyses.²⁵ Moreover, loss of insurance stemming from jobs that were disproportionately affected during the pandemic can amplify the effects of normal medical visits and screening to detect these comorbid conditions and cancers, especially among Black and Hispanic workers.²⁶

Whereas some of these changes in prostate cancer epidemiology are related to policy changes on screening and recent pandemic-related factors, there remains a host of other underlying problems affecting clinical care and even beneficial measures such as clinical trial participation. Standard-of-care benchmark treatments and clinical trials are vitally important parts of cancer care progress. Limited access to care, language barriers, transportation, and cost of care, even among insured patients, can also play a role in trial participation.²⁷ Patients who live farther from cancer centers have been shown to be less likely to enroll in clinical trials as well.²⁸ Underserved patients have also been shown to be less likely to regularly visit their physicians or enroll in interventional clinical trials.²⁹⁻³² Importantly, hurdles remain because of patient perception and medical mistrust among many affected high-risk groups.

Engaging local resources within respective communities may help provide culturally appropriate screening strategies and methods to address prostate cancer treatment. Surveyed men noted insufficient information regarding prostate cancer, medical mistrust, poor relationships with medical providers, and lack of sustained relationships from within the community as barriers to an emphasis on prostate health.³³ Embarrassment and fear of a positive diagnosis, reluctance to talk about sexually related complications, and beliefs that prostate cancer may stem from sexual behavior have also been cited during focus groups, which may affect continuity of cancer education and care.³⁴ Strong emphasis on a role for information from cancer survivors was noted.^{33,35,36} Successful outreach efforts have used community institutions such as churches and barbershops along with trusted community educators and local patients with cancer and contacts.³⁷⁻⁴¹ Indeed, familiarity with presenters has been shown to lead to more highly rated and effective engagement during educational ventures.^{42,43} Partners and spouses are also highly useful participants in educational efforts.

DIFFERENCES IN PATTERN OF AND RESPONSE TO TREATMENT: NOT JUST RACE

In the last several years, patients, the research community, and the press have appropriately paid an increasing amount of attention to disparities in outcomes based on race for prostate cancer and other malignancies. However, prostate cancer disparities also exist based on other factors, including rural versus urban location, socioeconomic status, ethnicity, clinical trial participation, and country of treatment. Here, we briefly discuss the multiple demographic

determinants of disparities in prostate cancer and focus on treatment and response to treatment rather than purely on outcomes. These disparities are complex in etiology and may be addressed in part by providers familiarizing themselves with where disparities exist and options for care,⁴⁴ improving communication skills,⁴² and standardizing treatment options.⁴⁵ Health care entities may also help by providing more broadly based support with navigators and other support mechanisms for clinical choices and presenting trial opportunities for patients.⁴⁶⁻⁴⁸

Race and Ethnicity

Patients with prostate cancer may receive different treatments based on stage, but there is a striking racial disparity in the treatment of localized disease. Using U.S. Surveillance, Epidemiology, and End Results data, Moses et al⁴⁵ reported that Black men were less likely than White men to receive definitive treatment by either prostatectomy or definitive radiation therapy for localized prostate cancer (odds ratio, 0.73; 95% CI, 0.71–0.75; $p < .001$). Although of a smaller magnitude, a significant disparity also existed between Hispanic and White patients, with fewer Hispanic patients receiving definitive treatment (odds ratio, 0.95; 95% CI, 0.92–0.98; $p < .001$). The racial disparity also seems to extend to the use of molecular imaging. In a single-center study, Black patients were more likely than White patients to receive the older fluciclovine PET/CT as opposed to the newer gallium-68 prostate-specific membrane antigen PET/CT to evaluate biochemically recurrent prostate cancer.⁴⁹ Although direct comparison studies do not exist, prostate-specific membrane antigen–based PET scans are generally agreed to be more sensitive than fluciclovine PET scans.⁵⁰ Although on average Black patients with prostate cancer receive less intensive treatment of localized disease, they unfortunately are more likely to have decisional regret afterward and may later wish they had opted for more aggressive approaches to their treatment.⁵¹ Lastly, even if assigned the same treatment, Black patients might be less likely to complete it. In a study of 25,727 Black and 126,199 White patients, 12.8% of Black men did not complete definitive radiation therapy for localized prostate cancer as compared with 11.8% of White men (odds ratio, 1.14; 95% CI, 1.09–1.19; $p < .001$).⁵²

Geographic Location

Other factors besides race and ethnicity are associated with disparities in prostate cancer treatment. Patients in non-urban areas are more likely than patients in urban areas to receive no treatment of prostate cancer. Conversely, patients in urban areas are more likely to receive radical prostatectomy than patients in nonurban areas.⁵³ Many researchers might expect that underserved patients treated at academic centers might receive more optimal or perhaps more aggressive care for prostate cancer than those patients

treated at nonacademic centers. However, this does not consistently seem to be the case. Black, Hispanic, and uninsured patients were all more likely to experience treatment delays than White patients at both academic and nonacademic centers.⁵⁴ Delays were actually slightly longer at academic centers, although academic and nonacademic centers were not directly compared. However, in a different study, patients at an academic center were more likely to be treated with radical prostatectomy (odds ratio, 2.57; 95% CI, 2.45–2.69; $p < .001$) as compared with community sites.⁵⁵

Financial and Socioeconomic Status

Another key area affecting treatment of prostate cancer comprises financial concerns and socioeconomic status. Sayyid et al⁵⁶ found in a U.S. population that high socioeconomic status was associated with an increased odds ratio for receipt of definitive treatment of localized disease. Socioeconomic status is interrelated with race, and the two can be difficult to disentangle. In a large series of patients from Detroit, Michigan, Black patients with prostate cancer had lower survival, but adjustment for treatment and socioeconomic status removed the survival difference.⁵⁷ However, even in a more homogenous population (Geneva, Switzerland), patients with prostate cancer of lower socioeconomic status had shorter survival. The survival difference was attributed to delayed diagnosis, different diagnostic workup, and less invasive treatment.⁵⁸ Prostate cancer treatment also differs on a wider scale, between rich and poor countries, as opposed to between patients of different socioeconomic status within a country. As an example, clinical trial participation varies greatly between countries. A recent study estimated that 96% of participants in clinical trials are White and that only 3% of African and Caribbean countries are even included in any clinical trials.⁵⁹ Cooperative group trials in the United States are somewhat better, but Black patients make up only approximately 9% of participants, less than the overall population and less than the overall percentage of patients with prostate cancer.^{60,61} The relatively low population of patients in clinical trials across many trial formats makes it challenging to apply trial results to a diverse population.

RESPONSE TO PROSTATE CANCER TREATMENT AND MITIGATION OF DISPARITIES

Despite the disparities in outcome discussed earlier and the differing treatment patterns outlined, one may argue that meaningful differences can be made by the practice patterns of individual physicians.^{44,62} Other points of view would support that often-touted biologic differences are minimal as opposed to large-scale societal issues that may address disparities.⁶³ Despite the complexity and multiple factors at play, mitigation of prostate cancer disparities will likely involve efforts such as enrollment in clinical trials that contribute toward better outcomes. Importantly, Black men in

particular seem to respond at least as well as White men to standardized prostate cancer treatments.

Black Patients Have Equal or Better Treatment Response

In the metastatic setting, Black men seem to respond better than or similar to White men to multiple different treatments. Among those with metastatic castration-resistant prostate cancer, Black patients have better and more durable PSA responses.^{64,65} In the area of immunotherapy, which has overall been disappointing in prostate cancer, the survival data in Black men are more encouraging. In a registry analysis, Black men treated with sipuleucel-T had a significant reduction in risk of death, with hazard ratios of 0.81 (95% CI, 0.68–0.97; $p = .03$) for all patients and 0.70 (95% CI, 0.57–0.86; $p < .001$) in patients with matched PSA values.⁶⁶ This pattern was corroborated on additional analyses.⁶⁷ Black men treated with docetaxel for metastatic castration-resistant prostate cancer had a similar survival to that of White men by raw numbers but had a lower risk of death when adjusted in a multivariable fashion within a large meta-analysis (HR, 0.81; 95% CI, 0.72–0.91; $p < .001$).⁶⁸ Differences have also been examined in the use of radium-223, a radiopharmaceutical agent approved in the castration-resistant prostate cancer setting. In a retrospective analysis of 318 patients receiving this agent, Black men had a lower risk of death from the time of radium-223 initiation (HR, 0.75; 95% CI, 0.57–0.99; $p = .045$).⁶⁹ Differences in treatment response have also been well elucidated with regard to oral novel androgen receptor pathway inhibitors. In the prechemotherapy castration-resistant prostate cancer setting, Black patients had a 53% rate of PSA decrease to greater than 90%, whereas only 31% of corresponding White patients had a similar reduction with abiraterone, a CYP-17 lyase inhibitor.⁷⁰ Statistical power in this study was limited by the low number of Black patients (28 of 1,088 total patients).⁷⁰ Patients treated in an equal access center had similar patterns of PSA decline with abiraterone, with 68.9% of Black patients demonstrating PSA level decline of 50% or greater versus 48.9% of White patients ($p = .028$).⁶⁴ A separate analysis of abiraterone or enzalutamide in castration-resistant prostate cancer showed improved overall survival of 918 days for Black patients versus 781 days over their White counterparts (HR, 0.826; 95% CI, 0.732–0.933).⁷¹ Importantly, this benefit of androgen-based therapies has also been analyzed in a prospective fashion, where PSA progression-free survival was approximately 16.6 months in Black patients (95% CI, 11.5 to not reached) versus 11.5 months in non-Black patients (95% CI, 8.5–19.3) treated for castration-resistant prostate cancer.⁶⁵ These various outcomes in prostate cancer for Black patients are summarized in [Table 1](#).⁷²

The reason for similar or enhanced responses in Black patients versus White patients with metastatic castration-

resistant prostate cancer is not completely understood. Genomic differences that may play a role in effects on various treatment pathways are explored more in depth later in this review. For example, in small cohorts of patients with metastatic castration-resistant prostate cancer, Black men demonstrated more tumor mutations in androgen receptor and DNA repair genes compared with other men.⁷³ Lastly, Black patients may have an equal or better response to therapy in localized disease as well, if they receive the same treatment as their White counterparts. As mentioned, in selected U.S. Surveillance, Epidemiology, and End Results analyses, Black men were more likely to receive no treatment at all or to receive radiotherapy versus radical prostatectomy when compared with White men (HR, 1.03; $p = .041$).⁶² The patients with similar risk profiles analyzed in this study had no difference in overall survival. In a separate analysis of data from the U.S. Veterans Administration, however, Black men had a lower 10-year all-cause mortality than White men who received definitive radiation therapy for localized prostate cancer.⁷⁴ The mortality racial differences by type of primary treatment seen in some series of patients with prostate cancer but not others require more study and analysis. Most analyses have been retrospective and may have been affected by various types of bias. Additional prospective analyses for localized prostate cancer treatment outcomes by race are necessary.

Treatment in Clinical Trials Mitigates Disparities

Black men and patients from other minority groups have a lower rate of participation in prostate cancer clinical trials, both in the United States⁷⁵ and globally.⁵⁹ Additionally, rural residents are less likely to enroll in clinical trials overall, although there are limited analyses specific to prostate cancer.⁷⁶ However, treatment in a clinical trial has been shown to eliminate differences in overall survival, both for Black patients with metastatic castration-resistant prostate cancer⁷⁷ and for patients with cancer in rural areas overall.⁷⁶ Several problematic issues exist even with large clinical trials that may confound trial availability and outcomes for marginalized patients. These may include site selection that favors more affluent populations, criteria that neglect comorbidities with real-world populations, distance from trial sites, and lack of insurance.

Importantly, additional confounding issues may also affect clinical trial availability. Lack of accrual has been shown to be a major reason for clinical trial closure and affects the presence of clinical treatment options for future patients.⁷⁸ Poor performance status is often a major reason for patients not qualifying for or being excluded from clinical trials.²⁸ Analyses of large phase III clinical trials demonstrated that 96% of patients enrolled across 600 analyzed trials had an Eastern Cooperative Oncology Group performance status of 0 or 1.⁷⁹ Analysis of clinical trial enrollment in

TABLE 1. Analyses Demonstrating Therapeutic Efficacy in Black Patients With Metastatic Prostate Cancer

Author	Agent Investigated	Trial and Analysis Type	Number of Patients	Endpoint	Outcomes
Halabi et al ⁶⁸	Docetaxel	Meta-analysis	8,820 (White, 7,528 [85%]; Black, 500 [6%])	Median OS and risk of death	Median OS, 21.0 vs. 21.2 months; (multivariable HR, 0.81; 95% CI, 0.72–0.91; p < .001)
Ramalingam et al ⁶⁴	Abiraterone	Case control analysis	135 (White, 90 [66%]; Black, 45 [33%])	PSA response	68.9%; ≥ 50% PSA level decline in Black patients vs. 48.9% in White patients (p = .028)
Efstathiou et al ⁷⁰	Abiraterone	Retrospective subset analysis	28 Black patients (of 1,088 total patients in COU-AA-302)	PSA response, radiographic PFS	> 90% PSA in 53% of Black patients vs. 31% of White patients; radiographic PFS, 16.6 months in Black patients vs. 11.1 in White patients
McNamara et al ⁷¹	Abiraterone or enzalutamide in CRPC	Retrospective medical record review of VA database	787 Black patients and 2,123 White patients with CRPC	Median OS and risk of death	Median OS, 918 days for Black patients and 781 days for White patients (multivariable HR, 0.826; 95% CI, 0.732–0.93; p = .0020)
George et al ⁶⁵	Abiraterone in metastatic CRPC	Prospective parallel group study	50 Black patients and 50 White patients	PSA, PFS, PSA response	Median PSA PFS, 16.6 months for Black patients vs. 11.5 for White patients; > 90% PSA decline in 48% of Black patients vs. 38% of White patients
Sartor et al, ⁶⁶ Higano et al ⁶⁷	Sipuleucel-T	Registry cohort analysis	1,976 (White, 1,649 [83.4%]; Black, 221 [11.1%])	Median OS and risk of death	Median OS, 25.8 vs. 35.3 months (HR, 0.81; 95% CI, 0.68–0.97; p = .03) in all patients (HR, 0.70; 95% CI, 0.57–0.86; p < .001) in PSA-matched set (HR, 0.60; 95% CI, 0.48–0.74; p < .001)
Zhao et al ⁶⁹	Radium-223	Retrospective medical record review of VA database	87 Black patients (27%) of 318 patients treated with radium-223	Risk of death	Black race was associated with decreased risk of mortality (HR, 0.75; 95% CI, 0.57–0.99; p = .045)

Abbreviations: OS, overall survival; PSA, prostate-specific antigen; PFS, progression-free survival; CRPC, castration-resistant prostate cancer; VA, Veterans Affairs.
Data adapted from Carthon et al.⁷²

a predominantly Black population also showed that these patients were often unable to take part in clinical trials because of comorbid conditions.⁸⁰ Although large clinical trials may help answer pertinent and relevant questions, they often exclude the very groups that may benefit most. These limitations in clinical trial design highlight the importance of including a diverse population of patients who are able to safely enroll.

Outreach, Communication, and Action Items

Individual physicians and other health care providers have the capacity to educate and help mitigate disparities in prostate cancer treatment and outcomes in their practice. Given that Black men have had similar or better responses to treatment than White men for both localized and metastatic prostate cancer, we recommend treatment for Black men should be as intensive as is safe and supported by the literature. This contrasts with a potential pitfall of treating Black patients more conservatively to avoid doing harm. Second, we recommend treatment in a clinical trial for any patient, but especially for underserved populations. Because Black men in particular have higher mistrust of the medical system in general and of clinical trials in particular, special efforts in communication may be required for Black patients. Although working to help rectify entrenched societal differences may seem daunting for an individual practitioner, recognizing that there are existing organizations in place can be the first step in countering systemic obstacles to care. These include the National Cancer Institute Geographic Management of Cancer Health Disparities and National Cancer Institute Center to Reduce Cancer Health Disparities.^{81,82} These entities not only support research but also provide assistance to cancer health professionals and patients and work to diversify the cancer care workforce.

Patient beliefs may also play a role in outcomes, both during screening and also once a patient is actually diagnosed with cancer and must undergo therapy. The exact contribution of patient beliefs (versus implicit or explicit bias) to systemic access issues is difficult to determine.^{83,84} Race alone has not been shown to be predictive of poor outcomes when examining multiple forms of treatment, including watchful waiting,⁸⁵ prostatectomy,⁸⁵ or even definitive radiation therapy.^{86,87} Various studies suggest that hurdles such as more adverse presenting features, negative patient beliefs, and systemic access issues may be overcome to some degree by receiving care in more equitable access environments or via other mechanisms.

Patient navigation is an opportunity to make use of nursing and other support professionals for better health outcomes. This also has the potential to provide increased access to clinical trial enrollment among diverse populations. This approach has been used in several cancers and has been

shown to help with screening and treatment planning in Black patients with prostate cancer. Men benefited by having more timely and increased rates of follow-up.^{43,88} Standard use of patient navigators may improve patient outcomes with regard to disparities in screening and overall outcomes in prostate cancer.

As we discussed, treatment in a clinical trial can help eliminate racial disparities,⁸⁹ but Black patients are less likely than White patients to participate in prostate cancer clinical trials.⁷⁵ Therefore, we encourage prostate cancer physicians to offer clinical trials to patients in all demographic groups. Additionally, the U.S. Food and Drug Administration has studied potential solutions to disparate clinical trial enrollment in patients from multiple demographic groups in part through workshops.⁹⁰ Multiple solutions were proposed in a nonbinding U.S. Food and Drug Administration guidance document,⁹¹ including loosening exclusion criteria throughout clinical trials, not copying overly restrictive phase II exclusion criteria in phase III trials, making trials less burdensome for patients by including more telehealth visits and reimbursing trial participants for travel expenses, conducting community outreach events, and including trial sites with a high percentage of underrepresented populations in patient pools. Although Black people make up approximately 12% of the U.S. population and approximately 22% of patients with cancer in the United States,⁶⁰ they constitute a small proportion of patients enrolled in pharmaceutical industry-sponsored trials (approximately 3%) and are enrolled less frequently in general in cooperative group (approximately 9%) and other types of trials.⁶¹ Therefore, in addition to individual physicians, authors of clinical trial protocols in academia and industry have an opportunity to lessen prostate cancer health disparities through thoughtful trial design.

PROSTATE CANCER DISPARITIES: GENOMIC DATA

A historical and persistent difficulty in the management of prostate cancer is being able to identify and distinguish indolent from aggressive disease.⁹²⁻⁹⁴ Prostate cancer incidence and mortality rates vary widely by ancestry, with men of African ancestry experiencing the greatest burden of disease, likely because of the interplay of socioeconomic factors, environmental exposures, and biologic/epigenetic phenomena.⁹⁵⁻¹⁰⁰ Decades of evidence have clearly established that Black men have a much greater burden of prostate cancer than men of European ancestry, including a nearly two-fold increased risk of developing prostate cancer and a more than 2.2-fold increased risk of dying as a result of prostate cancer.¹ As noted earlier, Black men present at earlier ages and with more advanced disease but are less likely to have access to screening and guideline-concordant care, when compared with other men.¹⁰¹

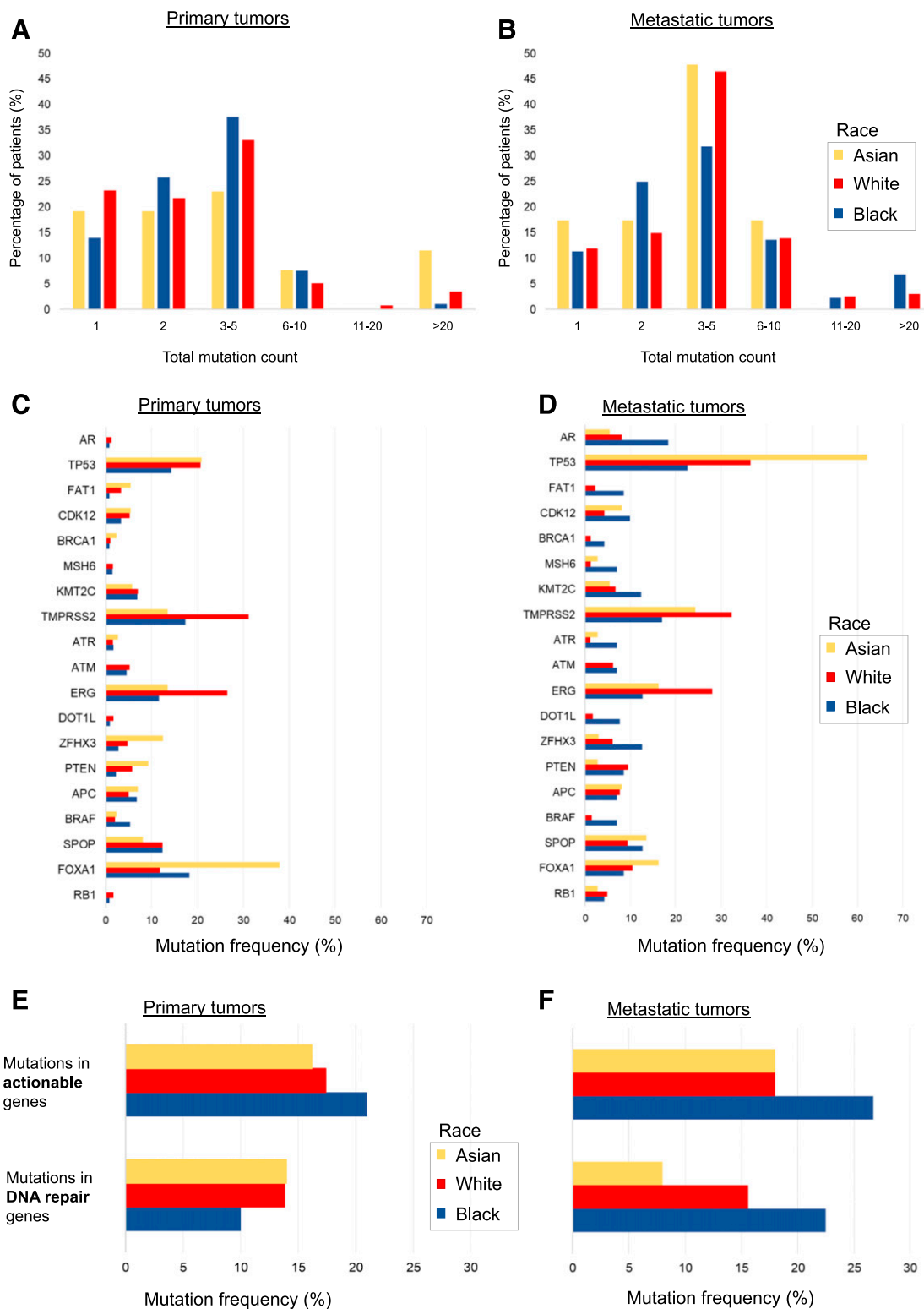


FIGURE 1. Tumor Mutation Profiles by Race in Primary and Metastatic Prostate Cancer

Tumor mutation profiles (MSK-IMPACT and Dana-Farber Sequencing) by race in 2,393 patients (2,109 White; 204 Black; 80 Asian) with primary (1,484 patients [1,308 White; 133 Black; 45 Asian]) or metastatic prostate cancer (909 patients [801 White; 71 Black; 37 Asian]). (A, B) Total mutation count was calculated in the MSK-468 cohort. (C, D) Mutation frequency in primary

FIGURE 1. (Continued). and metastatic tumors. (E, F) DNA repair genes include *ERCC5*, *MRE11*, *TP53BP1*, *POLE*, *RAD21*, *MSH2*, *MSH6*, *BRCA1/2*, *ATR*, and *ATM*. In metastatic cases, DNA repair gene mutations occurred more often in Black men (22.5%) compared with White men (15.6%; $p = .05$). Mutations in *ATR* and *MSH6* occurred more often in Black compared with White men (7.0% vs. 1.1%; $p = .0002$ for both). Actionable mutations include *ABL1*, *EGFR*, *ERBB2*, *BRAF*, *BRCA1/2*, *FGFR2/3*, *KIT*, *NTRK1/2/3*, *PDGFRA*, *RET*, *ROS1*, *ALK*, and *PIK3CA*. In metastatic cases, actionable gene mutations occurred more often in Black (26.7%) compared with White men (18.0%; $p = .05$).

The increasing use of precision genomics and medicine has the potential to improve outcomes for all men with prostate cancer; however, genomic efforts and clinical studies have been highly Eurocentric, and there is a risk of widening disparities in the precision medicine era if efforts continue to not include cohorts that are representative of local, national, and global populations.¹⁰²⁻¹⁰⁶ Efforts to address racial differences in prostate cancer outcomes have largely been focused on investigating the contribution of social versus biologic factors in high-risk populations.¹⁰⁷⁻¹⁰⁹ Now, there is increasing evidence that many genomic prognostic models and subsequent targeted therapies are most likely to benefit White patients and least likely to benefit Black patients with cancer and other diseases.¹⁰²⁻¹⁰⁶ Furthermore, there are no specific tumor-based biomarkers or tailored nomograms to guide workup and management of prostate cancer among the subset of patients of African descent who are known to have a higher risk of death resulting from prostate cancer.^{110,111} This is largely due to insufficient minority participation in cancer research, hence the present lack of validated predictive tools for this patient population.

This lack of inclusion of men of African descent is a particular potential hazard in prostate cancer, given the disease has some of the greatest disparities recorded to date. Clinically relevant alterations may occur at different frequencies across race that could have implications for prognosis, therapy response, and enrollment of minority populations in clinical trials and precision oncology studies. An alternative possibility for outcome disparities would suggest that outcome differences could be accounted for by differences in environment, socioeconomic differences, and/or contributors from structural racism. However, there may be a more complex biologic component to these outcomes as well. Preliminary studies in small cohorts of men with metastatic prostate cancer have demonstrated that Black men were more likely to have tumor mutations in androgen receptor, actionable mutations, and DNA repair genes compared with other men (Fig. 1).^{73,110,111} Nevertheless, conclusions cannot be drawn until appropriate

studies are conducted with large numbers of non-White patients and that include data on environmental exposures.

Of note, only 13% of the samples from a recent study examining genomic variants in prostate cancer were from Black patients.¹¹² Several issues complicate the availability of genomic clinical trials and next-generation sequencing to all patients. Insurance issues and cost may make these items financially unavailable. Patients may also refuse genomic testing because of a misunderstanding of terminology and hesitancy regarding what is believed to be genomic research.¹¹³ Availability of appropriate and standard genetic counseling may also provide a major impetus to overcoming such hurdles. Adherence to recent consensus meeting recommendations regarding genomic testing and utility of navigation may provide a way to definitely decrease the disparity in genomic analyses,¹¹⁴ but this will require resources to implement.

FUTURE DIRECTIONS

Despite the progress in prostate cancer survival, treatment, and disparity, much work remains. Because the etiology of these disparities is multifactorial and based not only on ethnicity, geographic location, and socioeconomic, the approach to address these disparities must also be multifaceted. We encourage and recommend:

1. More studies of novel therapies stratified by race
2. Use of patient navigation with clinical therapies and trial enrollment in underserved patient settings
3. Enhanced and guideline-driven use of genomic testing to personalize therapies
4. Standardization of treatment such that care is delivered in more equal access environments and pathways for optimal outcomes

It is hoped that ongoing community-based educational efforts using invested and familiar partners will continue to address the advances made in cancer therapies and approaches that have led to progress in eliminating prostate cancer disparities.

AFFILIATIONS

¹Karmanos Cancer Institute, Wayne State University, Detroit, MI

²Sylvester Comprehensive Cancer Center, University of Miami, Miami, FL

³Winship Cancer Institute, Emory University, Atlanta, GA

CORRESPONDING AUTHOR

Bradley Carthon, MD, PhD, Department of Hematology and Medical Oncology, Winship Cancer Institute, Emory University, 1365 Clifton Rd., Building B, Suite 4200, Atlanta, GA 30322; email: bcartho@emory.edu.

AUTHORS' DISCLOSURES OF POTENTIAL CONFLICTS OF INTEREST AND DATA AVAILABILITY STATEMENT

Disclosures provided by the authors and data availability statement (if applicable) are available with this article at DOI https://doi.org/10.1200/EDBK_321195.

REFERENCES

1. Siegel RL, Miller KD, Jemal A. Cancer statistics, 2020. *CA Cancer J Clin*. 2020;70:7-30.
2. Jemal A, Culp MB, Ma J, et al. Prostate cancer incidence 5 years after US Preventive Services Task Force recommendations against screening. *J Natl Cancer Inst*. 2020;113:64-71.
3. Pietro GD, Chornokur G, Kumar NB, et al. Racial differences in the diagnosis and treatment of prostate cancer. *Int Neurourol J*. 2016;20(suppl 2):S112-S119.
4. Noone AM, Lund JL, Mariotto A, et al. Comparison of SEER treatment data with Medicare claims. *Med Care*. 2016;54:e55-e64.
5. Leung AK, Hugar L, Patil D, et al. The clinical course of patients with prostate-specific antigen ≥ 100 ng/ml: insight into a potential population for targeted prostate-specific antigen screening. *Urology*. 2018;117:101-107.
6. Tsodikov A, Gulati R, de Carvalho TM, et al. Is prostate cancer different in black men? Answers from 3 natural history models. *Cancer*. 2017;123:2312-2319.
7. Miller EA, Pinsky PF, Black A, et al. Secondary prostate cancer screening outcomes by race in the Prostate, Lung, Colorectal, and Ovarian (PLCO) screening trial. *Prostate*. 2018;78:830-838.
8. Tewari AK, Gold HT, Demers RY, et al. Effect of socioeconomic factors on long-term mortality in men with clinically localized prostate cancer. *Urology*. 2009;73:624-630.
9. Ward E, Jemal A, Cokkinides V, et al. Cancer disparities by race/ethnicity and socioeconomic status. *CA Cancer J Clin*. 2004;54:78-93.
10. Singh GK, Jemal A. Socioeconomic and racial/ethnic disparities in cancer mortality, incidence, and survival in the United States, 1950-2014: over six decades of changing patterns and widening inequalities. *J Environ Public Health*. 2017;2017:2819372.
11. Dasgupta P, Baade PD, Aitken JF, et al. Geographical variations in prostate cancer outcomes: a systematic review of international evidence. *Front Oncol*. 2019;9:238.
12. Kim IE Jr., Jang TL, Kim S, et al. Abrogation of survival disparity between Black and White individuals after the USPSTF's 2012 prostate-specific antigen-based prostate cancer screening recommendation. *Cancer*. 2020;126:5114-5123.
13. National Cancer Institute Surveillance, Epidemiology, and End Results Program. SEER incidence data, 1975-2018: prostate cancer mortality. <https://seer.cancer.gov/data/>. Accessed March 30, 2021.
14. National Cancer Institute Surveillance, Epidemiology, and End Results Program. SEER incidence data, 1975-2017: prostate cancer incidence. <https://seer.cancer.gov/data/>. Accessed March 30, 2021.
15. Siegel DA, O'Neil ME, Richards TB, et al. Prostate cancer incidence and survival, by stage and race/ethnicity - United States, 2001-2017. *MMWR Morb Mortal Wkly Rep*. 2020;69:1473-1480.
16. Patel NH, Bloom J, Hillelsohn J, et al. Prostate cancer screening trends after United States Preventative Services Task Force guidelines in an underserved population. *Health Equity*. 2018;2:55-61.
17. Hu JC, Nguyen P, Mao J, et al. Increase in prostate cancer distant metastases at diagnosis in the United States. *JAMA Oncol*. 2017;3:705-707.
18. Bernstein AN, Shoag JE, Golan R, et al. Contemporary incidence and outcomes of prostate cancer lymph node metastases. *J Urol*. 2018;199:1510-1517.
19. Negoita S, Feuer EJ, Mariotto A, et al. Annual Report to the Nation on the Status of Cancer, part II: recent changes in prostate cancer trends and disease characteristics. *Cancer*. 2018;124:2801-2814.
20. Bakouny Z, Paciotti M, Schmidt AL, et al. Cancer screening tests and cancer diagnoses during the COVID-19 pandemic. *JAMA Oncol*. 2021;7:458-460.
21. Patt D, Gordan L, Diaz M, et al. Impact of COVID-19 on cancer care: how the pandemic is delaying cancer diagnosis and treatment for American seniors. *JCO Clin Cancer Inform*. 2020;4:1059-1071.
22. De Vincentiis L, Carr RA, Mariani MP, et al. Cancer diagnostic rates during the 2020 'lockdown', due to COVID-19 pandemic, compared with the 2018-2019: an audit study from cellular pathology. *J Clin Pathol*. 2021;74:187-189.
23. Wang Q, Berger NA, Xu R. Analyses of risk, racial disparity, and outcomes among US patients with cancer and COVID-19 infection. *JAMA Oncol*. 2021;7:220-227.
24. Andrasfay T, Goldman N. Reductions in 2020 US life expectancy due to COVID-19 and the disproportionate impact on the Black and Latino populations. *Proc Natl Acad Sci USA*. 2021;118:e2014746118.
25. Ssentongo P, Ssentongo AE, Heilbrunn ES, et al. Association of cardiovascular disease and 10 other pre-existing comorbidities with COVID-19 mortality: a systematic review and meta-analysis. *PLoS One*. 2020;15:e0238215.
26. Agarwal SD, Sommers BD. Insurance coverage after job loss - the importance of the ACA during the Covid-associated recession. *N Engl J Med*. 2020;383:1603-1606.

27. Ford JG, Howerton MW, Lai GY, et al. Barriers to recruiting underrepresented populations to cancer clinical trials: a systematic review. *Cancer*. 2008; 112:228-242.
28. Horn L, Keedy VL, Campbell N, et al. Identifying barriers associated with enrollment of patients with lung cancer into clinical trials. *Clin Lung Cancer*. 2013; 14:14-18.
29. Wasserman J, Flannery MA, Clair JM. Raising the ivory tower: the production of knowledge and distrust of medicine among African Americans. *J Med Ethics*. 2007;33:177-180.
30. Kennedy BR, Mathis CC, Woods AK. African Americans and their distrust of the health care system: healthcare for diverse populations. *J Cult Divers*. 2007; 14:56-60.
31. Shavers-Hornaday VL, Lynch CF, Burmeister LF, et al. Why are African Americans under-represented in medical research studies? Impediments to participation. *Ethn Health*. 1997;2:31-45.
32. Shavers VL, Brown ML. Racial and ethnic disparities in the receipt of cancer treatment. *J Natl Cancer Inst*. 2002;94:334-357.
33. Allen JD, Kennedy M, Wilson-Glover A, et al. African-American men's perceptions about prostate cancer: implications for designing educational interventions. *Soc Sci Med*. 2007;64:2189-2200.
34. Forrester-Anderson IT. Prostate cancer screening perceptions, knowledge and behaviors among African American men: focus group findings. *J Health Care Poor Underserved*. 2005;16(suppl A):22-30.
35. Vijaykumar S, Wray RJ, Jupka K, et al. Prostate cancer survivors as community health educators: implications for informed decision making and cancer communication. *J Cancer Educ*. 2013;28:623-628.
36. Wray RJ, Vijaykumar S, Jupka K, et al. Addressing the challenge of informed decision making in prostate cancer community outreach to African American men. *Am J Men Health*. 2011;5:508-516.
37. Frencher SK Jr., Sharma AK, Teklehaimanot S, et al. PEP talk: prostate education program, "cutting through the uncertainty of prostate cancer for Black men using decision support instruments in barbershops". *J Cancer Educ*. 2016;31:506-513.
38. Luque JS, Rivers BM, Kambon M, et al. Barbers against prostate cancer: a feasibility study for training barbers to deliver prostate cancer education in an urban African American community. *J Cancer Educ*. 2010;25:96-100.
39. Drake BF, Shelton RC, Gilligan T, et al. A church-based intervention to promote informed decision making for prostate cancer screening among African American men. *J Natl Med Assoc*. 2010;102:164-171.
40. Hill BC, Black DR, Shields CG. Barbershop prostate cancer education: factors associated with client knowledge. *Am J Men Health*. 2017;11:116-125.
41. Howard A, Morgan P, Fogel J, et al. A community/faith-based education: factors associated with client knowledge and shared decision making behavior for prostate cancer screening among Black men. *ABNF J*. 2018;29:61-68.
42. Walsh-Childers K, Odedina F, Poitier A, et al. Choosing channels, sources, and content for communicating prostate cancer information to Black men: a systematic review of the literature. *Am J Men Health*. 2018;12:1728-1745.
43. Troy C, Brunson A, Goldsmith A, et al. Implementing community-based prostate cancer education in rural South Carolina: a collaborative approach through a statewide cancer alliance. *J Cancer Educ*. Epub 2020 Jun 20.
44. Holmes JA, Bensen JT, Mohler JL, et al. Quality of care received and patient-reported regret in prostate cancer: analysis of a population-based prospective cohort. *Cancer*. 2017;123:138-143.
45. Moses KA, Orom H, Brasel A, et al. Racial/ethnic disparity in treatment for prostate cancer: does cancer severity matter? *Urology*. 2017;99:76-83.
46. Raich PC, Whitley EM, Thorland W, et al; Denver Patient Navigation Research Program. Patient navigation improves cancer diagnostic resolution: an individually randomized clinical trial in an underserved population. *Cancer Epidemiol Biomarkers Prev*. 2012;21:1629-1638.
47. Fouad MN, Acemgil A, Bae S, et al. Patient navigation as a model to increase participation of African Americans in cancer clinical trials. *J Oncol Pract*. 2016; 12:556-563.
48. Dobbs RW, Stinson J, Vasavada SR, et al. Helping men find their way: improving prostate cancer clinic attendance via patient navigation. *J Community Health*. 2020;45:561-568.
49. Bucknor MD, Lichtensztajn DY, Lin TK, et al. Disparities in PET imaging for prostate cancer at a tertiary academic medical center. *J Nucl Med*. Epub 2020 Sep 25.
50. Tan N, Oyoyo U, Bavadian N, et al. PSMA-targeted radiotracers versus ¹⁸F fluciclovine for the detection of prostate cancer biochemical recurrence after definitive therapy: a systematic review and meta-analysis. *Radiology*. 2020;296:44-55.
51. DeWitt-Foy ME, Gam K, Modlin C, et al. Race, decisional regret and prostate cancer beliefs: identifying targets to reduce racial disparities in prostate cancer. *J Urol*. 2021;205:426-433.
52. Dee EC, Muralidhar V, Arega MA, et al. Factors influencing noncompletion of radiation therapy among men with localized prostate cancer. *Int J Radiat Oncol Biol Phys*. 2021;109:1279-1285.
53. Maganty A, Sabik LM, Sun Z, et al. Under treatment of prostate cancer in rural locations. *J Urol*. 2020;203:108-114.
54. Bea M. National sociodemographic disparities in the treatment of high-risk prostate cancer: do academic cancer centers perform better than community cancers? *Cancer*. In press.
55. Agrawal V, Ma X, Hu JC, et al. Trends in diagnosis and disparities in initial management of high-risk prostate cancer in the US. *JAMA Netw Open*. 2020; 3:e2014674.

56. Sayyid RK, Klotz L, Benton JZ, et al. Influence of sociodemographic factors on definitive intervention among low-risk active surveillance patients. *Urology*. Epub 2021 Feb 10.
57. Schwartz K, Powell IJ, Underwood W 3rd, et al. Interplay of race, socioeconomic status, and treatment on survival of patients with prostate cancer. *Urology*. 2009;74:1296-1302.
58. Rapiti E, Fioretta G, Schaffar R, et al. Impact of socioeconomic status on prostate cancer diagnosis, treatment, and prognosis. *Cancer*. 2009;115:5556-5565.
59. Rencsok EM, Bazzi LA, McKay RR, et al. Diversity of enrollment in prostate cancer clinical trials: current status and future directions. *Cancer Epidemiol Biomarkers Prev*. 2020;29:1374-1380.
60. Loree JM, Anand S, Dasari A, et al. Disparity of race reporting and representation in clinical trials leading to cancer drug approvals from 2008 to 2018. *JAMA Oncol*. 2019;5:e191870.
61. Unger JM, Hershman DL, Osarogiagbon RU, et al. Representativeness of Black patients in cancer clinical trials sponsored by the National Cancer Institute compared with pharmaceutical companies. *JNCI Cancer Spectr*. 2020;4:pkaa034.
62. Moses KA, Orom H, Brasel A, et al. Racial/ethnic differences in the relative risk of receipt of specific treatment among men with prostate cancer. *Urol Oncol*. 2016;34:415.e7-415.e12.
63. Bach PB, Schrag D, Brawley OW, et al. Survival of Blacks and Whites after a cancer diagnosis. *JAMA*. 2002;287:2106-2113.
64. Ramalingam S, Humeniuk MS, Hu R, et al. Prostate-specific antigen response in Black and White patients treated with abiraterone acetate for metastatic castrate-resistant prostate cancer. *Urol Oncol*. 2017;35:418-424.
65. George DJ, Health EI, Sartor AO, et al. Abi Race: a prospective, multicenter study of black (B) and white (W) patients (pts) with metastatic castrate resistant prostate cancer (mCRPC) treated with abiraterone acetate and prednisone (AAP). *J Clin Oncol*. 2018;36:18s (suppl; abstr LBA5009).
66. Sartor O, Armstrong AJ, Ahaghotu C, et al. Survival of African-American and Caucasian men after sipuleucel-T immunotherapy: outcomes from the PROCEED registry. *Prostate Cancer Prostatic Dis*. 2020;23:517-526.
67. Higano CS, Armstrong AJ, Sartor AO, et al. Real-world outcomes of sipuleucel-T treatment in PROCEED, a prospective registry of men with metastatic castration-resistant prostate cancer. *Cancer*. 2019;125:4172-4180.
68. Halabi S, Dutta S, Tangen CM, et al. Overall survival of Black and White men with metastatic castration-resistant prostate cancer treated with docetaxel. *J Clin Oncol*. 2019;37:403-410.
69. Zhao H, Howard LE, De Hoedt A, et al. Racial discrepancies in overall survival among men treated with ²²³radium. *J Urol*. 2020;203:331-337.
70. Efsthathiou EDH, George D, Joshua AM, et al. An exploratory analysis of efficacy and safety of abiraterone acetate (AA) in black patients (pts) with metastatic castration-resistant prostate cancer (mCRPC) without prior chemotherapy (ctx). *Cancer Res*. 2014;74(19 Suppl):Abstract nr CT313.
71. McNamara MAGD, Ramaswamy K, Lechpammer S, et al. Overall survival by race in chemotherapy-naïve metastatic castration-resistant prostate cancer (mCRPC) patients treated with abiraterone acetate or enzalutamide. *J Clin Oncol*. 2019;27:7s (suppl; abstr 212).
72. Carthon B, Sibold HC, Blee S, et al. Prostate cancer: disparities in diagnosis and treatment, and community education. *Oncologist*. Epub 2021 Mar 8.
73. Mahal BA, Alshalalfa M, Kensler KH, et al. Racial differences in genomic profiling of prostate cancer. *N Engl J Med*. 2020;383:1083-1085.
74. McKay RR, Sarkar RR, Kumar A, et al. Outcomes of Black men with prostate cancer treated with radiation therapy in the Veterans Health Administration. *Cancer*. 2021;127:403-411.
75. Balakrishnan AS, Palmer NR, Fergus KB, et al. Minority recruitment trends in phase III prostate cancer clinical trials (2003 to 2014): progress and critical areas for improvement. *J Urol*. 2019;201:259-267.
76. Kim SH, Tanner A, Friedman DB, et al. Barriers to clinical trial participation: a comparison of rural and urban communities in South Carolina. *J Community Health*. 2014;39:562-571.
77. Spratt DE, Chen YW, Mahal BA, et al. Individual patient data analysis of randomized clinical trials: impact of Black race on castration-resistant prostate cancer outcomes. *Eur Urol Focus*. 2016;2:532-539.
78. Khunger M, Rakshit S, Hernandez AV, et al. Premature clinical trial discontinuation in the era of immune checkpoint inhibitors. *Oncologist*. 2018;23:1494-1499.
79. Abi Jaoude J, Kouzy R, Mainwaring W, et al. Performance status restriction in phase III cancer clinical trials. *J Natl Compr Canc Netw*. 2020;18:1322-1326.
80. Adams-Campbell LL, Ahaghotu C, Gaskins M, et al. Enrollment of African Americans onto clinical treatment trials: study design barriers. *J Clin Oncol*. 2004;22:730-734.
81. Springfield SA, Van Duyn MAS, Aguila HN, et al. The NCI Center to Reduce Cancer Health Disparities: moving forward to eliminate cancer health disparities and diversify the cancer biomedical workforce. *J Natl Med Assoc*. 2020;112:308-314.
82. Wells KJ, Lima DS, Meade CD, et al; Region 3 GMAp/BMaP investigators. Assessing needs and assets for building a regional network infrastructure to reduce cancer related health disparities. *Eval Program Plann*. 2014;44:14-25.
83. Dovidio JF, Penner LA, Albrecht TL, et al. Disparities and distrust: the implications of psychological processes for understanding racial disparities in health and health care. *Soc Sci Med*. 2008;67:478-486.
84. Boulware LE, Cooper LA, Ratner LE, et al. Race and trust in the health care system. *Public Health Rep*. 2003;118:358-365.
85. Kosciuszka M, Hatcher D, Christos PJ, et al. Impact of race on survival in patients with clinically nonmetastatic prostate cancer who deferred primary treatment. *Cancer*. 2012;118:3145-3152.

86. Johnstone PA, Kane CJ, Sun L, et al. Effect of race on biochemical disease-free outcome in patients with prostate cancer treated with definitive radiation therapy in an equal-access health care system: radiation oncology report of the Department of Defense Center for Prostate Disease Research. *Radiology*. 2002; 225:420-426.
87. Kupelian PA, Buchsbaum JC, Patel C, et al. Impact of biochemical failure on overall survival after radiation therapy for localized prostate cancer in the PSA era. *Int J Radiat Oncol Biol Phys*. 2002;52:704-711.
88. Allen JD, Akinyemi IC, Reich A, et al. African American Women's Involvement in Promoting Informed Decision-Making for Prostate Cancer Screening Among Their Partners/Spouses. *Am J Mens Health*. 2018;12:884-893.
89. Unger JM, Moseley A, Symington B, et al. Geographic distribution and survival outcomes for rural patients with cancer treated in clinical trials. *JAMA Netw Open*. 2018;1:e181235.
90. U.S. Food and Drug Administration. Public Workshop: Evaluating Inclusion and Exclusion Criteria in Clinical Trials—Workshop Report. <https://www.fda.gov/media/134754/download>. Accessed April 1, 2021.
91. U.S. Food and Drug Administration. Enhancing the Diversity of Clinical Trial Populations - Eligibility Criteria, Enrollment Practices and Trial Designs Guidance for Industry. <https://www.fda.gov/regulatory-information/search-fda-guidance-documents/enhancing-diversity-clinical-trial-populations-eligibility-criteria-enrollment-practices-and-trial>. Accessed April 1, 2021.
92. Partin AW, Kattan MW, Subong EN, et al. Combination of prostate-specific antigen, clinical stage, and Gleason score to predict pathological stage of localized prostate cancer. A multi-institutional update. *JAMA*. 1997;277:1445-1451.
93. D'Amico AV, Whittington R, Malkowicz SB, et al. Biochemical outcome after radical prostatectomy, external beam radiation therapy, or interstitial radiation therapy for clinically localized prostate cancer. *JAMA*. 1998;280:969-974.
94. Carroll PH, Mohler JL. NCCN Guidelines Updates: Prostate Cancer and Prostate Cancer Early Detection. *J Natl Compr Canc Netw*. 2018;16:620-623.
95. Siegel RL, Miller KD, Jemal A. Cancer statistics, 2018. *CA Cancer J Clin*. 2018;68:7-30.
96. Sundi D, Ross AE, Humphreys EB, et al. African American men with very low-risk prostate cancer exhibit adverse oncologic outcomes after radical prostatectomy: should active surveillance still be an option for them? *J Clin Oncol*. 2013;31:2991-2997.
97. Mahal BA, Aizer AA, Ziehr DR, et al. Trends in disparate treatment of African American men with localized prostate cancer across National Comprehensive Cancer Network risk groups. *Urology*. 2014;84:386-392.
98. Mahal BA, Chen YW, Muralidhar V, et al. Racial disparities in prostate cancer outcome among prostate-specific antigen screening eligible populations in the United States. *Ann Oncol*. 2017;28:1098-1104.
99. Taksler GB, Keating NL, Cutler DM. Explaining racial differences in prostate cancer mortality. *Cancer*. 2012;118:4280-4289.
100. Hamilton RJ, Aronson WJ, Presti JC Jr., et al. Race, biochemical disease recurrence, and prostate-specific antigen doubling time after radical prostatectomy: results from the SEARCH database. *Cancer*. 2007;110:2202-2209.
101. Presti J Jr., Alexeff S, Horton B, et al. Changes in prostate cancer presentation following the 2012 USPSTF screening statement: observational study in a multispecialty group practice. *J Gen Intern Med*. 2020;35:1368-1374.
102. Spratt DE, Yousefi K, Dehesi S, et al. Individual patient-level meta-analysis of the performance of the decipher genomic classifier in high-risk men after prostatectomy to predict development of metastatic disease. *J Clin Oncol*. 2017;35:1991-1998.
103. Zhao SG, Chang SL, Erho N, et al. Associations of luminal and basal subtyping of prostate cancer with prognosis and response to androgen deprivation therapy. *JAMA Oncol*. 2017;3:1663-1672.
104. Beltran H, Rickman DS, Park K, et al. Molecular characterization of neuroendocrine prostate cancer and identification of new drug targets. *Cancer Discov*. 2011; 1:487-495.
105. Grasso CS, Wu Y-M, Robinson DR, et al. The mutational landscape of lethal castration-resistant prostate cancer. *Nature*. 2012;487:239-243.
106. Pritchard CC, Mateo J, Walsh MF, et al. Inherited DNA-repair gene mutations in men with metastatic prostate cancer. *N Engl J Med*. 2016;375:443-453.
107. Taksler GB, Keating NL, Cutler DM. Explaining racial differences in prostate cancer mortality. *Cancer*. 2012;118:4280-4289.
108. Vastola ME, Yang DD, Muralidhar V, et al. Laboratory eligibility criteria as potential barriers to participation by black men in prostate cancer clinical trials. *JAMA Oncol*. 2018;4:413-414.
109. Mahal AR, Mahal BA, Nguyen PL, et al. Prostate cancer outcomes for men aged younger than 65 years with Medicaid versus private insurance. *Cancer*. 2018; 124:752-759.
110. Yamoah K, Johnson MH, Choeurng V, et al. Novel biomarker signature that may predict aggressive disease in African American men with prostate cancer. *J Clin Oncol*. 2015;33:2789-2796.
111. Huang FW, Mosquera JM, Garofalo A, et al. Exome sequencing of African-American prostate cancer reveals loss-of-function *ERF* mutations. *Cancer Discov*. 2017;7:973-983.
112. Kwon DH-M, Borno HT, Cheng HH, et al. Ethnic disparities among men with prostate cancer undergoing germline testing. *Urol Oncol*. 2020;38:80.e1-80.e7.
113. Rogers CR, Rovito MJ, Hussein M, et al. Attitudes toward genomic testing and prostate cancer research among black men. *Am J Prev Med*. 2018; 55:S103-S111.
114. Szymaniak BM, Facchini LA, Giri VN, et al. Practical considerations and challenges for germline genetic testing in patients with prostate cancer: recommendations from the germline Genetics Working Group of the PCCTC. *JCO Oncol Pract*. 2020;16:811-819.

Amendment.....	1
Personnel Information.....	2
Species.....	7
General Questions.....	11
Are you using?.....	12
Funding.....	16
Purpose and Value.....	17
Animal Use Justification.....	18
Animal Breeding, Housing & Care.....	21
Procedures.....	25
Non-Surgical Procedure Details.....	33
Surgery Relationships.....	37
Schedule of Procedures.....	38
Euthanasia.....	39
Attachments.....	41

July 02, 2021

Wayne State University
INSTITUTIONAL ANIMAL CARE AND USE COMMITTEE (IACUC)
 Animal Research Protocol

Protocol #
 IACUC-20-07-2485

Protocol Title: The Hippo pathway in prostate cancer dormancy and recurrence
Protocol Type: IACUC
Approval Period: Draft
Important Note: This Print View may not reflect all comments and contingencies for approval. Please check the comments section of the online protocol.

***** Amendment *****

Amendment

1. **Is this an amendment to add personnel?** Y
 This person will need to have all required training completed prior to amendment approval, which will not allow any additional amendments to be submitted until that time.
2. **Is this a general amendment?** N
 Review General Amendment Requests for guidance. All changes must be incorporate into this protocol application.
 - a. **Describe why this amendment is necessary and how it integrates with the original protocol (and approved amendments).**
 - b. **Does this amendment include new procedures that may require additional training of personnel by DLAR (e.g. oral gavage, i.v. injection)?**
 Please list the person/people and procedure(s):

July 02, 2021

Wayne State University
INSTITUTIONAL ANIMAL CARE AND USE COMMITTEE (IACUC)
 Animal Research Protocol

Protocol #
 IACUC-20-07-2485

Protocol Title: The Hippo pathway in prostate cancer dormancy and recurrence
Protocol Type: IACUC
Approval Period: Draft
Important Note: This Print View may not reflect all comments and contingencies for approval. Please check the comments section of the online protocol.

***** Personnel Information *****

Principal Investigator

Name:	Cackowski, Frank	Degree:	MD, PhD
University Title:	Asst Prof (Clinical Scholar)	WSU Access ID:	hf7160
Department:	Oncology	Division:	Hematology & Oncology
Office Address:	Hudson-Webber	Office Phone:	313-576-8321
E-mail Address:	hf7160@wayne.edu	Laboratory Phone:	313-576-8321
Emergency Phone:			

Training Details			
Course ID	Course	Course Completion Date	Course Expiration Date
100	Ani Con Questionnaire	2020-07-22 00:00:00	
73559	Animal Allergy Exposure Reduction	2020-07-22 10:50:00	2023-07-22
27185	Aseptic surgery	2020-07-22 14:06:00	
27086	Biomedical Investigators	2020-05-14 18:04:00	2023-05-14
27090	Biomedical Responsible Conduct of Research Course 1.	2020-05-15 14:42:00	
99756	Biosafety/Bloodborne Pathogens	2020-07-17 11:33:00	2021-07-17
27089	CITI Good Clinical Practice Course	2020-05-14 16:42:00	2023-05-14
27177	CITI Health Information Privacy and Security (HIPS) for Clinical Investigators	2020-05-15 11:49:00	
62527	Conflicts of Interest	2020-05-15 13:56:00	2024-05-14
203	DLAR Mouse	1900-01-01 00:00:00	
119473	GS0900 RCR Core Topics Course	2020-05-15 15:13:00	2024-05-14
99755	Laboratory Safety Training	2020-07-18 23:15:00	2021-07-18
130575	Principal Investigators: NIH Guidelines involving Recombinant or Synthetic Nucleic Acid Molecules	2020-07-17 13:34:00	2023-07-17
132965	Radiation Awareness (Non-users)	2021-01-13 16:36:00	
133087	Radiation Generating Machine	2021-01-13 16:34:00	2022-01-13
27184	Reducing Pain and Distress in Laboratory Mice and Rats	2020-07-22 11:45:00	

July 02, 2021

**Wayne State University
INSTITUTIONAL ANIMAL CARE AND USE COMMITTEE (IACUC)
Animal Research Protocol**

Protocol #
IACUC-20-07-2485

Protocol Title: The Hippo pathway in prostate cancer dormancy and recurrence
Protocol Type: IACUC
Approval Period: Draft
Important Note: This Print View may not reflect all comments and contingencies for approval. Please check the comments section of the online protocol.

27187	Working with Mice in Research	2020-07-22 14:56:00	
27182	Working with the IACUC	2020-07-22 12:57:00	2023-07-22

Working with animal models?

Y

Describe Previous Experience and Responsibilities for this Protocol: Identify the responsibilities of this individual, his/her experience with the procedures and the animal species, and who will train personnel on the procedures for work specific to this protocol.

Dr. Cackowski has experience with most of the techniques in this protocol and will serve as the lead for animal techniques in addition to overall scientific direction as PI. Of particular importance, he became proficient in the intracardiac injections of tumor cells proposed in this protocol during his 5 years of research experience as a clinical fellow and junior faculty member at the University of Michigan. He did almost all of the intracardiac injections for the group (PI. Dr. Russ Taichman) during this time and has performed the procedure over 500 times. In the course of these studies, he also gained experience with monitoring for adverse effects from the intracardiac injection procedure and monitoring animals for signs of pain or distress from tumor growth. Also of particular importance for this protocol, Dr. Cackowski did the majority of the intraperitoneal luciferin injection and bioluminescence imaging for the Taichman group during his time at University of Michigan. Additionally, Dr. Cackowski also has experience with mouse euthanasia using carbon dioxide, intra-tibial (intraosseous) injections of tumor cells, surgical castration, tail vein blood collection, post-mortem tissue harvest, and subcutaneous injections.

Is this person an emergency contact? Emergency contacts need to be able to authorize treatment or euthanasia of sick animals. Y

Can prepare the Protocol and can be responsible for all animal work

Co-Investigator

Name: Zielske, Steven
University Title: Research Scientist
Department: Oncology
Office Address:
E-mail Address: en9282@wayne.edu

Degree: PhD
WSU Access ID: en9282
Division:
Office Phone:
Laboratory Phone:

Emergency Phone:

July 02, 2021

**Wayne State University
INSTITUTIONAL ANIMAL CARE AND USE COMMITTEE (IACUC)
Animal Research Protocol**

Protocol #
IACUC-20-07-2485

Protocol Title: The Hippo pathway in prostate cancer dormancy and recurrence
Protocol Type: IACUC
Approval Period: Draft
Important Note: This Print View may not reflect all comments and contingencies for approval. Please check the comments section of the online protocol.

Training Details			
Course ID	Course	Course Completion Date	Course Expiration Date
100	Ani Con Questionnaire	2020-07-21 00:00:00	
73559	Animal Allergy Exposure Reduction	2020-07-16 16:00:00	2023-07-16
27185	Aseptic surgery	2020-07-15 12:24:00	
27086	Biomedical Investigators	2020-07-15 11:23:00	2023-07-15
27090	Biomedical Responsible Conduct of Research Course 1.	2020-07-13 09:54:00	
99756	Biosafety/Bloodborne Pathogens	2020-07-13 11:47:00	2021-07-13
203	DLAR Mouse	1900-01-01 00:00:00	
99755	Laboratory Safety Training	2020-07-10 14:35:00	2021-07-10
130575	Principal Investigators: NIH Guidelines involving Recombinant or Synthetic Nucleic Acid Molecules	2020-07-13 12:18:00	2023-07-13
133087	Radiation Generating Machine	2020-12-23 10:42:00	2021-12-23
27184	Reducing Pain and Distress in Laboratory Mice and Rats	2020-07-16 12:25:00	
27187	Working with Mice in Research	2020-07-15 12:46:00	
27182	Working with the IACUC	2020-07-15 12:19:00	2023-07-15

Working with animal models?

Y

Describe Previous Experience and Responsibilities for this Protocol: Identify the responsibilities of this individual, his/her experience with the procedures and the animal species, and who will train personnel on the procedures for work specific to this protocol.

I have worked with animals in biomedical research since 1992 in studies about gene therapy, radiotherapy, and cancer while at the University of Iowa, Case Western Reserve University, the University of Michigan, the University of Minnesota, and at Wayne State University. Overall, I have conducted animal research for 14 years, most of that time with mouse models. Procedures that have been routinely performed include anesthesia, intraperitoneal injections, oral gavage, sub-cutaneous injections, blood collection, tail vein injections, restraint, ear tagging and notching, irradiation, bioluminescent imaging, and euthanasia. I have received training and instruction in these techniques from veterinary technicians and lab staff at the various institutions. In addition to a proficiency in these hands-on procedures, I have written animal protocols at various institutions, including Wayne State University, and have undergone online and in-class instruction regarding animal use procedures.

Cardiac injection training will be provided by Dr. Frank Cackowski, the lab PI, who is proficient in this technique.

For this protocol, I will be responsible for co-supervising the work (together with Dr. Cackowski) and performing the work.

Is this person an emergency contact? Emergency contacts need to be able to authorize treatment or euthanasia of sick animals.

Y

July 02, 2021

**Wayne State University
INSTITUTIONAL ANIMAL CARE AND USE COMMITTEE (IACUC)
Animal Research Protocol**

Protocol #
IACUC-20-07-2485

Protocol Title: The Hippo pathway in prostate cancer dormancy and recurrence
Protocol Type: IACUC
Approval Period: Draft
Important Note: This Print View may not reflect all comments and contingencies for approval. Please check the comments section of the online protocol.

**Can prepare the Protocol
Lab Manager**

Name:	Ibrahim, Kristina	Degree:	MS
University Title:	Research Associate	WSU Access ID:	ap0156
Department:	Oncology	Division:	
Office Address:	Hudson-Webber Rm 715	Office Phone:	+1 313-576-8232
E-mail Address:	ap0156@wayne.edu	Laboratory Phone:	313-576-8232
Emergency Phone:			

Training Details			
Course ID	Course	Course Completion Date	Course Expiration Date
100	Ani Con Questionnaire	2021-03-17 00:00:00	
73559	Animal Allergy Exposure Reduction	2021-02-26 09:43:00	2024-02-26
27090	Biomedical Responsible Conduct of Research Course 1.	2021-01-04 14:59:00	
99756	Biosafety/Bloodborne Pathogens	2021-01-05 11:20:00	2022-01-05
99755	Laboratory Safety Training	2021-01-04 15:29:00	2022-01-04
27184	Reducing Pain and Distress in Laboratory Mice and Rats	2021-02-26 09:14:00	
27187	Working with Mice in Research	2021-02-25 13:03:00	
27182	Working with the IACUC	2021-02-24 14:58:00	2024-02-24

Working with animal models?

Y

Describe Previous Experience and Responsibilities for this Protocol: Identify the responsibilities of this individual, his/her experience with the procedures and the animal species, and who will train personnel on the procedures for work specific to this protocol.

No previous experience with laboratory mice. Kristina will be trained on the procedures in this protocol by Drs. Cackowski and Zielske. Her degree of responsibility will increase as she becomes more proficient in animal handling and procedures.

Is this person an emergency contact? Emergency contacts need to be able to authorize treatment or euthanasia of sick animals. Y

Research Staff

If this person does not have a WSU Access ID, please contact IACUC administration

Non-WSU (or Affiliate) Collaborator

July 02, 2021

Wayne State University
INSTITUTIONAL ANIMAL CARE AND USE COMMITTEE (IACUC)
 Animal Research Protocol

Protocol #
 IACUC-20-07-2485

Protocol Title: The Hippo pathway in prostate cancer dormancy and recurrence
Protocol Type: IACUC
Approval Period: Draft
Important Note: This Print View may not reflect all comments and contingencies for approval. Please check the comments section of the online protocol.

A proxy may be listed if the Chair is the PI or a member of the research team.

Department Chair (or signatory official)

Name:	Bepler, Gerold	Degree:	MD, PhD
University Title:	Associate Dean	WSU Access ID:	ej3086
Department:	Oncology	Division:	
Office Address:		Office Phone:	+1 313-576-8665
E-mail Address:	ej3086@wayne.edu	Laboratory Phone:	
Emergency Phone:			

Emergency Contacts

Name	Emergency Phone
Cackowski, Frank	
Zielske, Steven	
Ibrahim, Kristina	

July 02, 2021

**Wayne State University
INSTITUTIONAL ANIMAL CARE AND USE COMMITTEE (IACUC)
Animal Research Protocol**

Protocol #
IACUC-20-07-2485

Protocol Title: The Hippo pathway in prostate cancer dormancy and recurrence
Protocol Type: IACUC
Approval Period: Draft
Important Note: This Print View may not reflect all comments and contingencies for approval. Please check the comments section of the online protocol.

*** * * Species * * ***

NUMBER OF ANIMALS - If this is an initial submission of a multi-year grant beyond the three year protocol period, all the work and number of animals must be included in this protocol application. For all other submissions, list the total number of animals to be used over the 3 YEAR PERIOD of this protocol (or for the life of the project if less than 3 years)

Species to be used

Species	Mouse
Scientific Name	Mus musculus
Strain	C.B-17 Scid
Animal Sex	Male
Weight Range	15 - 30 gm(s)
Age Range	3 - 36 Week(s)
USDA Category	D
Source of these animals	Purchased
Can be purchased from any approved DLAR vendor	
Number of animals for three year project period	290

Species	Mouse
Scientific Name	Mus musculus
Strain	FVB
Animal Sex	Male
Weight Range	15 - 30 gm(s)
Age Range	3 - 36 Week(s)
USDA Category	D
Source of these animals	Purchased
Can be purchased from any approved DLAR vendor	
Number of animals for three year project period	60

Please review the detailed Explanation of USDA Reporting Codes.

Brief examples:

Category B: Animals being bred but not used for experimental purposes.

Category C: Experimental animals that will experience no pain or distress.

Category D: Experimental animals where anesthetic or analgesic agents are used to avoid pain or distress.

Category E: Experimental animals where anesthetic or analgesic agents cannot be used to avoid pain or distress.

1. USDA CATEGORY E: Identify the condition that places the animals in Category E and provide scientific justification for withholding alleviation of pain/distress. Describe any non-pharmaceutical methods that will be used to minimize pain and distress.

NOTE: If animals may die as a result of experimental procedures (e.g., infectious disease or oncology studies), or because an endpoint is used that allows the animals to experience significant pain or distress, justify why an alternate endpoint (e.g., weight loss, clinical signs, tumor size) cannot be used prior to death or pain or distress.

2. Indicate how the total number of animals needed for this study was reached for each USDA category (group size X groups in each experiment X number of experiments). Provide the number and type of experimental and control groups in each experiment, the

July 02, 2021

**Wayne State University
INSTITUTIONAL ANIMAL CARE AND USE COMMITTEE (IACUC)
Animal Research Protocol**

Protocol #
IACUC-20-07-2485

Protocol Title:	The Hippo pathway in prostate cancer dormancy and recurrence
Protocol Type:	IACUC
Approval Period:	Draft
Important Note:	This Print View may not reflect all comments and contingencies for approval. Please check the comments section of the online protocol.

number of experiments planned, and the number of animals in each group. Include all animals in each USDA category, including those that will be needed for training and those that will be culled.

The number and category of animals in this section must match the animal tables above.

DO NOT cut and paste your experimental aims from your grant proposal.

Details of each procedure are to be described in the appropriate section, NOT here.

For survival analyses using the log-rank test, the sample size of 20 per group was calculated using the following parameters; type 1 error 5%, 80% power, 50% of animals in each group, relative hazard 0.25, and no control animals without metastases at the end of the experiment.

All animals will be in USDA category D, except experiment 5, which will have 30 CB17 SCID animals in USDA category C.

For all USDA category D animals, anesthesia will be with inhalational isoflurane. Analgesia if needed will be with carprofen.

Experiment 1:

Control 1: This group will have 20 male CB17 SCID mice. We will inject 100 uL of 5x10⁵ luciferase labeled PC3 or Du-145 cells stably expressing empty pENTR into the left ventricle of the heart. This control group will receive a standard laboratory diet.

Control 2: This group will have 20 male CB17 SCID mice. We will inject 100 uL of 5x10⁵ luciferase labeled PC3 or Du-145 cells stably expressing empty pENTR into the left ventricle. This control group will receive 625 mg/kg doxycycline in the food pellets.

Treatment 1: This group will have 20 male CB17 SCID mice. We will inject 100 uL 5x10⁵ luciferase labeled PC3 or Du-145 cells stably expressing active YAP1 into the left ventricle. This group group will receive 625 mg/kg doxycycline in the food pellets.

Treatment 2: This group will have 20 male CB17 SCID mice. We will inject 100 uL 5x10⁵ luciferase labeled PC3 or Du-145 cells stably expressing active TAZ into the left ventricle. This group will receive 625 mg/kg doxycycline in the food pellets.

Experiment 1 details: This experiment will use a total of 80 male CB17 SCID mice. All groups will have weekly bioluminescence imaging under isoflurane anesthesia. All groups will receive an IP injection of 150 mg/kg luciferin prior to imaging. Experiment 1 will determine if YAP1, TAZ, or both regulate prostate cancer dormancy and metastatic site relapse.

Experiment 2:

Control: This group will have 20 male FVB mice. We will inject 100 uL of 1x10⁶ tdTomato labeled Myc-CaP cells expressing empty vector into the left ventricle.

Treatment 1: This group will have 20 male FVB mice. We will inject 100 uL of 1x10⁶ tdTomato labeled Myc-CaP cells expressing inducible YAP1 into the left ventricle.

Treatment 2: This group will have 20 male FVB mice. We will inject 100 uL of 1x10⁶ tdTomato labeled Myc-CaP cells expressing inducible TAZ into the left ventricle.

Experiment 2 details: This experiment will use a total of 60 male FVB mice. All groups will receive 625 mg/kg doxycycline in the food pellets. All groups will be treated with 100 mg/kg BrdU by IP injection the day after intraventricular injection. All groups will receive 1 mg/mL BrdU in drinking water for seven days. All groups will have weekly bioluminescence imaging under isoflurane anesthesia. All groups will receive an IP injection of 150 mg/kg luciferin prior to imaging. Experiment 2 will be used to validate our findings from the xenograft model. We will use FVB Myc-CaP immune competent, hormone dependent model of prostate cancer bone metastases.

Experiment 3:

Control: This group will have 20 male CB17 SCID mice. We will inject 100 uL of PC3 or Du-145 GFP-luciferase cells expressing empty pENTR into the left ventricle.

Treatment 1: This group will have 20 male CB17 SCID mice. We will inject 100 uL of PC3 or Du-145 GFP-luciferase cells expressing MST1 or MST2 into the left ventricle.

Treatment 2: This group will have 20 male CB17 SCID mice. We will inject 100 uL of PC3 or Du-145 GFP-luciferase cells expressing LATS1 or LATS2 into the left ventricle.

July 02, 2021

Wayne State University
INSTITUTIONAL ANIMAL CARE AND USE COMMITTEE (IACUC)
 Animal Research Protocol

Protocol #
 IACUC-20-07-2485

Protocol Title:	The Hippo pathway in prostate cancer dormancy and recurrence
Protocol Type:	IACUC
Approval Period:	Draft
Important Note:	This Print View may not reflect all comments and contingencies for approval. Please check the comments section of the online protocol.

luciferase cells expressing LATS1 or LATS2 into the left ventricle.

Experiment 3 details: This experiment will use a total of 60 male CB17 SCID mice. All groups will receive 625 mg/kg doxycycline in the food pellets. All groups will have weekly bioluminescence imaging under isoflurane anesthesia. All groups will receive an IP injection of 150 mg/kg luciferin prior to imaging. In experiment 3 we will determine the effect of gene excision on the cell cycle, specifically after arrival of disseminated tumor cells in the bone marrow niche to assess dormancy escape. Experiments 1-3 will determine which member(s) of the hippo pathway are important for prostate cancer dormancy escape.

Experiment 4:

Control: This group will have 20 male CB17 SCID mice. We will inject 100 uL of luciferase labeled PC3 or Du-145 cells into the left ventricle. This group will not receive BAPN injections.

Treatment: This group will have 20 male CB17 SCID mice. We will inject 100 uL of luciferase labeled PC3 or Du-145 cells into the left ventricle. This group will receive IP injections of BAPN at 100 mg/kg starting the day after intraventricular injection.

Experiment 4 details: This experiment will use a total of 40 male CB17 SCID mice. Both groups will have weekly bioluminescence imaging under isoflurane anesthesia. Both groups will receive an IP injection of 150 mg/kg luciferin prior to imaging. Experiment 4 will examine the impact of matrix stiffness on dormancy escape. After validation of the use of the inhibitor BAPN, we will verify effectiveness of inhibition in the context of cancer dormancy.

Experiment 5: USDA category C

This experiment will use 30 male CB17 SCID mice. All mice will be euthanized for tissue harvest. Both tibia (60 total bones) will be harvested for a bone explant model where they will be transfected with RHOA siRNA1, RHOA siRNA2, or control siRNA.

Experiment 6:

Control: This group will have 20 male CB17 SCID mice. We will inject 100 uL of PC3 or Du-145 GFP-luciferase cells that are not bearing a control CRISPR/Cas9 system into the left ventricle.

Treatment: This group will have 20 male CB17 SCID mice. We will inject 100 uL of PC3 or Du-145 GFP-luciferase cells that are bearing the inducible CRISPR/Cas9 system into the left ventricle.

Experiment 6 details: This experiment will use a total of 40 male CB17 SCID mice. Both groups will receive 625 mg/kg doxycycline in the food pellets. Both groups will have weekly bioluminescence imaging under isoflurane anesthesia. Both groups will receive an IP injection of 150 mg/kg luciferin prior to imaging. Experiment 6 will be complementary to experiment 4. We will excise RHOA to specifically study the effect of RHOA excision on inhibition and dormancy escape after arrival of disseminated tumor cells in the bone marrow niche. Experiments 4-6 will determine if tissue mechanics regulate prostate cancer dormancy escape through the actin cytoskeleton and YAP1 or TAZ. This will elucidate an upstream mechanism for regulation of prostate cancer recurrence.

Experiment 7:

Control: This group will have 20 male CB17 SCID mice. We will inject 100 uL of PC3 or Du-145 cells with SNHG1 expression into the left ventricle. This group will receive a standard laboratory diet.

Treatment: This group will have 20 male CB17 SCID mice. We will inject 100 uL of PC3 or Du-145 cells with SNHG1 expression into the left ventricle. This group will receive 625 mg/kg doxycycline in the food pellets.

Experiment 7 details: Both groups will have weekly bioluminescence imaging under isoflurane anesthesia. Both groups will receive an IP injection of 150 mg/kg luciferin prior to imaging. In experiment 7 we will study regulation of hippo pathway RNA as a novel potential mechanism of prostate cancer recurrence regulation, concentrating on long non-coding RNA SNHG1.

Animal Use justification: Lit Search and Q1d incomplete –are there alternatives to intra-cardiac injection procedure? Considerations are well documented elsewhere (non-surgical procedural detail section) so findings/justifications should be congruent with lit search.

-One article (Kuchimaru et al., 2018) indicates that a possible alternative to intracardiac injection in a bone

July 02, 2021

Wayne State University
INSTITUTIONAL ANIMAL CARE AND USE COMMITTEE (IACUC)
Animal Research Protocol

Protocol #
IACUC-20-07-2485

Protocol Title:	The Hippo pathway in prostate cancer dormancy and recurrence
Protocol Type:	IACUC
Approval Period:	Draft
Important Note:	This Print View may not reflect all comments and contingencies for approval. Please check the comments section of the online protocol.

metastasis model is a caudal artery tail injection. The injection into the tail artery forces the cells back up to the femoral artery branch point where they can then travel to the bones of the legs. There is limited data with caudal artery tail injections in a bone metastasis model so we intend to do a small pilot study to determine if this technique is a potential replacement for the intracardiac injection. We have no experience with this technique so we cannot switch over to it without further investigation. Please refer to the attachment "Email Communication".

July 02, 2021

Wayne State University
INSTITUTIONAL ANIMAL CARE AND USE COMMITTEE (IACUC)
 Animal Research Protocol

Protocol #
 IACUC-20-07-2485

Protocol Title: The Hippo pathway in prostate cancer dormancy and recurrence
Protocol Type: IACUC
Approval Period: Draft
Important Note: This Print View may not reflect all comments and contingencies for approval. Please check the comments section of the online protocol.

***** General Questions *****

General Questions

1. **Is this protocol replacing an expiring protocol?** N
 The number of the expiring protocol is:
 - a. Provide a brief summary of the work completed under the expiring protocol. It may be helpful to include the number of animals that were used/bred related to how many were approved in the expiring protocol; DLAR can provide you with a report, call 577-1107.
 - b. Describe any unexpected adverse events that resulted in increased pain, distress or death rates to animals that were not described in the original protocol. Include how these were managed and what steps were taken to prevent recurrence (if applicable). Please make sure that any additional adverse effects, expected mortality, pain category changes, humane endpoints, etc. have been incorporated into this application.
 - c. Do you have animals currently in-house that will be transferred to this renewal protocol upon approval?
If yes, please include them in species section
2. **Is this VA research (i.e. conducted in VA facilities, funded by the VA)?** N
 Please affirm that you understand that this research cannot be initiated until after the John D. Dingell VAMC, Detroit, MI (station number 553) R&D Committee approval.
3. **Will this protocol be submitted to the VA Central Office for approval (formerly submitted on an ACORP)?** N
4. **Will this research involve students/visitors (not listed as Research Staff)?** N
 If yes, the guideline will need to be affirmed
 Describe the nature of the potential participation:
5. **Is this a teaching protocol?** N
 How many classes are held per year?
 Approximately how many students participate in each class?
6. **Is this a collaboration protocol with another institution via a WSU Memorandum of Understanding?** N
 Institution Name:
 Institution Protocol Number:
 The institution's protocol and approval letter must be attached to this application
 Describe the experimental procedures that will be conducted at WSU in this protocol application
7. **Is this wildlife field research?** N

July 02, 2021

**Wayne State University
INSTITUTIONAL ANIMAL CARE AND USE COMMITTEE (IACUC)
Animal Research Protocol**

Protocol #
IACUC-20-07-2485

Protocol Title: The Hippo pathway in prostate cancer dormancy and recurrence
Protocol Type: IACUC
Approval Period: Draft
Important Note: This Print View may not reflect all comments and contingencies for approval. Please check the comments section of the online protocol.

***** Are you using? *****

Are you using?

1. BIOLOGICAL HAZARDS - Does this research involve the use of any recombinant DNA, mammalian viruses, biological toxins, infectious agents, human blood, human cell lines, human tissue, and/or transgenic animals? Y
 - a. Transgenic/Knockout/Knockin/GEM Animals N
Detailed information regarding transgenic animals must be provided in the "Animal Breeding, Housing and Care" section.
 - b. CDC Select Agents and Biotoxins (see the list of CDC select agents) N
Note : Use of Select agents and Biotoxins requires an Institutional Biosafety Committee(IBC) Protocol application.
IBC Protocol ID:
 - c. Other Toxins (non CDC select agent toxin with LD50<100ng/kg) N
Note : Use of toxins requires an Institutional Biosafety Committee(IBC) Protocol application.
IBC Protocol ID:
 - d. Human or non-human primate cell lines, tumors, blood, tissues, etc. Y
- Human Cell Lines, Tumors, Blood, Tissues, etc.**
- | | |
|-------------------------|-------------|
| Specify material:* | Cell Lines |
| Describe Material:* | PC3 |
| Primary \ Established: | Established |
| Used in which species:* | Mouse |
- Human Cell Lines, Tumors, Blood, Tissues, etc.**
- | | |
|-------------------------|-------------|
| Specify material:* | Cell Lines |
| Describe Material:* | Myc-CaP |
| Primary \ Established: | Established |
| Used in which species:* | Mouse |
- Human Cell Lines, Tumors, Blood, Tissues, etc.**
- | | |
|-------------------------|-------------|
| Specify material:* | Cell Lines |
| Describe Material:* | DU-145 |
| Primary \ Established: | Established |
| Used in which species:* | Mouse |
- Human Cell Lines, Tumors, Blood, Tissues, etc.**
- | | |
|-------------------------|--|
| Specify material:* | Cell Lines |
| Describe Material:* | PC3 (overexpressed with YAP1, TAZ, MST1, MST2, LATS1, LATS2, CRISPR/Cas9 system, or SNHG1) |
| Primary \ Established: | Established |
| Used in which species:* | Mouse |
- Human Cell Lines, Tumors, Blood, Tissues, etc.**
- | | |
|--------------------|------------|
| Specify material:* | Cell Lines |
|--------------------|------------|

July 02, 2021

Wayne State University
INSTITUTIONAL ANIMAL CARE AND USE COMMITTEE (IACUC)
 Animal Research Protocol

Protocol #
 IACUC-20-07-2485

Protocol Title: The Hippo pathway in prostate cancer dormancy and recurrence
Protocol Type: IACUC
Approval Period: Draft
Important Note: This Print View may not reflect all comments and contingencies for approval. Please check the comments section of the online protocol.

Describe Material:* DU-145 (overexpressed with YAP1, TAZ, MST1, MST2, LATS1, LATS2, CRISPR/Cas9 system, or SNHG1)
Primary \ Established: Established
Used in which species:* Mouse
Human Cell Lines, Tumors, Blood, Tissues, etc.
Specify material:* Cell Lines
Describe Material:* Myc-CaP (overexpressed with YAP1 or TAZ)
Primary \ Established: Established
Used in which species:* Mouse

e. Infectious Agents ONLY (if you will be using viral vectors to express rDNA proceed to the next question) Y

Infectious Agents

Infectious Agent:* Lentivirus
Administered to animals (potential DLAR staff exposure)* N
Species:*

Note : Use of Infectious Agents requires an Institutional Biosafety Committee(IBC) Protocol application.
 IBC Protocol ID: IBC-20-07-2486

f. Non-plasmid rDNA, shRNA N

Note : Use of Non-plasmid rDNA shRNA requires an Institutional Biosafety Committee(IBC) Protocol application.
 IBC Protocol ID:

g. Plasmid recombinant (NIH Exempt) DNA N
 Type:

(Please verify by reviewing the NIH exempt explanation)

2. CHEMICAL HAZARDS - Does this research involve the use of any hazardous chemicals (e.g. CFA), chemotherapeutic drugs or gas anesthetic agents (e.g. isoflurane)? (If you are uncertain, you can refer to Chemical Hazards Definition and Examples) Y

a. Hazardous chemicals/chemotherapeutic drugs Y

Hazardous chemicals/chemotherapeutic drugs

Hazardous chemical/drug:* Other
 Doxycycline
Administered to animals (potential DLAR staff exposure)* Y
Species:* Mouse

Hazardous chemicals/chemotherapeutic drugs

Hazardous chemical/drug:* Other
 Bromodeoxyuridine (BrdU)
Administered to animals (potential DLAR staff exposure)* Y
Species:* Mouse

July 02, 2021

Wayne State University
INSTITUTIONAL ANIMAL CARE AND USE COMMITTEE (IACUC)
 Animal Research Protocol

Protocol #
 IACUC-20-07-2485

Protocol Title: The Hippo pathway in prostate cancer dormancy and recurrence
Protocol Type: IACUC
Approval Period: Draft
Important Note: This Print View may not reflect all comments and contingencies for approval. Please check the comments section of the online protocol.

Hazardous chemicals/chemotherapeutic drugs

Hazardous chemical/drug:* Other
 beta-aminopropionitrile (BAPN)
Administered to animals (potential DLAR staff exposure)* Y
Species:* Mouse

b. Gas anesthetic agents Y

Gas anesthetic agents

Gas anesthetic:* Isoflurane

b1. Gas scavenging system? Y

Gas scavenging system

Indicate type of control measures:* Induction chamber with charcoal canister/
 scrubber

If induction chamber or "other", describe the scavenging method (e.g. passive or active) passive

Use Location* Elliman

Room* unknown

If No, please explain

3. Radiation Hazard - Does this research involve the use of ionizing/non-ionizing equipment, radioisotopes in vivo or the use of irradiators? N

a. Non-Ionizing radiation equipment-Examples include: Lasers, Infrared, Microwaves, MRI.

b. Ionizing radiation equipment-Examples include: PET scanner, CT scanner, SPECT, Fluoroscopy, Radiography and other imaging equipment

Note: Use of Ionizing Radiation Equipment requires a Radiation Safety Committee(RSC) Protocol application.

RSC Protocol ID:

c. Sealed Source / X-ray irradiators

d. Radioisotopes

Note: Use of Radioisotopes requires a Radiation Safety Committee(RSC) protocol application.

RSC Protocol ID:

4. PHYSICAL or OTHER HAZARDS - Does this research involve the use of any physical/other hazards (e.g. nanoparticles, noise, cryogens)? N

5. CONTROLLED SUBSTANCES - Does this research involve the use of Controlled Substances (if you are uncertain you can check the DEA CS list: Controlled Substances - by CSA Schedule)? N

Note : Use of Controlled Substance requires a Controlled Substance(CS) Committe Protocol application.

July 02, 2021

Wayne State University
INSTITUTIONAL ANIMAL CARE AND USE COMMITTEE (IACUC)
Animal Research Protocol

Protocol #
IACUC-20-07-2485

Protocol Title: The Hippo pathway in prostate cancer dormancy and recurrence
Protocol Type: IACUC
Approval Period: Draft
Important Note: This Print View may not reflect all comments and contingencies for approval. Please check the comments section of the online protocol.

CS Protocol ID:

6. OCCUPATIONAL HEALTH CONCERNS - Are there any non-routine measures, such as special vaccines or additional health screening techniques that would potentially benefit staff (e.g. research, husbandry, veterinary) that participate in or support this project? Routine measures included in the Occupational Health and Safety Program (vaccination for tetanus, rabies, and hepatitis B, and TB screening) need not be mentioned here. N

Describe:

7. **Use of Non-Pharmaceutical Grade Compounds**

- a. **Are any of the drugs, biologics or reagents being used in these procedures non-pharmaceutical grade (neither human nor veterinary)?** Y

Identify the non-pharmaceutical grade drugs, biologics or reagents that will be administered to animals. Provide scientific justification for their use and describe methods that will be used to ensure appropriate preparation and administration.

BAPN and BrdU are not available as pharmaceutical grade. We will obtain >98% pure BAPN or BrdU and dissolve in sterile PBS for administration. Sterile filtration will be used for sterilization prior to administration.

July 02, 2021

Wayne State University
INSTITUTIONAL ANIMAL CARE AND USE COMMITTEE (IACUC)
 Animal Research Protocol

Protocol #
 IACUC-20-07-2485

Protocol Title: The Hippo pathway in prostate cancer dormancy and recurrence
Protocol Type: IACUC
Approval Period: Draft
Important Note: This Print View may not reflect all comments and contingencies for approval. Please check the comments section of the online protocol.

*** * * Funding * * ***

Funding Checklist

Funding - Grants/Contracts

Funding Source:* U.S. Department Of Defense

Principal Investigator* Cackowski, Frank

Grant/Contract Title* Regulation of Prostate Cancer Dormancy and Recurrence by Hippo Signaling

Sponsor (or internal) Grant ID* W81XWH2010394

What is the status of this proposal?* Awarded

Are all the procedures in this Grant/Contract described in this protocol?* Y

NOTE: Federal agencies require that all procedures using animals described in the grant/proposal must be approved by the IACUC. If this is an initial submission of a multi-year grant beyond the three year protocol period, all the work and number of animals must be included in this protocol application.

If no, list any animal experiments in the associated document(s) that are NOT described in this protocol, and explain their exclusion in the box below. This may include work that has already been completed, work that will not be conducted (the granting agency must already be aware of the exclusion), or work that will be performed by collaborators at other institutions.

Is this protocol supported by a Master Protocol or Core/Program/Consortium Project?* N

Title

Funding - Other

Other Funding (e.g. Start-up funds)

Other Fund Name* Cackowski, Frank: Start-up Funds

July 02, 2021

Wayne State University
INSTITUTIONAL ANIMAL CARE AND USE COMMITTEE (IACUC)
 Animal Research Protocol

Protocol #
 IACUC-20-07-2485

Protocol Title: The Hippo pathway in prostate cancer dormancy and recurrence
Protocol Type: IACUC
Approval Period: Draft
Important Note: This Print View may not reflect all comments and contingencies for approval. Please check the comments section of the online protocol.

*** * * Purpose and Value * * ***

PURPOSE AND POTENTIAL VALUE OF STUDY

Official Project Title

The Hippo pathway in prostate cancer dormancy and recurrence

In non-technical, everyday language that a senior high school student would understand, BRIEFLY state the research or development question to be addressed in this protocol. Also, explain the potential value of this study and the ways the proposed animal use might benefit human or animal health, the advancement of knowledge, education and training, or the good of society.

A scientific abstract from a grant or funding proposal is not acceptable. Do not describe experiments or procedures, or use abbreviations. The information provided in this section could be used for possible press release.

Prostate cancer is the cause of death in about 30,000 men in the U.S. per year. Approximately 2/3 of the deaths result from recurrence after initial surgery or radiation. An improved understanding of the biology of prostate cancer recurrence and strategies to prevent it are critically needed. This protocol seeks to determine how prostate cancer cells lie dormant, and then become active again to cause fatal metastases at a distant site (particularly in bone marrow). The particular focus of these experiments will be on finding the mechanisms that regulate cancer cells escape from dormancy. We will use established animal models of metastasis and dormancy to answer this question.

July 02, 2021

**Wayne State University
INSTITUTIONAL ANIMAL CARE AND USE COMMITTEE (IACUC)
Animal Research Protocol**

Protocol #
IACUC-20-07-2485

Protocol Title: The Hippo pathway in prostate cancer dormancy and recurrence
Protocol Type: IACUC
Approval Period: Draft
Important Note: This Print View may not reflect all comments and contingencies for approval. Please check the comments section of the online protocol.

*** * * Animal Use Justification * * ***

Animal Use Justification

The US Animal Welfare Act (AWA) and USDA Policy #12 regulations require principal investigators to consider alternatives to procedures that may cause more than momentary or slight pain or distress to animals, and provide a written narrative of the methods used and sources consulted to determine the availability of alternatives, including refinements, reductions, and replacements (the 3Rs).

Examples of Refinement: The use of most appropriate anesthetics and analgesics, the use of remote telemetry to increase the quality and quantity of data gathered, and humane endpoints.

Examples of Reduction: The use of shared control groups, preliminary screening in non-animal systems, innovative statistical packages or a consultation with a statistician.

Examples of Replacement: Alternatives such as tissue culture models, or computer-based simulations. Alternative animal models lower on the phylogenetic scale (i.e. using a mouse model in lieu of a non-human primate model).

1. Consideration of Alternatives and the Prevention of Unnecessary Duplication. Complete items below. Keep copies of computer database search results in your files to demonstrate your compliance with the law if regulatory authorities or the IACUC should choose to audit your project.

The USDA webpage Literature Searching and Databases contains links to excellent resources that can help you better understand the requirements and organize your search for alternatives.

WSU Medical School Contact Shiffman Medical Library via askmed@wayne.edu or 313-577-1094

WSU General Libraries visit ASK-A-LIBRARIAN; subject specialists are available.

- a. Investigators must consider less painful or less stressful alternatives to procedures, and provide assurance that proposed research does not unnecessarily duplicate previous work. You should perform one or more database searches to meet these mandates unless compelling justifications can be made without doing so. Complete the table below for each database search you conduct to answer the questions below.

The literature search must not be older than 3 months at time of submission of this protocol application.

Search Data

Search Range From*	1900	(YYYY)
To*	2020	(YYYY)
Search Date*	07/08/2020	(MM/DD/YYYY)

Keywords* YAP, YAP1, TAZ, Prostate cancer, bioluminescence, hippo pathway

Because this is a search for alternatives to painful or distressful procedures, you are advised to use the word "alternative" as a search term along with words that describe the painful procedures described in this protocol.

Databases Searched*

Agricola Data Base		Alternatives to Animal Use in Research, Testing and Education
Animal Welfare Info Center		ATLA (Alternatives to Laboratory Animal Journal)
Benchmarks		BioOne
BIOSIS		CAB Abstracts
Current Contents		Google Scholar
Medline	X	Pubmed
Quick Biblio. Series		TOXLINE
Web of Science		Other

Indicate which alternative mandate(s) this search was conducted for:

- X Computer models or in vitrotechniques
- X Use of less-sentient species
- X Use of less stressful model or methods, or fewer animals

July 02, 2021

Wayne State University
INSTITUTIONAL ANIMAL CARE AND USE COMMITTEE (IACUC)
Animal Research Protocol

Protocol #
IACUC-20-07-2485

Protocol Title: The Hippo pathway in prostate cancer dormancy and recurrence
Protocol Type: IACUC
Approval Period: Draft
Important Note: This Print View may not reflect all comments and contingencies for approval. Please check the comments section of the online protocol.

X Lack of unnecessary duplication

- b. Could any of the animal procedures described in this protocol be replaced by non-animal models, such as mathematical models, computer simulations, or in vitro biological systems? Indicate below if such replacement is or is not possible, and provide a narrative as on how you came to your conclusion.

No, the current state of scientific knowledge and the applicable guidelines do not provide acceptable alternatives, in vitro or otherwise, to the use of live animals to accomplish the purpose of this study. "The development of knowledge necessary for the improvement of the health and well-being of humans as well as other animals requires in vivo experimentation with a wide variety of animal species." (NIH: OLAW) "Whole animals are essential in research and testing because they best reflect the dynamic interactions between the various cells, tissues, and organs comprising the human body." (NIH Guide)

- c. Could a smaller, less sentient mammalian species or a non-mammalian species (e.g. fish, invertebrates) substitute for the mammals in any of the experiments planned? Indicate below if such substitution is or is not possible and provide a narrative on how you came to your conclusion.

No, the xenograft mouse model was previously used to demonstrate differential gene expression of the hippo pathway being studied in these experiments. No acceptable alternative procedures exist for the proposed experiments in less sentient non-mammalian species.

- i. Describe the biological characteristics that make each species, strain and sex selected the most appropriate for this project. If you will use transgenic, knockout or knockin animals, describe the unique feature(s) of each. Cost is not an acceptable consideration.

This study will address the regulation of prostate cancer dormancy and recurrence by hippo signaling. Male CB17 SCID immunodeficient mice will be used for most studies. Females lack a prostate so male mice must be used. Immunodeficient mice lack both T and B cells and accept xenogeneic cells. The use of male CB17 SCID mice is crucial for the growth of xenografts containing active YAP1 or TAZ. We will also use male FVB mice for a syngeneic and immune competent tumor model.

- d. Could a different animal model or different animal procedure that involves (1) less distress, pain, or suffering, or (2) fewer animals substitute for any proposed animal model or animal procedure planned? Indicate below if such replacement is or is not possible, and provide a narrative on how you came to your conclusion:

No, luciferase labeled PC3 or Du-145 cells (wildtype or modified form) will only be injected one time. Animals will be anesthetized during this procedure to minimize pain and distress. Animals will receive imaging via bioluminescence weekly and will be anesthetized during this procedure to minimize distress. All other procedures are routine husbandry or laboratory procedures and will not be expected to induce pain or unnecessary distress.

Using fewer animals could potentially underpower the statistical analysis. For survival analyses using the log-rank test, the sample size of 20 per group was calculated using the following parameters; type 1 error 5%, 80% power, 50% of animals in each group, relative hazard 0.25, and no control animals without metastases at the end of the experiment.

- e. Does the proposed research unnecessarily duplicate previous work? Indicate below if the proposed work unnecessarily duplicates previous work and provide a narrative on how you came to your conclusion:

No, the hippo pathway was delineated relatively recently (2003) in the history of biomedical research and has recently been shown to be involved in prostate cancer. No previous research has been conducted to determine which hippo pathway components stimulate or inhibit dormancy escape in vivo.

2. Indicate the METHOD(S) used to determine the group size of animals needed for this study.

Note: The Guide states that whenever possible, the number of animals requested should be justified statistically. A power analysis is strongly encouraged to justify group sizes when appropriate. Please provide this information.

- a. X Group sizes determined statistically. State what statistical analysis was performed and give the power function. The variance may be estimated from similar previously published studies. Software such as that available at www.poweranalysis.com or www.statistics.com may be helpful.

For survival analyses using the log-rank test, the sample size of 20 per group was calculated using the following parameters: type 1 error 5%, 80% power, 50% of animals in each group, relative hazard 0.25, and no control animals without metastases at the end of the experiment.

- b. Group sizes based on quantity of harvested cells or amount of tissue required. Elaborate. (Note: A statement such as "The study

July 02, 2021

Wayne State University
INSTITUTIONAL ANIMAL CARE AND USE COMMITTEE (IACUC)
Animal Research Protocol

Protocol #
IACUC-20-07-2485

Protocol Title:	The Hippo pathway in prostate cancer dormancy and recurrence
Protocol Type:	IACUC
Approval Period:	Draft
Important Note:	This Print View may not reflect all comments and contingencies for approval. Please check the comments section of the online protocol.

requires 50 experiments" is not sufficient.)

- c.** Pilot study or preliminary project, group variances unknown at present. Minimal number of animals should be requested. You must provide justification for the number of animals you are requesting. State the basis for your request.

- d.** Other Elaborate and justify criteria used to determine group size.

July 02, 2021

**Wayne State University
INSTITUTIONAL ANIMAL CARE AND USE COMMITTEE (IACUC)
Animal Research Protocol**

Protocol #
IACUC-20-07-2485

Protocol Title: The Hippo pathway in prostate cancer dormancy and recurrence
Protocol Type: IACUC
Approval Period: Draft
Important Note: This Print View may not reflect all comments and contingencies for approval. Please check the comments section of the online protocol.

***** Animal Breeding, Housing & Care *****

Animal Breeding, Housing and Care

1. Breeding: Will animals be bred in-house?

YES

X NO

All animals bred in-house must be listed in the "Species" section including any excess or unsuitable animals that will not be used for experiments. For complicated breeding schemes, please consider including an attachment (see "Attachments" tab above)

a. Review the Rodent Breeding and Weaning Policy and complete the table below.

	Pair mating		Pups weaned at 21 days
	Trio mating		Other (describe below):
	Other (describe below):		

b. Will the offspring be genotyped?

	Tail biopsy	Review Rodent Tail Biopsy
	Toe clipping	Review Rodent Toe Clipping (please justify below)
Toe clip ping enable		
	Other:	

2. Rodent Identification Method (e.g. ear punch, tattoo, ear notch) See Rodent Identification for guidance.

Not Applicable

None

X List:

ear punch/notch

3. Will Transgenic, Knockout and Knockin animals be used?

X YES (review the Genetically-Modified Animals Guideline)

NO

a. Describe any special care or monitoring that the animals will require, or need for special breeding systems.

No special care required

X Special care required (describe below):

SPF housing required for immunodeficient SCID mice.

b. For each strain: what is the inserted or knocked-out gene (avoid abbreviations; for an inserted gene, indicate the source species, wild-type or mutant; if mutant, indicate how) and what is the function of the wild-type gene product?

This is not a transgeneic animal per se, as the mutation causing immunodeficiency was spontaneous and not lab-generated. The mutation is in Prkdc, which is a DNA repair gene.

c. Will these modifications to the genome cause an increased risk for the animal to shed intentionally introduced infectious agents, biological toxins, hazardous chemical agents, radioisotopes or create other hazards for the animal handlers and research staff?

YES Explain the hazard the animal will present to staff handling the animals and provide safety precautions required to be observed in housing and handling these animals in the space below.

X NO

July 02, 2021

**Wayne State University
INSTITUTIONAL ANIMAL CARE AND USE COMMITTEE (IACUC)
Animal Research Protocol**

Protocol #
IACUC-20-07-2485

Protocol Title: The Hippo pathway in prostate cancer dormancy and recurrence
Protocol Type: IACUC
Approval Period: Draft
Important Note: This Print View may not reflect all comments and contingencies for approval. Please check the comments section of the online protocol.

- d. Are two or more different strains of transgenic animals being bred?

YES

☒ **NO**

- i. Which strains are being bred?

- ii. What is the expected biological characteristic(s) or outcome of the novel strain(s)?

- iii. Will the novel strain(s) pose any additional risks to staff? If yes, please explain.

4. Housing Outside DLAR Facilities: Will animals need to be maintained outside the DLAR facilities for more than 12 hours?

YES (Review Overnight and Long-Term Housing of Animals in Investigator Laboratories)

☒ **NO**

>12 hours but <=24 hours

>24 hours

If animals are housed more than 24 hours in a laboratory, the room is designated as a satellite animal housing facility and must comply with all pertinent regulations as if it was a DLAR facility. If this room has not been set up as such, contact the IACUC office immediately.

Building:

Room:

DLAR will provide all husbandry and oversight.

DLAR and PI will share the responsibilities for husbandry and oversight.

PI will be responsible for all husbandry and oversight. Provisions for care and housing, animal monitoring and environmental monitoring will meet or exceed standard DLAR SOPs.

All outside housing requests require a Husbandry Agreement between the DLAR and PI. A scanned signed agreement must be attached to this protocol, See attachments tab in the Protocol information.

In the Training Checklist section, please select the persons responsible for taking care of animals outside of DLAR facilities.

- a. Which animals will be housed outside of the DLAR facilities? Please include species and specific information about which animals will be housed (e.g. post-op animals, animals undergoing behavioral testing).

- b. How many animals will be housed outside the DLAR facilities at one time?

- c. How long will the animals be maintained outside of the DLAR facilities?

- d. Justify why it is necessary to house animals outside of the DLAR facilities?

5. Caging Requirements

☒ Standard housing (appropriate for species, including sterile for immunocompromised animals)

Special housing needs required (e.g. suspended wire mesh flooring, non-standard size) for some or all animals on this protocol. Provide justification and describe circumstances below:

July 02, 2021

Wayne State University
INSTITUTIONAL ANIMAL CARE AND USE COMMITTEE (IACUC)
 Animal Research Protocol

Protocol #
 IACUC-20-07-2485

Protocol Title: The Hippo pathway in prostate cancer dormancy and recurrence
Protocol Type: IACUC
Approval Period: Draft
Important Note: This Print View may not reflect all comments and contingencies for approval. Please check the comments section of the online protocol.

6. Social Housing: The Guide states: "Single housing of social species should be the exception and justified based on experimental requirements or veterinary-related concerns about animal well-being."

☒ Standard social housing

Single housing will be required for some or all animals on this protocol. Provide justification and describe circumstances below; include the duration of time animals will be singly housed:

7. Environmental Enrichment: The Guide states: "The primary aim of environmental enrichment is to enhance animal well-being by providing animals with sensory and motor stimulation, through structures and resources that facilitate the expression of species-typical behaviors and promote psychological well-being through physical exercise, manipulative activities, and cognitive challenges according to species-specific characteristics"

☐ Species-specific enrichment will be provided (see Environmental Enrichment and Behavioral and Social Management of Research Animals Policy/Guideline)

Enrichment will not be provided for some or all animals on this protocol. Provide justification and describe circumstances below:

8. State the period of time animals will be allowed to acclimate following arrival at WSU and prior to the initiation of experimental or breeding procedures (Review the Acclimation of Animals Guideline).

1 week

9. Will photographs and/or videos of animals be taken in an animal holding facility (i.e. DLAR)? Review the Security Policy/Guideline.

YES, list building(s) and room number(s) and describe:

☒ NO

10. Will animals be transported between buildings for procedures?

☐ YES Review the Transportation of Animals Policy/SOP

☒ NO

To ensure humane animal handling and protect against disease spread, IACUC/DLAR requires that special provisions be met regarding the transportation of animals between WSU buildings or off campus locations. Transportation arrangements can be made through DLAR by calling 313-577-1343.

1. State the species and number of animals to be transported at one time:

2. Identify the building and room numbers involved in the transport:

Note: If animals will be taken into a medical center area hospital for a procedure, you must have prior approval from the authorizing persons at that hospital.

3. State the purpose of the transportation, indicate if it may be necessary to do this more than once with the same or different groups of animals, and the length of the stay at each site (e.g., 1 hour, 6 hours, overnight, permanent).

4. Authorization to bring animals into WSU locations such as hospitals, clinics or access equipment in the WSU campus area used for human patients. Provide details of authorization to use the facilities by the person responsible for the area(s). Include the name and title of the individual(s), and the date authorization was obtained. Also describe how animal use locations/equipment will be cleaned following use. An authorization letter can be attached in the "Attachments" tab above.

NA

July 02, 2021

**Wayne State University
INSTITUTIONAL ANIMAL CARE AND USE COMMITTEE (IACUC)
Animal Research Protocol**

Protocol #
IACUC-20-07-2485

Protocol Title: The Hippo pathway in prostate cancer dormancy and recurrence
Protocol Type: IACUC
Approval Period: Draft
Important Note: This Print View may not reflect all comments and contingencies for approval. Please check the comments section of the online protocol.

5. If animals are being transported to WSU buildings, will they come into contact with, or be housed in the same room as other animals already residing at the destination?

Yes (provide details below):

No

6. Will the animals need to be sedated or anesthetized prior to or during transportation? Note that large animals (e.g. dogs) usually require sedation prior to transportation. Please consult a veterinarian if this was not previously approved by the IACUC.

Yes (provide details below):

No

7. Will the animals be transported by DLAR?

You are encouraged to make arrangements with DLAR to transport your animals free of charge by calling 313-577-1452 if you are considering using a personal vehicle.

Yes

No, provide details below. You will be required to select the person(s) responsible for transporting the animals in the Training Checklist.

- a. If you and/or your staff will be transporting the animals, please assure the Committee that:

- Animals will be transported in an appropriate climate controlled vehicle. (i.e. air conditioned/heated). The use of personal vehicles is discouraged, as it can result in allergen exposure to the occupant and future occupants of the car, as the car can serve as a potential reservoir of animal pathogens. During regular business hours, arrangements can be made with DLAR to transport animals free of charge.
- Animals will be transported expeditiously in a draped cage or cart by an approved route (out of public view avoiding personnel areas such that no one is aware that an animal is being taken into the hospital area).
- Animals will be hand carried between WSU buildings (the use of carts is discouraged due to uneven pavement conditions on walkways).
- Rodents will be transported in clean filtered microisolator cages and water bottles Inverted to prevent leakage.
- Rodent cages will be sanitized at the destination. Rodent cage exteriors must be sprayed with bleach solution (1 part bleach to 20 parts water) when they reach their destination. Cages cannot be opened until the bleach solution has been on the cage for 10 minutes.
- DLAR facility leaders will be notified at least 24 hrs in advance of the return of the animals.

I will comply with the transportation requirements outlined above and have reviewed the Transportation of Animals Policy/SOP

- b. Briefly describe transportation route below.

July 02, 2021

Wayne State University
INSTITUTIONAL ANIMAL CARE AND USE COMMITTEE (IACUC)
 Animal Research Protocol

Protocol #
 IACUC-20-07-2485

Protocol Title: The Hippo pathway in prostate cancer dormancy and recurrence
Protocol Type: IACUC
Approval Period: Draft
Important Note: This Print View may not reflect all comments and contingencies for approval. Please check the comments section of the online protocol.

* * * Procedures * * *

* * * Procedures * * *

Addition of Agents to Food or Water Supply

Procedure Type:	Addition of Agents to Food or Water Supply	Procedure Title:	Addition of doxycycline to food pellets
Species:	Mouse	Pain/Distress Category:	C
Use Location:	Elliman	Location Type:	DLAR Facility
Room:			

Every procedure must be added individually and then described in the Non-Surgical Procedure Details section.

* * * Add any/all anesthetic agents, analgesics, drugs, etc. that will be used for this procedure. * * *

Anesthetic Agents

Analgesic Agents

Other Agents

Agent Name	Other
	Doxycycline
Dosage (in mg/kg if possible)	625 mg/kg
Route	Other (OTH)
	625 mg/kg doxycycline will be offered in food pellets
Duration and Frequency of Administration	Daily

July 02, 2021

Wayne State University
INSTITUTIONAL ANIMAL CARE AND USE COMMITTEE (IACUC)
 Animal Research Protocol

Protocol #
 IACUC-20-07-2485

Protocol Title: The Hippo pathway in prostate cancer dormancy and recurrence
Protocol Type: IACUC
Approval Period: Draft
Important Note: This Print View may not reflect all comments and contingencies for approval. Please check the comments section of the online protocol.

Addition of Agents to Food or Water Supply

Procedure Type:	Addition of Agents to Food or Water Supply	Procedure Title:	Addition of BrdU to water
Species:	Mouse	Pain/Distress Category:	C
Use Location:	Elliman	Location Type:	DLAR Facility
Room:			

Every procedure must be added individually and then described in the Non-Surgical Procedure Details section.

*** Add any/all anesthetic agents, analgesics, drugs, etc. that will be used for this procedure. ***

Anesthetic Agents

Analgesic Agents

Other Agents

Agent Name	Other
	Bromodeoxyuridine (BrdU)
Dosage (in mg/kg if possible)	1 mg/kg
Route	Other (OTH)
	1 mg/kg BrdU will be offered in drinking water
Duration and Frequency of Administration	Daily

Tumor Transplantation (non-surgical)

Procedure Type:	Tumor Transplantation (non-surgical)	Procedure Title:	Injection of tumor cells
Species:	Mouse	Pain/Distress Category:	D

July 02, 2021

Wayne State University
INSTITUTIONAL ANIMAL CARE AND USE COMMITTEE (IACUC)
Animal Research Protocol

Protocol #
IACUC-20-07-2485

Protocol Title: The Hippo pathway in prostate cancer dormancy and recurrence
Protocol Type: IACUC
Approval Period: Draft
Important Note: This Print View may not reflect all comments and contingencies for approval. Please check the comments section of the online protocol.

Use Location: Elliman **Location Type:** DLAR Facility
Room:

Every procedure must be added individually and then described in the Non-Surgical Procedure Details section.

July 02, 2021

Wayne State University
INSTITUTIONAL ANIMAL CARE AND USE COMMITTEE (IACUC)
 Animal Research Protocol

Protocol #
 IACUC-20-07-2485

Protocol Title: The Hippo pathway in prostate cancer dormancy and recurrence
Protocol Type: IACUC
Approval Period: Draft
Important Note: This Print View may not reflect all comments and contingencies for approval. Please check the comments section of the online protocol.

* * * Add any/all anesthetic agents, analgesics, drugs, etc. that will be used for this procedure. * * *

Anesthetic Agents

Agent Name	Isoflurane
Dosage (in mg/kg if possible)	Concentration of 2-5% isoflurane
Route	Inhalation (INH)
Maintenance Dosage	Concentration of 0.5-2.0% isoflurane
Duration and Frequency of Administration	
Once for injection.	

Analgesic Agents

Agent Name	Carprofen
Dosage (in mg/kg if possible)	5 mg/kg
Route	Subcutaneous (SQ)
Duration and Frequency of Administration	Once daily for any sign of pain, until signs of pain resolve or euthanasia

Other Agents

Agent Name	Other
	Tumor cells
Dosage (in mg/kg if possible)	500,000 cells
Route	Other (OTH)
	Intracardiac (left ventricle)
Duration and Frequency of Administration	Once

Administration of Study Drugs, Hormones, Chemicals, or Cytotoxic Substances

July 02, 2021

**Wayne State University
INSTITUTIONAL ANIMAL CARE AND USE COMMITTEE (IACUC)
Animal Research Protocol**

Protocol #
IACUC-20-07-2485

Protocol Title: The Hippo pathway in prostate cancer dormancy and recurrence
Protocol Type: IACUC
Approval Period: Draft
Important Note: This Print View may not reflect all comments and contingencies for approval. Please check the comments section of the online protocol.

Procedure Type:	Administration of Study Drugs, Hormones, Chemicals, or Cytotoxic Substances	Procedure Title:	Injection of BrdU
Species:	Mouse	Pain/Distress Category:	C
Use Location:	Elliman	Location Type:	DLAR Facility
Room:			

Every procedure must be added individually and then described in the Non-Surgical Procedure Details section.

* * * Add any/all anesthetic agents, analgesics, drugs, etc. that will be used for this procedure. * * *

Anesthetic Agents

Analgesic Agents

Other Agents

Agent Name	Other
	Bromodeoxyuridine (BrdU)
Dosage (in mg/kg if possible)	100 mg/kg
Route	Intraperitoneal (IP)
Duration and Frequency of Administration	Once

Administration of Study Drugs, Hormones, Chemicals, or Cytotoxic Substances

Procedure Type:	Administration of Study Drugs, Hormones, Chemicals, or Cytotoxic Substances	Procedure Title:	Injection of BAPN
Species:	Mouse	Pain/Distress Category:	C

July 02, 2021

Wayne State University
INSTITUTIONAL ANIMAL CARE AND USE COMMITTEE (IACUC)
 Animal Research Protocol

Protocol #
 IACUC-20-07-2485

Protocol Title: The Hippo pathway in prostate cancer dormancy and recurrence
Protocol Type: IACUC
Approval Period: Draft
Important Note: This Print View may not reflect all comments and contingencies for approval. Please check the comments section of the online protocol.

Use Location: Elliman **Location Type:** DLAR Facility
Room:

Every procedure must be added individually and then described in the Non-Surgical Procedure Details section.

* * * Add any/all anesthetic agents, analgesics, drugs, etc. that will be used for this procedure. * * *

Anesthetic Agents

Analgesic Agents

Other Agents

Agent Name	Other
	Beta-aminopropionitrile (BAPN)
Dosage (in mg/kg if possible)	100 mg/kg
Route	Intraperitoneal (IP)
Duration and Frequency of Administration	Once

Administration of Study Drugs, Hormones, Chemicals, or Cytotoxic Substances

Procedure Type:	Administration of Study Drugs, Hormones, Chemicals, or Cytotoxic Substances	Procedure Title:	Injection of luciferin
Species:	Mouse	Pain/Distress Category:	C
Use Location:	Elliman	Location Type:	DLAR Facility
Room:			

Every procedure must be added individually and then described in the Non-Surgical Procedure Details section.

July 02, 2021

Wayne State University
INSTITUTIONAL ANIMAL CARE AND USE COMMITTEE (IACUC)
 Animal Research Protocol

Protocol #
 IACUC-20-07-2485

Protocol Title: The Hippo pathway in prostate cancer dormancy and recurrence
Protocol Type: IACUC
Approval Period: Draft
Important Note: This Print View may not reflect all comments and contingencies for approval. Please check the comments section of the online protocol.

* * * Add any/all anesthetic agents, analgesics, drugs, etc. that will be used for this procedure. * * *

Anesthetic Agents

Analgesic Agents

Other Agents

Agent Name	Other
	Luciferin
Dosage (in mg/kg if possible)	150 mg/kg
Route	Intraperitoneal (IP)
Duration and Frequency of Administration	Weekly, luciferin will be injected prior to bioluminescence imaging

Imaging / Scans (CAT, MRI, MRS, PET, etc.)

Procedure Type:	Imaging / Scans (CAT, MRI, MRS, PET, etc.)	Procedure Title:	Bioluminescence
Species:	Mouse	Pain/Distress Category:	D
Use Location:	Elliman	Location Type:	DLAR Facility
Room:			

Every procedure must be added individually and then described in the Non-Surgical Procedure Details section.

July 02, 2021

Wayne State University
INSTITUTIONAL ANIMAL CARE AND USE COMMITTEE (IACUC)
Animal Research Protocol

Protocol #
IACUC-20-07-2485

Protocol Title: The Hippo pathway in prostate cancer dormancy and recurrence
Protocol Type: IACUC
Approval Period: Draft
Important Note: This Print View may not reflect all comments and contingencies for approval. Please check the comments section of the online protocol.

***** Add any/all anesthetic agents, analgesics, drugs, etc. that will be used for this procedure. *****

Anesthetic Agents

Agent Name	Isoflurane
Dosage (in mg/kg if possible)	Concentration of 2-5% isoflurane
Route	Inhalation (INH)
Maintenance Dosage	Concentration of 0.5-2.0% isoflurane
Duration and Frequency of Administration	
Weekly, will be conducted prior to bioluminescence imaging.	

Analgesic Agents

Other Agents

July 02, 2021

**Wayne State University
INSTITUTIONAL ANIMAL CARE AND USE COMMITTEE (IACUC)
Animal Research Protocol**

Protocol #
IACUC-20-07-2485

Protocol Title: The Hippo pathway in prostate cancer dormancy and recurrence
Protocol Type: IACUC
Approval Period: Draft
Important Note: This Print View may not reflect all comments and contingencies for approval. Please check the comments section of the online protocol.

***** Non-Surgical Procedure Details *****

Non-Surgical Procedure Details

Procedures

Species	Procedure Title	Procedure Type	Pain Category
Mouse	Addition of BrdU to water	Addition of Agents to Food or Water Supply	C
Mouse	Addition of doxycycline to food pellets	Addition of Agents to Food or Water Supply	C
Mouse	Injection of BAPN	Administration of Study Drugs, Hormones, Chemicals, or Cytotoxic Substances	C
Mouse	Injection of BrdU	Administration of Study Drugs, Hormones, Chemicals, or Cytotoxic Substances	C
Mouse	Injection of luciferin	Administration of Study Drugs, Hormones, Chemicals, or Cytotoxic Substances	C
Mouse	Bioluminescence	Imaging / Scans (CAT, MRI, MRS, PET, etc.)	D
Mouse	Injection of tumor cells	Tumor Transplantation (non-surgical)	D

DESCRIBE ALL NON-SURGICAL PROCEDURES: Summarize in a narrative what procedures will be done. Include only those experiments where animals are directly involved. When animals are used as donors of organs, tissues, or cells, only describe how the organs, tissues or cells will be obtained. Do not describe what will be done with those organs, tissues or cells once they have been removed from the animal.

1. **Describe every procedure.**

Intracardiac injection of tumor cells: Most experiments will include an intracardiac (left ventricle) injection of PC3, Du-145, or Myc-CaP prostate cancer cells. This route of administration is chosen to allow systemic inoculation of tumor cells so that the time period of initial growth (dormancy escape) can be studied. On the day prior to injection, the hair of the chest will be removed with Nair. On the day of the procedure, the mice will be anesthetized using inhalant isoflurane 2% in oxygen prior to stereostatic injection. The induction box will be placed on a heating pad set on "low." Once sufficient anesthesia is obtained, each mouse will be transferred to a nose cone to maintain isoflurane anesthesia and positioned supine. The chest will be cleaned and sterilized with isopropanol. 100 microliters of PBS containing 500,000 tumor cells will be loaded into a 30 gauge insulin syringe, which will be placed in a mechanical injection apparatus. Using the cardiac pulsations and anatomic landmarks, the needle will be slowly inserted into the left ventricle. Bright red pulsatile flow will be used to verify correct positioning. Then the cells will be injected over 30 seconds. Each mouse will then be transferred to a recovery cage on a heating pad set to "low" and monitored until complete recovery from anesthesia. The mice will be checked again 2 hours after the procedure and again the following morning, with special attention paid to exam for neurologic deficits. The animals will then be checked at least three times per week for signs of tumor development.

Justification: Although there is risk of complications, the intracardiac (left ventricle) route of injection is selected to physiologically model disseminated prostate cancer, which metastasizes primarily to bone. To create this pattern of metastases, this route of injection is commonly used in the prostate cancer literature. Inoculation of tumor cells to the arterial circulation ensures that the first capillary beds the cells encounter are in the systemic (left heart) circulation, including the skeleton. In other metastatic models, where lung metastases are required (commonly for breast cancer), the tail vein is chosen as the site for inoculation. Although the risk of complications with tail vein injections is much lower, this route would not produce a metastatic pattern representative of prostate cancer because the cells would enter the right heart circulation

July 02, 2021

Wayne State University
INSTITUTIONAL ANIMAL CARE AND USE COMMITTEE (IACUC)
 Animal Research Protocol

Protocol #
 IACUC-20-07-2485

Protocol Title: The Hippo pathway in prostate cancer dormancy and recurrence
Protocol Type: IACUC
Approval Period: Draft
Important Note: This Print View may not reflect all comments and contingencies for approval. Please check the comments section of the online protocol.

metastatic pattern representative of prostate cancer because the cells would enter the right heart circulation and land in the capillary beds downstream of the pulmonary artery. For cell lines capable of growing in lung, this would result in primarily lung metastases. For cell lines not capable of growing in lung, it would result in graft failure. Please see the references below. Copies of these files have also been added to the attachments section.

Review of prostate cancer bone metastasis models, including intracardiac injection:

Park, S.H., M.R. Eber, and Y. Shiozawa, *Models of Prostate Cancer Bone Metastasis*. Methods Mol Biol, 2019. **1914**: p. 295-308.

Example of our experience with the intracardiac injection model:

Cackowski, F.C., et al., *Mer Tyrosine Kinase Regulates Disseminated Prostate Cancer Cellular Dormancy*. J Cell Biochem, 2017. **118**(4): p. 891-902.

Bioluminescence imaging: Luciferin will be injected intraperitoneally immediately prior to each bioluminescence imaging session. A 28 gauge (or smaller) needle will be inserted into the abdominal cavity and 100 microliters of luciferin will be slowly injected into the intraperitoneal cavity. The needle will then be removed and discarded. Immediately after luciferin injection, the animals will go under anesthesia to allow imaging. They will be placed in an induction box infused with 2% isoflurane in oxygen. After sufficient anesthesia is obtained, they will be transferred to the bioluminescence imager with a nose cone to maintain anesthesia. Images will be obtained for one minute prone and one minute supine. After imaging, they will recover in a cage placed on a heating pad set on "low." Bioluminescence imaging will occur weekly. Tumors will be monitored through this weekly imaging. Once tumors are easily detected by imaging, animals will be euthanized.

BrdU administration: BrdU will be injected intraperitoneally in experiment 2 for detection of proliferative cells. This will occur once on the day after intraventricular injection. A 28 gauge (or smaller) needle will be inserted into the abdominal cavity and BrdU will be slowly injected into the intraperitoneal cavity. The needle will then be removed and discarded. In experiment 2, BrdU will be added to the drinking water. BrdU treated water and tap water will be changed at least every three days.

BAPN administration: BAPN treatment will be injected intraperitoneally the day after intraventricular injection occurs in experiment 4. This will occur for 5 days weekly for up to 8 weeks or until tumor detection occurs. A 21 gauge (or smaller) needle will be inserted into the abdominal cavity and BAPN will be slowly injected into the intraperitoneal cavity. The needle will then be removed and discarded.

Doxycycline administration: Doxycycline will be added to the food pellets in experiments 1, 2, 3, 6, and 7. In experiment 2, all animals will receive the doxycycline diet as well as BrdU treated water. The doxycycline diet will contain 625 mg/kg of doxycycline which is expected to deliver a daily dose of 2-3 mg of doxycycline based on consumption of 4-5 g/day by a mouse. Animals will remain on the doxycycline diet and BrdU treated water until tumor detection occurs. Doxycycline treated pellets will be changed at least once weekly.

2. How will the animals be monitored for adverse effects? Describe any likely effects.

The most dangerous procedure in this protocol is the intracardiac injections. However, the PI is very experienced with these and typically has > 90% of animals without morbidity or mortality. If complications do occur they typically follow one of two patterns: 1. Animals do not awake from anesthesia - possibly due to bleeding or 2. Focal neurological deficits arise - possibly due to embolic stroke. In addition to monitoring immediately after the procedure, the mice will be examined in 2 hrs and the morning after the procedure. Any mice displaying neurologic deficits will be euthanized - as these deficits do not typically improve. Complications do not typically arise more than one day after the procedure until tumors begin to form several weeks later. Therefore, the mice will be examined for signs of tumor formation 3x per week. We plan to euthanize animals once tumors are easily detected by imaging; i.e. these are not survival studies. The use of imaging will permit the detection of experimental endpoints (tumor formation) that precede the development of significant clinical signs that would otherwise result in morbidity, moribundity, or mortality. Mice are expected to be asymptomatic at endpoint, but any mice that exhibit tumor burden symptoms will be euthanized. Tumor burden symptoms include significant weight loss or decreasing body condition, hunched posture or unkempt appearance, neurological symptoms, difficulty with ambulation that might interfere with food or water acquisition, or ulceration or necrosis of visible tumors. If necessary we will administer carprofen for any signs of pain either from the injection or from tumor formation.

Metastasis is expected to be observed in the distal femur, proximal tibia, mandible, vertebrae, adrenal gland, mediastinum, and lungs.

For all procedures requiring anesthesia, the mice will be monitored until complete neurologic recovery. Occasionally mice might receive excess anesthesia and not recover. However, this has not been a major problem in our past experience.

July 02, 2021

**Wayne State University
INSTITUTIONAL ANIMAL CARE AND USE COMMITTEE (IACUC)
Animal Research Protocol**

Protocol #
IACUC-20-07-2485

Protocol Title: The Hippo pathway in prostate cancer dormancy and recurrence
Protocol Type: IACUC
Approval Period: Draft
Important Note: This Print View may not reflect all comments and contingencies for approval. Please check the comments section of the online protocol.

Decreased water and food consumption may occur in groups with BrdU treated water or doxycycline treated food pellets. Body weight and general health will be monitored to ensure adequate food/water intake. A veterinarian will be consulted if significant weight loss or dehydration occur.

Anesthetic Agents

Species	Procedure Title	Agent	Dosage (in mg/kg if possible)	Route
Mouse	Bioluminescence	Isoflurane	Concentration of 2-5% isoflurane	Inhalation (INH)
Mouse	Injection of tumor cells	Isoflurane	Concentration of 2-5% isoflurane	Inhalation (INH)

Analgesic Agents

Species	Procedure Title	Agent	Dosage (in mg/kg if possible)	Route
Mouse	Injection of tumor cells	Carprofen	5 mg/kg	Subcutaneous (SQ)

Other Agents

Species	Procedure Title	Agent	Dosage (in mg/kg if possible)	Route
Mouse	Addition of BrdU to water	Other - Bromodeoxyuridine (BrdU)	1 mg/kg	Other (OTH) - 1 mg/kg BrdU will be offered in drinking water
Mouse	Addition of doxycycline to food pellets	Other - Doxycycline	625 mg/kg	Other (OTH) - 625 mg/kg doxycycline will be offered in food pellets
Mouse	Injection of BAPN	Other - Beta-aminopropionitrile (BAPN)	100 mg/kg	Intraperitoneal (IP)
Mouse	Injection of BrdU	Other - Bromodeoxyuridine (BrdU)	100 mg/kg	Intraperitoneal (IP)
Mouse	Injection of luciferin	Other - Luciferin	150 mg/kg	Intraperitoneal (IP)
Mouse	Injection of tumor cells	Other - Tumor cells	500,000 cells	Other (OTH) - Intracardiac (left ventricle)

Indicate what parameters will be used to determine the need for additional doses of anesthesia.

The isoflurane concentration will be increased if there is a response to a toe or tail pinch after the initial administration of isoflurane. Isoflurane will be administered at a concentration of 2-5% for induction and at 0.5%-2.0% for maintenance of general anesthesia.

3. Post-Anesthetic Care of Rodents

Review and affirm the Post Operative/ Post Anesthetic Care of Rodents in the Guidelines section. If it will not be followed then the variance must be justified in that section.

4. Post-Anesthetic Care of Non-Rodents

Describe supportive care and monitoring provided during immediate anesthetic recovery period (from cessation of anesthesia until sternal recumbency is regained) and intermediate recovery period (from sternal recumbency until the animal is able to walk).

--

July 02, 2021

Wayne State University
INSTITUTIONAL ANIMAL CARE AND USE COMMITTEE (IACUC)
Animal Research Protocol

Protocol #
IACUC-20-07-2485

Protocol Title: The Hippo pathway in prostate cancer dormancy and recurrence
Protocol Type: IACUC
Approval Period: Draft
Important Note: This Print View may not reflect all comments and contingencies for approval. Please check the comments section of the online protocol.

July 02, 2021

Wayne State University
INSTITUTIONAL ANIMAL CARE AND USE COMMITTEE (IACUC)
Animal Research Protocol

Protocol #
IACUC-20-07-2485

Protocol Title:	The Hippo pathway in prostate cancer dormancy and recurrence
Protocol Type:	IACUC
Approval Period:	Draft
Important Note:	This Print View may not reflect all comments and contingencies for approval. Please check the comments section of the online protocol.

*** * * Surgery Relationships * * ***

1. Will this project include multiple survival surgeries on the same animal? N

1a. Multiple survival surgeries will be conducted on an animal, review the Multiple Survival Surgeries Policy and provide justification below.

2. Will this project include multiple major survival surgeries on the same animal?

3. Describe the sequence and timing of the surgeries and how they relate to each other. If multiple surgeries will be conducted on some or all of the animals use enough details to allow the reviewers to understand what each animal will undergo.

July 02, 2021

**Wayne State University
INSTITUTIONAL ANIMAL CARE AND USE COMMITTEE (IACUC)
Animal Research Protocol**

Protocol #
IACUC-20-07-2485

Protocol Title: The Hippo pathway in prostate cancer dormancy and recurrence
Protocol Type: IACUC
Approval Period: Draft
Important Note: This Print View may not reflect all comments and contingencies for approval. Please check the comments section of the online protocol.

*** * * Schedule of Procedures * * ***

Schedule of Procedures

Species	Procedure Title	Procedure Type	Pain Category
Mouse	Addition of BrdU to water	Addition of Agents to Food or Water Supply	C
Mouse	Addition of doxycycline to food pellets	Addition of Agents to Food or Water Supply	C
Mouse	Injection of BAPN	Administration of Study Drugs, Hormones, Chemicals, or Cytotoxic Substances	C
Mouse	Injection of BrdU	Administration of Study Drugs, Hormones, Chemicals, or Cytotoxic Substances	C
Mouse	Injection of luciferin	Administration of Study Drugs, Hormones, Chemicals, or Cytotoxic Substances	C
Mouse	Bioluminescence	Imaging / Scans (CAT, MRI, MRS, PET, etc.)	D
Mouse	Injection of tumor cells	Tumor Transplantation (non-surgical)	D

Schedule of procedures for experimental groups: State or list in chronological order all procedures for each experimental group, their frequency, and time points over the course of the experiment. Details of each procedure are to be described in the appropriate sections, NOT here. A diagram or chart may be helpful to explain complex designs, which can be added in the "Attachments" tab above.

Please see the following attachments:

- Experiment 1 Chronological Order
- Experiment 2 Chronological Order
- Experiment 3 Chronological Order
- Experiment 4 Chronological Order
- Experiment 5 Chronological Order
- Experiment 6 Chronological Order
- Experiment 7 Chronological Order

Details for each procedure can be found in previous sections.

July 02, 2021

**Wayne State University
INSTITUTIONAL ANIMAL CARE AND USE COMMITTEE (IACUC)
Animal Research Protocol**

Protocol #
IACUC-20-07-2485

Protocol Title: The Hippo pathway in prostate cancer dormancy and recurrence
Protocol Type: IACUC
Approval Period: Draft
Important Note: This Print View may not reflect all comments and contingencies for approval. Please check the comments section of the online protocol.

*** * * Euthanasia * * ***

1. **STATE the SPECIFIC CRITERIA for the euthanasia of abnormal or moribund animals (assume someone may have to euthanize animals IN YOUR ABSENCE). Review the Defining Humane Endpoints and End-stage Illness Guideline.**

Not Applicable (e.g. animals are used for tissue harvesting only and will not undergo any procedures prior to death)

- X Weight loss of 20% or more
 X Other conditions (examples may include, but are not limited to: a clinical condition that does not respond to treatment, such as an infected surgical site; any condition that a veterinarian deems severe enough to warrant euthanizing the animal). Please describe below:

Neurologic deficits (suspected stroke) after intracardiac injection. Any mice displaying neurological deficits will be euthanized - as these deficits do not typically improve. Complications do not typically arise more than one day after the procedure until tumors begin to form several weeks later. Therefore, the mice will be examined for signs of tumor formation 3x per week. We plan to euthanize animals once tumors are easily detected by imaging. Tumor growth is expected around 30-60 days post injection.
 Mice are expected to be asymptomatic at endpoint (including models studying metastasis), but any mice that exhibit tumor burden symptoms will be euthanized. Tumor burden symptoms include significant weight loss or decreasing body condition, hunched posture or unkempt appearance, neurological symptoms, difficulty with ambulation that might interfere with food or water acquisition, or ulceration or necrosis of visible tumors.
 Any condition that a veterinarian deems severe enough to warrant euthanizing the animal.

PHS Policy on Humane Care and Use of Laboratory Animals requires the IACUC to use the recommendations of the AVMA Guidelines for the Euthanasia of Animals: 2020 Edition; please refer to it when necessary. If anesthetic overdose or CO2 narcosis is used, a secondary procedure such as bilateral pneumothorax, severing the aorta, or removal of a critical organ must be used to assure that the animal will not recover.

Euthanasia

Species	Mouse
Primary Method of Euthanasia	Carbon dioxide
Route of Administration	Inhalation (INH)
Dosage (in mg/kg if possible)	Gradual fill method with a displacement rate from 10-30% of the chamber volume/min
Secondary Method of Euthanasia	Thoracotomy

2. **Is the method consistent with the AVMA Guidelines for the Euthanasia of Animals: 2020 Edition**

Y

If no, please provide scientific justification for the use of the method below.

3. **Who will be responsible for performing euthanasia?**

Personnel Details

Personnel Responsible

Name* Zielske, Steven

Does this person have prior experience performing this/these method(s) of euthanasia in this species?* Y

If no, describe the training plan to assure proficiency.

Personnel Responsible

Name* Cackowski, Frank

Does this person have prior experience performing this/these method(s) of euthanasia in this species?* Y

If no, describe the training plan to assure proficiency.

July 02, 2021

Wayne State University
INSTITUTIONAL ANIMAL CARE AND USE COMMITTEE (IACUC)
 Animal Research Protocol

Protocol #
 IACUC-20-07-2485

Protocol Title: The Hippo pathway in prostate cancer dormancy and recurrence
Protocol Type: IACUC
Approval Period: Draft
Important Note: This Print View may not reflect all comments and contingencies for approval. Please check the comments section of the online protocol.

Personnel Responsible

Name*

Ibrahim, Kristina

Does this person have prior experience performing this/these method(s) of euthanasia in this species?*

N

If no, describe the training plan to assure proficiency.

Kristina will be trained by Drs. Cackowski and Zielske until she is proficient. She will be observed after teaching to ensure she demonstrates consistent and accurate technique.

4. **Does this research include the euthanasia of mouse and/or rat fetuses and neonates?** N
 Review and affirm the Euthanasia of Mouse and Rat Fetuses and Neonates in the Guidelines section. If it will not be followed then the variance must be justified in that section.
5. **Will all animals be euthanized at the end of this study?** Y
 If no, state their final disposition:

July 02, 2021

**Wayne State University
INSTITUTIONAL ANIMAL CARE AND USE COMMITTEE (IACUC)
Animal Research Protocol**

Protocol #
IACUC-20-07-2485

Protocol Title: The Hippo pathway in prostate cancer dormancy and recurrence
Protocol Type: IACUC
Approval Period: Draft
Important Note: This Print View may not reflect all comments and contingencies for approval. Please check the comments section of the online protocol.

***** Attachments *****

Document Type	Attachment(s)	Document Name	Attached Date	Submitted Date
Funding/Grant Proposal	TechAbs Narrative Refs	TechAbs Narrative Refs	07/23/2020	07/27/2020
Other, supplemental information	Meth Mol Bio 2019	Meth Mol Bio 2019	08/13/2020	08/13/2020
Other, supplemental information	J Cell Biochem 2017 MERTK	J Cell Biochem 2017 MERTK	08/13/2020	08/13/2020
Explanatory Diagram	Experiment 1 Chronological Order	Experiment 1 Chronological Order	09/09/2020	09/10/2020
Explanatory Diagram	Experiment 2 Chronological Order	Experiment 2 Chronological Order	09/09/2020	09/10/2020
Explanatory Diagram	Experiment 3 Chronological Order	Experiment 3 Chronological Order	09/09/2020	09/10/2020
Explanatory Diagram	Experiment 4 Chronological Order	Experiment 4 Chronological Order	09/09/2020	09/10/2020
Explanatory Diagram	Experiment 5 Chronological Order	Experiment 5 Chronological Order	09/09/2020	09/10/2020
Explanatory Diagram	Experiment 6 Chronological Order	Experiment 6 Chronological Order	09/09/2020	09/10/2020
Explanatory Diagram	Experiment 7 Chronological Order	Experiment 7 Chronological Order	09/09/2020	09/10/2020
Other, supplemental information	Email Communication	Email Communication	09/10/2020	09/10/2020
Other, supplemental information	A reliable murine model of bone metastasis by injecting cancer cells through caudal arteries	A reliable murine model of bone metastasis by injecting cancer cells through caudal arteries	09/10/2020	09/10/2020
Other, supplemental information	ApprovalLetter_IBC	ApprovalLetter_IBC	09/30/2020	09/30/2020
Husbandry Documents	ahafii_form	ahafii_form	09/30/2020	09/30/2020
Husbandry Documents	ahaf-chemical	ahaf-chemical	10/06/2020	10/06/2020

Protocol Title: The Hippo pathway in prostate cancer dormancy and recurrence
Protocol Type: IACUC
Approval Period: **Draft**
Important Note: This Print View may not reflect all comments and contingencies for approval. Please check the comments section of the online protocol.

Disclaimer: The generated PDF may not duplicate the original format completely. We do not warrant the accuracy of the changed format.

***** Attached Document *****

Document Name	Created Date
TechAbs Narrative Refs.pdf	01/05/2021

TECHNICAL ABSTRACT: “Regulation of Prostate Cancer Dormancy and Recurrence by Hippo Signaling”

BACKGROUND and PRELIMINARY DATA: Prostate cancer disseminated tumor cells (DTCs) are thought by many investigators to display a dormant phenotype and to act as an important reservoir for distant recurrence after curative intent surgery or radiation – which makes the disease incurable^{5,15-18}. To identify additional dormancy regulators, we analyzed the TCGA dataset of localized PCa samples and found that expression of hippo signaling pathway components correlates with *MAPK14* (p38 MAPK), which has been shown to regulate dormancy in multiple studies^{7-9,15,19}. We also found that the hippo pathway was differentially expressed between G0 and G1 PCa cells and between DTCs vs. macroscopic tumors. We subsequently found in the TCGA data that high expression of TAZ (which is negatively regulated by the hippo pathway) correlated with early biochemical recurrence, the clinical manifestation of dormancy escape. In cell lines, we inhibited the TAZ paralog *YAP1* and observed G0 arrest. Critically, in mice, *YAP1* knockdown prevented PCa growth after left ventricular injection, confirming the importance of the pathway for the growth of DTCs.

RESEARCH PLAN: Based on these preliminary studies, we hypothesize that; **inhibition of hippo signaling or YAP1 and TAZ activation stimulates dormancy escape in PCa.**

Aim 1: *Determine which hippo pathway components stimulate or inhibit dormancy escape in vivo.* **(1A):** We will first examine human PCa primary tumor tissue microarrays (TMAs) and the corresponding patient data to compare nuclear level of YAP1 and TAZ to biochemical recurrence free survival. **(1B):** Our preliminary results establish a role for hippo signaling in regulation of PCa recurrence. However, it remains unclear which pathway components specifically regulate PCa escape from dormancy at metastatic sites. To address this question, we will inducibly express *wild type*, constitutively active, or dominant negative mutants of hippo pathway components and measure tumor formation after metastasis in a mouse xenograft model of PCa recurrence.

Aim 2: *Delineate how tissue mechanics regulate PCa dormancy through the hippo pathway.* We find that mechanical properties such as extra-cellular elasticity can regulate hippo signaling in PCa cells, which often metastasize to the bone and enter dormancy. Yet, it is unknown how tissue mechanics at metastatic sites affect PCa dormancy, and which cytoskeletal cues might be responsible for dormancy *in vivo*. **(2A):** We will examine how changes in substrate stiffness alter PCa cell cycle entry using innovative acoustic tweezing cytometry²⁰ and culture on stiff vs. pliable substrates. We will examine the role of bone matrix stiffness on PCa dormancy *in vivo*, by modulation of lysyl oxidase²¹. **(2B):** We will determine if cellular mechanics regulate PCa dormancy through the actin cytoskeleton using inhibitors of f-actin and the small GTPase RHOA.

Aim 3: *Investigate how non-coding RNAs regulate PCa dormancy escape through the hippo pathway.* Canonical hippo regulation occurs through protein localization and stability, but newer work is beginning to reveal modulation of hippo components through mRNA stability²²⁻³⁴. We found that a non-coding RNA reported to regulate hippo signaling, *SNHG1*²⁹, was also strongly correlated with early PCa biochemical recurrence. **(3A):** We will determine the effect of knockdown and over-expression of *SNHG1* on the cell cycle and on hippo signaling in PCa cells. **(3B):** We will then inducibly excise *SNHG1* and evaluate the fraction of quiescent (G0) cells and time to recurrence *in vivo*.

PERSONNEL: Frank Cackowski, PI. As a PCa physician scientist I aim to understand the biology of PCa DTCs and develop treatments to eradicate cancer from PCa patients with a temporarily low disease burden, but ultimately lethal disease. To do this, I will gain independence through active mentorship by the following team members, followed by the expected contributions for each: Evan T. Keller, Primary Mentor; bone microenvironment, single cell studies, overall career guidance, Russell S. Taichman, Co-Mentor; Dormancy, microenvironment, communication, career development, Laura Buttitta, Co-Mentor; Cell cycle studies, hippo signaling, genome editing techniques. Todd M. Morgan, Co-Mentor; DTCs, biomarkers, clinical context, therapeutic application, Jianping Fu, Consultant; Hippo signaling especially in relation to mechanical regulation, Arul Chinnaiyan, Consultant; Hippo signaling, non-coding RNAs, analysis of multi ‘omics data.

IMPACT: Successful completion of these studies will determine how the hippo pathway regulates DTCs to cause PCa dormancy maintenance vs. escape and subsequent distant recurrence – which is uniformly fatal. Therefore, these studies directly address the Overarching Challenge; “Define the biology of lethal PCa to reduce death.” Successful completion of these studies will also directly lead to subsequent work which will address the Overarching Challenge; “Develop treatments that improve outcomes for men with lethal PCa” because the results of these studies can be used to develop treatments to prevent PCa relapse.

NARRATIVE: “Regulation of Prostate Cancer Dormancy and Recurrence by Hippo Signaling”

Principal Investigator: Frank Cackowski, MD, PhD. I am a Clinical Lecturer, physician-scientist, and medical oncologist at the University of Michigan Rogel Cancer Center Genitourinary Oncology Clinic. My long term career goal is an independent academic career, which will continue to focus the majority of my effort on laboratory based research in prostate cancer (PCa) dormancy and recurrence with a smaller portion of my time spent in clinical care of patients with PCa. I expect my research work to be essential for my colleagues and I to develop treatment strategies to prevent PCa recurrence. During the course of this award, I will gain skills used to interrogate signaling of disseminated tumor cells including modulation by mechanical forces, communication and managerial skills and launch my successful independent career. In addition to the skills gained from this award, the salary support will ensure that I have adequate protected research time to allow my success.

Primary Mentor: Evan T. Keller, DVM, PhD. Dr. Keller is a PCa laboratory researcher and Univ. of Michigan Prof of Urology and has mentored over 35 trainees at various levels. Several of his trainees have developed their own research program in academia and progressed from Assistant Professors through Full Professors at various institutes, including: Zheng Fu, Associate Professor, Virginia Commonwealth University; Dr. Peter Smith, Associate Professor, Yale; Jian Zhang Professor, Guangxi Medical University. Dr. Keller has been continuously NIH-funded for over 20 years. He is PI of a highly competitive NCI-funded Program Project (P01, now in year 15) focused on PCa Skeletal Metastasis, Co-director of the Cancer Center Urologic Oncology Program and Co-director of the Single Cell Sequencing Core at The University of Michigan Rogel Cancer Center. He currently has a project in the Prostate Cancer SPORC and is PI on an R01, and CoI on another R01. He plans to meet with Dr. Cackowski weekly to review data and planned experiments. Dr. Keller expects to be particularly involved with single cell analysis, bone tumor models, and coaching on communication skills.

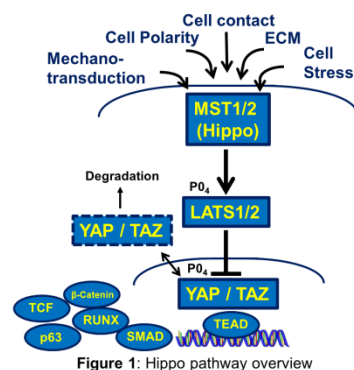
Co-Mentor: Russell S. Taichman, DMD, DMSc. Dr. Taichman was Dr. Cackowski’s primary mentor until recently when he accepted the position of Dean of the Dentistry at Univ. of Alabama at Birmingham. Although they will soon be separated geographically, he will continue to play an active role in Dr. Cackowski’s mentorship and will Skype with him weekly. Dr. Taichman has over 20 years of experience in PCa research, much of which has been focused on dissemination to bone marrow, dormancy and stemness. Current funding includes a Challenge Award from the Prostate Cancer Foundation, and as PI for one of the projects on the P01 chaired by Dr. Keller. Among his many trainees are the other Co-Mentor for this application, Dr. Todd Morgan, Dr. Yusuke Shiozawa, Assistant Professor at Wake Forest University and DoD Idea Award recipient, and Dr. Ann Decker, previously a resident and graduate student and recently appointed to the University of Michigan Dental School Faculty. In recognition of his mentorship efforts, Dr. Taichman received the University of Michigan Institute for Clinical & Health Research Distinguished Mentor Award in 2016.

Co-Mentor: Todd M. Morgan, MD. Dr. Morgan is a urologic oncology surgeon, translational researcher and Associate Professor of Urology at the University of Michigan. He is also proud to be a previous recipient of the DoD PCRP Physician Research Award. He directs projects focused on identifying meaningful biomarkers in genitourinary malignancies; in particular (CTCs) and disseminated tumor cells (DTCs) in men with PCa. Current funding includes Co-I on the P01 chaired by Dr. Keller, site PI for an R01, and multiple foundation grants and industry partnerships. His most recent R01 application was competitively score at NCI with a funding decision pending. Dr. Morgan has been involved with Dr. Cackowski’s training since shortly after he joined Dr. Taichman’s laboratory in 2015. This began with serving on his research mentoring committee as a fellow. He plans to continue to meet with Dr. Cackowski weekly. Several of his prior mentees have now been promoted to Assistant Professor including Drs; Tudor Borza (Univ of Wisconsin), Simpa Salami (Univ. of Michigan), Paul Womble (Eastern VA Medical School), and Takahiro Osawa (Hokkaido Univ.).

RESEARCH PROJECT - BACKGROUND: Approximately 2/3 of the deaths from prostate cancer (PCa) result from recurrence after initial curative intent surgery or radiation – about 20,000 men in the U.S. per year^{1,2}. Therefore, an improved understanding of the biology of PCa recurrence and strategies to prevent it are critically needed. Some cancers, especially PCa and ER⁺ breast cancer, have the potential to recur years or even decades after initial treatment⁶. This clinical observation suggests that cancer cells spread early in the disease process, lie dormant, and then escape from dormancy to cause fatal distant metastases¹⁹. The cells which spread early from the primary tumor to distant sites are termed disseminated tumor cells (DTCs) or disseminated cancer cells (DCCs) and are thought to start growing at the sites where metastases are later detected clinically – often bone

for PCa patients. Therefore, DTCs from localized PCa patients have most often been studied in the bone marrow because of this metastasis pattern and likely because patient bone marrow samples are more easily obtained than specimens from other tissues (excepting blood). I recently reviewed the literature on detection of DTCs from bone marrow of patients with localized PCa⁵ and developed novel methods for the detection and isolation of viable DTCs from localized PCa patients, which is currently submitted for publication¹⁷. Now that we can isolate DTCs, I am focused on finding the mechanisms that regulate their escape from dormancy. As described below, I arrived at the Hippo signaling pathway as a dormancy regulator by three independent approaches.

The Hippo pathway was delineated relatively recently (2003) in the history of biomedical research¹¹, yet interest in this pathway has increased exponentially with 2620 PubMed citations as of this writing. The core of the pathway consists of upstream “hippo” kinases; MST1 & MST2 (STK3), their targets the LATS kinases; LATS1 & LATS2, which in turn inhibit the activity of transcriptional co-activator orthologous proteins YAP1 and TAZ through phosphorylation (**Figure 1**). The hippo pathway lacks a cell membrane receptor, and instead integrates multiple potential upstream inputs, many of which concern cell-cell contact, extracellular matrix and tissue mechanics³⁵. YAP1 and TAZ, the hippo pathway effectors are transcriptional co-activators that complex predominantly with transcription factors of the TEAD family, but also can bind SMADs, TCFs and others. Hippo signaling impacts cell proliferation, survival, and adhesion leading to extensive work on this pathway in the field of cancer biology, most often in the areas of tumorigenesis and treatment resistance^{12,13}. Although it is not commonly altered at the DNA level, the hippo pathway has recently been shown to be involved in PCa³⁶⁻³⁸.



However, it has no known role in dormancy regulation in prostate or other cancers. Here we take advantage of our experience in studying PCa dormancy to explore a likely role for the hippo pathway in regulation of PCa recurrence specifically after cells have arrived at metastatic sites as discussed in the experimental plan below.

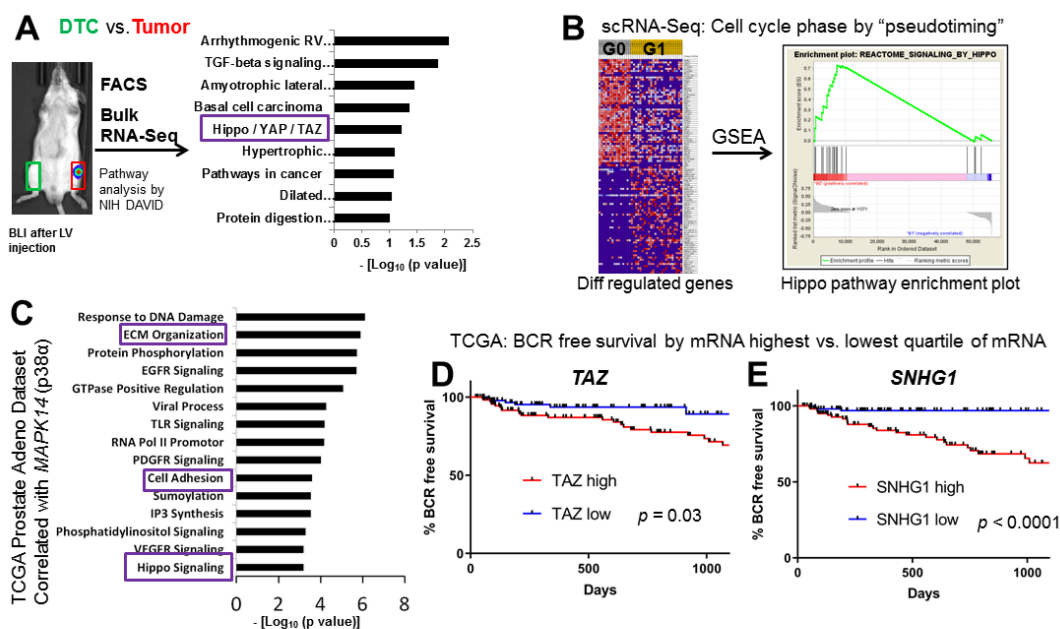


Figure 2: Data suggesting a role for the hippo pathway in regulation of PCa recurrence. (**A**) Du145 PCa cells were isolated by FACS from bones either with or without and compared by bulk RNA-Seq followed by KEGG pathway analysis using NIH DAVID software. (**B**) Single cell RNA-Seq data was acquired from non-synchronized C42B cells and used to predict the cell cycle phase of each cell by pseudotiming. Whole transcriptome data of cells predicted to be in G0 vs. G1 was compared by GSEA analysis. (**C**) Expression data from the TCGA Prostate Adenocarcinoma dataset was used to perform NIH DAVID software gene ontology analysis of the 500 genes with expression most correlated with MAPK14 (p38 MAPK). (**D,E**) TCGA Prostate Adenocarcinoma dataset gene expression and outcomes data used to compare biochemical recurrence (BCR) free survival in patients in the top vs. bottom quartiles of TAZ mRNA (**D**) or SNHG1 mRNA (**E**).

PRELIMINARY DATA: To identify novel mechanisms for PCa dormancy regulation, we injected SCID mice with PCa Du145 xenografts in the left ventricle and serially imaged them for tumor formation using bioluminescence (BLI) (**Figure 2A**). To compare cancer cells in a dormant “DTC-like” environment vs. a “tumor like” environment, we used FACS to isolate tumor cells from paired bones from two mice either with or without tumor detectable by BLI. We compared DTCs and macroscopic tumor cells by bulk cell RNA-Seq and performed pathway analysis using NIH DAVID software and found the hippo pathway to be one of the top differentially expressed pathways. Next, we adapted bioinformatics methods to predict cell cycle phase from single cell PCa RNA-Seq data – an approach we refer to as cell cycle-pseudotiming^{39,40} (**Figure 2B**). We

performed GSEA analysis of C42B cells predicted by pseudotiming to be in either the G0 vs. G1 phase and found that hippo signaling was the sixth most differentially expressed pathway. Next, we used the TCGA Prostate Adenocarcinoma Dataset to examine gene expression data from 489 untreated primary prostate tumors for genes co-expressed with *MAPK14* (p38 MAPK), a kinase with a well-established role in dormancy regulation for prostate and other cancers^{7-9,15,19} (**Figure 2C**). After gene ontology analysis using NIH DAVID software, we again found the hippo pathway to be one of the top differentially expressed groups. We then mapped individual patient outcomes data back to the TCGA gene expression data to determine if expression of hippo pathway components was correlated with time to biochemical recurrence (BCR). Importantly, we found that high expression of the Hippo pathway effector TAZ is correlated with statistically significantly shorter BCR free survival (**Figure 2D**). We also used this valuable dataset to look for novel modes of hippo pathway regulation in PCa dormancy. We examined several non-coding RNAs reported to regulate hippo signaling in other disease contexts²²⁻³⁴ and identified the long non-coding RNA *SNHG1*, to be significantly correlated with cancer recurrence (**Figure 2E**). *SNHG1* has been reported to increase YAP1 transcription but has no known role in dormancy regulation and is the subject of only two primary investigations in PCa^{29,41,42}.

Next, we experimentally tested the role of the hippo pathway in PCa dormancy regulation through cell cycle analysis *in vitro* and metastasis free

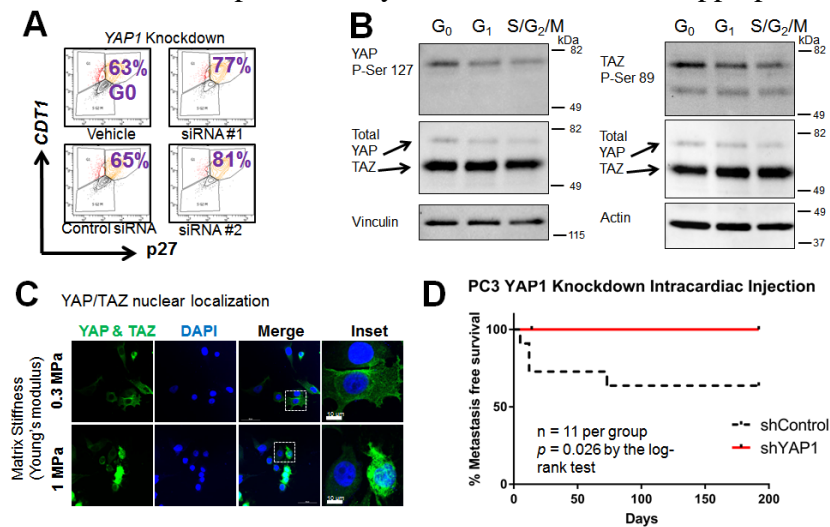


Figure 3: Experimental manipulation of the hippo pathway supports a role in PCa dormancy regulation. (A) PC3 cells containing reporters for p27 (Venus) and CDT1 (mCherry) transfected with siRNA against YAP1 and analyzed by flow cytometry – with dual positivity indicating G0. (B) PC3 cells were FACS sorted by cell cycle phase using the Venus-Cherry reporters and western blotted for inactivating phosphorylations of YAP1 or TAZ. (C) PC3 cells cultured on fibronectin coated matrices of the indicated stiffness and IF labeled with an antibody recognizing YAP1 and TAZ. (D) YAP1 was stably knocked down in luciferase labeled PC3 cells. Metastasis free survival was analyzed for tumors detected by serial bioluminescence imaging.

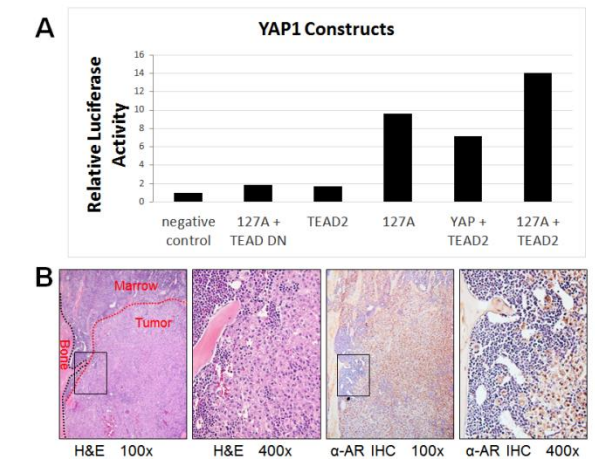


Figure 4: Tools developed for dormancy analysis: (A) Initial expression of the constructs used for hippo pathway analysis in 293T cells. Luciferase activity indicates YAP/TAZ signaling and is derived from a TEAD binding luciferase construct. (B) Bone metastases after left ventricle injection of parental FVB Myc-CaP cells are stained with H&E or IHC for androgen receptor to identify the cancer cells.

survival analysis after left ventricular injection of PC3 cells into SCID mice. For some of these analyses, we used “Venus-Cherry” PCa cell lines with fluorescent reporters to indicate cell cycle phase; p27 conjugated to venus and CDT1 conjugated to mCherry. With these reporters, dual positivity indicates G0, mCherry single positive indicates G1, and dual negative indicates S, G2 or M phases. We first found that *YAP1* siRNA silencing increased the percentage of cells in G0 – which conversely is consistent with promotion of dormancy escape and cell cycle progression by YAP1 activity (**Figure 3A**). We also used these reporters to sort cells by cell cycle phase and subsequently western blotted for the inactivating phosphorylations of YAP1 and TAZ. We found increased phosphorylated and inactive YAP1 and TAZ in G0 cells (**Figure 3B**). Because matrix stiffness is reported to induce YAP/TAZ activity and nuclear localization, we cultured PC3 cells on fibronectin coated silicone of varying stiffness and found YAP/TAZ nuclear localization induced by the stiffer substrate (**Figure 3C**). Lastly, we stably knocked down *YAP1* by shRNA in PC3 cells and found it prevented tumor formation after intra-cardiac injection (**Figure 3D**). All of this data is consistent with Hippo signaling promoting dormancy and upregulation of YAP/TAZ activity leading to dormancy escape.

We have developed tools to analyze the role of Hippo signaling in PCa dormancy. We have acquired wild-type and dominant negative inducible YAP1 and TEAD constructs and confirmed they modulate a Hippo pathway reporter. (**Figure 4A**). Also, to develop a AR-dependent, immune-competent model of PCa bone dissemination we have found that the Myc-CaP cell line⁴³ forms bone metastases after left ventricle injection, confirmed tumor cell identity by IHC for AR (**Figure 4B**).

EXPERIMENTAL DESIGN: From existing literature and our preliminary data, we have developed the following **Central Hypothesis: inhibition of hippo signaling or YAP1 and TAZ activation stimulates dormancy escape in PCa**. Subsequent hypotheses will be tested in the following specific aims (Figure 5).

Specific Aim 1: Determine which hippo pathway components stimulate or inhibit dormancy escape in vivo.

Rationale: Our bulk RNA-Seq from a xenograft model, single cell RNA-Seq and analysis of TCGA data all highlighted differential expression of the hippo pathway. Further, our knock down of *YAP1* caused quiescence *in vitro* and prevented growth of DTCs *in vivo*. However, which hippo pathway member(s) are predominantly responsible for our observations remains poorly defined. Here we will determine if protein level and localization of the hippo pathway downstream transcriptional co-activators YAP1 and TAZ predicts time to biochemical recurrence in patients, using tissue microarray samples from the Prostate Cancer Biorepository Network (1A). Next we will use inducible mutants of individual hippo pathway components to study the regulation of distant relapse by hippo signaling after cells have had time to home to metastatic sites (1B).

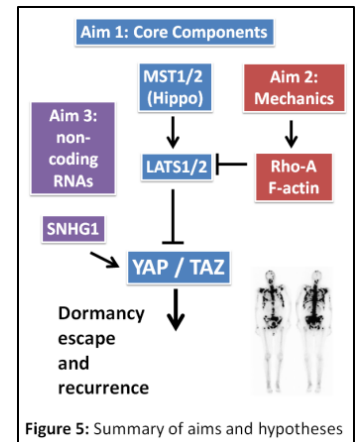
Sub-aim 1A: Primary prostate tumor YAP/TAZ nuclear localization and time to recurrence.

Using existing prostate tissue from a rapid autopsy (currently in our possession) we will first optimize dual immunofluorescence methods for PSA to prostate epithelial and cancer cells (Abcam #140337) paired with an antibody specific to either YAP1 (Abcam #52771) or TAZ (Abcam #242313). General immunofluorescence methods will be as in our preliminary data and as we previously reported except that no decalcification is required^{44,45}. After establishing immunofluorescence protocols, we will label YAP1 and TAZ separately along with PSA on the tissue microarray “726 Case PSA Progression TMA” from the Prostate Cancer Biorepository Network. We will identify PCa cells as PSA positive cells in morphologically abnormal glands and score the percentage of cancer cells with predominantly nuclear YAP1 or TAZ for each patient. We will then use the accompanying clinical data in Kaplan Meier analyses of BCR free survival in patients with >50% YAP1 or TAZ nuclear localization vs. patients with <50% YAP1 or TAZ nuclear localization.

Sub-aim 1B: Determine which core hippo pathway genes regulate dormancy at distant metastatic sites.

Sub-aim 1B-1; Importance of downstream co-activators YAP1 vs. TAZ: Initial studies for this sub-aim will focus on the transcriptional co-activators *YAP1* and *TAZ*. In the preliminary data we showed expression of constructs for; wild type *YAP1*, constitutively active *YAP^{S127A}*, wild type *TEAD2*, dominant negative *TEAD2* (reported as a dominant negative for YAP1 and TAZ) and the 8xGT-Ilc reporter construct for YAP/TAZ activity⁴⁶⁻⁴⁸. We are currently producing tetracycline inducible cell lines with these mutants by Directional TOPO cloning into the pENTR vector. Because TAZ may also be important, we will next create the analogous tetracycline inducible cell lines in luciferase labeled PC3 (human, castration resistant) or FVB Myc-CaP (mouse, castration sensitive) cells for wild type TAZ and constitutively active *TAZ^{S89A}* constructs using the same system. These *TAZ* mutants are reported and are available from AddGene⁴⁷. We will first confirm the inducible expression and *in vitro* phenotype of the inducible constructs. We will collect lysates from cells cultured with or without 1 µg/ml tetracycline for two days and then examine transgene expression level by both qRT-PCR (cataloged Taqman primer/probe mixes from ThermoFisher) and western blotting with a total YAP1 and TAZ dual specific antibody (Cell Signaling Technology #8418). We will also confirm nuclear localization of the constitutively active constructs (*YAP1^{S127A}* and *TAZ^{S89A}*) using the same antibody used for the preliminary data. Then, to determine the effect of these constructs on the cell cycle we will use flow cytometry for both Ki67 (BioLegend antibody #652406 or #350514) or cell cycle phases DAPI for DNA content and a fluorescent conjugated antibody against BrdU incorporated into DNA (BD #552598), as we previously performed⁴⁹.

After validation of constructs, we will determine if YAP1, TAZ or both regulate PCa dormancy and metastatic site relapse in mouse models. We will inject 5×10^5 luciferase labeled PC3 cells stably expressing empty pENTR, constitutively active *YAP1^{S127A}* or *TAZ^{S89A}* into the left ventricle of 20 male CB17 SCID mice per group. We will induce expression of the trans-gene with doxycycline in the drinking water and then image



by bioluminescence (BLI) weekly and evaluate metastasis free survival by Kaplan Meier analysis. This assay is our group's most frequently utilized measure of time to PCa relapse as described previously⁴⁹. To validate our findings from the xenograft model, we will also use our newly developed FVB Myc-CaP immune competent, hormone dependent model of PCa bone metastases. We will perform left ventricle injections of 1×10^6 tdTomato labeled Myc-CaP cells expressing empty vector, or inducible *YAP1*^{S127A} or *TAZ*^{S89A} in 20 mice per group, induce transgene expression with doxycycline the day after injection, and treat the mice with BrdU by intraperitoneal injection and in the drinking water for 7 days for subsequent detection of proliferative cells. After RBC lysis, marrow cells from these mice will be fixed, permeabilized, and labeled with an antibody against BrdU incorporated into DNA (BD #552598). We will identify cancer cells as described in the preliminary data and use the % of BrdU positive cells to indicate the proliferation during the treatment period.

Sub-aim 1B-2; Importance of the hippo pathway kinases: After determining which of the downstream co-activators are important for PCa recurrence, we will examine the four core kinases of the hippo pathway - the "hippo" kinases; *MST1* and *STK3* (*MST2*), and the LATS kinases; *LATS1* and *LATS2*. In addition to dissection of the signaling mechanism, it is important to investigate the upstream kinases for two potentially translational or therapeutic reasons; (1) As enzymes, the kinases are more easily inhibited with drugs than the transcriptional co-activators YAP1 and TAZ, and (2) YAP1 and TAZ can be activated by hippo independent (non-canonical) mechanisms^{50,51}. Because the hippo and LATS kinases negatively regulate YAP1 and TAZ, we will conduct loss of function experiments. We will excise each of the four genes using a tetracycline inducible CRISPR/Cas9 system as reported.⁵² and as applied in the Takara Lenti-X Tet-On 3G CRISPR-Cas9 System. Briefly, Transfected clones will be screened with the Cell1 assay to detect mutations followed by sequencing. Final clones will be verified by qRT-PCR and Western blot. After validation, we will determine the effect gene excision on the cell cycle *in vitro* as described for the *YAP1* and *TAZ* mutants. Subsequently, PC3 GFP-luciferase cells bearing the inducible CRISPR/Cas9 system will be injected in CB17 SCID mice prior to doxycycline treatment. To specifically study effects of excision after arrival of DTCs in the bone marrow niche, mice will be treated continuously with doxycycline starting 1 day after cancer cell inoculation. Kaplan Meier analysis of metastasis free survival will be used to assess dormancy escape.

Statistical Methods (for all 3 aims): Analyses will be conducted with GraphPad or Stata SE software. For *in vitro* studies, data will be first tested for normality using the Shapiro-Wilk test. For normally distributed data, the equal variance, two tailed Student's t-test will be used to compare two groups and one-way ANOVA with Tukey's HSD post-hoc testing will be used for multiple groups. For non-normally distributed data, two groups will be compared with the Mann-Whitney-U test and multiple groups will be compared with the Kruskal-Wallis test. Experiments examining the nuclear localization of YAP or TAZ will be analyzed with Fisher's exact test with a sample size of 150 cells. This sample size calculation presumes 5% type 1 error, 80% power, 0.25 nuclear fraction in the control group, and a two-fold change with genetic manipulation. For survival analyses using the log-rank test, the sample size of 20 per group was calculated using the following parameters; type 1 error 5%, 80% power, 50% of animals in each group, relative hazard 0.25, and no control animals without metastases at the end of the experiment.

Aim 1 Anticipated Results: **Sub-aim 1A:** We expect that high nuclear localization of YAP1 and/or TAZ will significantly correlate with a shorter biochemical recurrence free survival. Based on our preliminary data of TAZ mRNA expression, nuclear TAZ may predict early biochemical recurrence. However, posttranscriptional regulation of YAP1 localization may also drive recurrence. **Sub-aim 1B:** We expect that induction of YAP1 and/or TAZ activity after tumor cell homing to metastatic sites will shorten metastasis free survival. We also expect inducible excision of hippo pathway core kinases to shorten metastasis-free survival.

Aim 1 Potential Pitfalls & Alternative Strategies: We designed this aim to uncover novel roles, thus any outcome will be informative. **Sub-aim 1A:** If problems with immunofluorescence arise, we try alternative antibody clones. If there is a problem with the technical quality of the TMA its self, we could switch to the "235 Case Natural History of PCa" also from PCBN. **Sub-aim 1B:** If there are unmanageable technical problems with the inducible CRISPR/Cas9 system, we will switch to an inducible shRNA system such as Dharmacon SMARTvector. We may encounter "leaky expression" issues with the TET-inducible system. In this case, we will use tamoxifen inducible systems. Because there are two paralogs for each hippo kinase (i.e. two LATS genes and two MST genes) inactivation of one may not be sufficient for a phenotype. If this is the case, we will knock down one paralog with a shRNA and the other with an inducible CRISPR as described.

Rigor and Reproducibility (for all 3 aims): All *in vitro* studies will be carried out using STR fingerprinting verified, mycoplasma free cell lines and three biological replicates each with at least quadruplicate technical replicates for each. Results from a representative experiment will be shown for publication. We will repeat STR fingerprinting and mycoplasma testing yearly. *In vivo* experiments will be analyzed by a blinded observer. Raw data from any large datasets will be deposited in the NCBI GEO Omnibus. All stable cell lines will be available upon request or deposited in AddGene if requests are frequent.

Aim 1 Summary: Successful completion of aim 1 will determine which member(s) of the hippo pathway are important for PCa dormancy escape. This will allow targeting in subsequent pre-clinical or clinical studies.

Specific Aim 2: Delineate how tissue mechanics regulate PCa dormancy through the hippo pathway.

Rationale: The hippo pathway is reported to be regulated by mechanical properties in other settings²⁰, which we confirmed for PCa in our preliminary data. Our preliminary data also shows the ECM and cell adhesion gene groups to be co-expressed with p38 MAPK (*MAPK14*) – a key dormancy regulator^{7,9}. In other normal biology or pathologic contexts, matrix stiffness has been shown to inhibit the hippo pathway by way of actin polymerization, activation of RHOA and other GTPases, inhibition of LATS kinases (hippo pathway inhibition), and activation of YAP and/or TAZ⁵³⁻⁵⁵. Therefore, we hypothesize that cellular mechanics acting through actin cytoskeleton associated proteins are an important upstream regulatory mechanism for PCa dormancy and recurrence regulated by the hippo pathway. We found this hypothesis especially compelling because of the stiffness of bone matrix, and the observation that over 90% of men with fatal metastatic PCa have bone metastases⁵⁶. We have a unique opportunity here at Michigan with Drs. Fu and Deng, to use innovative acoustic tweezing cytometry (ATC) to modulate cell mechanics and study YAP/TAZ activation²⁰.

Sub-aim 2A: Effect of cellular mechanics on the PCa cell cycle and dormancy:

Sub-aim 2A-1; Matrix stiffness, YAP/TAZ activation and cell cycle in PCa cells: We will first expand on our preliminary data showing PCa cell YAP/TAZ nuclear localization in response to culture on stiff PDMS (silicone) fibronectin coated matrix. We will first optimize our IF labeling for antibodies specific to YAP1 (Abcam #52771) or TAZ (Abcam #242313), rather than the YAP/TAZ bi-specific antibody utilized in the preliminary data. In addition to PC3 cells, we will also analyze the human LNCaP and mouse Myc-CaP PCa cell lines. In order to better model dormancy and dormancy escape, we will serum starve the cells for one day before seeding and culture on the fibronectin coated silicone matrixes of varying stiffness for one day in 1% serum media after seeding. In parallel experiments, we will also determine the effect of matrix stiffness on the cell cycle by flow cytometric analyses for Ki67 and DNA content and incorporated BrdU. Lastly, we will determine if YAP1 and TAZ are required for the effects on the cell cycle using two independent methods: (1) *YAP1* or *TAZ* silencing by siRNA as we have previously performed⁴⁹ and (2) culture with or without tetracycline of cells containing the inducible TEAD2 dominant negative construct as described in Specific Aim 1.

Sub-aim 2A-2; Acoustic tweezing cytometry (ATC) and PCa cell cycle: To study mechanical modulation of the cell cycle in real time we will subject serum starved, quiescent PCa cells to control conditions or ATC as described in studies from Dr. Fu and Deng²⁰. For these experiments, we will use PCa cells containing the p27-Venus and CDT1-mCherry (Venus-Cherry) reporters described in the preliminary data to allow identification of cells in either; G0, G1 or the combination of S, G2 and M cell cycle phases. This also allows live cell imaging of phase transitions. First, we will determine which experimental conditions cause YAP1 and TAZ nuclear localization in PC3, LNCaP, and Myc-CaP cells. We will culture on either rigid (1.2 MPa) or soft (1 KPa) substrate and with or without ATC stimulation. We anticipate YAP1 and TAZ nuclear localization to be induced at 5 hours, but will also fix samples (with paraformaldehyde) for YAP1 or TAZ immunofluorescence at 2 hours and 10 hours. Then, after establishing the conditions for YAP1 and TAZ activation, we will perform live cell imaging of PCa cells with the Venus-Cherry reporters. Next, we will perform four color IF fixed cell imaging to compare the cell cycle phase in cells with nuclear YAP1 or TAZ to cells with cytoplasmic YAP1 or TAZ. To allow visualization of the Venus and Cherry reporters on the FITC and Texas Red channels, we will perform immunofluorescence with Alexa 405 Zenon secondary reagents (ThermoFisher #Z25013) and nuclear labeling with far red DRAQ5 (ThermoFisher #62251). Lastly, we will determine if YAP1 or TAZ is required for cell cycle change using siRNA and the TEAD2 dominant negative as described in Sub-aim 2A-1 above.

Sub-aim 2A-3; Matrix stiffness and dormancy escape in vivo: To examine the impact of matrix stiffness on dormancy escape, we will use lysyl oxidase as a modifiable target. This family of enzymes crosslink

collagen, and in so doing increases matrix stiffness. It is a proposed therapeutic target and has been chemically inhibited in a rat orthotopic PCa mode²¹. Overexpression of lysyl oxidase increases colon cancer dissemination and metastasis formation⁵⁷. However, it has never been studied in the context of cancer dormancy. We will first establish methods for modulation of bone mechanical properties in mice using lysyl oxidase inhibitor Beta-aminopropionitrile (BAPN). To verify effectiveness of inhibition, bone will be examined Masson-Trichrome stain (performed by the University of Michigan Dental School histology core). We will also cut thick (50 µm) fresh, frozen sections of femorae from PBS or BAPN treated mice and analyze their mechanical properties using high frequency spectral ultrasound imaging as previously performed by consultant, Dr. Deng⁵³. After validation of the use of the inhibitor, we will perform left ventricle injections of luciferase labeled PC3 cells into SCID mice. Starting the day after injection, the mice will be treated with BAPN. Tumors will be detected with BLI and metastasis free survival will be analyzed by the Kaplan-Meier method as described in Aim 1.

Sub-aim 2B: Role of the actin cytoskeleton associated signaling:

Sub-aim 2B-1; actin skeleton signaling *in vitro* and *ex vivo*: In parallel with the studies in Sub-aim 2A, we will first verify that stiff matrix and ATC causes actin polymerization in parallel with YAP1 or TAZ activation by labeling filamentous actin with phalloidin conjugated to rhodamine (ThermoFisher #R415) or other fluorophores as needed for color compatibility. In the same set of samples, we will also assay RHOA activity using an active Rho detection kit (Cell Signaling Technology #8820). Likewise, we will determine LATS1 and LATS2 activity by Western blotting with a phospho-specific antibody (Abcam #ab111344). We will first determine if general inhibition of actin cytoskeletal dynamics with cytochalasin D (Sigma-Aldrich #C2618) blocks PCa cell cycle change induced by matrix stiffness and measured by flow cytometry for DNA content and BrdU. Then, we will determine if these cell cycle dynamics are blocked by siRNA against *RHOA*. We will test for a role of this pathway in a more physiological model of dormancy escape – our mouse bone explant model as recently published⁵⁸. Using the Venus-Cherry reporters, we will sort G0 phase cells and transiently transfect them with *RHOA* siRNA or control siRNA. We will then inject the cells in bone explants and determine their cell cycle phase two days later using the Venus-Cherry reporters.

Sub-aim 2B-2; Rho-A inhibition and dormancy escape *in vivo*: To complement the *in vivo* studies in aim 2A using the dominant negative construct, we will excise *RHOA* using a tetracycline inducible CRISPR/Cas9 system as described under Sub-aim 1B-2. PC3 GFP-luciferase cells bearing the inducible CRISPR/Cas9 system will be injected in CB17 SCID mice prior to doxycycline treatment. To specifically study the effect of *RHOA* excision after arrival of DTCs in the bone marrow niche, mice will be treated continuously with doxycycline starting 1 day after cancer cell inoculation. Kaplan-Meier analysis of metastasis free survival will be used to assess dormancy escape. To confirm the extent and durability of the *RHOA* excision, tumors from euthanized animals will be evaluated by *RHOA* expression by WB and qRT-PCR.

Anticipated Results: **Sub-aim 2A:** We expect both stiff substrate and ATC to cause YAP1 and /or TAZ nuclear localization and an increase % of cells in the S, G2, and M cell cycle phases. We hypothesize that a stiff bone matrix favors YAP1 or TAZ activation and subsequent dormancy escape. Therefore, we expect that inhibition of collagen cross linking with the lysyl oxidase inhibitor BAPN will delay time to recurrence and increase metastasis free survival. **Sub-aim 2B:** We expect that matrix stiffness and acoustic tweezing will cause formation of filamentous actin and that this will be blocked by cytochalasin D or *RHOA* silencing to inhibit cell cycle entry. Similarly, we expect that *RHOA* excision will increase metastasis free survival *in vivo*.

Potential Pitfalls & Alternative Strategies: In this aim we have complimentary approaches; *i.e.* both matrix stiffness and acoustic tweezing *in vitro*, and both matrix stiffness modulation by lysyl oxidase inhibition and inducible excision of *RHOA* with CRISPR/Cas9 *in vivo*. Although these approaches do answer slightly different scientific questions, they are related and nevertheless reduce the risk of technical problems halting progress. For example, if creation of the inducible CRISPR/Cas9 system is delayed, we can study the same question *in vitro* in the meantime, and the *in vivo* work with lysyl oxidase inhibition will partially compensate.

Aim 2 Summary: We will determine if tissue mechanics regulate PCa dormancy escape through the actin cytoskeleton and YAP1 or TAZ. This will elucidate an upstream mechanism for regulation of PCa recurrence.

Specific Aim 3: Investigate how non-coding RNAs regulate PCa dormancy escape through the hippo pathway.

Rationale: Canonical hippo regulation is by control of protein localization and stability, but investigators in other fields are beginning to show modulation of the stability of hippo pathway mRNAs²²⁻³⁴. Therefore we

examined expression data for these non-coding RNAs in the TCGA data-set. Patients in the top quartile of long non-coding RNA *SNHG1* expression had a much higher risk of early BCR. Small Nucleolar RNA Host Gene 1 (*SNHG1*) was first reported in 2013 and is reported to be an oncogene in several cancers but has received even less attention in PCa – and is only mentioned in two primary research publications when combined with prostate cancer in a PubMed search^{41,42,59-61}. Therefore, we hypothesize that *SNHG1* contributes to PCa dormancy escape by increasing YAP1 and/or TAZ expression.

Sub-aim 3A: Regulation of the PCa cell cycle *in vitro* by *SNHG1*:

Sub-aim 3A-1; *SNHG1* expression by cell cycle phase at single cell resolution: In related studies, we have made progress in predicting cell cycle phase from Fluidigm single-cell RNA sequencing (RNA-Seq) data of non-synchronized PCa cells – a process referred to as pseudotiming^{39,40}. However, definition of the G0 population remains somewhat less well-defined. We will improve our pseudotiming methods by acquiring single cell RNA-Seq data from LNCaP cells brightly expressing the Venus-Cherry vectors vs. cells in other phases of the cell cycle. We are not using serum starvation to synchronize cells because of the multiple possible other effects of serum starvation. Using this data-set, we will determine if *SNHG1* expression varies by cell cycle phase – and expect it to be highest in the S, G2 and M phases. We will then determine if *SNHG1* mRNA level predicts mRNA level of the six core hippo pathway genes.

Sub-aim 3A-2; *SNHG1* regulation of the PCa cell cycle *in vitro* through YAP1 or TAZ mRNA: We will first purchase a *SNHG1* clone in the pORF vector (ABM #ORF032663), transform in to bacteria and prepare plasmid DNA. The insert identity and sequence will be confirmed by Sanger sequencing performed by the core facility. We will then transfect into PCa cells using the Lipofectamine 3000 system (ThermoFisher #L3000). We will verify the induced *SNHG1* gene expression by comparing *SNHG1* and empty vector transfected cells by qRT-PCR. In the same samples, we will determine any downstream effects on the mRNA level for; *MIR375*, *MIR199A1*, *CDK7*, *YAP1*, *TAZ*, *LATS1*, *LATS2*, *MST1*, and *STK3 (MST2)*. Then, we will determine if *SNHG1* expression induces cell cycle entry of quiescent PCa cells. Lastly, we will determine if YAP1 or TAZ expression is required for cell cycle changes induced by *SNHG1* expression by two independent methods: (1) if siRNAs targeting YAP1 or TAZ block *SNHG1*'s effects, and (2) if the effects are blocked by induced expression of the dominant negative *TEAD* system described in Specific aim 1.

Sub-aim 3B: Regulation of recurrence *in vivo* by *SNHG1*: Lastly, we will determine if excision of *SNHG1* delays PCa recurrence *in vivo*. First, using CRISPR/Cas9 technology described under Specific aim 1, we will create a PC3 PCa cell line with *SNHG1* excision induced by tetracycline. We will inject these cells in the left ventricle of CB17 SCID mice and treat with or without tetracycline starting the day after injection. We will perform bioluminescence imaging and Kaplan Meier analysis of metastasis free survival as described above. After completion of the experiment, we will isolate the tumors and verify lack of expression of *SNHG1* and any changes in expression of *MIR375*, *MIR199A1*, *CDK7*, *YAP1*, *TAZ*, *LATS1*, *LATS2*, *MST1*, and *STK3 (MST2)* by qRT-PCR.

Anticipated Results: Sub-aim 3A: We expect induced *SNHG1* expression to decrease expression of *MIR375* and *MIR199A1*, and increase expression of *YAP1* and *TAZ* to cause PCa cell cycle entry. In the single cell RNA-Seq pseudotiming studies, we anticipate that *SNHG1* expression will be lowest in the G0 phase of the cell cycle. Sub-aim 3B: We expect that induced *SNHG1* excision will prolong metastasis free survival and reduce expression of *YAP1* and *TAZ*.

Potential Pitfalls & Alternative Strategies: Overall, we view this third aim as being of higher risk, but potentially higher reward than the other two aims. While our preliminary data for *SNHG1* is less abundant than the preliminary data for the other two aims, we are confident that, if not *SNHG1*, then another non-coding RNA will regulate PCa dormancy – as both hippo signaling and non-coding RNAs are receiving increasing attention in the literature. The single cell RNA-Seq work may be challenging from a bioinformatics perspective. However, the broader goal of this work (to develop a PCa G0 gene signature) is a goal of several members of the mentoring team and will be high impact. We think that as Co-Director of the single cell core, Dr. Keller has the experience and resources to move these studies forward.

Aim 3 Summary: We will study regulation of hippo pathway RNA as a novel potential mechanism of PCa recurrence regulation, concentrating on long non-coding RNA *SNHG1*. In addition to studying this mechanism, we will develop a gene expression signature for quiescent PCa cells.

REFERENCES

1. SEER Cancer Statistics Factsheets: Prostate Cancer. National Cancer Institute. Bethesda, MD. 2019. <https://seer.cancer.gov/statfacts/html/prost.html> (accessed December 9, 2016).
2. ZERO The End of Prostate Cancer. 2019. <https://zerocancer.org>.
3. Brookman-May SD, Campi R, Henriquez JDS, et al. Latest Evidence on the Impact of Smoking, Sports, and Sexual Activity as Modifiable Lifestyle Risk Factors for Prostate Cancer Incidence, Recurrence, and Progression: A Systematic Review of the Literature by the European Association of Urology Section of Oncological Urology (ESOU). *Eur Urol Focus* 2018.
4. NCCN Clinical Practice Guidelines in Oncology. April 17, 2019 2019. https://www.nccn.org/professionals/physician_gls/pdf/prostate.pdf.
5. Cackowski FC, Taichman RS. Minimal Residual Disease in Prostate Cancer. *Adv Exp Med Biol* 2018; **1100**: 47-53.
6. Pound CR, Partin AW, Eisenberger MA, Chan DW, Pearson JD, Walsh PC. Natural history of progression after PSA elevation following radical prostatectomy. *JAMA* 1999; **281**(17): 1591-7.
7. Aguirre-Ghiso JA, Ossowski L, Rosenbaum SK. Green fluorescent protein tagging of extracellular signal-regulated kinase and p38 pathways reveals novel dynamics of pathway activation during primary and metastatic growth. *Cancer Res* 2004; **64**(20): 7336-45.
8. Sosa MS, Parikh F, Maia AG, et al. NR2F1 controls tumour cell dormancy via SOX9- and RARbeta-driven quiescence programmes. *Nat Commun* 2015; **6**: 6170.
9. Bragado P, Estrada Y, Parikh F, et al. TGF-beta2 dictates disseminated tumour cell fate in target organs through TGF-beta-RIII and p38alpha/beta signalling. *Nat Cell Biol* 2013; **15**(11): 1351-61.
10. Ledford H. Cancer researchers target the dormant cells that seed tumours. *Nature* 2018; **558**(7710): 355-6.
11. Wu S, Huang J, Dong J, Pan D. hippo encodes a Ste-20 family protein kinase that restricts cell proliferation and promotes apoptosis in conjunction with salvador and warts. *Cell* 2003; **114**(4): 445-56.
12. Buttitta LA, Edgar BA. How size is controlled: from Hippos to Yorkies. *Nat Cell Biol* 2007; **9**(11): 1225-7.
13. Calses PC, Crawford JJ, Lill JR, Dey A. Hippo Pathway in Cancer: Aberrant Regulation and Therapeutic Opportunities. *Trends Cancer* 2019; **5**(5): 297-307.
14. de Bono JS, Logothetis CJ, Molina A, et al. Abiraterone and increased survival in metastatic prostate cancer. *N Engl J Med* 2011; **364**(21): 1995-2005.
15. Chery L, Lam HM, Coleman I, et al. Characterization of single disseminated prostate cancer cells reveals tumor cell heterogeneity and identifies dormancy associated pathways. *Oncotarget* 2014; **5**(20): 9939-51.
16. Morgan TM, Lange PH, Porter MP, et al. Disseminated tumor cells in prostate cancer patients after radical prostatectomy and without evidence of disease predicts biochemical recurrence. *Clin Cancer Res* 2009; **15**(2): 677-83.
17. Cackowski FC WY, Decker JT, Sifuentes C, Weindorf S, Jung Y, Decker AM, Yumoto K, Szerlip N, Buttitta L, Pienta KJ, Morgan TM, and Taichman RS Detection and Isolation of Disseminated Tumor Cells in Bone Marrow of Patients with Clinically Localized Prostate Cancer. *The Prostate* 2019; **Submitted**.
18. Cackowski FC, Taichman RS. Parallels between hematopoietic stem cell and prostate cancer disseminated tumor cell regulation. *Bone* 2019; **119**: 82-6.
19. Sosa MS, Bragado P, Aguirre-Ghiso JA. Mechanisms of disseminated cancer cell dormancy: an awakening field. *Nat Rev Cancer* 2014; **14**(9): 611-22.
20. Xue X, Hong X, Li Z, Deng CX, Fu J. Acoustic tweezing cytometry enhances osteogenesis of human mesenchymal stem cells through cytoskeletal contractility and YAP activation. *Biomaterials* 2017; **134**: 22-30.
21. Nilsson M, Adamo H, Bergh A, Halin Bergstrom S. Inhibition of Lysyl Oxidase and Lysyl Oxidase-Like Enzymes Has Tumour-Promoting and Tumour-Suppressing Roles in Experimental Prostate Cancer. *Sci Rep* 2016; **6**: 19608.
22. Gokey JJ, Snowball J, Sridharan A, et al. MEG3 is increased in idiopathic pulmonary fibrosis and regulates epithelial cell differentiation. *JCI Insight* 2018; **3**(17).

23. Li Z, Wang Y, Hu R, Xu R, Xu W. LncRNA B4GALT1-AS1 recruits HuR to promote osteosarcoma cells stemness and migration via enhancing YAP transcriptional activity. *Cell Prolif* 2018; **51**(6): e12504.
24. Mou K, Liu B, Ding M, et al. lncRNA-ATB functions as a competing endogenous RNA to promote YAP1 by sponging miR-590-5p in malignant melanoma. *Int J Oncol* 2018; **53**(3): 1094-104.
25. Oh HJ, Kim MJ, Song SJ, et al. MST1 limits the kinase activity of aurora B to promote stable kinetochore-microtubule attachment. *Curr Biol* 2010; **20**(5): 416-22.
26. Yan H, Li H, Li P, et al. Long noncoding RNA MLK7-AS1 promotes ovarian cancer cells progression by modulating miR-375/YAP1 axis. *J Exp Clin Cancer Res* 2018; **37**(1): 237.
27. Yu M, Luo Y, Cong Z, Mu Y, Qiu Y, Zhong M. MicroRNA-590-5p Inhibits Intestinal Inflammation by Targeting YAP. *J Crohns Colitis* 2018; **12**(8): 993-1004.
28. Zhong X, Lu M, Wan J, Zhou T, Qin B. Long noncoding RNA kcna3 inhibits the progression of colorectal carcinoma through down-regulating YAP1 expression. *Biomed Pharmacother* 2018; **107**: 382-9.
29. Gao L, Cao H, Cheng X. A positive feedback regulation between long noncoding RNA SNHG1 and YAP1 modulates growth and metastasis in laryngeal squamous cell carcinoma. *Am J Cancer Res* 2018; **8**(9): 1712-24.
30. Jin D, Guo J, Wang D, et al. The antineoplastic drug metformin downregulates YAP by interfering with IRF-1 binding to the YAP promoter in NSCLC. *EBioMedicine* 2018; **37**: 188-204.
31. Kaowinn S, Yawut N, Koh SS, Chung YH. Cancer upregulated gene (CUG)2 elevates YAP1 expression, leading to enhancement of epithelial-mesenchymal transition in human lung cancer cells. *Biochem Biophys Res Commun* 2019; **511**(1): 122-8.
32. Wang HY, Long QY, Tang SB, et al. Histone demethylase KDM3A is required for enhancer activation of hippo target genes in colorectal cancer. *Nucleic Acids Res* 2019; **47**(5): 2349-64.
33. Liu G, Huang K, Jie Z, et al. CircFAT1 sponges miR-375 to promote the expression of Yes-associated protein 1 in osteosarcoma cells. *Mol Cancer* 2018; **17**(1): 170.
34. Zhang Q, Fang X, Zhao W, Liang Q. The transcriptional coactivator YAP1 is overexpressed in osteoarthritis and promotes its progression by interacting with Beclin-1. *Gene* 2019; **689**: 210-9.
35. Hansen CG, Moroishi T, Guan KL. YAP and TAZ: a nexus for Hippo signaling and beyond. *Trends Cell Biol* 2015; **25**(9): 499-513.
36. Jiang N, Ke B, Hjort-Jensen K, et al. YAP1 regulates prostate cancer stem cell-like characteristics to promote castration resistant growth. *Oncotarget* 2017; **8**(70): 115054-67.
37. Nguyen LT, Tretiakova MS, Silvis MR, et al. ERG Activates the YAP1 Transcriptional Program and Induces the Development of Age-Related Prostate Tumors. *Cancer Cell* 2015; **27**(6): 797-808.
38. Guo Y, Cui J, Ji Z, et al. miR-302/367/LATS2/YAP pathway is essential for prostate tumor-propagating cells and promotes the development of castration resistance. *Oncogene* 2017; **36**(45): 6336-47.
39. Campbell KR, Yau C. Order Under Uncertainty: Robust Differential Expression Analysis Using Probabilistic Models for Pseudotime Inference. *PLoS Comput Biol* 2016; **12**(11): e1005212.
40. Reid JE, Wernisch L. Pseudotime estimation: deconfounding single cell time series. *Bioinformatics* 2016; **32**(19): 2973-80.
41. Li J, Zhang Z, Xiong L, et al. SNHG1 lncRNA negatively regulates miR-199a-3p to enhance CDK7 expression and promote cell proliferation in prostate cancer. *Biochem Biophys Res Commun* 2017; **487**(1): 146-52.
42. Wan X, Huang W, Yang S, et al. Identification of androgen-responsive lncRNAs as diagnostic and prognostic markers for prostate cancer. *Oncotarget* 2016; **7**(37): 60503-18.
43. Watson PA, Ellwood-Yen K, King JC, Wongvipat J, Lebeau MM, Sawyers CL. Context-dependent hormone-refractory progression revealed through characterization of a novel murine prostate cancer cell line. *Cancer Res* 2005; **65**(24): 11565-71.
44. Jung Y, Cackowski FC, Yumoto K, et al. CXCL12gamma Promotes Metastatic Castration-Resistant Prostate Cancer by Inducing Cancer Stem Cell and Neuroendocrine Phenotypes. *Cancer Res* 2018; **78**(8): 2026-39.
45. Shiozawa Y, Berry JE, Eber MR, et al. The marrow niche controls the cancer stem cell phenotype of disseminated prostate cancer. *Oncotarget* 2016.

46. Zhao B, Ye X, Yu J, et al. TEAD mediates YAP-dependent gene induction and growth control. *Genes Dev* 2008; **22**(14): 1962-71.
47. Lei QY, Zhang H, Zhao B, et al. TAZ promotes cell proliferation and epithelial-mesenchymal transition and is inhibited by the hippo pathway. *Mol Cell Biol* 2008; **28**(7): 2426-36.
48. Diepenbruck M, Waldmeier L, Ivanek R, et al. Tead2 expression levels control the subcellular distribution of Yap and Taz, zyxin expression and epithelial-mesenchymal transition. *J Cell Sci* 2014; **127**(Pt 7): 1523-36.
49. Cackowski FC, Eber MR, Rhee J, et al. Mer Tyrosine Kinase Regulates Disseminated Prostate Cancer Cellular Dormancy. *J Cell Biochem* 2017; **118**(4): 891-902.
50. Feng X, Degese MS, Iglesias-Bartolome R, et al. Hippo-independent activation of YAP by the GNAQ uveal melanoma oncogene through a trio-regulated rho GTPase signaling circuitry. *Cancer Cell* 2014; **25**(6): 831-45.
51. Chan SW, Lim CJ, Chong YF, Pobbati AV, Huang C, Hong W. Hippo pathway-independent restriction of TAZ and YAP by angiomin. *J Biol Chem* 2011; **286**(9): 7018-26.
52. Liu KI, Ramli MN, Woo CW, et al. A chemical-inducible CRISPR-Cas9 system for rapid control of genome editing. *Nat Chem Biol* 2016; **12**(11): 980-7.
53. Ranganathan K, Hong X, Cholak D, et al. High-frequency spectral ultrasound imaging (SUSI) visualizes early post-traumatic heterotopic ossification (HO) in a mouse model. *Bone* 2018; **109**: 49-55.
54. Sun Y, Yong KM, Villa-Diaz LG, et al. Hippo/YAP-mediated rigidity-dependent motor neuron differentiation of human pluripotent stem cells. *Nat Mater* 2014; **13**(6): 599-604.
55. Wang L, Luo JY, Li B, et al. Integrin-YAP/TAZ-JNK cascade mediates atheroprotective effect of unidirectional shear flow. *Nature* 2016; **540**(7634): 579-82.
56. Bubendorf L, Schopfer A, Wagner U, et al. Metastatic patterns of prostate cancer: an autopsy study of 1,589 patients. *Hum Pathol* 2000; **31**(5): 578-83.
57. Reynaud C, Ferreras L, Di Mauro P, et al. Lysyl Oxidase Is a Strong Determinant of Tumor Cell Colonization in Bone. *Cancer Res* 2017; **77**(2): 268-78.
58. Decker AM, Jung Y, Cackowski FC, Yumoto K, Wang J, Taichman RS. Sympathetic Signaling Reactivates Quiescent Disseminated Prostate Cancer Cells in the Bone Marrow. *Mol Cancer Res* 2017; **15**(12): 1644-55.
59. Chaudhry MA. Expression pattern of small nucleolar RNA host genes and long non-coding RNA in X-rays-treated lymphoblastoid cells. *Int J Mol Sci* 2013; **14**(5): 9099-110.
60. Thin KZ, Tu JC, Raveendran S. Long non-coding SNHG1 in cancer. *Clin Chim Acta* 2019; **494**: 38-47.
61. Yu Y, Yang J, Yang S, et al. Expression level and clinical significance of SNHG1 in human cancers: a meta-analysis. *Onco Targets Ther* 2019; **12**: 3119-27.

Protocol Title: The Hippo pathway in prostate cancer dormancy and recurrence
Protocol Type: IACUC
Approval Period: Draft
Important Note: This Print View may not reflect all comments and contingencies for approval. Please check the comments section of the online protocol.

*** Attached Document ***

Document Name	Created Date
Meth Mol Bio 2019.pdf	01/05/2021



Published in final edited form as:

Methods Mol Biol. 2019 ; 1914: 295–308. doi:10.1007/978-1-4939-8997-3_16.

Models of Prostate Cancer Bone Metastasis

Sun Hee Park, Matthew Robert Eber, Yusuke Shiozawa

Department of Cancer Biology and Wake Forest Baptist Comprehensive Cancer Center, Wake Forest University Health Sciences, Winston-Salem, NC, USA

Abstract

More than 180% of patients with advanced prostate cancer (PCa) experience bone metastasis, which negatively impacts overall survival and patient quality of life. Various mouse models have been used to study the mechanisms of bone metastasis over the years; however, there is currently no model that fully recapitulates what happens in humans because bone metastasis rarely occurs in spontaneous PCa mouse models. Nevertheless, animal models of bone metastasis using several different tumor inoculation routes have been developed to help study bone metastatic progression, which occurs particularly in late-stage PCa patients. This chapter describes the protocols commonly used to develop models of bone metastatic cancer in mice using different percutaneous injection methods (Intracardiac and Intraosseous). These models are useful for understanding the molecular mechanisms of bone metastatic progression, including tumor tissue tropism and tumor growth within the bone marrow microenvironment. Better understanding of the mechanisms involved in these processes will clearly lead to the development of new therapeutic strategies for PCa patients with bone métastasés.

Keywords

Bone metastasis; Bone marrow microenvironment; Mouse model; Intracardiac injection; Intraosseous injection

1 Introduction

Bone metastasis is the major cause of both increased mortality and reduced mobility of patients with advanced cancer, which is due in large part to its resilience to current treatments [1]. In fact, approximately 80% of advanced prostate cancer (PCa) metastasizes to bone, yet the mechanisms of its selectiveness and growth in bone remain unclear [2]. What is clear however, is that the mechanisms of metastatic tumor growth within the bone must be better understood before the development of effective therapies is possible. Although in vitro cell culture systems allow for a reductionist approach to achieving parts of this goal, our best tools in this pursuit are animal models that recapitulate the bone metastatic progression we observe in human patients. However, just like the ideal treatments for bone metastatic PCa, the ideal animal models of bone metastatic PCa remain elusive.

A large number of animal models have been developed to aid in the study of the molecular pathways of PCa metastasis, to varying degrees of utility. For instance, orthotopic models of primary human PCa and transgenic models of spontaneous PCa in mice have been beneficial for the study of PCa progression specifically within the primary site [3–6]. However,

studying bone metastasis using these models has been challenging in part due to their low frequencies of spontaneous skeletal metastasis [4, 6–8]. In addition, most of the experimental animals will die from complications involving the primary tumor long before any overt bone lesions develop [4, 6–8]. Therefore, distinct approaches from these to effectively recapitulate the process of bone metastasis are needed. There are several xenograft and syngeneic animal models that allow us to study bone metastatic progression utilizing conceptually simple, but technically difficult injection strategies. This chapter describes detailed procedures for two of these strategies: the intra-cardiac and intraosseous routes of injection.

As with the orthotopic and transgenic models, the intracardiac and intraosseous models have limitations. The intracardiac route of injection infuses high numbers of cancer cells directly into the blood stream, which bypass the lungs and ultimately settle and grow into tumors at other common metastatic sites, including bone [9–11]. Therefore, the intracardiac injection strategy is useful in studying the cellular and molecular mechanisms of metastatic site tropism; however, the sites where tumors grow can be unpredictable in this model. On the other hand, intraosseous injections allow the implantation of tumor cells directly into a specific site of interest, such as the femur or tibia [12]. Since these tumors grow locally by design, the intraosseous injection is a very reliable and reproducible model to study the interaction between tumor cells and the bone marrow microenvironment, resulting in subsequent tumor growth. However, this model does not enable us to address the mechanisms of the dissemination process. Moreover, both of these models allow for the detection and analysis of bone metastases in a relatively short period of time; however, neither are capable of addressing the early stages of metastasis that occur in the primary tumor.

In this chapter, we describe the routinely used protocols of both the intracardiac and intraosseous injection in mice. Neither model is fully adequate to explain the complete mechanisms of bone metastasis, but each provides a means to study the unknown drivers of PCa bone metastatic progression, resulting in the development of effective therapeutic strategies for the PCa patients who suffer from bone metastases.

2 Materials

2.1 Animals

4–8-week-old immunodeficient mice (BALB/c nu/nu and CB17 SCID) or immunocompetent mice (C57BL/6) can be used (Jackson laboratory) for xenograft or syngeneic mouse models, respectively.

2.2 Cell Lines

1. Listed below are several popular cell lines used as models of PCa. There are many factors that must be considered when selecting the best cell line for any given study, but an exhaustive list of these factors and cell lines is beyond the scope of this chapter. However, a small review of considerations can be found in Table 1.

- Human PCa cell lines: PC-3, PC-3M, DU145, LNCaP, LNCaP C4–2, LNCaP C4–2B, LuCaP23.1, and LuCaP35.
 - Mouse PCa cell line: RM1.
 - Dog cell line: Ace-1.
2. Cells can be transduced to stably express firefly luciferase to allow for the quantification of in vivo tumor growth in the bone using bioluminescence imaging (BLI) with the IVIS system (see Subheading 3.5). Detailed protocols for the generation of lentiviral particles and transduction of firefly luciferase into cancer cells have been described many times elsewhere [13] (see Note 1).
 3. For the intracardiac inoculation model of PCa, a highly metastatic cancer cell line (e.g., PC-3 and DU145) typically gives rise to multiple metastases, whereas very few or no metastases will be detected from a poorly metastatic cancer cell line (e.g., LNCaP). For the intraosseous injection model, bone metastases should be detected in the bone between 4 and 6 weeks after tumor injection, but this time frame is also cell line dependent.

2.3 Reagents

1. 0.05% Trypsin-EDTA (Gibco, #25300054).
2. Dulbecco's Phosphate-Buffered Saline (PBS) without Calcium and Magnesium (Gibco, #14190250).
3. Roswell Park Memorial Institute (RPMI) 1640 (Gibco, #11875119) or Dulbecco's Modified Eagle Medium (DMEM) (Gibco, #11995073): Add 100 U/ml penicillin-streptomycin (Gibco, #15140122), and 10% (V/V) fetal bovine serum (FBS) (Sigma-Aldrich, #F2442).

2.4 Equipment and Tools

1. Sterile tissue culture flasks or dishes (Thermo Scientific, #130190 and #130182).
2. Sterile 15 ml or 50 ml sterile conical tubes (Corning, #352098).
3. Sterile 1.5 ml microcentrifuge tubes (Fisherbrand, #05–408–129).
4. Sterile 40 µm cell strainers (Fisherbrand, #22–363–547).
5. 0.4% Trypan Blue Solution (Gibco, #15250061).
6. Hemacytometer (Hausser Scientific Partnership, #1475).
7. Electric hair clipper or chemical hair remover (Nair).
8. Cotton-Tipped Applicators (Fisherbrand, #23–400–106).
1 ml syringes (Becton Dickinson, #309628) with 27G needles, ½ in. (Becton Dickinson, #305109).
9. 0.5 ml insulin syringes with 28G needles, ½ in. (Becton Dickinson, #329461).
10. Povidone-iodine, 5% (Betadine).

11. Alcohol Swabs (Fisherbrand, #06–669–62).
12. Isoflurane.
13. Oxygen tank.
14. Isoflurane/oxygen-based anesthesia system fitted with an induction chamber and a nose cone for mice.
15. Ophthalmic ointment.
16. Heating pad.
17. 0.2 μ m syringe filter unit (Corning, #431222).
18. 40 mg/ml D-Luciferin (Perkin-Elmer, #122799) in PBS.
19. In vivo imaging system (Xenogen IVIS, Perkin-Elmer).

3 Methods

3.1 Preparing the Inoculum

1. Passage the cells 1–2 days prior to harvest so that they are about 70–80% confluent on the day of inoculation.
2. Perform the following cell preparation steps in a laminar flow hood using a proper aseptic technique.
3. Grow the cells on 10 cm dishes and harvest as follows: aspirate the growth media; gently wash with PBS; add 1 ml of 0.05% Trypsin-EDTA; and incubate at 37 °C for 1–3 min to detach the cells.
4. Inactivate the trypsin by adding 4–5 ml of fresh growth media.
5. Pass the cells through a 40 μ m cell strainer to exclude any large cell aggregates.
6. Count the total number of live and dead cells with a hemocytometer using the trypan blue exclusion assay; and calculate both cell concentration and viability. Cell viability should be >90% prior to inoculation.
7. Calculate the number of cells required for the experiment; and transfer at least twice the required amount of cell suspension to a new 15 ml conical tube (see Note 2).
8. Spin the cell suspension in a swinging bucket centrifuge at 4 °C ($100\text{--}400 \times g$ for 3 min).
9. Aspirate the supernatant; resuspend the cell pellet in an appropriate volume of PBS, and transfer to a sterile microcentrifuge tube (see Note 2).
10. Place the cell suspension (inoculum) on ice and bring immediately to the surgery room (see Note 3).

3.2 Preparing the Mice for Surgery (See Note 4)

1. Place and arrange all necessary equipment and materials in a laminar flow hood.

2. Turn on the anesthesia machine, and allow the induction chamber to fill completely with 2% isoflurane/98% oxygen.
3. Place a mouse in the induction chamber, and wait until it is anesthetized and no longer moving (~3–5 min).
4. Transfer the mouse to the surgery platform, and insert its head (nose) into the nose cone supplied with a constant flow of 2% isoflurane/98% oxygen for the duration of the procedure and ensure depth of anesthesia before operating by performing a toe pinch (Fig. 1a and see Note 5).
5. Apply ophthalmic ointment, and remove any hair with electrical clippers or chemical hair remover, if needed.

3.3 Intracardiac Injection

This section describes the protocol for injecting tumor cells directly into the left ventricle of the heart. Once in circulation, the tumor cells will disseminate to various tissues depending on the cell line used. We have found the PCa cell lines recommended above often form tumors in the long bones of mice. Other sites of metastasis include mandibles, brain, spine, lymph nodes, and adrenal glands. Tissue tropism, time to tumor formation, and frequency are cellline and mouse strain dependent and as such will require individual characterization.

1. Place the mouse in a supine position (Fig. 1a).
2. Disinfect the chest area with povidone iodine followed by an alcohol swab.
3. Push and withdraw the plunger of an insulin syringe until the plunger moves without resistance; slowly load 120 μ l of inoculum; and mix by gentle flicking until the cell suspension is homogenous. Retain a small air bubble between the plunger and inoculum.
4. Hold the syringe in your dominant hand.
5. Use the index and middle finger of your non-dominant hand to gently hold down the limbs of the mouse, being sure to secure and position it flat on its back (Fig. 1b).
6. Locate the injection point 1–2 mm from the midline on the animal's left halfway between the clavicle and xiphoid process (Fig. 1b). A heart beat can often be seen at this point.
7. Insert the needle perpendicular into the injection point about 7–8 mm deep; then carefully move your non-dominant hand to the plunger; and pull up very slightly without moving the position of the needle. If the needle is in the correct position a small pulse of bright red blood will flush into the syringe (Fig. 1c and see Note 6).
8. Slowly inject the cell suspension (~30 s for 100 μ l). During the injection, slightly aspirate the plunger several times and check for a pulse of blood to confirm that the needle is still correctly placed in the left ventricle.
9. Gently and slowly remove the needle from the injection site.

10. Place the mouse in a clean cage on a heating pad until fully recovered. Monitor the mouse until movement, breathing, heart rate, and eating and drinking return to normal.
11. Measure in vivo luciferase activity by BLI using the IVIS system within 2 h to confirm successful systemic tumor cell inoculation (Fig. 3a and see Note 7).

3.4 Intraosseous Injection (Intratibial or Intrafemoral)

Here, we describe two ways to perform intraosseous injections: tumor cells injected directly into the mouse tibia or femur. Intraosseous injections are invasive and as such the injection channels can be observed in histological sections. We, therefore, recommend that any studies that may be affected by a physical defect in the bone should also contain sham injected mice as negative controls.

1. Place the mouse in a supine position.
2. Disinfect the hind limb with povidone iodine followed by an alcohol swab.
3. Using thumb and index finger of your non-dominant hand, hold the ankle of the leg to be injected, and bend the knee (Fig. 2a).
4. With your dominant hand, insert a 27G needle attached to an empty syringe (drilling needle) into the appropriate area of the knee joint to generate a hole for tumor cell inoculation.
 - For the intratibial injection, insert the drilling needle through the patellar tendon and joint space into the tibial plateau. Using a gentle drilling motion and pressure toward the tuberosity, bore a hole into the tibia (Fig. 2b).
 - For the intrafemoral injection, insert the drilling needle near the patellar groove of the distal femur and bore a hole using a gentle drilling motion and pressure toward the femoral shaft (Fig. 2c).
5. Gently move the needle back and forth to confirm the needle is in the right space. If the needle tip is in the correct position, the syringe will be secure on its own. Faxitron X-ray images may be taken at this step to confirm the correct positioning of the needle within the trabecular bone.
6. Remove the drilling needle.
7. Load an insulin syringe with the inoculum as mentioned before.
8. Place the needle in the hole bored by the drilling needle, and slowly inject 10 μ l of the inoculum (see Note 7).
9. Remove the needle while pressing the injection site with a cotton swab. Alternatively, drilled holes can be sealed with bone wax or dental amalgam to prevent cancer cell migration from the medullary cavity.

10. Place the mouse in a clean cage on a heating pad until fully recovered. Monitor the mouse until movement, breathing, heart rate, and eating and drinking return to normal.

3.5 Imaging

This section describes the protocol for measuring BLI signal in the mice using a IVIS system.

1. The monitoring of tumor growth is commonly done by BLI using the IVIS system, which is a well-established technique used to locate and track metastatic foci within living animals. This system is sensitive enough to detect photons emitted from luciferase-expressing cells deep within the bones and other tissues of live mice. We recommend imaging once or twice a week after injection.
2. PCa bone metastatic lesions can also be detected by small animal diagnostic imaging (microcomputed tomography (micro CT), magnetic resonance imaging, or Faxitron cabinet X-ray systems). While BLI imaging is useful to detect the metastatic sites of the animal, micro CT or Faxitron X-ray systems can be used to detect the type of bone lesion (osteoblastic or osteolytic) as well as the location of metastatic lesions inside bone. If both BLI and other imaging techniques are not available, histopathological examination of metastatic nodules after necropsy is the best approach.
3. Prepare a stock solution of D-luciferin in PBS (40 mg/ml); and sterilize using a 0.2 μ m syringe filter unit.
4. Using an insulin syringe, inject the appropriate dose of d-luciferin into the intraperitoneal cavity (150 μ g/g), and then place the mouse back in its cage.
5. After 6 min, transfer the mouse to an induction chamber connected to 2% isoflurane mixed with 98% oxygen until fully anesthetized (~3–5 min).
6. Transfer the mouse to the IVIS cabinet with its face in a nose cone and its body on its side or supine/prone.
7. Acquire bioluminescence images (Fig. 3).

4 Notes

1. The most important thing to consider when generating a luciferase expressing cell line is the method of selection. If gene alteration of your cell line is a desired downstream application, choose a method of antibiotic selection for the luciferase gene that does not overlap with the gene of interest or gene alteration method. Alternatively, dual expression of luciferase and a fluorescent protein reporter allows for routine and quick purification by fluorescence-activated cell sorting (FACS). This is a convenient selection method only if a FACS machine is easily accessible.
2. The number of cells to be injected depends on the metastatic ability of the cell line and the inoculation model. The recommended number of cells for each

inoculation route is below. It is important to prepare 2–4 times the required number of cells for the experiment due to the loss of inoculum in the syringe dead space.

- Intracardiac injection: 1×10^5 – 1×10^6 cells/100 μ l of PBS per mouse
 - Intraosseous injection: 5×10^3 – 5×10^5 cells/10 μ l of PBS per mouse
3. It is important to perform the injections immediately after the preparation of the inoculum to maintain cell viability. We recommend that the inoculum is stored on ice for no longer than 2 h prior to injection.
 4. All experimental mice should be monitored regularly and according to the procedures for the care and use of laboratory animals required by an Institutional Animal Care and Use Committee (IACUC). The experimental mice should be diligently euthanized if any clinical sign meets the humane endpoints, including rapid weight loss and any condition interfering with daily activities, such as eating or drinking, ambulation, or elimination.
 5. To test if the mouse is properly anesthetized, pinch the paw skin between the toes of one hind paw. The mouse is fully anesthetized when it does not respond to this stimulus and the procedure can begin. However, if the mouse responds in any way to the stimulus, it is not fully anesthetized and must be placed back in the anesthesia induction chamber.
 6. If the needle is properly inserted in the left ventricle, bright red blood (oxygenated arterial blood) will be pumped back into the cell suspension and pulsation should be visible from the air bubble remaining in the syringe. If the needle is not placed in the left ventricle, darker venous blood from the right ventricle can be detected. If there is no blood pumping back or dark red blood observed, retract, and re-insert the needle, but no more than three attempts should be carried out within 24 h.
 7. If the tumor cells were correctly injected into the left ventricle, bioluminescence signals will be observed throughout the whole body. Otherwise, signals will be concentrated mainly in the chest area near the injection site (Fig. 3a).

Acknowledgment

This work is directly supported by National Cancer Institute (CA163124, Y. Shiozawa), Department of Defense (W81XWH-14-1-0403 and W81XWH-17-1-0541, Y. Shiozawa), the Wake Forest Baptist Comprehensive Cancer Center Internal Pilot Funding (Y. Shiozawa), and the Wake Forest School of Medicine Internal Clinical and Translational Science Institute Pilot Funding (Y. Shiozawa). Y. Shiozawa is supported as the Translational Research Academy which is supported by the National Center for Advancing Translational Sciences (NCATS), National Institutes of Health, through Grant Award Number UL1TR001420. This work is also supported by the National Cancer Institute's Cancer Center Support Grant award number P30CA012197 issued to the Wake Forest Baptist Comprehensive Cancer Center. The content is solely the responsibility of the authors and does not necessarily represent the official views of the National Institutes of Health.

References

1. Saad F, Olsson C, Schulman CC (2004) Skeletal morbidity in men with prostate cancer: quality-of-life considerations throughout the continuum of care. *Eur Urol* 46(6):731–739; discussion 739–740. 10.1016/j.eururo.2004.08.016 [PubMed: 15548440]
2. Bubendorf L, Schöpfer A, Wagner U, Sauter G, Moch H, Willi N, Gasser TC, Mihatsch MJ (2000) Metastatic patterns of prostate cancer: an autopsy study of 1,589 patients. *Hum Pathol* 31(5):578–583 [PubMed: 10836297]
3. Pettaway CA, Pathak S, Greene G, Ramirez E, Wilson MR, Killion JJ, Fidler IJ (1996) Selection of highly metastatic variants of different human prostatic carcinomas using orthotopic implantation in nude mice. *Clin Cancer Res* 2 (9):1627–1636 [PubMed: 9816342]
4. Gingrich JR, Barrios RJ, Morton RA, Boyce BF, DeMayo FJ, Finegold MJ, Angelopoulou R, Rosen JM, Greenberg NM (1996) Metastatic prostate cancer in a transgenic mouse. *Cancer Res* 56(18):4096–4102 [PubMed: 8797572]
5. Thalmann GN, Anezinis PE, Chang SM, Zhou HE, Kim EE, Hopwood VL, Pathak S, von Eschenbach AC, Chung LW (1994) Androgen-independent cancer progression and bone metastasis in the LNCaP model of human prostate cancer. *Cancer Res* 54 (10):2577–2581 [PubMed: 8168083]
6. Hurwitz AA, Foster BA, Allison JP, Greenberg NM, Kwon ED (2001) The TRAMP mouse as a model for prostate cancer. *Curr Protoc Immunol* Chapter 20:Unit 20 25. 10.1002/0471142735.im2005s45
7. Wang S, Gao J, Lei Q, Rozengurt N, Pritchard C, Jiao J, Thomas GV, Li G, Roy-Burman P, Nelson PS, Liu X, Wu H (2003) Prostate-specific deletion of the murine Pten tumor suppressor gene leads to metastatic prostate cancer. *Cancer Cell* 4(3):209–221 [PubMed: 14522255]
8. An Z, Wang X, Geller J, Moossa AR, Hoffman RM (1998) Surgical orthotopic implantation allows high lung and lymph node metastatic expression of human prostate carcinoma cell line PC-3 in nude mice. *Prostate* 34 (3):169–174 [PubMed: 9492844]
9. Kalikin LM, Schneider A, Thakur MA, Fridman Y, Griffin LB, Dunn RL, Rosol TJ, Shah RB, Rehemtulla A, McCauley LK, Pienta KJ (2003) In vivo visualization of metastatic prostate cancer and quantitation of disease progression in immunocompromised mice. *Cancer Biol Ther* 2(6):656–660 [PubMed: 14688471]
10. Drake JM, Gabriel CL, Henry MD (2005) Assessing tumor growth and distribution in a model of prostate cancer metastasis using bioluminescence imaging. *Clin Exp Metastasis* 22 (8):674–684. 10.1007/s10585-006-9011-4 [PubMed: 16703413]
11. Arguello F, Baggs RB, Frantz CN (1988) A murine model of experimental metastasis to bone and bone marrow. *Cancer Res* 48 (23):6876–6881 [PubMed: 3180096]
12. Corey E, Quinn JE, Bladou F, Brown LG, Roudier MP, Brown JM, Buhler KR, Vessella RL (2002) Establishment and characterization of osseous prostate cancer models: intra-tibial injection of human prostate cancer cells. *Prostate* 52(1):20–33. 10.1002/pros.10091 [PubMed: 11992617]
13. Carceles-Cordon M, Rodriguez-Fernandez I, Rodriguez-Bravo V, Cordon-Cardo C, Domingo-Domenech J (2016) In vivo bioluminescence imaging of luciferase-labeled cancer cells. *Bio-protocol* 6(6). 10.21769/BioProtoc.1762
14. Schneider A, Kalikin LM, Mattos AC, Keller ET, Allen MJ, Pienta KJ, McCauley LK (2005) Bone turnover mediates preferential localization of prostate cancer in the skeleton. *Endocrinology* 146(4):1727–1736. 10.1210/en.2004-1211 [PubMed: 15637291]
15. Wu TT, Sikes RA, Cui Q, Thalmann GN, Kao C, Murphy CF, Yang H, Zhou HE, Balian G, Chung LW (1998) Establishing human prostate cancer cell xenografts in bone: induction of osteoblastic reaction by prostate-specific antigen-producing tumors in athymic and SCID/bg mice using LNCaP and lineage-derived metastatic sublines. *Int J Cancer* 77(6):887–894 [PubMed: 9714059]
16. Nemeth JA, Harb JF, Barroso U Jr, He Z, Grignon DJ, Cher ML (1999) Severe combined immunodeficient-hu model of human prostate cancer metastasis to human bone. *Cancer Res* 59(8):1987–1993 [PubMed: 10213511]
17. Kozlowski JM, Fidler IJ, Campbell D, Xu ZL, Kaighn ME, Hart IR (1984) Metastatic behavior of human tumor cell lines grown in the nude mouse. *Cancer Res* 44(8):3522–3529 [PubMed: 6744277]

18. Morrissey C, Kostenuik PL, Brown LG, Vessella RL, Corey E (2007) Host-derived RANKL is responsible for osteolysis in a C4-2 human prostate cancer xenograft model of experimental bone metastases. *BMC Cancer* 7:148 10.1186/1471-2407-7-148 [PubMed: 17683568]
19. Hall CL, Bafico A, Dai J, Aaronson SA, Keller ET (2005) Prostate cancer cells promote osteoblastic bone metastases through Wnts. *Cancer Res* 65(17):7554–7560. 10.1158/0008-5472.CAN-05-1317 [PubMed: 16140917]
20. LeRoy BE, Thudi NK, Nadella MV, Toribio RE, Tannehill-Gregg SH, van Bokhoven A, Davis D, Corn S, Rosol TJ (2006) New bone formation and osteolysis by a metastatic, highly invasive canine prostate carcinoma xenograft. *Prostate* 66(11):1213–1222. 10.1002/pros.20408 [PubMed: 16683269]
21. McCabe NP, Madajka M, Vasanji A, Byzova TV (2008) Intraosseous injection of RM1 murine prostate cancer cells promotes rapid osteolysis and periosteal bone deposition. *Clin Exp Metastasis* 25(5):581–590. 10.1007/s10585-008-9175-1 [PubMed: 18506587]
22. Power CA, Pwint H, Chan J, Cho J, Yu Y, Walsh W, Russell PJ (2009) A novel model of bone-metastatic prostate cancer in immunocompetent mice. *Prostate* 69(15):1613–1623. <https://doi.org/10.1002/pros.21010> [PubMed: 19585491]

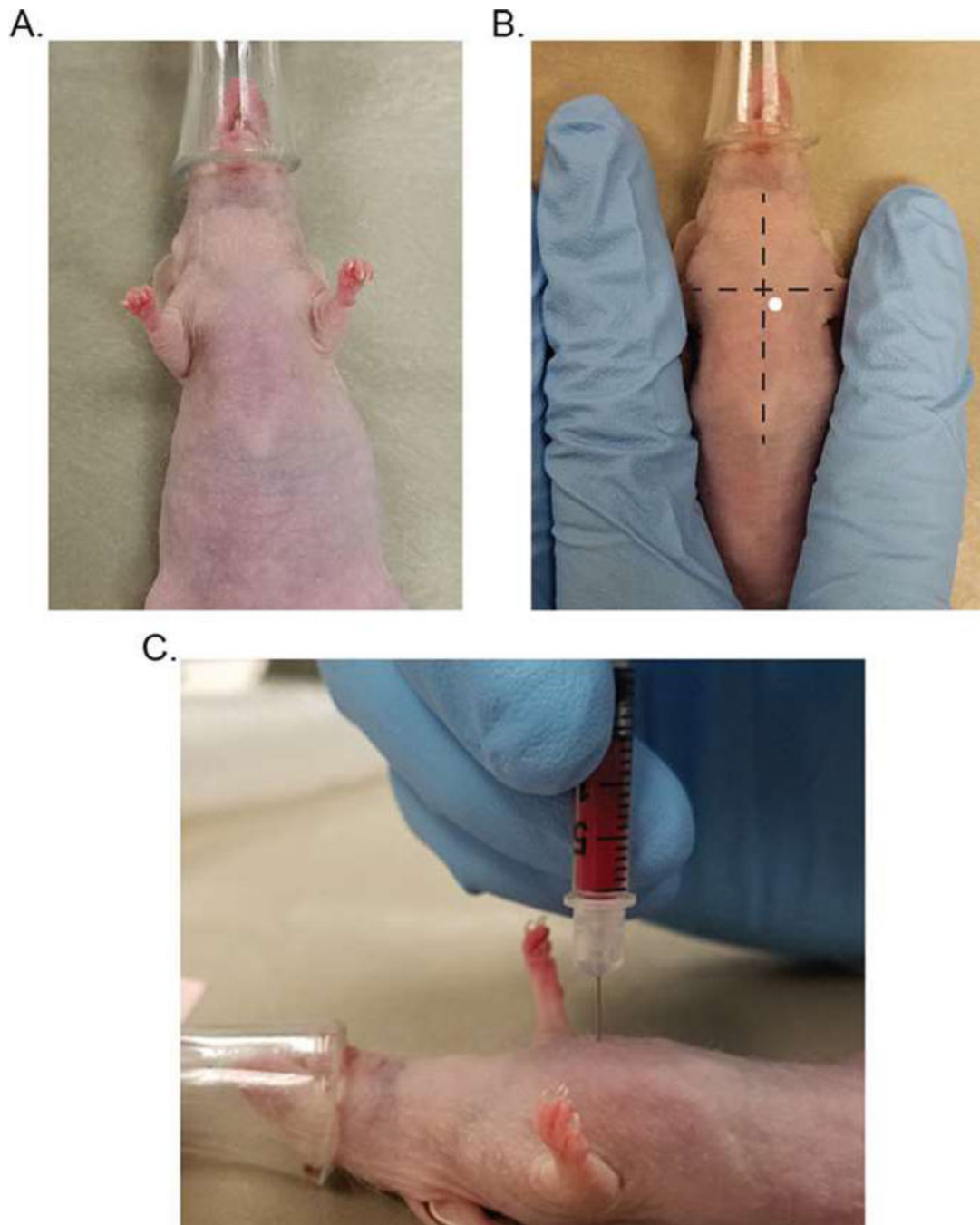


Fig. 1.

The intracardiac injection, (a) Visualization of an anesthetized mouse with its body in the correct position for the intracardiac injection and its face in a nose cone supplied with a constant flow of 2% isoflurane mixed with 98% oxygen, (b) The upper limbs of the mouse are gently held down with the index and middle fingers to secure the torso of the mouse. The location of the injection point, 1–2 mm from the midline on the animal's left, is shown as a white dot. (c) A side view of the mouse with a 28G insulin syringe inserted in the left

ventricle. Correct needle insertion is evidenced by the mixing of bright red blood with the inoculum in the syringe

Author Manuscript

Author Manuscript

Author Manuscript

Author Manuscript

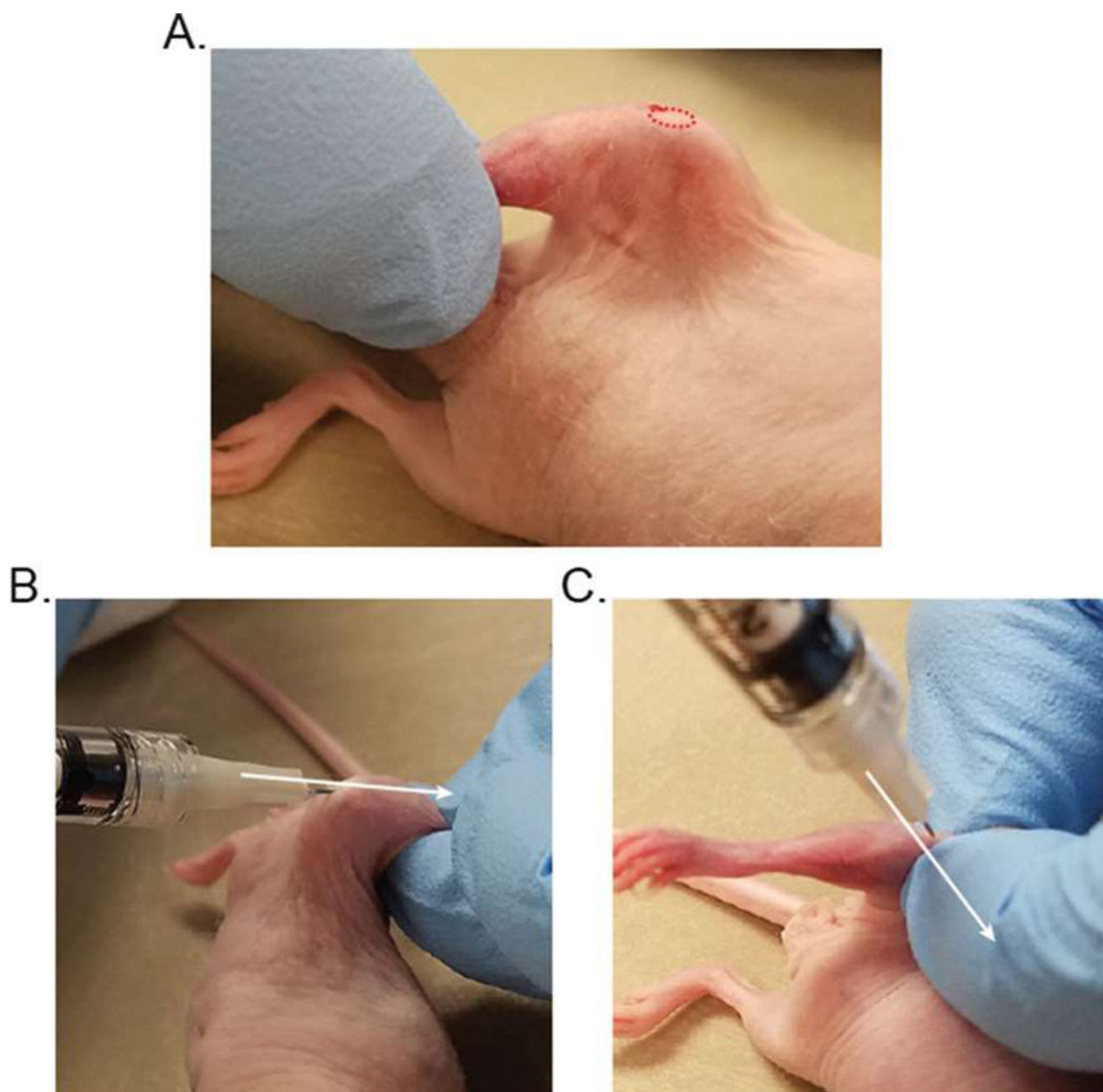


Fig. 2.

The intraosseous injection, (a) Correct positioning and visualization of the left leg of a mouse is shown. The ankle of the leg is tightly held to bend the knee to position both femur and tibia for the injection. Clear visualization of the knee joint (red dotted circle) is shown, (b) A 27G needle attached to a 1 ml syringe is inserted into the proximal tuberosity of tibia through the joint with drilling motion to generate a hole for intratibial tumor inoculation, (c) Visualization of the correct manipulation of the leg for the intrafemoral injection. A 27G needle attached to a 1 ml syringe is inserted into the patellar groove of the femur toward the shaft. The needle-syringe is in line with the long axis of tibia and femur (white arrow)

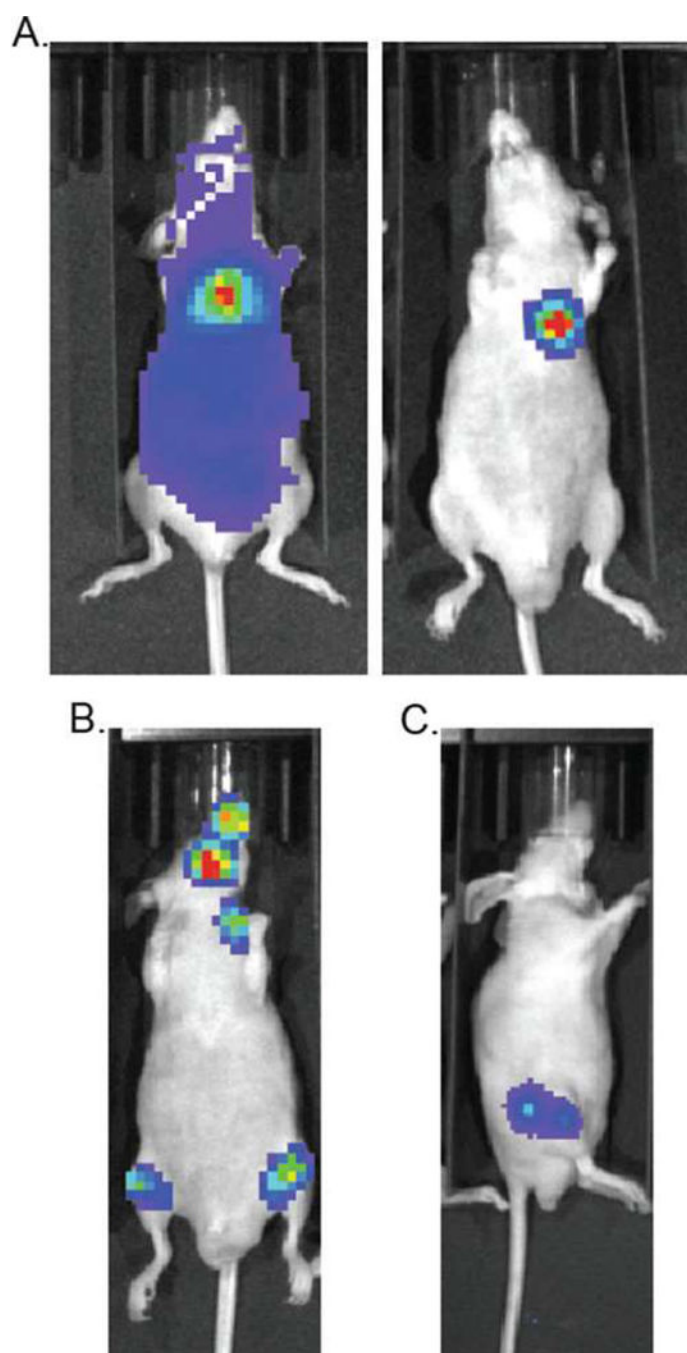


Fig. 3. Bioluminescence imaging of the tumor inoculated mice, (a) A mouse was imaged with bioluminescence imaging (BLI) 2 h after luciferase expressing cancer cell inoculation into the left ventricle. (Left) BLI signals detected throughout the whole body are indicative of a successful intracardiac injection, and (Right) intense signals limited to the thoracic region are indicative of injection failure, (b) Detection of skeletal metastases 4 weeks after intracardiac tumor injection of luciferase-expressing PC-3 cells, (c) Visualization of tumor

growth in the femur by BLI 4 weeks after intrafemoral injection of luciferase-expressing PC-3 cells

Author Manuscript

Author Manuscript

Author Manuscript

Author Manuscript

Table 1

Prostate cancer cell lines used for skeletal metastasis mice model

Animal	Cell lines	IO growth	IC growth	Type if bone metastasis	Mouse strain	References
	PC-3	+	+	Osteolytic	BALB/c	[14–16]
	PC-3M	+	+	Osteolytic	nu/nu	[17]
	DU145	+	–	Osteolytic		[16]
Human	LNCap	+	+	Mixed	or	[15]
	LNCap C4–2	+	+	Mixed	CB17 SCID	[5,15,18]
	LNCap C4–2B	+	+	Mixed		[5,15,19]
	LuCaP23.1	+	–	Osteoblastic		[12]
	LuCaP35	+	–	Osteolytic		[12]
Dog	Ace-1	+	+	Mixed	BALB/c	[20]
Mouse	RM1	+	+	Mixed	C57BL/6	[21,22]

IO Intravenous, IC Intracardiac

Protocol Title: The Hippo pathway in prostate cancer dormancy and recurrence
Protocol Type: IACUC
Approval Period: **Draft**
Important Note: This Print View may not reflect all comments and contingencies for approval. Please check the comments section of the online protocol.

***** Attached Document *****

Document Name	Created Date
J Cell Biochem 2017 MERTK.pdf	01/05/2021

Mer Tyrosine Kinase Regulates Disseminated Prostate Cancer Cellular Dormancy

Frank C. Cackowski,^{1,2} Matthew R. Eber,^{1,3} James Rhee,¹ Ann M. Decker,¹ Kenji Yumoto,¹ Janice E. Berry,^{1§} Eunsohl Lee,¹ Yusuke Shiozawa,³ Younghun Jung,¹ Julio A. Aguirre-Ghiso,⁴ and Russell S. Taichman^{1*}

¹Department of Periodontics and Oral Medicine, University of Michigan School of Dentistry, Ann Arbor, Michigan

²Division of Hematology and Oncology, Department of Medicine, University of Michigan School of Medicine, Ann Arbor, Michigan

³Department of Cancer Biology and Comprehensive Cancer Center, Wake Forest University School of Medicine, Winston-Salem, North Carolina

⁴Division of Hematology and Oncology, Tisch Cancer Institute, Departments of Medicine, Otolaryngology, and Black Family Stem Cell Institute, Icahn School of Medicine at Mount Sinai, New York, New York

ABSTRACT

Many prostate cancer (PCa) recurrences are thought to be due to reactivation of disseminated tumor cells (DTCs). We previously found a role of the TAM family of receptor tyrosine kinases TYRO3, AXL, and MERTK in PCa dormancy regulation. However, the mechanism and contributions of the individual TAM receptors is largely unknown. Knockdown of MERTK, but not AXL or TYRO3 by shRNA in PCa cells induced a decreased ratio of P-Erk1/2 to P-p38, increased expression of p27, NR2F1, SOX2, and NANOG, induced higher levels of histone H3K9me3 and H3K27me3, and induced a G1/G0 arrest, all of which are associated with dormancy. Similar effects were also observed with siRNA. Most importantly, knockdown of MERTK in PCa cells increased metastasis free survival in an intra-cardiac injection mouse xenograft model. MERTK knockdown also failed to inhibit PCa growth in vitro and subcutaneous growth in vivo, which suggests that MERTK has specificity for dormancy regulation or requires a signal from the PCa microenvironment. The effects of MERTK on the cell cycle and histone methylation were reversed by p38 inhibitor SB203580, which indicates the importance of MAP kinases for MERTK dormancy regulation. Overall, this study shows that MERTK stimulates PCa dormancy escape through a MAP kinase dependent mechanism, also involving p27, pluripotency transcription factors, and histone methylation. *J. Cell. Biochem.* 118: 891–902, 2017. © 2016 Wiley Periodicals, Inc.

KEY WORDS: MERTK; AXL; TYRO3; PROSTATE CANCER; DORMANCY; DISSEMINATED TUMOR CELL

Prostate cancer patients often have long time periods between curative intent surgery or radiation therapy until the time of biochemical recurrence or metastatic disease visible with current imaging, which marks incurable disease with current treatment options. For example, in a large series of patients treated with radical prostatectomy, nearly 20% recurrences occurred at least 5 years after surgery [Amling et al., 2000]. Greater than half of prostate cancer patients with no evidence of disease, soon after radical prostatectomy were found to have disseminated prostate tumor cells (DTCs) in their bone marrow, which are thought to be a major source of distant

recurrences [Morgan et al., 2009]. This finding implies that many of these tumor cells die, never grow, or grow very slowly. Many investigators refer to this ability of cancer cells to remain viable but not have detectable growth as “cellular dormancy.”

There is significant interest in regulators of cancer cellular dormancy. Several studies have identified a low ratio of phosphorylated MAPK3/MAPK1 (Erk 1/2) to phosphorylated MAPK14 (p38) as marking dormant tumor cells. TGFβ2 (TGF-β2) was proposed to be the major ligand responsible for dormant behavior of head and neck squamous cell carcinoma cells. The cell cycle inhibitor CDKN1B

§Deceased on February 4, 2016.

Grant sponsor: NIH/NCI; Grant number: P01-CA093900; Grant sponsor: NIH/NCI Tumor Microenvironment Network; Grant number: U54-CA163124; Grant sponsor: Department of Defense; Grant numbers: W81XWH-14-1-0403, W81XWH-15-1-0637, W81XWH-15-1-0413; Grant sponsor: NIH/NCI T32; Grant number: 5T32CA009357-32; Grant sponsor: Prostate Cancer Foundation Grant (PCF); Grant number: 2016CHAL1503.

*Correspondence to: Russell S. Taichman, D.M.D., D.M.Sc., University of Michigan School of Dentistry, 1011 North University Avenue, Ann Arbor, MI 48109. E-mail: rtaich@umich.edu

Manuscript Received: 17 October 2016; Manuscript Accepted: 17 October 2016

Accepted manuscript online in Wiley Online Library (wileyonlinelibrary.com): 17 October 2016

DOI 10.1002/jcb.25768 • © 2016 Wiley Periodicals, Inc.

(p27) and transcription factor BHLHE41 (DEC2) were implicated as nuclear signals [Bragado et al., 2013]. More recently, pluripotency associated transcription factors NR2F1, SOX2, SOX9, NANOG, and RARB were identified as transcriptional regulators of dormancy in head and neck, prostate and breast cancers [Sosa et al., 2015]. Similarly, others have shown that TGF- β family member BMP7 maintains prostate cancer dormancy through autocrine SPARC [Kobayashi et al., 2011; Sharma et al., 2016]. A role of the epigenome in regulating cellular dormancy is also becoming apparent. Histone H3 tri-methylated lysine 9 and tri-methylated lysine 27 were shown to identify and to be important for dormant cells, primarily in head and neck cancer [Sosa et al., 2015].

Our group has established a role of the TYRO3, AXL, and MERTK (TAM) family of receptors and one of their ligands, growth arrest-specific 6 (GAS6), in regulation of prostate cancer cell dormancy in the bone marrow [Shiozawa et al., 2010; Jung et al., 2012; Taichman et al., 2013]. We also found that GAS6 and MERTK are important for cancer stem like cell formation [Jung et al., 2016; Shiozawa et al., 2016]. This receptor family has an established role in the regulation of the innate immune system, but more recently has been shown to be important for cancer growth and metastasis as well. For example, MERTK was recently identified in a screen of wild-type kinases as a mediator of prostate cancer metastasis [Faltermeier et al., 2015]. The TAM family of receptors have a high degree of homology, but have been shown to have different functions, which might relate to differences in ligand binding affinities and downstream pathways [Graham and DeRyckere, 2014]. There are at least four vitamin K dependent γ -carboxylated protein ligands that bind to at least one of the TAM receptors including GAS6, Protein S (PROS1), Tubby (TUB), and Tubby like protein 1 (TULP1) [Caberoy, 2010]. We found that GAS6 decreased prostate cancer proliferation and protected the cells from chemotherapy induced apoptosis [Shiozawa et al., 2010; Lee et al., 2016]. We also found that prostate cancer bone metastases grew larger in the absence of GAS6 [Jung et al., 2012].

However, these studies did not identify which of the TAM receptors are responsible for the ability of GAS6 to slow prostate cancer growth, while also preventing apoptosis—findings which are consistent with cellular dormancy. However, the role of TYRO3 and MERTK remained unclear. To begin to answer this question, we previously studied the relative expression level TYRO3 and AXL in prostate cancer primary tumors, DTCs, and in gross metastases. However, MERTK was not included in these studies. We found that TYRO3 was expressed highly in the primary tumors, but that AXL was expressed highly in disseminated but dormant disease [Taichman et al., 2013]. Based on these results, we hypothesized that TYRO3 might play a role when prostate cancer was actively growing but that AXL might play a role when it is dormant. However, these studies did not include experiments to test this hypothesis further than gene expression. Most recently, in work that is currently in press, we reported that AXL is required for TGF- β 2 to induce prostate cancer dormancy [Yumoto et al., 2016]. However, the contributions of MERTK and TYRO3 remain unclear.

In the current study, we took an unbiased approach to discern which of the TAM receptors, including MERTK, are required for prostate cancer dormancy escape. With shRNA and siRNA technology, we knocked down the expression of each of the three receptors in

three different prostate cancer cell lines. We found that loss of MERTK, but not the other receptors decreased the ratio of P-Erk to P-p38, increased the expression of p27 and pluripotency associated transcription factors, increased the levels of dormancy associated histone H3 and caused accumulation of cells in the G1 and G0 phases of the cell cycle, and decreased apoptosis, all of which characterize dormant cells. Importantly, the effect of MERTK on the cell cycle and histone H3 post-translational modifications was reversed by altering MAP kinase signaling with a p38 inhibitor. We also found that MERTK knockdown increased metastasis free survival in an intra-cardiac injection mouse prostate cancer xenograft model, but did not inhibit in vitro cell growth or subcutaneous tumor growth showing that it did not compromise global growth characteristics. Thus, our studies implicate MERTK in stimulation of prostate cancer dormancy escape by a mechanism particular to the metastatic microenvironment and involving MAP kinases.

MATERIALS AND METHODS

CELL CULTURE

Human PCa cell lines, PC3, Du145, and LNCaP C4-2B (C4-2B) were obtained from American Type Culture Collection (Rockville, MD [PC3 and Du145]) and UroCor (Oklahoma City, OK [C4-2B]). PCa cells were maintained in RPMI 1640 with 10% fetal bovine serum (FBS) and 1% penicillin/streptomycin (P/S) in a humidified incubator with 5% CO₂. For in vitro assays, unless indicated otherwise, cells were seeded at a density 1×10^5 /ml, allowed to rest for 1 day in 10% serum and then changed to reduced serum concentrations as indicated. For the p38 inhibitor experiments, cells were first cultured for 14 days under routine conditions with 10% serum and 5 μ M SB203580 (EMD Millipore #A8254) dissolved in DMSO or 0.05% DMSO control.

TAM RECEPTOR STABLE shRNA KNOCKDOWNS

GFP and luciferase expressing PCa cell lines (PC3^{GFP}, Du145^{GFP}, and C4-2B^{GFP} cells) were first established by lentiviral transduction. Stable knockdowns of the TAM receptors (TYRO3, AXL, and MERTK) were then generated by lentiviral infection. Lentiviruses were constructed by the University of Michigan Vector Core using pGIPZ lentiviral vectors containing either a shRNA targeting one of the TAM receptors or a nonsilencing (shControl) shRNA (Open Biosystems). Stable lines were selected with puromycin. Knockdown of greater than 80% was verified by Western blotting and qRT-PCR. qRT-PCR gene expression data are presented as mean \pm SEM of independent cultures.

MerTK TRANSIENT siRNA KNOCKDOWNS

siRNAs targeting MerTK (# s20474, s20473, and s20472) and control siRNA (siControl) (# 4390843) were purchased from Thermo-Fisher Scientific. Transient transfection in C4-2B and PC3 cells was performed using 10 mM of each siRNA with Lipofectamine RNAiMAX reagent (Thermo-Fisher) using the reverse transfection protocol, followed by 3 days incubation. Knockdown was verified by real time qRT-PCR. Data are presented as mean \pm SEM of triplicate PCR reactions.

WESTERN BLOTTING

Cells were serum starved overnight unless indicated otherwise. Lysates were prepared in cOmplete lysis M (Roche #04 719 956 001) supplemented with proteinase inhibitor Mini cOmplete Tablets (Roche #04705378) and phosphatase inhibitor PhosSTOP EASYpack Tablets (Roche #04 906 837 001). Protein concentration was determined by the BCA method. Twenty micrograms of total protein was added per lane of 4–20% reducing SDS polyacrylamide Tris-Glycine gels after sample preparation in Laemmli sample buffer. The samples were transferred to PVDF membranes and blocked for 1 h in 5% dry milk in TBS with 0.1% Tween-20 (TBST). Antibodies for phosphorylated proteins were applied at 4°C overnight in 5% BSA TBST, washed, and visualized with a horseradish peroxidase conjugated anti-rabbit IgG secondary antibody (Cell Signalling #7074S) and SuperSignal West Dura Chemiluminescent Substrate (Thermo Scientific #34075). Images were acquired with a ChemoDoc Touch imager (BioRad). Membranes were stripped with Restore PLUS stripping buffer (Thermo Scientific #46430). They were blocked and re-probed for antibodies to total proteins, and again striped and re-probed for GAPDH or β -actin to normalize for protein loading. All primary antibodies were monoclonal rabbit from Cell Signaling Technology. Catalog numbers and dilutions were as follows; Phosphorylated-Erk 1/2 (P-Erk) Y204(#4377S, diluted 1:500), total Erk (#4695, 1:500), Phospho-p38 (P-p38) T190/Y182 (#4511, 1:500), total p38, (#9212, total Axl (#4939, 1:500), total Tyro3 (#5585, 1:500), total MerTK (#4319, 1:500), Sox2 (# 3579, 1:500), Caspase-9 (#9502, 1:1000), β -actin (#4970, 1:2000), and GAPDH (#2118, 1:2000). Images representative of biological replicates are shown and cropped for presentation. For P-Erk, P-p38, and p27 quantification, images from five independent experiments were quantified relative to each vehicle treated scrambled shRNA control with BioRad ImageLab software and then normalized to housekeeping gene expression. The P-Erk to P-p38 ratio was obtained by dividing the normalized P-Erk and P-p38 values for each independent experiment. All data are shown as fold change from control.

REAL TIME REVERSE TRANSCRIPTASE PCR (qRT-PCR)

Cells were lysed and RNA was harvested using the Qiagen RNeasy kit followed by reverse transcription using Invitrogen SuperScript II Reverse Transcriptase. Real time qPCR was performed using TaqMan Universal PCR Master Mix and Gene Expression Assays on a Applied Biosystems ViiA 7 instrument. TaqMan MGB probes (Applied Biosystems) were as follows: *MERTK* (Hs00179024_m1), *p27/CDKN1B* (Hs00153277), *SOX2* (Hs01053049_s1), and *NANOG* (Hs02387400). We designed primers and a probe to specifically detect *NR2F1/TFCOU1*: forward; CAAAGCCATCGTGCTGTTCAC, reverse; CCTGCAGGCTCTCGATGT, and probe; TCA-GACGCCTGTGGCCTG. β -actin (Hs01060665_g1) was used as an internal control for the normalization of target gene expression.

FLOW CYTOMETRY FOR HISTONE POST-TRANSLATIONAL MODIFICATIONS AND Ki67

Cell pellets were fixed and permeabilized with dropwise addition of 1 ml of cold 70% ethanol and then incubated overnight. All steps were at 4°C or on ice. Samples were then washed, blocked, and

incubated for 1 h in flow buffer (PBS with 2% FBS and 2 mM EDTA) with each of the following antibodies; Alexa 647 conjugated rabbit anti histone H3 tri-methylated lysine 27 diluted 1:50 (Cell Signaling Technology #12158), unconjugated rabbit polyclonal anti histone H3 tri-methylated lysine 9 (Abcam #8898), or APC conjugated rabbit anti-human Ki-67 antibody (Biolegend #350513). Cells were washed twice with flow buffer. The unconjugated histone H3 tri-methylated lysine 9 antibody was detected with an Alexa 647 conjugated anti-rabbit IgG diluted 1:250 (Cell Signaling Technology #4414). Data were acquired with a three laser (405, 488, and 640 nm) Becton Dickinson FACS Aria IIu flow cytometer. Gating was forward scatter versus side scatter, single cells (linear on FSC-A vs. FSC-H), then the 670/30 filter (APC or Alexa 647) versus forward scatter or histogram. An isotype control antibody was used for setting the gates. Negative and dim cells were selected for methylated histones. Negative cells were selected for Ki67. Data are presented as representative plots or mean \pm SEM of triplicate wells from replicate experiments.

CELL CYCLE ANALYSIS

Cells were cultured for 3 days as indicated and pulsed with 10 μ M bromodeoxyuridine (BrdU) for 30 min. The cells were collected with trypsin as necessary and then fixed and stained for total DNA with 7-AAD and BrdU incorporated into DNA using the Becton Dickinson APC BrdU flow kit (#552598). Data were acquired with a Becton Dickinson FACS Aria IIu flow cytometer. Gating was forward scatter versus side scatter, single cells (linear on FSC-A vs. FSC-H), then APC (BrdU) versus 7-AAD (DNA).

LEFT VENTRICLE INTRACARDIAC INJECTION XENOGRFT MODEL OF PROSTATE CANCER METASTASIS

Stable shRNA infected PC3^{GFP} (1×10^6) or Du145^{GFP} (2×10^5) prostate cancer cells were suspended in 100 μ l of PBS and injected into male CB.17. SCID mice (6–8 weeks of age; Charles River Labs) by left ventricle intracardiac injection. For analysis of metastasis free survival, bioluminescence images were acquired after injection of luciferin twice weekly using a PerkinElmer IVIS 2000 system. Animals that had a large portion of the signal in the lungs (indicative of a right ventricle injection) were removed from analysis a priori. After removing mice that had a right ventricular injections or did not survive the procedure, the following numbers of animals were analyzed; PC3 shControl; 6, PC3 shMER; 7, Du145 shControl; 20, and Du145 shMER; 18. Time to metastasis formation visible by bioluminescence (or death in rare cases) was then determined from the images. The data were analyzed by Kaplan–Meier analysis. For analysis of transit to the bone marrow, different mice, five mice per group, were sacrificed 24 h after tumor cell injection, and their pelvis, femora, and tibiae were harvested. The bones were crushed with a mortar and pestle and strained to remove debris. All steps used PBS buffer with 2% FBS unless otherwise noted. Cells were first depleted of mouse cells with a Mouse Cell Depletion Kit magnetic labeling system (Miltenyi Biotec # 130-104-694) and anti-Biotin MicroBeads and an AutoMACS machine (Miltenyi Biotec). The enriched cells were incubated with an APC-Cy7 conjugated anti-HLA-ABC antibody (BioLegend #311426) and a PerCP-Cy5.5 conjugated anti-mouse lineage cocktail (CD3e, CD11b, B220, Ter-119, Ly-6G, and Ly-6C) (BD Biosciences #561317), for an hour at 4°C, washed and resuspended in

PBS with 2% FBS, 2 mM EDTA and 0.5 $\mu\text{g/ml}$ DAPI. Thereafter, the percentage of disseminated prostate cancer cells (DTCs) was determined by gating on single, viable, lineage negative, HLA⁺ cells with a FACS Aria IIu flow cytometer. Mice injected with PBS rather than PCa cells were used as a negative control for flow cytometry. Data represents three independent experiments.

PROSTATE CANCER SUBCUTANEOUS TUMOR MODEL

One million prostate cancer cells suspended in 50 μl complete media were mixed with an equal volume of cold collagen solution and then slowly injected under the skin of the back of SCID mice; five mice per group. Bioluminescence images were acquired weekly. Animals were sacrificed before tumors grew to 1 cm^3 . All experimental procedures were approved by the University of Michigan Committee for the Use and Care of Animals.

PROSTATE CANCER CELL VIABILITY/MTS ASSAY

Prostate cancer cells were seeded at 2000 cells per well in 96 well plates and rested for 1 day in 10% FCS RPMI media. The media was subsequently changed to the indicated serum concentrations and the cells were cultured for an additional 3 days. The total viable cell number was then assayed with the Cell Titer Aqueous One Solution

MTS Proliferation Assay System (Promega #G3580) by absorbance at 490 nm. Data represent means of three independent experiments.

STATISTICAL ANALYSES

The type I error rate (α) was set to 0.05 for all analyses. Two-sample, two-tailed Student's *t*-tests were used to compare means of two groups. One-way repeated measures analysis of variance (ANOVA) with Bonferroni post-hoc testing was used for data normalized to housekeeping genes (blots and PCR). Standard one-way ANOVA with Tukey's Honest Significant Difference post-hoc testing was used for multiple comparisons in other experiments. The Log-rank test was used for Kaplan–Meier survival analyses. Growth curves for subcutaneous tumors were analyzed with a mixed design (split plot) ANOVA with repeated measures. All analyses were conducted with SPSS software, except for *t*-tests, which were performed in Microsoft Excel.

RESULTS

MERTK KNOCKDOWN CAUSES DORMANCY ASSOCIATED CHANGES IN MAPK ACTIVITY AND p27 EXPRESSION

To study the importance of TAM signaling on dormancy, each TAM receptor was stably knocked down with shRNA in PC3, Du145, and

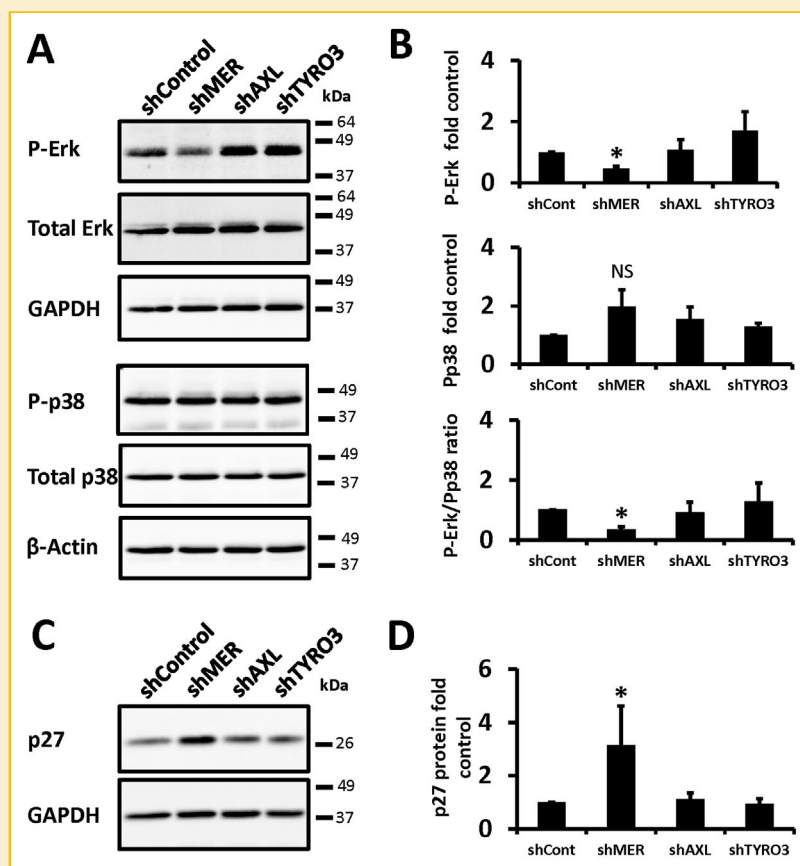


Fig. 1. TAM receptor knockdown and dormancy associated pathways in prostate cancer cells. (A) Representative Western blots of PC3 cells with each of the TAM receptors knocked down by shRNA probed for phosphorylated or total p38 and Erk 1/2 or housekeeping proteins. (B) Quantification of the samples in panel A for P-Erk, P-p38 or the ratio of P-Erk to P-p38 relative to the values for the scrambled shRNA control and normalized to the housekeeping proteins. (C) Representative Western blot for p27 of the PC3 cells. (D) Quantification of the data in C. All data is presented normalized to control. Error bars represent mean \pm SEM. *Represents $P < 0.05$ compared to shRNA control cells.

C4-2B prostate cancer cell lines. Protein expression of each receptor was decreased by at least 80% (Fig. S1). A decreased ratio of P-Erk 1/2 to P-p38 MAPK marks cellular dormancy in prostate and other cancers [Kobayashi et al., 2011; Bragado et al., 2013; Chery et al., 2014]. Therefore, we first examined P-Erk1/2 and P-p38 levels in PC3 cells with each of the TAM receptors knocked down. The ratio of P-Erk 1/2 to P-p38 was significantly decreased in serum starved MERTK knockdown cells, but not in TYRO3 or AXL knockdown cells (Fig. 1A and B). Similarly, the cell cycle inhibitor p27 was also previously found to be a dormancy marker [Kobayashi et al., 2011; Bragado et al., 2013]. In agreement with the Erk and p38 data, we found higher basal p27 protein expression in the MERTK knockdown cells (Fig. 1C and D). These data are consistent with a dormant phenotype in prostate cancer cells as a result of chronically reduced expression of MERTK.

MERTK KNOCKDOWN CAUSES EXPRESSION OF DORMANCY AND PLURIPOTENCY ASSOCIATED TRANSCRIPTION FACTORS

Transcription factors first studied in embryonic stem cells have been found to promote cancer dormancy [Sosa et al., 2015]. Therefore, we determined the basal expression level of three of these transcription factors in PC3 cells with each of the TAM receptors knocked down by shRNA. In parallel with the MAP kinase and p27 data, we saw marked upregulation of SOX2 message and protein in shMER but not shAXL or shTYRO3 cells (Fig. 2A and B). Similarly, we also observed increased expression of SOX2 in shMER C4-2B cells (Fig. 2A). We also observed increased NR2F1 and NANOG mRNA in shMER, but not shAXL or shTYRO3 cells (Fig. 2C and D). Because of the possibility of off target effects of shRNAs, we performed analogous studies with siRNA rather than shRNA and found that a siRNA targeting MERTK increased expression of SOX2 and NANOG in PC3 and C4-2B cells.

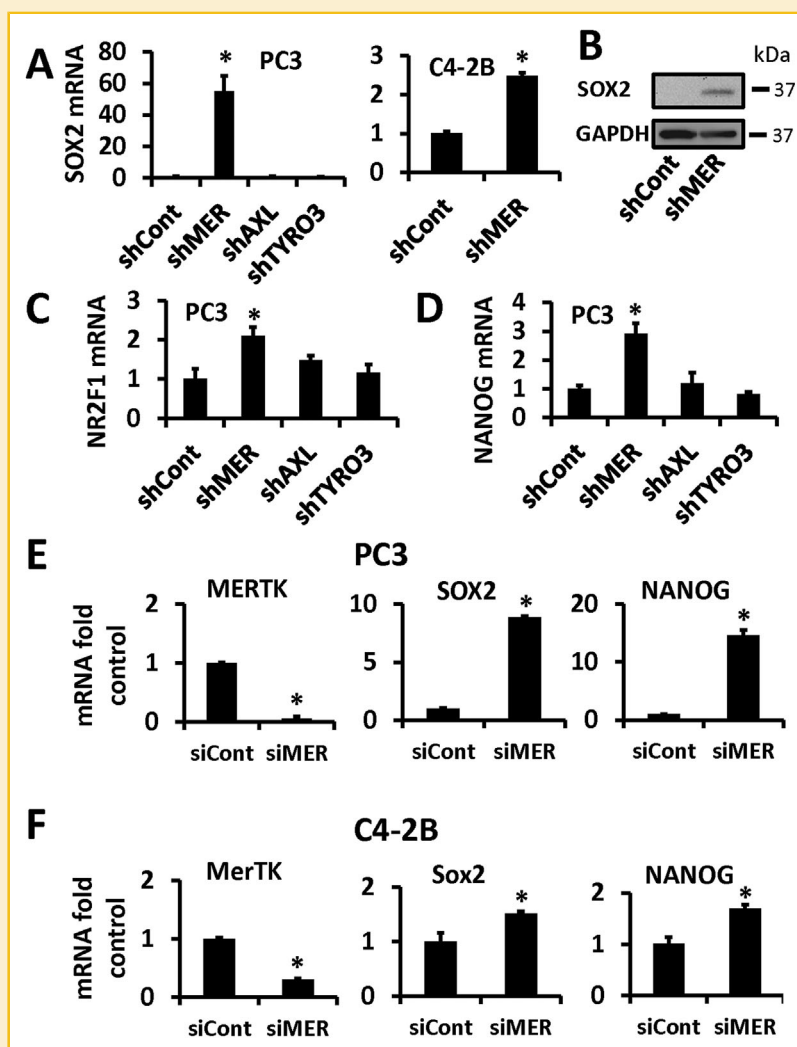


Fig. 2. TAM receptor knockdown and expression of dormancy and pluripotency associated transcription factors. (A) PC3 cells with each of the TAM receptors knocked down by shRNA or C4-2B cells with MERTK knocked down, analyzed for SOX2 expression by qPCR. (B) Representative SOX2 Western blot of shControl and shMER PC3 cells. (C and D) PC3 TAM receptor shRNA cells with expression of NR2F1 or NANOG respectively, quantified by qPCR. (E) PC3 cells with MerTK knocked down by siRNA and quantified for expression of SOX2 and NANOG by qPCR. (F) C4-2B cells with MERTK knocked down by siRNA and quantified for expression of SOX2 and NANOG by qPCR. All data are presented normalized to control. Error bars represent mean \pm SEM. *Represents $P < 0.05$ compared to shRNA or siRNA control cells.

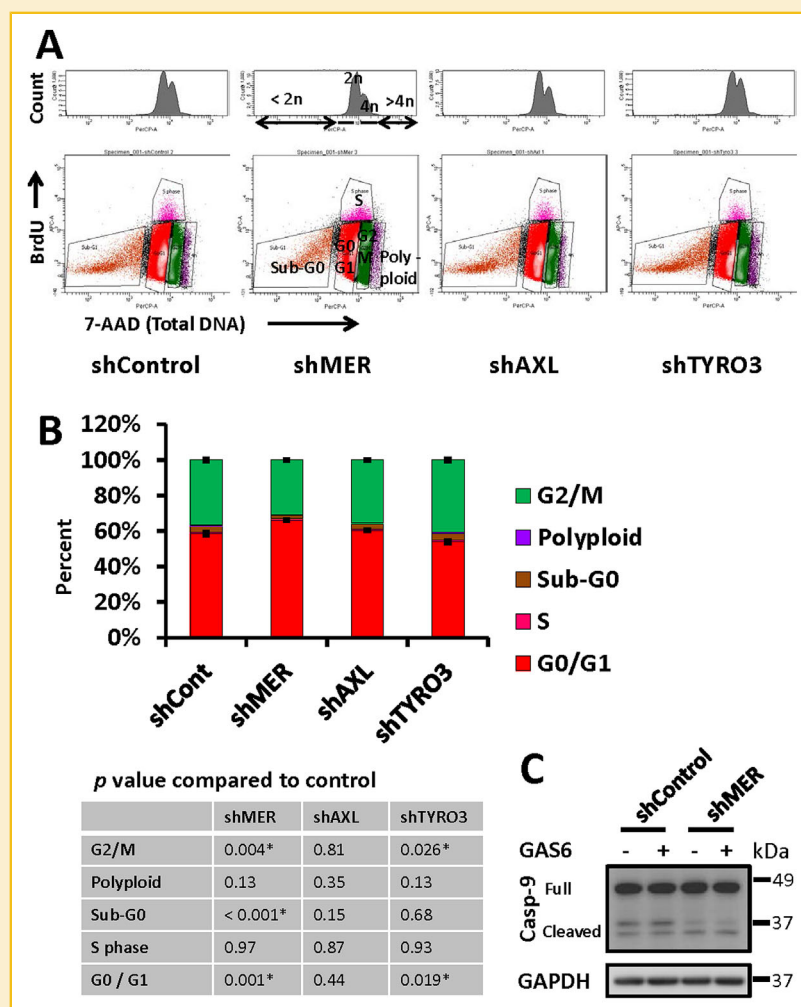


Fig. 3. Cell cycle analysis of TAM receptor knockdown PC3 cells by flow cytometry with BrdU and total DNA labeling. (A) Example flow plots for each cell type. Top: histograms of total DNA content labeled with 7-AAD. Bottom: BrdU versus total DNA plots. The significance of each population is as follows: <2n DNA and BrdU negative; Sub-G0 (apoptotic and necrotic), 2n DNA and BrdU negative; G0 and G1 phases, 4n DNA and BrdU negative; G2 and M phases, BrdU positive; S-phase, >4n DNA; polyploid cells. (B) Quantification of the above cell cycle data. The table lists P values for each cell type compared to control with significant comparisons marked with an asterisk. Error bars are shown for the G0G1 and G2M populations and represent mean \pm SEM. * Represents $P < 0.05$ compared to shRNA control cells. (C) Western blots for total caspase-9 to verify the changes in Sub-G0 cells observed by flow cytometry.

MERTK KNOCKDOWN INDUCES CELL CYCLE CHANGES ASSOCIATED WITH CELLULAR DORMANCY

Cellular dormancy and decreased Erk 1/2 activity are also characterized by arrest in the G1 and G0 phases of the cell cycle [Aguirre-Ghiso et al., 2004]. Therefore, we compared cell cycle characteristics of TAM receptor knockdown PC3 cells cultured in 0.1% serum using flow cytometry to detect antibody labeled pulsed bromodeoxyuridine (BrdU) incorporated into DNA and 7-AAD to quantify total DNA content. This assay identifies BrdU positive cells as S-phase, less than 2n DNA as apoptotic or necrotic cells, 2n BrdU negative cells as G1 and G0 phases, 4n BrdU negative cells as G2 and M phases and cells with >4n DNA as polyploid (Fig. 3A). In agreement with our other data, MERTK knockdown cells showed a pattern consistent with dormancy, with a higher percentage of cells in G0/G1 and lower percentage in G2/M compared to control (Fig. 3B). Curiously, TYRO3 knockdown cells

showed the opposite pattern with fewer cells in G0/G1 and more cells in the G2 and M phases. We did not convincingly see other analogous results for TYRO3 in our other experiments. We did not see differences between the different TAM knockdown cells in the percentage of cells in S-phase, but note that there are very few cells in S-phase in this study because of the low serum conditions. However, we did observe a reduction in the sub-G0 (apoptotic and necrotic) population in the shMER cells. Further, Western blots showed decreased levels of cleaved Caspase-9 in the shMER cells, thus suggesting that this reduced sub-G0 population represented reduced apoptosis. There is precedence in the literature for correlation of reduced apoptosis with a dormant phenotype [Aguirre-Ghiso et al., 2004]. Further, p38 stimulated cellular dormancy and reduced apoptosis have been proposed to be adaptive responses to allow DTCs to survive when conditions are not conducive to growth [Ranganathan et al., 2006].

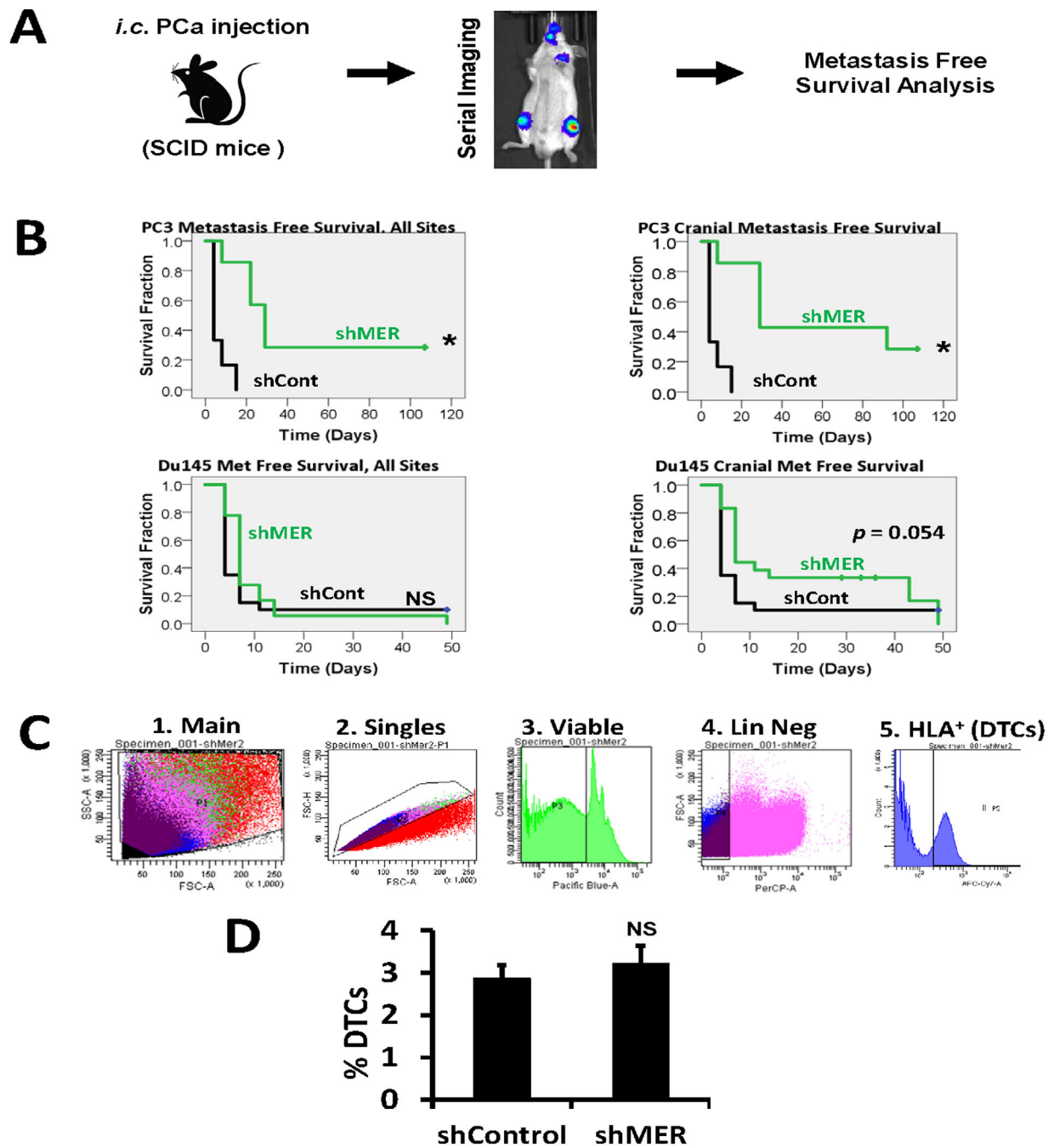


Fig. 4. MERTK knockdown and metastasis free survival in a prostate cancer left ventricle injection xenograft model. (A) Experimental design. (B) Kaplan–Meier analysis of time to formation of metastases visible by bioluminescence imaging or death in mice injected with luciferase labeled control or shMER PC3 or Du145 cells. Left panels: metastases to any site. Right panels: cranial metastases only. * Indicates $P < 0.05$ versus control cells. (C) Strategy for quantification of the percentage of DTCs in mouse bone marrow by flow cytometry after first depleting the number of mouse cells with immunomagnetic beads. (D) Comparison of the percentage of DTCs in mouse bone marrow in control versus shMER PC3 cells 1 day after intracardiac injection. Error bars represent mean \pm SEM.

DEPLETION OF MERTK INCREASES METASTASIS FREE SURVIVAL IN VIVO

We next tested the importance for MERTK for dormancy escape in vivo. GFP and luciferase labeled control shRNA or MERTK shRNA PC3 or Du145 PCa cells were injected in the left ventricle of SCID

mice and time to metastases visible by bioluminescence imaging, or death in rare cases, was evaluated with Kaplan–Meier analysis (Fig. 4A). Metastases are primarily to bone with both cell lines. Metastasis free survival in this model is established in the literature as a measure of dormancy [Kobayashi et al., 2011]. In agreement

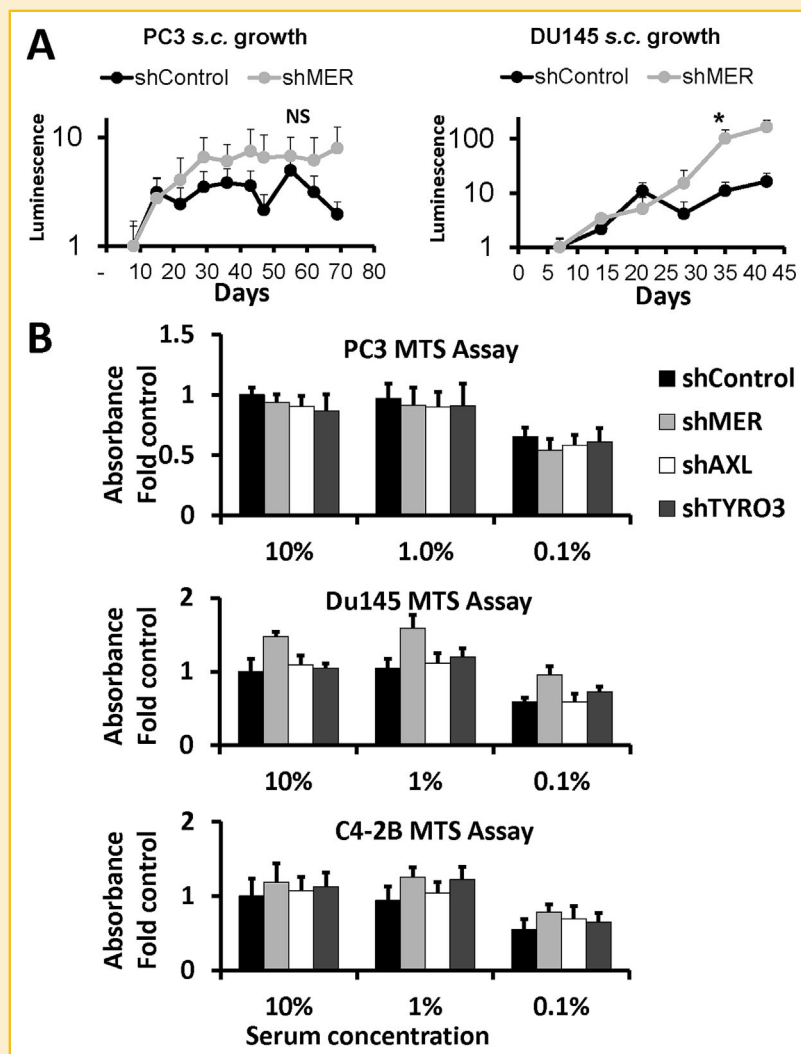


Fig. 5. Effect of MERTK knockdown on growth of prostate cancer cells in culture and in subcutaneous tumors. (A) Subcutaneous tumor growth of control or shMER PC3 or Du145 cells as measured by bioluminescence imaging. * Indicates $P < 0.05$ versus shcontrol group. (B) Relative cell number quantified by XTT assay after 3 days of culture in 10%, 1%, or 0.1% serum for PC3, Du145, and C4-2B cells with each of the TAM receptors knocked down. Data are presented as mean \pm SEM. No pairwise comparisons were statistically significant.

with the in vitro data, metastasis free survival was prolonged in mice injected with shMER PC3 cells relative to control cells (Fig. 4B, top left). With Du145 cells, the increase in metastasis free survival with MERTK knockdown was small and not statistically significant (Fig. 4B, lower left). However, we noted that shMER Du145 cells appeared to develop metastases to the head more slowly, which approached statistical significance (Fig. 4B, lower right). Time to cranial metastases was again significantly different with PC3 cells. A defect in transit to the bone marrow could also explain delayed metastasis formation but would not involve dormancy escape. Therefore, in separate experiments, we used flow cytometry to quantify the percentage of control or shMER PC3 cells in marrow 1 day after injection and found no difference (Fig. 4C and D). This further supports the conclusion that MERTK is selectively important for dormancy escape rather than transit to the bone marrow in this model.

MERTK KNOCKDOWN DOES NOT DECREASE PROSTATE CANCER GROWTH IN VITRO OR AT A SUBCUTANEOUS SITE IN VIVO

We hypothesized that the role of MERTK was somewhat specific to cellular dormancy and therefore, it should not greatly affect overall cellular growth in vitro or in vivo at a site not dependent on the usual microenvironment, such as a subcutaneous site with an artificial extracellular matrix. Indeed, other groups who have derived dormant and tumorigenic cancer cell lines have observed similar growth in culture [Bragado et al., 2013; Sharma et al., 2016]. In agreement with these expectations, we saw no difference in subcutaneous growth in vivo between control and shMER PC3 cells and saw slightly higher growth of Du145 shMER cells compared to control (Fig. 5A). Similarly, we saw no significant differences in relative cell number, as measured by MTS assay, between any of the TAM shRNA knockdowns in PC3, Du145, and C4-2B cells cultured for 3 days in 0.1%, 1%, or 10% serum (Fig. 5B). The Du145 shMER

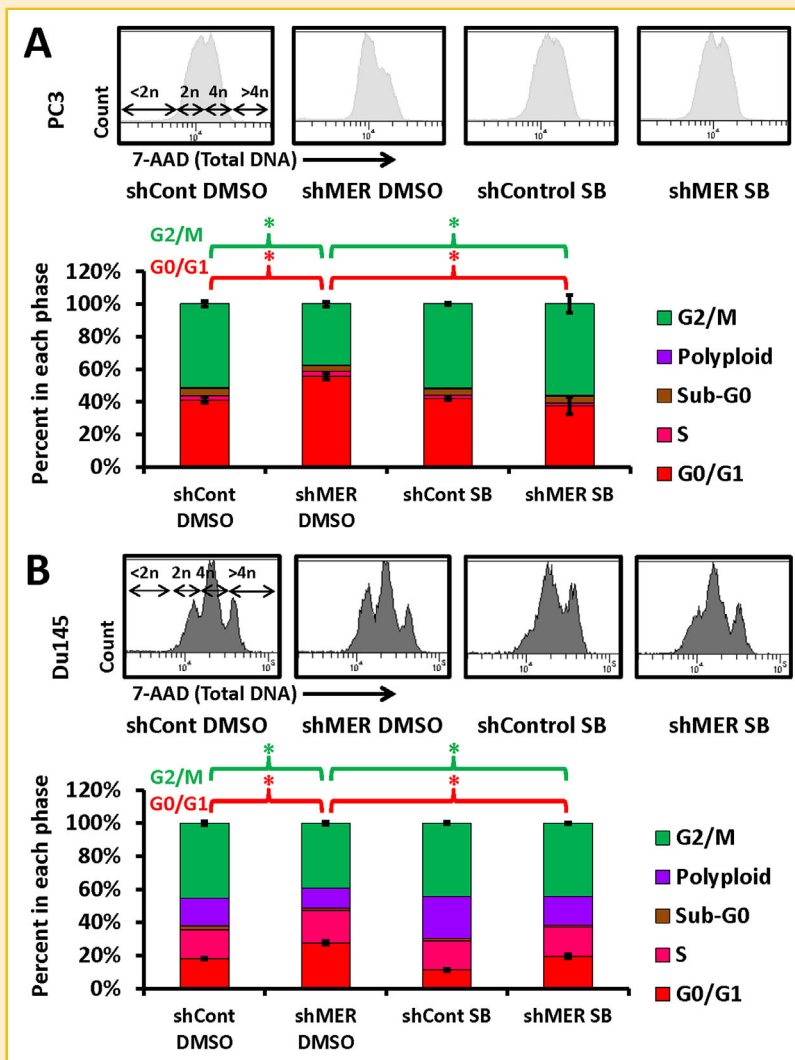


Fig. 6. Reversal of the shMER cell cycle phenotype with long term p38 inhibition. (A) Control or shMER PC3 cells cultured with 5 μ M SB203580 or 0.05% DMSO solvent control for 14 days in 10% serum and 3 days in 0.1% serum followed by cell cycle analysis with total DNA and BrdU labeling as described for Figure 3. Top: Total DNA flow cytometry histograms. Bottom: Quantified data. Error bars are shown for the G0/G1 and G2M populations and represent mean \pm SEM. *Represents $P < 0.05$ for comparisons of interest. (B) Cell cycle analysis as above of Du145 cells grown for 17 days in 10% serum with or without SB203580.

cells trended toward higher relative cell number but did not reach statistical significance after multiple comparison testing.

CELL CYCLE CHANGES OF MERTK KNOCKDOWN ARE MAP KINASE DEPENDENT

Because of the well-established role of MAP kinases in regulation of cancer cellular dormancy, we investigated if p38 was required for the dormancy associated cell cycle changes induced by knockdown of MERTK. In appreciation of the known role of epigenetic changes in dormancy regulation and the time period required for these changes to occur, we cultured control and MERTK shRNA PC3 and Du145 cells with p38 inhibitor SB203580 or 0.05% DMSO solvent control for 2 weeks before performing experiments [Sosa et al., 2015]. The expected compensatory increase in P-p38 in response to p38 active site inhibition was observed by Western blot (Fig. S2A). We again observed an increased percentage of G0/G1 and decreased percentage

of G2/M cells with MERTK knockdown both in PC3 and Du145 cells (Fig. 6). This change induced by MERTK knockdown was completely reversed by p38 inhibition, thus showing involvement of MAP kinases. Similarly, we also observed a increased percentage of Ki67 negative cells (non-cycling) with MERTK knockdown in PC3 cells, which was also reversed by p38 inhibition (Fig. S2C). Curiously, we did not observe reversal of shMER induced p27 upregulation with p38 inhibition (Fig. S2B). This suggests that not all of the effects of MERTK knockdown are MAP kinase dependent.

MERTK KNOCKDOWN INDUCES DORMANCY ASSOCIATED CHANGES IN HISTONE H3 METHYLATION BY A MAP KINASE DEPENDENT MECHANISM

Lastly, we used flow cytometry with specific antibodies to determine the effect of shRNA knockdown in PC3 cells of each of the TAM receptors on histone H3 tri-methylated lysine 9 (H3 K9 me3) and

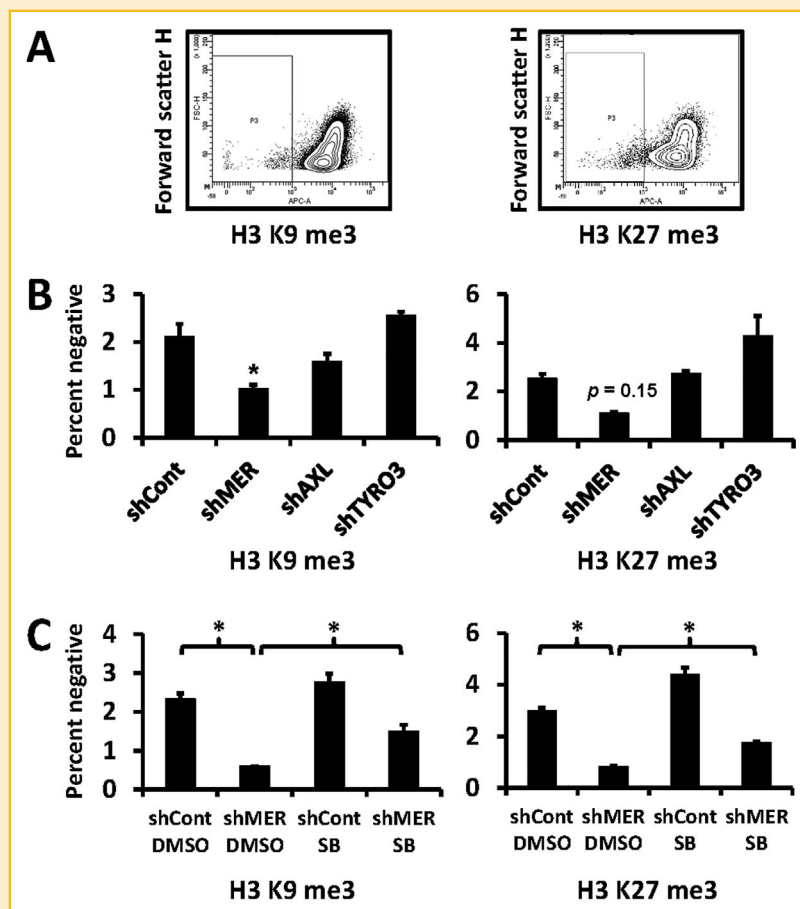


Fig. 7. Presence and MAP kinase dependence of dormancy associated histone H3 post-translational modifications in TAM receptor knockdown prostate cancer cells. (A) Example plots for percentage of cells negative or dim for histone H3 tri-methylated lysine 9 and tri-methylated lysine 27 evaluated by flow cytometry. (B) Percent of PC3 cells with each TAM receptor knocked down by shRNA negative for each histone H3 tri-methylation. (C) Control or shMER PC3 cells cultured for 14 days with or without p38 inhibitor SB203580 (as in Fig. 6) negative or dim for tri-methylated histone H3 lysine 9 or lysine 27. Error bars represent mean \pm SEM. * Represents $P < 0.05$ compared to control for panel B, or for comparisons of interest for panel C.

histone H3 tri-methylated lysine 27 (H3 K27 me3). Both of these histone marks are increased in dormant cells [Sosa et al., 2015]. Because the majority of cells were positive, we gated on the negative and dim populations rather than the positive population (Fig. 7A). We observed the expected dormancy associated change in H3 K9me3, and a trend toward significance for H3 K27me3 with MERTK knockdown but no significant differences for AXL or TYRO3 knockdown (Fig. 7B). In cells treated with the p38 inhibitor SB203580 or solvent control, we saw significant dormancy associated changes with MERTK knockdown, which were partially reversed by p38 inhibition (Fig. 7C).

DISCUSSION

Overall, these studies implicate MERTK in prostate cancer dormancy escape through a MAP kinase dependent mechanism linked to transcriptional and epigenetic regulation. Knockdown of MERTK consistently induced the changes expected for dormant cells; a decreased ratio of P-Erk to P-p38, increased p27 expression,

expression of dormancy, and pluripotency associated transcription factors, and G0/G1 arrest. Further, these findings translated to an increased metastasis free survival in vivo. This identifies MERTK as being important for the process whereby one or a few cancer cells progress to a small tumor (i.e., escape from cellular dormancy). As expected, MERTK knockdown did not inhibit growth in culture or growth of subcutaneous tumors implanted in an artificial matrix. This lack of a general growth inhibitory effect of MERTK knockdown suggests specificity for dormancy regulation in bone and a requirement for a signal from the microenvironment rather than dysregulation of multiple cellular processes.

Our data do not identify which signal(s) from the microenvironment interact with MERTK to regulate dormancy. The four other TAM receptor ligands, other than GAS6 (Tubby, Tubby like protein 1, Galectin 2, and Protein S), may also play a role. Although not a MERTK ligand, retinoic acid may be indirectly involved as well because it has been shown to stimulate cancer dormancy through NR2F1 and also interacts indirectly with MERTK in immune cells [Garabuczi, 2015; Sosa et al., 2015]. Because no recombinant protein or other treatment other than low serum conditions was required for

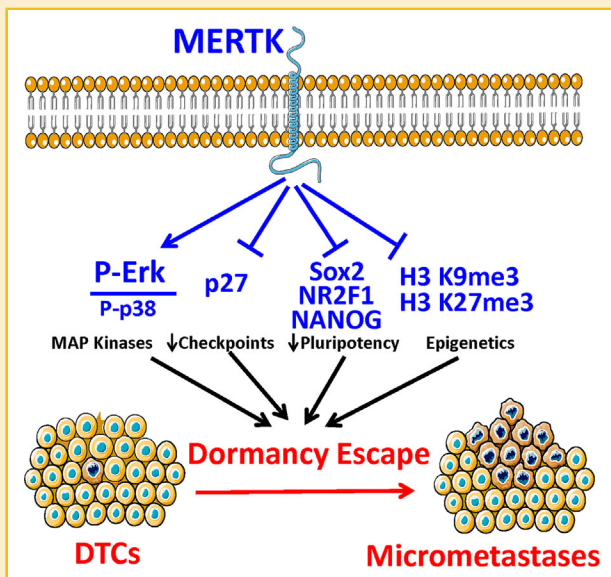


Fig. 8. Results summary for MERTK stimulates PCa dormancy escape through a MAP kinase dependent mechanism, also involving p27, pluripotency transcription factors, and histone methylation.

our observed in vitro effects, knockdown of MERTK may have caused epigenetic reprogramming of the cells as a result of chronic alterations in signaling from autocrine TAM receptor ligands. Prostate cancer cells are known to express MERTK ligands GAS6 and PROS1 [Jung et al., 2016; Ning et al., 2016]. The observed changes in histone H3 methylation also suggests that part of the effects of MERTK may be due to epigenetic reprogramming rather than through a more immediate response to ligands.

Previously, we examined the expression of TYRO3 and AXL, but not MERTK in disseminated tumor cells (DTCs) versus prostate cancer primary tumors and gross metastases [Taichman et al., 2013]. We reported higher expression of AXL in DTCs and higher expression of TYRO3 in primary tumors and gross metastases. Thus, we hypothesized that AXL might be important for maintenance of dormancy and TYRO3 might be important for escape from dormancy or growth of a gross tumor. In retrospect, it would have been useful to include MERTK in these studies. Our most recent work, currently in press, confirms the earlier hypothesis regarding AXL and shows that AXL is required for TGF- β 2 induced prostate cancer dormancy [Yumoto et al., 2016]. However, prior to the current work, the contribution of MERTK to prostate cancer dormancy remained completely unclear. Here, we took an unbiased approach and were consistently guided by the data to focus on MERTK. However, our data does not rule out contributions from AXL or TYRO3 in stimulation of dormancy escape. For example, the percent knockdown might have been insufficient to observe effects with shAXL or shTYRO3.

We recently reported a role for MERTK in formation of prostate cancer stem-like cells (CSCs) [Jung et al., 2016; Shiozawa et al., 2016]. However, the proliferative rate of CSCs was not examined in these studies and other literature reports that CSCs can be either slowly or rapidly cycling [Sharma et al., 2016; Takeishi and

Nakayama, 2016]. Additionally, others identified MERTK in an unbiased screen of over 100 kinases as a stimulator of prostate cancer metastasis. Therefore, our data showing a new role for MERTK in dormancy escape combined with the other studies implicating MERTK in CSC formation and metastasis, suggests that MERTK plays a role in prostate cancer progression by regulating several processes.

In summary, we are beginning to understand the roles of the TAM kinases in prostate cancer dormancy regulation. AXL plays a role in dormancy maintenance through TGF- β 2 and microenvironment dependent effects. The role of TYRO3 remains less clear. Conversely, this study provides the first evidence that MERTK stimulates prostate cancer dormancy escape. Our studies with a p38 inhibitor show MAP kinases are required for MERTK to stimulate dormancy escape. Furthermore, MERTK causes changes observed in histone H3 methylation, pluripotency associated transcription factors and cell cycle regulatory proteins observed in dormancy regulation of other cancers (Fig. 8). Thus, MERTK appears to reprogram DTCs to grow rather than remain dormant. This understanding of the role of MERTK should inform future studies of prostate cancer dormancy and may provide a therapeutic target for prevention of recurrence.

ACKNOWLEDGMENTS

The authors wish to thank Taocong Jin with assistance with primer design and qRT-PCR. Portions of Figure 8 are derived from the Servier powerpoint image bank.

REFERENCES

- Aguirre-Ghiso JA, Ossowski L, Rosenbaum SK. 2004. Green fluorescent protein tagging of extracellular signal-regulated kinase and p38 pathways reveals novel dynamics of pathway activation during primary and metastatic growth. *Cancer Res* 64(20):7336–7345.
- Amling CL, Blute ML, Bergstralh EJ, Seay TM, Slezak J, Zincke H. 2000. Long-term hazard of progression after radical prostatectomy for clinically localized prostate cancer: Continued risk of biochemical failure after 5 years. *J Urol* 164(1):101–105.
- Bragado P, Estrada Y, Parikh F, Krause S, Capobianco C, Farina HG, Schewe DM, Aguirre-Ghiso JA. 2013. TGF- β 2 dictates disseminated tumour cell fate in target organs through TGF- β -RIII and p38 α /p38 β signalling. *Nat Cell Biol* 15(11):1351–1361.
- Caberoy NB, Zhou Y, Li W. 2010. Tubby and tubby-like protein 1 are new MerTK ligands for phagocytosis. *EMBO J* 29(23):3898–3910.
- Chery L, Lam HM, Coleman I, Lakely B, Coleman R, Larson S, Aguirre-Ghiso JA, Xia J, Gulati R, Nelson PS, Montgomery B, Lange P, Snyder LA, Vessella RL, Morrissey C. 2014. Characterization of single disseminated prostate cancer cells reveals tumor cell heterogeneity and identifies dormancy associated pathways. *Oncotarget* 5(20):9939–9951.
- Faltermeier CM, Drake JM, Clark PM, Smith BA, Zong Y, Volpe C, Mathis C, Morrissey C, Castor B, Huang J, Witte ON. 2015. Functional screen identifies kinases driving prostate cancer visceral and bone metastasis. *Proc Natl Acad Sci USA* 113(2):E172–E181.
- Garabuczi E, Sarang Z, Szondy Z. 2015. Glucocorticoids enhance prolonged clearance of apoptotic cells by upregulating liver X receptor, peroxisome proliferator-activated receptor- δ and UCP2. *Biochim Biophys Acta* 1853(3):573–582.
- Graham DK, DeRyckere D, Davies KD, Earp HS. 2014. The TAM family: Phosphatidylserine sensing receptor tyrosine kinases gone awry in cancer. *Nat Rev Cancer* 14(12):769–785.

- Jung Y, Decker AM, Wang J, Lee E, Kana LA, Yumoto K, Cackowski FC, Rhee J, Carmeliet P, Buttitta L, Morgan TM, Taichman RS. 2016. Endogenous GAS6 and Mer receptor signaling regulate prostate cancer stem cells in bone marrow. *Oncotarget* 7(18):25698–25711.
- Jung Y, Shiozawa Y, Wang J, McGregor N, Dai J, Park SI, Berry JE, Havens AM, Joseph J, Kim JK, Patel L, Carmeliet P, Daignault S, Keller ET, McCauley LK, Pienta KJ, Taichman RS. 2012. Prevalence of prostate cancer metastases after intravenous inoculation provides clues into the molecular basis of dormancy in the bone marrow microenvironment. *Neoplasia* 14(5):429–439.
- Kobayashi A, Okuda H, Xing F, Pandey PR, Watabe M, Hirota S, Pai SK, Liu W, Fukuda K, Chambers C, Wilber A, Watabe K. 2011. Bone morphogenetic protein 7 in dormancy and metastasis of prostate cancer stem-like cells in bone. *J Exp Med* 208(13):2641–2655.
- Lee E, Decker AM, Cackowski FC, Kana LA, Yumoto K, Jung Y, Wang J, Buttitta L, Morgan TM, Taichman RS. 2016. Growth arrest-specific 6 (GAS6) promotes prostate cancer survival by G1 Arrest/S phase delay and inhibition of apoptotic pathway during chemotherapy in bone marrow. *J Cell Biochem* 117(12):2815–2824.
- Morgan TM, Lange PH, Porter MP, Lin DW, Ellis WJ, Gallaher IS, Vessella RL. 2009. Disseminated tumor cells in prostate cancer patients after radical prostatectomy and without evidence of disease predicts biochemical recurrence. *Clin Cancer Res* 15(2):677–683.
- Ning P, Zhong JG, Jiang F, Zhang Y, Zhao J, Tian F, Li W. 2016. Role of protein S in castration-resistant prostate cancer-like cells. *Endocr Relat Cancer* 23(8):595–607.
- Ranganathan AC, Adam AP, Zhang L, Aguirre-Ghiso JA. 2006. Tumor cell dormancy induced by p38SAPK and ER-stress signaling: An adaptive advantage for metastatic cells? *Cancer Biol Ther* 5(7):729–735.
- Sharma S, Xing F, Liu Y, Wu K, Said N, Pochampally R, Shiozawa Y, Lin HK, Balaji KC, Watabe K. 2016. Secreted protein acidic and rich in cysteine (SPARC) mediates metastatic dormancy of prostate cancer in the bone. *J Biol Chem* 291(37):19351–19363.
- Shiozawa Y, Berry JE, Eber MR, Jung Y, Yumoto K, Cackowski FC, Yoon HJ, Parsana P, Mehra R, Wang J, McGee S, Lee E, Negrath S, Pienta KJ, Taichman RS. 2016. The marrow niche controls the cancer stem cell phenotype of disseminated prostate cancer. *Oncotarget*. doi: 10.18632/oncotarget.9251 [Epub ahead of print].
- Shiozawa Y, Pedersen EA, Patel LR, Ziegler AM, Havens AM, Jung Y, Wang J, Zalucha S, Loberg RD, Pienta KJ, Taichman RS. 2010. GAS6/AXL axis regulates prostate cancer invasion, proliferation, and survival in the bone marrow niche. *Neoplasia* 12(2):116–127.
- Sosa MS, Parikh F, Maia AG, Estrada Y, Bosch A, Bragado P, Ekin E, George A, Zheng Y, Lam HM, Morrissey C, Chung CY, Farias EF, Bernstein E, Aguirre-Ghiso JA. 2015. NR2F1 controls tumour cell dormancy via SOX9- and RARbeta-driven quiescence programmes. *Nat Commun* 6:6170.
- Taichman RS, Patel LR, Bedenis R, Wang J, Weidner S, Schumann T, Yumoto K, Berry JE, Shiozawa Y, Pienta KJ. 2013. GAS6 receptor status is associated with dormancy and bone metastatic tumor formation. *PLoS ONE* 8(4):e61873.
- Takeishi S, Nakayama KI. 2016. To wake up cancer stem cells, or to let them sleep, that is the question. *Cancer Sci* 107(7):875–881.
- Yumoto K, Eber M, Wang J, Cackowski F, Lee E, Nobre AR, Aguirre-Ghiso J, Jung Y, Taichman R. 2016. Axl is required for TGF- β 2-induced dormancy of prostate cancer cells in the bone marrow. *Sci Rep* 6:36520. doi: 10.1038/srep36520

SUPPORTING INFORMATION

Additional supporting information may be found in the online version of this article at the publisher's web-site.

Protocol Title: The Hippo pathway in prostate cancer dormancy and recurrence
Protocol Type: IACUC
Approval Period: **Draft**
Important Note: This Print View may not reflect all comments and contingencies for approval. Please check the comments section of the online protocol.

*** Attached Document ***

Document Name	Created Date
Email Communication.pdf	01/05/2021

From: [Steven Zielske](#)
To: [Antonio Marietti](#)
Subject: Fw: Forgot to add one comment - Protocol 20-07-2485 Cackowski
Date: Thursday, September 10, 2020 9:25:32 AM

From: Institutional Animal Care and Use Committee <iacuc@wayne.edu>
Sent: Wednesday, September 9, 2020 3:03 PM
To: Steven Zielske <en9282@wayne.edu>
Cc: Frank Cackowski <Cackowski@wayne.edu>; Institutional Animal Care and Use Committee <iacuc@wayne.edu>
Subject: RE: Forgot to add one comment - Protocol 20-07-2485 Cackowski

Hello Steve,

The best option would be to wait until the current protocol is approved and once approved you may submit an amendment to do a small pilot study. You should include the information you've provided in your email strand below, including submitting an amendment for a pilot study, as your answer to Q1d.

Kind regards,
Sue

From: Steven Zielske
Sent: Wednesday, September 9, 2020 10:06 AM
To: Institutional Animal Care and Use Committee <iacuc@wayne.edu>
Subject: Re: Forgot to add one comment - Protocol 20-07-2485 Cackowski

Regarding this comment about alternatives/justification for intra-cardiac injection, we have a question. We recently discovered (past couple weeks) a potential alternative to this that has been published as a bone metastasis model. It is injection into the tail artery (quick enough to force cells back up to the femoral artery branch point where they can then reach the leg bones). We have no experience with this technique so cannot switch over to it without further investigation.

If we wanted to do a small, pilot study of this technique as a potential replacement of intra-cardiac, should we write a new animal protocol for it, or add it as a new experiment to our existing protocol under review?

Regards,

Steve

Steven Zielske, PhD
Research Scientist

Department of Oncology
Wayne State University
Detroit, MI
Ph: (313)576-8320

From: Institutional Animal Care and Use Committee <iacuc@wayne.edu>
Sent: Friday, September 4, 2020 5:44 PM
To: Frank Cackowski <Cackowski@wayne.edu>
Cc: Institutional Animal Care and Use Committee <iacuc@wayne.edu>; Steven Zielske <en9282@wayne.edu>; Antonio Marietti <hg1121@wayne.edu>
Subject: Forgot to add one comment - Protocol 20-07-2485 Cackowski

Hello Dr. Cackowski,

One of the reviewer's forgot to add a comment and I already sent the comments to your dashboard. Please see comment below:

Animal Use justification: Lit Search and Q1d incomplete – are there alternatives to intra-cardiac injection procedure? Considerations are well documented elsewhere (non-surgical procedural detail section) so findings/justifications should be congruent with lit search.

If you could cut and paste this question to your response in the Species section (so it's recorded) and note you've addressed the concern that would be much appreciated.

Thank you kindly,

Sue Bonarek
IACUC Research Compliance Administrator

Protocol Title: The Hippo pathway in prostate cancer dormancy and recurrence
Protocol Type: IACUC
Approval Period: **Draft**
Important Note: This Print View may not reflect all comments and contingencies for approval. Please check the comments section of the online protocol.

***** Attached Document *****



Document Name	Created Date
A reliable murine model of bone metastasis by injecting cancer cells through caudal arteries.pdf	01/05/2021

ARTICLE

DOI: 10.1038/s41467-018-05366-3

OPEN

A reliable murine model of bone metastasis by injecting cancer cells through caudal arteries

Takahiro Kuchimaru¹ , Naoya Kataoka¹, Kenji Nakagawa¹, Tatsuhiko Isozaki¹, Hitomi Miyabara¹, Misa Minegishi¹, Tetsuya Kadonosono¹ & Shinae Kizaka-Kondoh¹ 

Although the current murine model of bone metastasis using intracardiac (IC) injection successfully recapitulates the process of bone metastasis, further progress in the study of bone metastasis requires a new model to circumvent some limitations of this model. Here, we present a new murine model of bone metastasis achieved by injecting cancer cells through the intra-caudal arterial (CA). This model does not require high technical proficiency, predominantly delivers cancer cells to bone marrow of hind limbs with much higher efficiency than IC injection, and greatly shortens the period of overt bone metastasis development. Moreover, CA injection barely causes acute death of mice, enabling us to inject a larger number of cancer cells to further accelerate the development of bone metastasis with a wide variety of cell lines. Our model may open a new avenue for understanding the bone metastatic processes and development of drugs preventing bone metastasis and recurrence.

¹School of Life Science and Technology, Tokyo Institute of Technology, 4259-B60, Nagatsuta-cho, Midori-ku, Yokohama 226-8501, Japan. Correspondence and requests for materials should be addressed to S.K.-K. (email: skondoh@bio.titech.ac.jp)

Bone is one of the most common sites of metastasis for various primary tumors including prostate, breast, lung, and kidney cancers^{1,2}. Although bone metastasis is associated with increased morbidity and mortality, promising therapy to prevent bone metastasis is currently unavailable. This deficiency emphasizes the need for new therapeutic approaches targeting molecular mechanisms that regulate bone metastasis and for new models to study this disease phenomenon.

Murine models of bone metastasis using intracardiac (IC) and intratibial injections have been instrumental in revealing molecular mechanisms underlying metastatic processes and translational studies for drug development^{3,4}. During the past two decades, IC injection has been the gold standard to develop bone metastasis in mice^{5–9} by injecting cancer cells into the left ventricle to disseminate them to the whole body including bone marrow tissue via the arterial bloodstream, which eventually develop into metastatic colonies in the bone and other organs¹⁰. Unlike intratibial injection that severely damages the tibia, IC injection recapitulates the bone metastasis process, including survival of cancer cells in the bloodstream, extravasation, micro-colony formation, and metastatic progression in the intact bone marrow, and thus provides more relevant information for drug development. IC injection, however, is insufficient for rapid studies in this field, mainly owing to its requirement for high technical proficiency to exactly insert a syringe needle into the left ventricle of a mouse, causing severe cardiac stresses^{3,4}. This limits the number of cancer cells that can be injected at one time, leading to limited delivery of cancer cells to the bone. Thereby analysis with IC model may bias toward cancer cell lines with relatively high metastatic ability. Furthermore, cancer cells are preferably delivered to organs other than bone, such as the lungs and liver, and often develop into lethal cancers in other organs, hampering or even terminating studies of bone metastasis with cell lines with relatively slow metastasis development. New models overcoming such limitations would accelerate basic studies and drug development for bone metastasis.

Here, we present the establishment of a new murine model that predominantly develops bone metastasis in the hind limbs at high frequency. In this model, cancer cells are injected via the caudal artery (CA) in the tail, and the technique is as easy as tail vein injection. CA injection rarely causes acute death and facilitates the injection of a large number of cancer cells, thereby greatly increasing the frequency of bone metastasis for various types of cancer cells. Therefore, CA injection provides an easy-to-use murine model to develop overt bone metastasis in a short time and could greatly facilitate studies to understand bone metastasis and to prevent them.

Results

CA as a new route for injection. To develop a novel murine bone metastasis model, we searched for an alternative arterial route to deliver cancer cells to bone marrow in mice. The CA was the most easily accessible route to inject cancer cells without any surgical procedures (Fig. 1a). Although cell distribution after IC injection has been well studied, no study has assessed CA-injection route. Therefore, to examine whether this route could be practically used for injection, we injected fluorescent nanoparticles emitting near-infrared II (NIR-II) fluorescence (maximum emission at 1530 nm)^{11,12}. Because the nanoparticles injected via CA were thought to eventually travel to the tail vein, we compared their distributions after CA and intravenous (IV) injection by video-rate fluorescence imaging. Surprisingly, CA-injection exhibited totally different routes from IV injection: Injecting nanoparticles into the CA quickly illuminated the capillary bed in the lower body of mice, whereas nanoparticles

injected via the tail vein resulted in slow and modest illumination (Fig. 1b and Supplementary Movies 1 and 2). This result implied that the CA can be a practical injection route and may be suitable for delivery of cancer cells to the bone of hind limbs. To track the fate of cancer cells after CA injection, we used murine lung carcinoma LLC cells constitutively expressing firefly luciferase (LLC/luc). In vivo bioluminescence (BL) imaging revealed predominant delivery of LLC/luc cells to the lower body by CA injection that is technically as easy as tail vein injection (Fig. 1c and Supplementary Movie 3). CA injection delivered cancer cells three-fold more efficiently to hind-limb bone marrow than IC injection, as revealed by luciferase activity in the bone marrow 30 min after injection of LLC/luc cells (Fig. 1d). This result was well correlated to the one of ex vivo bone imaging acquired just after dissection (Supplementary Fig. 1). In addition, ex vivo BL imaging of representative organs confirmed dominant delivery of cancer cells to organs of the lower body after CA injection; in contrast, IC injection resulted in dissemination of cancer cells to various tissues (Fig. 1e and Supplementary Fig. 2). These results indicated that CA injection provides a preferable model to study bone metastasis.

Cancer cell distribution after CA injection. We next compared the efficacy of bone metastasis development in mice, between CA and IC injections, by comparing luciferase activity over time after transplanting LLC/luc cells. BL intensities in the hind limbs were significantly higher after CA injection than after IC injection (Fig. 2a). Over time, growth rates were similar between these models throughout the development of bone metastasis (Fig. 2a and Supplementary Fig. 3), indicating that differences in stress between the methods, during injection and dissemination, did not affect cell proliferation in the bone marrow. Histological analysis confirmed an increase in the number of bone metastatic lesions in CA-injected mice 7 days after the injection of LLC/luc cells (Fig. 2b and Supplementary Fig. 4). In addition, significantly larger tumors were observed in the hind-limb bones of CA-injected mice at 14 days after LLC/mKO2-Rluc cell injection (Fig. 2c and Supplementary Fig. 5). X-ray micro-computed tomography (CT) imaging revealed a decrease in bone mass in CA-injected mice compared to that in IC-injected animals (Fig. 2d and Supplementary Fig. 6), confirming enhanced bone metastasis in CA-injected mice. CA injection enabled observation for more than 32 days after cancer cell injection. In contrast, IC-injected mice became weak and could not be observed after day 25 due to death (Fig. 2e). Ex vivo BL imaging of representative organs at 32 days after CA injection of LLC/luc cells revealed the development of metastasis predominantly in the hind-limb bones and some nonlethal micrometastases in vesicular glands (Fig. 2f). Most importantly, we obtained essentially similar BL imaging results in all CA-injected mice without failure.

Improved bone metastasis development by CA injection. Furthermore, we were able to inject a larger number of cancer cells (1×10^6 cells) via CA injection without any acute death, overcoming one of the limitations of IC injection model (Supplementary Table 1). Cancer cells delivered to bone marrow in the femur increased as the number of cancer cells injected through the CA was increased (Fig. 3a). The delivery efficiency directly reflected the efficiency of bone metastasis development (Fig. 3b).

These results motivated us to examine other cancer cell lines, because cancer cell lines applicable to the IC bone metastasis model has been limited. Notably, CA-injected MCF7, which has been recognized as a non-metastatic human breast cancer cell line^{13,14}, developed bone metastasis (Fig. 4a and Supplementary Fig. 7a). We further applied CA injection of several human cancer

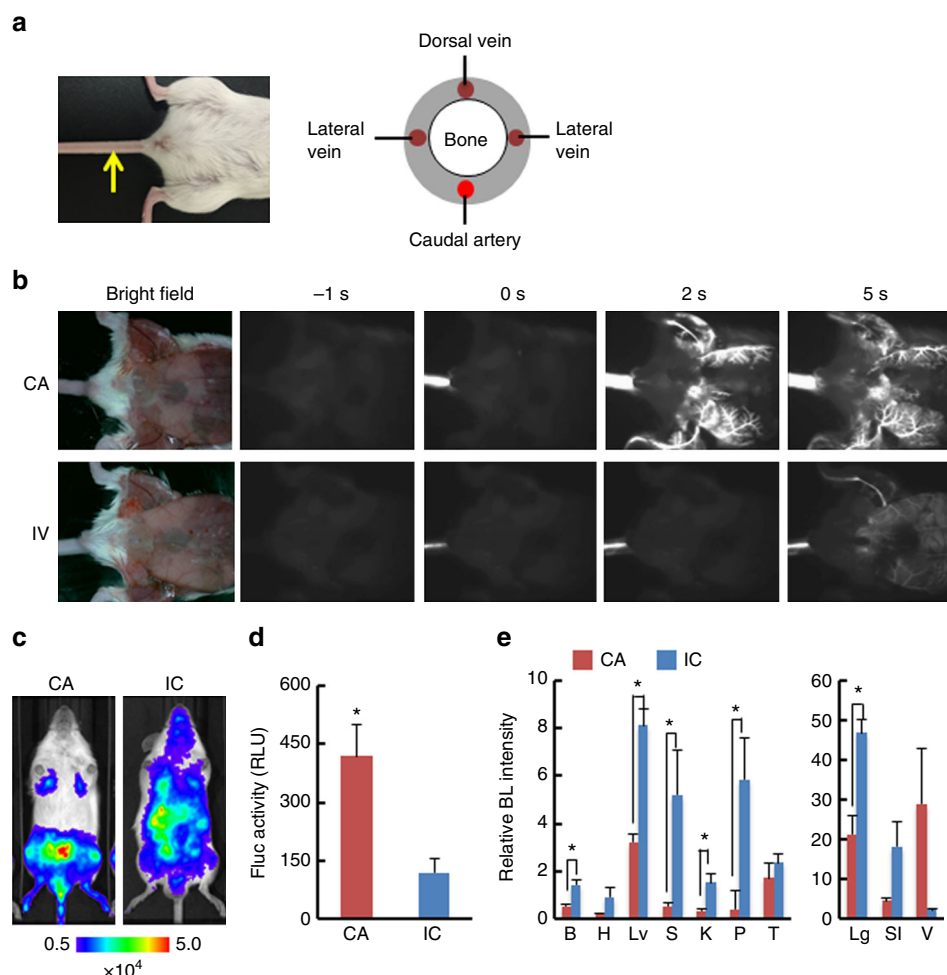


Fig. 1 CA injection efficiently delivered cancer cells to bone marrow of a hind limb. **a** Location of caudal artery in a mouse (left) and a schematic of cross section of mouse tail (right). A yellow arrow indicates the caudal artery along the tail. **b** Comparison of fluorescence images after intra-caudal artery (CA) or tail vein (IV) injection of near-infrared II nanoparticles. **c** Representative BL images at 30 min after injecting LLC/luc cells through caudal artery (CA) or left ventricle (IC). **d** BL intensity of LLC/luc cells harvested from bone marrow of hind limbs at 30 min after CA or IC injection. $n = 8$, $^*P < 0.05$ (two-side student's t -test). Error bars indicate s.e.m. **e** Biodistribution of LLC/luc cells after CA or IC injection. Major organs were removed at 30 min after injecting LLC/luc cells and ex vivo BL imaging was performed. BL intensity of each organ was quantitatively analyzed and its relative BL intensity to the one in hind limb is shown. B brain, H heart, Lv liver, S spleen, K kidney, P pancreas, T testis, Lg lung, St stomach and intestine, V vesicular gland. $n = 3$, $^*P < 0.05$ (two-side student's t -test)

cell lines including breast (MDA-MB-231), prostate (PC-3), and kidney (786-O) cancers as well as osteosarcoma (143B). These cancers often metastasize to the bone in patients. In addition, syngeneic mouse models were examined using three cell lines including breast carcinoma E0771 that is first described here in a bone metastasis model. In vivo BL imaging confirmed that these cell lines developed bone metastasis after CA injection (Fig. 4b and Supplementary Fig. 7b). It is noteworthy that we could detect bone metastasis by 5–12 days after CA injection of all the cell line examined. Overall, the results demonstrated that CA injection provides a reliable method to develop bone metastasis by increasing the delivery efficiency of a wide variety of cancer cell lines to the bone marrow of the hind limbs in mice.

Discussion

Here, we present a new method to establish a murine model of bone metastasis by caudal artery injection of cancer cells. The reliability (almost no failures) and easiness of this method minimize animal use and distress. The reliability is the result of the following features. (1) Because the caudal artery is visible on

the body surface, injection into the caudal artery is as easy as tail vein injection. (2) Failure of CA injection is immediately detectable by low resistance upon pushing the plunger or leakage at the needle tip, and reinjection is possible at different points of the caudal artery closer to the body. (3) Successful injection can be confirmed by BL in the lower body of the mouse immediately after CA injection (Fig. 1c).

Although we first thought that the cells injected into the CA would eventually go to the tail vein, they were delivered to the bone marrow of hind limbs via a route very different from IV injection (Fig. 1b). In the CA injection model, injected cancer cells were forced to move upstream against the flow of the CA by strongly pushing them in a short time (0.1 mL per 3 s), allowing them to enter the femoral artery through the common iliac artery (see Supplementary Fig. 8)¹⁵. Then they rarely move further upstream to reach the interior mesenteric artery because a high BL signal was not detected in the liver, stomach, or spleen after CA injection (Fig. 1e and Supplementary Fig. 2). During these processes, cancer cells might be exposed to severe shear stresses. The in vivo growth rates, however, were similar between CA-injected and IC-injected cells (Fig. 2a and Supplementary Fig. 3).

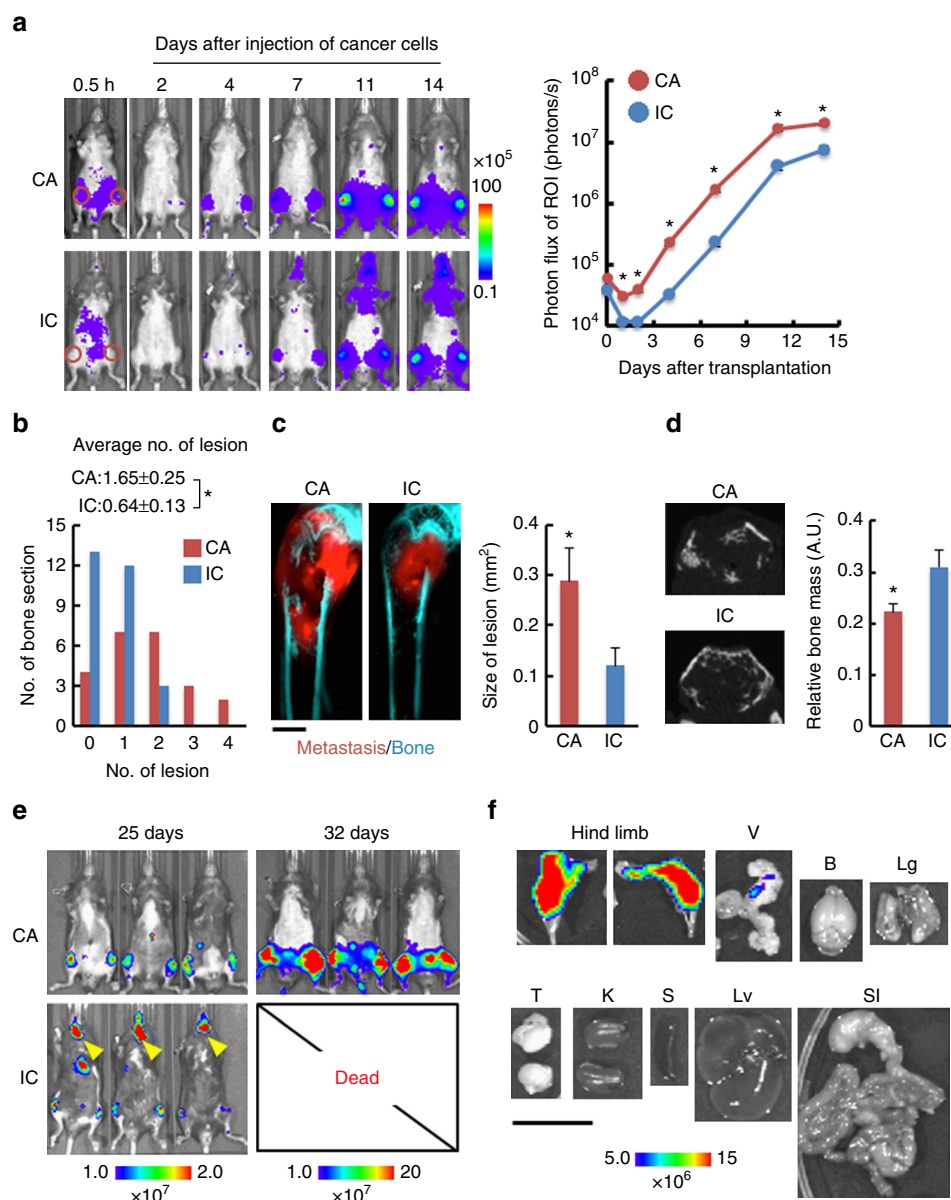


Fig. 2 CA injection accelerated development of bone metastasis in a hind limb. **a** Representative BL images (left) and BL intensity in region of interest (ROI) (right) at indicated days after LLC/luc cells injection by CA ($n = 16$) or IC injection ($n = 12$). Red circles in the images of 0.5 h indicate ROI. $*P < 0.05$ (two-side student's t -test). Error bars indicate s.e.m. **b** Metastatic lesions in hind limb at 7 days after CA or IC injection of LLC/luc cells. The average number of a metastatic lesion per bone section was shown above the bar graph. $n = 23$ (CA), $n = 28$ (IC), $*P < 0.05$ (two-side student's t -test). **c** Representative fluorescence images (left) and quantitative analysis of bone metastasis in femur bones at 14 days after injecting LLC/mKO2-Rluc8.6 cells via CA or IC. Metastasis and bone were visualized with mKO2 fluorescence (red) and tissue autofluorescence (cyan), respectively. A scale bar is 500 μm . $n = 8$ (CA), $n = 6$ (IC). $*P < 0.05$ (two-side student's t -test). **d** X-ray micro CT imaging (left) and quantitative analysis (right) of bone volume in the femur at 14 days after CA or IC injection of LLC/mKO2-Rluc8.6 cells. Representative images are transverse plane of femurs shown in **c**. $n = 8$ (CA), $n = 6$ (IC). $*P < 0.05$ (two-side student's t -test). **e** Representative BL images of mice at 25 and 32 days after CA or IC injection of LLC/luc cells. The representative image of mice at 32 days after IC injection are not shown because all IC-injected mice died before the day. **f** Representative ex vivo BL images of organs harvested from a mouse at 32 days after CA injection of LLC/luc cells. A scale bar is 10 mm. V vesicular gland, B brain, Lg lung, T testis, K kidney, S spleen, Lv liver, SI stomach and intestine

These data suggest that the cellular stress by CA-injection was, if any, similar to the one by IC injection and that the injection methods did not influence the growth of cancer cell after their delivery to the bone marrow. In addition, CA injection barely caused acute death of mice even at injection of a large number of cancer cells, allowing more cancer cells to be delivered to the bone marrow (Supplementary Table 1 and Fig. 3a). Increased delivery efficiency by CA injection increases the chance of successful colonization of cancer cells. For example, MCF7, which has been

recognized as a non-metastatic cell line^{13,14}, successfully developed bone metastasis as soon as 8 days after CA-injection, suggesting that the non-metastatic phenotype of these cells might be due to low homing efficiency. Further analysis will reveals the effect of hormone pre-treatment, which makes MCF7 metastatic¹⁶, on bone metastasis. This result suggests that our model might open up new avenues for exploring key events in bone metastasis by enabling analyses that were previously impossible using current models.

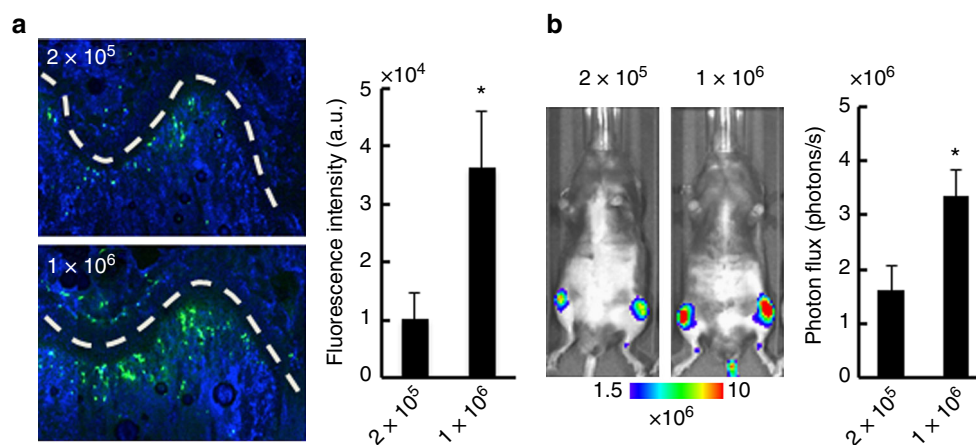


Fig. 3 Injection of larger number of cancer cells enhances bone metastasis development. **a** Fluorescence microscopic analysis of cancer cells in bone marrow of the femur. Representative fluorescence images of the femur (left) and fluorescent intensities of cancer cells (right) at 30 min after CA injection of green-fluorescently labeled LLC/luc cells (2.0×10^5 or 1.0×10^6 cells). Cells were stained with Hoechst dyes (blue). White-dashed lines indicate growth plates. A scale bar is 200 μm . $n = 4$, * $P < 0.05$ (two-side student's t -test). **b** Development of bone metastasis after injection of different number of LLC/luc cells. Representative BL images (left) and BL intensity in hind limbs (right) at 14 days after CA injection of LLC/luc cells (2.0×10^5 or 1.0×10^6 cells). $n = 8$, * $P < 0.05$ (two-side student's t -test). Error bars indicate s.e.m.

The fact that CA-injection delivers cancer cells to the organs downstream of the common iliac artery (Supplementary Fig. 8) limits the investigation for systemic effect of injected cancer cells or the development of metastasis in the bones located upper sites of the body such as skull. In contrast, this model enables the investigation of bone metastasis for a much longer time than that with the IC-injection model because of reduced incidence of lethal metastasis in other organs (Fig. 2f). This represents a great advantage for investigating cancer cell dormancy, which are key issues for bone metastasis.

Recently, intra-iliac artery (IIA) injection was described to selectively deliver cancer cells to bone marrow of a hind limb in mice, allowing efficient immunohistological analysis of metastatic colonies at the early stage of bone metastasis¹⁷. Although delivery efficiency to the bone might be higher by IIA injection than CA injection, the requirement of a surgical procedure and microscopic observation of IIA injection is not suitable for experiments with large numbers of mice¹⁸. In addition, inflammation at the site of surgery may influence the analysis of bone metastasis.

CA injection might facilitate a particular scope of studies to understand bone metastatic processes. For example, interactions between cancer cells and platelets might be a key event in bone metastasis and remain to be fully understood^{19,20}. A previous study raised the issue that IC injection often causes death of transgenic mice with platelet dysfunction, probably due to lasting bleeding from the left ventricle²¹. The CA injection model may solve this problem by direct hemostasis at the injection site, enabling investigation of bone metastasis in mice with platelet dysfunction or depletion.

In the CA injection model using LLC/luc cells, metastatic formation was often detected in vesicular glands, probably because of the efficient delivery of cancer cells (Figs. 1e, 2f), but this metastasis was not lethal. Although further studies will need to reveal organotropism of various cell lines injected via the CA, our new model could represent a powerful tool for the development of drugs that target bone metastasis, in addition to facilitating research on the molecular mechanisms regulating the initiation and progression of bone metastasis.

Methods

Cell lines. The murine lung carcinoma cell LLC, human breast cancer cell MDA-MB-231 and MCF7, human prostate cancer cell PC-3, human renal cell

adenocarcinoma 786-O, human osteosarcoma 143B and murine breast cancer cell 4T1 were obtained from ATCC (Rockville, MD, USA). Murine breast cancer cell E0771 was purchased from C3H BioSystems (Buffalo, NY, USA). Isolation of LLC/luc and MDA-MB-231/luc were described previously^{9,22}. Similarly, PC-3/luc, 786-O/luc, 143B/luc, and 4T1/luc were isolated after transfection with plasmid pEF/luc by calcium phosphate method²³. E0771 and MCF7 were stably transduced with luc2 fused with monomer KusabiraOrange2 (mKO2) using *Sleeping Beauty* transposon system²⁴. To utilize the system, first pT2/CMV-MSC-SVNeo. was constructed by amplifying a fragment of CMV promoter-multi cloning site (MSC)-poly A using pcDNA3.1 plasmids (Invitrogen, Carlsbad, CA, USA) as a template and inserting the fragment into Addgene plasmid #26553. Then pcDNA/mKO2-luc2 was constructed by inserting a luc2-mKO2 fused cDNA fragment amplified from pGL4.32 (Promega, Madison, WI, USA) and Addgene plasmid #67661 as templates, respectively and inserting the fragment into pT2/CMV-MSC-SVNeo using In-Fusion HD Cloning Kit (Clontech, Palo Alto, CA, USA). E0771 and MCF7 were co-transfected with pT2/CMV-mKO2-luc2-SVNeo and pCMV(CAT)T7-SB100 (Addgene plasmid #34879) using NEPA21 electroporator (NEPA gene, Chiba, Japan). The fluorescence/bioluminescence dual reporter-introduced cells E0771/mKO2-luc2 and MCF7/mKO2-luc2 were established from a single colony after antibiotic selection. LLC/mKO2-Rluc8.6 was established using the *Sleeping Beauty* transposon system. To construct pT2/mKO2-Rluc8.6, Rluc8.6 cDNA was amplified from pGEX/PTD-ODD-Rluc8.6 as described previously²⁵. LLC/luc, LLC/mKO2-Rluc8.6, MDA-MB-231/luc, 786-O/luc, and 143B/luc were maintained at 37 °C in 5% FCS-DMEM (Nacalai Tesque, Kyoto, Japan) supplemented with penicillin (100 U/mL) and streptomycin (100 $\mu\text{g/mL}$). PC-3/luc, E0771/mKO2-luc2, and 4T1/luc were maintained at 37 °C in 10% FCS-RPMI (Nacalai Tesque, Kyoto, Japan) supplemented with penicillin (100 U/mL) and streptomycin (100 $\mu\text{g/mL}$). The cells were regularly checked for mycoplasma contamination by a mycoplasma check kit (Lonza, Basel, Switzerland) and were independently stored and recovered from the original stock every time for each experiment.

Mice. C57B/6 mice (male), C57B/6 albino mice (male), NOD-SCID mice (female), SCID mice (male and female), BALB/c mice (female), and BALB/c-nu nude mice (male) were obtained from Charles River Laboratory Japan (Yokohama, Japan). All mice used were provided access to food and water ad libitum, and were housed in the animal facilities at Tokyo Institute of Technology. All the experimental procedures using mice were approved by the Animal Experiment Committees of Tokyo Institute of Technology (authorization number 2010006-3 and 2014005) and carried out in accordance with relevant national and international guidelines.

NIR-II fluorescence imaging. NIR-II fluorescence images were acquired with SAI-1000 (SHIMADZU, Kyoto, Japan). Mice were injected with 50 μL OTN ceramic probe Y (Katayama Chemical Industries, Osaka, Japan) via cannulate line connected to caudal artery or tail vein, respectively. NIR-II fluorescence images were obtained using following settings: excitation/emission wavelength = 980 nm/1530 nm, laser power = 10.5 mW, and camera exposure time = 500 ms.

In vitro analysis of cancer cells from the bone marrow. Hind-limb bones were harvested and crushed in a mortar with PBS. The bone marrow extract was centrifuged to obtain the cell pellet and the pellet was suspended into 100 μL of Passive

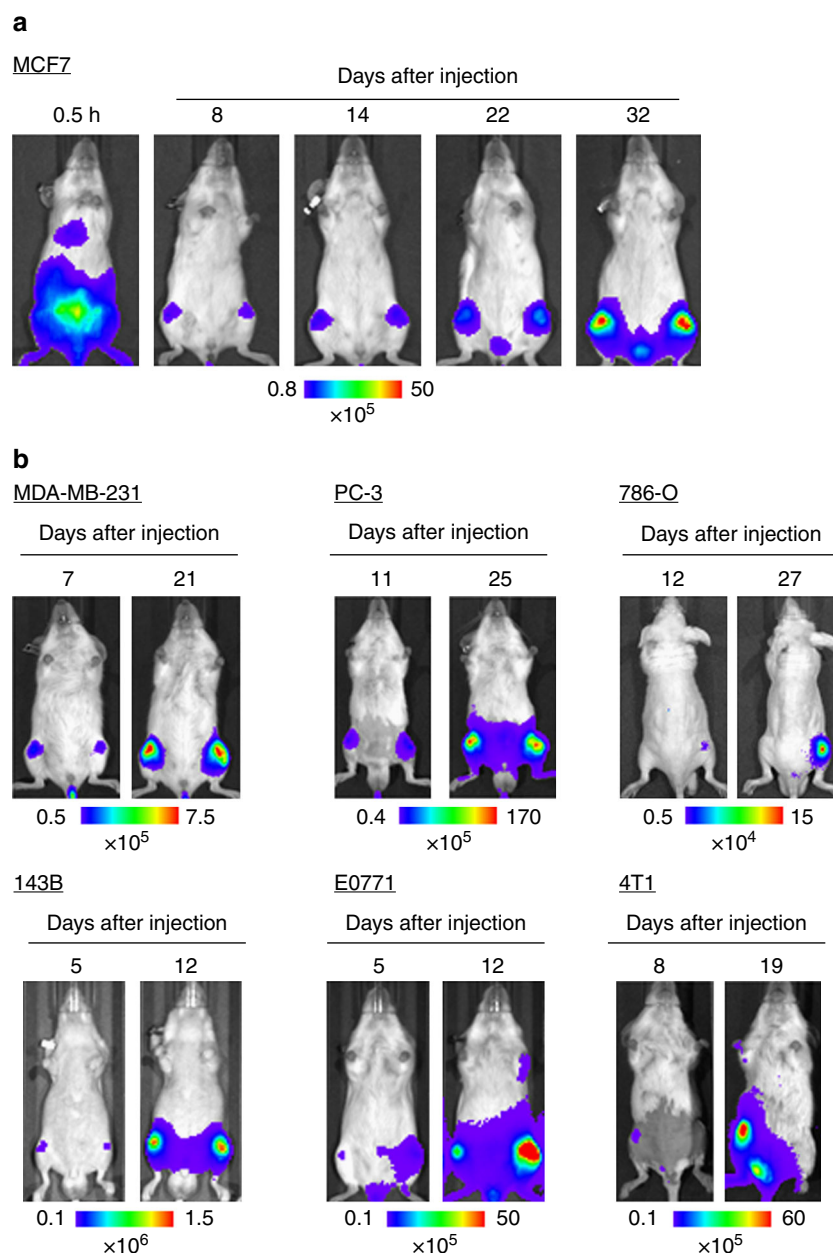


Fig. 4 Efficient bone metastasis development with various cancer cell lines by CA injection. **a** Representative BL images at indicated days after CA injection of MCF7 constitutively expressing firefly luciferase. **b** Representative BL images at indicated days after CA injection of cancer cell lines (MDA-MB-231, PC-3, 786-O, 143B, E0771, and 4T1) constitutively express firefly luciferase

Lysis Buffer (Promega). Fifty μL of cell lysate was mixed with an equal volume of Luciferase Assay Reagent (Promega) in a 96-well plate and then BL imaging was performed using IVIS Spectrum (PerkinElmer, Boston, MA, USA). The BL images were analyzed by Living Image 4.3 software (PerkinElmer) specialized for IVIS.

Bone metastasis models. For CA injection, LLC/luc (2×10^5 or 1×10^6 cells to male C57B/6), MDA-MB-231/luc (5×10^5 cells to female NOD-SCID), PC-3/luc (1×10^6 cells to male SCID), 786-O/luc (1×10^6 cells to male BALB/c-nu), 143B/luc (5×10^5 cells to male BALB/c-nu), E0771/mKO-luc2 (2×10^5 cells to female C57B/6 albino), 4T1/luc (1×10^3 cells to female BALB/c), or MCF7 (1.5×10^6 cells to female SCID) suspended in 100 μL PBS was injected into the caudal artery of anesthetized mice using 29 G syringe needle in a short time (<3 s). IC injection was performed as described previously^{4,5}. LLC/luc (2×10^5 cells) suspended in 100 μL PBS and was injected into left cardiac ventricle of 5-week-old-male C57B/6 mice. IC injection is well established and CA injection is technically as easy as IV injection. Therefore, >8 samples are adequate sample size for evaluation of metastasis growth in each experiment. Randomization and blind tests were not performed during the experiments.

In vivo bioluminescence imaging. BL images of tumor bearing mice were acquired with IVIS Spectrum at 15 min after intraperitoneal injection of D-luciferin (50 mg/kg). The following conditions were used for image acquisition: open emission filter, exposure time = 60 s, binning = medium: 8, field of view = 12.9×12.9 cm, and f/stop = 1. The BL images were analyzed by Living Image 4.3 software (PerkinElmer) specialized for IVIS.

Ex vivo bioluminescence imaging. A mouse was sacrificed immediately after in vivo BL imaging and major organs were removed. BL images of the organs were obtained with following conditions: open emission filter, exposure time = 30 s, binning = medium: 8, field of view = 12.9×12.9 cm, and f/stop = 1. The BL images were analyzed by Living Image 4.3 software (PerkinElmer) specialized for IVIS.

Histological analysis. The isolated bone of a hind limb was fixed in 70% ethanol for 48 h, decalcified in 10% EDTA for 2 weeks, processed, and embedded in paraffin. Sectioned bones (10 μm thickness) were then stained with hematoxylin-eosin. To detect bone metastasis of mKO2-expressing cancer cells, isolated bones were embedded in OCT compound (Leica Microsystems, Wetzlar,

Germany), and cryosections of the embedded bones were prepared by using CM3050 Cryostat (Leica BIOSYSTEMS), stained with Hoechst and observed under a confocal fluorescence microscope (LSM700, Carl Zeiss, Oberkochen, Germany). To quantitatively evaluate the formation of bone metastatic lesions, multiple sections were prepared from eight bones dissected from CA and IC-injected mice and metastatic lesions in each section were counted. The size of bone metastasis was quantified by measuring area with mKO2 fluorescence with ImageJ software.

X-ray micro CT imaging. X-ray micro CT imaging was performed using CosmoScan GX II system (Rigaku Corp., Tokyo, Japan). Dissected hind-limb bones were imaged using following parameters: 90 KV of X-ray tube voltage, 88 μ A of X-ray tube current. For quantitative analysis of bone mass, X-ray CT images of transverse plane at 0.7 mm from the growth plate were analyzed using ImageJ software.

Imaging of cancer cells in the bone marrow. Femur bones were harvested from mice at 30 min after CA injection of LLC/luc cells labeled with CellTracker Green CMFDA Dye (Thermo Fisher Scientific, San Jose, CA, USA). Also, mice were injected with Hoechst 33342 dyes (50 mg/kg) (Wako, Tokyo, Japan) at 5 min before isolation of bones. The isolated bone was then embedded into OCT compound to freeze it at -80°C . The bone marrow of a femur bone was exposed using CM3050 Cryostat (Leica BIOSYSTEMS, Wetzlar, Germany) and mounted to confocal microscope (Carl Zeiss, Oberkochen, Germany) for fluorescence imaging of cancer cells in the bone marrow. Total intensity of green fluorescence in 0.5 mm from the growth plate was quantified using ImageJ 1.47.

Statistical analysis. Data sets with similar variance were statistically analyzed. Data are presented as means \pm standard error of the mean (s.e.m.) and were statistically analyzed with a two-side student's *t*-test. *P* values of <0.05 were considered statistically significant.

Data availability. The data that support the findings of this study are available from the corresponding author upon request.

Received: 5 February 2017 Accepted: 26 June 2018

Published online: 30 July 2018

References

- Weilbaecher, K. N., Guise, T. A. & McCauley, L. K. Cancer to bone: a fatal attraction. *Nat. Rev. Cancer* **11**, 411–425 (2011).
- Johnson, R. W., Schipani, E. & Giaccia, A. J. Pharmacology & Therapeutics HIF targets in bone remodeling and metastatic disease. *Pharmacol. Ther.* **150**, 169–177 (2015).
- Simmons, J. K. et al. Animal models of bone metastasis. *Vet. Pathol.* **52**, 827–841 (2015).
- Dai, J., Hensel, J., Wang, N., Julio, M. K. & Shiozawa, Y. Mouse models for studying prostate cancer bone metastasis. *Bone Rep.* **5**, 1–10 (2016).
- Sasaki, A. et al. Bisphosphonate risedronate reduces metastatic human breast cancer burden in bone in nude mice. *Cancer Res.* **55**, 3551–3557 (1995).
- Kang, Y. et al. A multigenic program mediating breast cancer metastasis to bone. *Cancer Cell* **3**, 537–549 (2003).
- Shiozawa, Y. et al. Human prostate cancer metastases target the hematopoietic stem cell niche to establish footholds in mouse bone marrow. *J. Clin. Invest.* **121**, 1298–1312 (2011).
- Lu, X. et al. VCAM-1 promotes osteolytic expansion of indolent bone micrometastasis of breast cancer by engaging $\alpha 4 \beta 1$ -positive osteoclast progenitors. *Cancer Cell* **20**, 701–714 (2011).
- Kuchimaru, T. et al. Bone resorption facilitates osteoblastic bone metastatic colonization by cooperation of insulin-like growth factor and hypoxia. *Cancer Sci.* **105**, 553–559 (2014).
- Yoneda, T. Arterial microvascularization and breast cancer colonization in bone. *Histol. Histopathol.* **12**, 1145–1149 (1997).
- Zako, T. et al. Development of near infrared-fluorescent nanophosphors and applications for cancer diagnosis and therapy. *J. Nanomater.* **2010**, 491471 (2010).
- Wei, Y. et al. High-sensitive in vivo imaging for tumors using a spectral up-conversion nanoparticle NaYF₄: Yb³⁺, Er³⁺ in cooperation with a microtubulin inhibitor. *Nanoscale* **4**, 3901–3909 (2012).
- Vlodavsky, I. et al. Mamalian heparanase: Gene cloning, expression and function in tumor progression and metastasis. *Nat. Med.* **5**, 793–802 (1999).
- Praptap, J. et al. The Runx2 osteogenic transcriptional factor regulates matrix metalloproteinase 9 in bone metastatic cancer cells and controls cell invasion. *Mol. Cell Biol.* **25**, 8581–8591 (2005).
- Cook, M. J. *The Anatomy of the Laboratory Mouse* (Academic Press, New York, 1965).
- Ogba, N. et al. Luminal breast cancer metastases and tumor arousal from dormancy are promoted by direct actions of estradiol and progesterone on the malignant cells. *Breast Cancer Res.* **16**, 489 (2014).
- Wang, H. et al. Osteogenic niche promotes early-stage bone colonization of disseminated breast cancer cells. *Cancer Cell* **27**, 1–18 (2015).
- Yu, C. et al. Intra-iliac artery injection for efficient and selective modeling of microscopic bone metastasis. *J. Vis. Exp.* **115**, e53982 (2016).
- Suva, L. J., Washam, C., Nicholas, R. W. & Griffin, R. J. Bone metastasis: mechanisms and therapeutic opportunities. *Nat. Rev. Endocrinol.* **7**, 208–218 (2011).
- Suva, L. J. et al. Platelet Dysfunction and a high bone mass phenotype in a murine model of platelet-type von Willebrand disease. *Am. J. Pathol.* **172**, 430–439 (2008).
- Bakewell, S. J. et al. Platelet and osteoclast β_3 integrins are critical for bone metastasis. *Proc. Natl Acad. Sci. USA* **100**, 14205–14210 (2003).
- Kuchimaru, T. et al. A luciferin analogue generating near-infrared bioluminescence achieves highly sensitive deep-tissue imaging. *Nat. Commun.* **7**, 11856 (2016).
- Chen, C., & Okayama, H. High-efficiency transformation of mammalian cells by plasmid DNA. *Mol. Cell Biol.* **7**, 2745–2752 (1987).
- Mátés, L. et al. Molecular evolution of a novel hyperactive *Sleeping Beauty* transposase enables robust stable gene transfer in vertebrates. *Nat. Genet.* **41**, 753–761 (2009).
- Kuchimaru, T. et al. A novel injectable BRET-based in vivo imaging probe for detecting the activity of hypoxia-inducible factor regulated by the ubiquitin-proteasome system. *Sci. Rep.* **6**, 34311 (2016).

Acknowledgements

We are grateful to Shigeaki Watanabe and Machiko Horiuchi (Summit Pharmaceuticals International Corporation, Tokyo, Japan) for discussion and technical support of IVIS, SAI-1000, and CosmoScan GX II system. We thank Doreen Chan (California Institute of Technology) for assistance in animal imaging. We also thank Biomaterials Analysis Division, Technical Department of Tokyo Institute of Technology for DNA sequencing analysis. This research was supported by a Grant-in-Aid for Scientific Research on Innovative Areas “Integrative Research on Cancer Microenvironment Network” from the “Ministry of Education, Culture, Sports, Science and Technology of Japan” (S.K.-K.), Grant-in-Aid for Young Scientist (B) (T.Ku.).

Author contributions

T.Ku. and K.N. conceived CA injection. S.K.-K. designed and managed the overall project. T.Ku., N.K., K.N., T.I., H.M., M.M., and T.Ka. performed experiments. T.Ku. and N.K. analyzed data. T.Ku. and S.K.-K. wrote the manuscript.

Additional information

Supplementary Information accompanies this paper at <https://doi.org/10.1038/s41467-018-05366-3>.

Competing interests: The authors declare no competing interests.

Reprints and permission information is available online at <http://npg.nature.com/reprintsandpermissions/>

Publisher's note: Springer Nature remains neutral with regard to jurisdictional claims in published maps and institutional affiliations.



Open Access This article is licensed under a Creative Commons Attribution 4.0 International License, which permits use, sharing, adaptation, distribution and reproduction in any medium or format, as long as you give appropriate credit to the original author(s) and the source, provide a link to the Creative Commons license, and indicate if changes were made. The images or other third party material in this article are included in the article's Creative Commons license, unless indicated otherwise in a credit line to the material. If material is not included in the article's Creative Commons license and your intended use is not permitted by statutory regulation or exceeds the permitted use, you will need to obtain permission directly from the copyright holder. To view a copy of this license, visit <http://creativecommons.org/licenses/by/4.0/>.

© The Author(s) 2018

Protocol Title: The Hippo pathway in prostate cancer dormancy and recurrence
Protocol Type: IACUC
Approval Period: **Draft**
Important Note: This Print View may not reflect all comments and contingencies for approval. Please check the comments section of the online protocol.

*** Attached Document ***

Document Name	Created Date
ApprovalLetter_IBC.pdf	01/05/2021



Institutional Biosafety Committee

5425 Woodward Ave., Suite 300

Detroit, MI 48202

Phone: (313) 577-1200

<http://research.wayne.edu/oehs/bio-safety/index.php>

September 15, 2020

Re: Protocol # **IBC-20-07-2486**

Dear Cackowski, Frank,

The Wayne State University Biosafety Committee grants approval for experiments described in your protocol titled The Hippo pathway in prostate cancer dormancy and recurrence. This protocol will expire after 3 years, September 14, 2023.

If you require any additional information, please contact Richard Pearson (Biosafety Officer) or me.

Sincerely,

A handwritten signature in black ink, appearing to read "Thomas A. Kocarek".

Kocarek, Thomas

Thomas A. Kocarek, Ph.D., Chair

Wayne State University Institutional Biosafety Committee